FREEZING PROCESS OPTIMISATION OF PHARMACEUTICAL FORMULATIONS
FOR FREEZE DRYING

ADEKUNBI AYO-OKANLAWON

Master of Philosophy

ASTON UNIVERSITY

June 2014

Aston University

Freezing Process Optimisation of Pharmaceutical Formulations for Freeze Drying
By
Adekunbi Ayo-Okanlawon
MPhil, 2014

THESIS SUMMARY

The body of work presented in this thesis are in three main parts: [1] the effect of ultrasound on freezing events of ionic systems, [2] the importance of formulation osmolality in freeze drying, and [3] a novel system for increasing primary freeze drying rate. Chapter 4 briefly presents the work on method optimisation, which is still very much in its infancy.

Aspects of freezing such as nucleation and ice crystal growth are strongly related with ice crystal morphology; however, the ice nucleation process typically occurs in a random, non-deterministic and spontaneous manner. In view of this, ultrasound, an emerging application in pharmaceutical sciences, has been applied to aid in the acceleration of nucleation and shorten the freezing process. The research presented in this thesis aimed to study the effect of sonication on nucleation events in ionic solutions, and more importantly how sonication impacts on the freezing process. This work confirmed that nucleation does occur in a random manner. It also showed that ultrasonication aids acceleration of the ice nucleation process and increases the freezing rate of a solution.

Cryopreservation of animal sperm is an important aspect of breeding in animal science especially for endangered species. In order for sperm cryopreservation to be successful, cryoprotectants as well as semen extenders are used. One of the factors allowing semen preservation media to be optimum is the osmolality of the semen extenders used. Although preservation of animal sperm has no relation with freeze drying of pharmaceuticals, it was used in this thesis to make a case for considering the osmolality of a formulation (prepared for freeze drying) as a factor for conferring protein protection against the stresses of freeze drying. The osmolalities of some common solutes (mostly sugars) used in freeze drying were determined (molal concentration from 0.1m to 1.2m). Preliminary investigation on the osmolality and osmotic coefficients of common solutes were carried out. It was observed that the osmotic coefficient trend for the sugars analysed could be grouped based on the types of sugar they are. The trends observed show the need for further studies to be carried out with osmolality and to determine how it may be of importance to protein or API protection during freeze drying processes.

Primary drying is usually the longest part of the freeze drying process, and primary drying times lasting days or even weeks are not uncommon; however, longer primary drying times lead to longer freeze drying cycles, and consequently increased production costs. Much work has been done previously by others using different processes (such as annealing) in order to improve primary drying times; however, these do not come without drawbacks. A novel system involving the formation of a frozen vial system which results in the creation of a void between the formulation and the inside wall of a vial has been devised to increase the primary freeze drying rate of formulations without product damage. Although the work is not nearly complete, it has been shown that it is possible to improve and increase the primary drying rate of formulations without making any modifications to existing formulations, changing storage vials, or increasing the surface area of freeze dryer shelves.

DEDICATION

To my husband, Ayobami, thank you for your continued support and encouragement. You were there with me through the highs and the lows. Your words of advice pulled me through many tough times.

To my daughter, Eunice, thank you for being such a good girl and for the joy and laughter you always bring.

To my parents, Tokunboh and Foluke, I will forever be grateful for your support in every single way from the very beginning of my programme. I will never be able to say thank you enough.

To my grandma, Lydia, your calls and prayers can never be forgotten.

To my sisters, Bukola and Kemi, you both have always been on the side lines cheering me on and supporting me every way you can. You are both awesome!

ACKNOWLEDGEMENTS

First and foremost, I would like to thank the Lord God Almighty, without Whom I would not have been able to make it through my programme.

A heartfelt thank you goes to Dr Andrew Ingham for his guidance, help, advice and particularly patience throughout my research programme. I will forever be grateful to you!

Many thanks also to Jiteen Ahmed for all laboratory related help and sometimes lending an ear to listen. I will never forget!

To my colleagues in MB328, it's been such a privilege working side by side with each of you. Thank you!

LIST OF CONTENTS

LIST OF TABLES

LIST OF FIGURES

16

CHAPTER 1: INTRODUCTION

Therapeutic proteins have now become a significant and highly important product class in the pharmaceutical industry (Maltesen & van de Weert, 2008). Compared with more conventional, low molecular weight drugs, therapeutic proteins have higher activity and specificity, making them more effective and better at treating life-threatening diseases such as cancer, diabetes and rheumatoid arthritis (Sarmento, 2008).

The sensitivity of proteins has been an issue of concern for well over a decade. This is due, in part, to the fact that a change in the structure of a protein can negatively impact its therapeutic effect and consequently lead to adverse immune reactions to the drug formulation (Roumeliotis, 2006). The delicate nature of the majority of proteins as well poor long term stability has brought about a challenge for the pharmaceutical industry causing a focus on finding methods capable of stabilising proteins (Maltesen & van de Weert, 2008).

Lyophilisation has long been known as a common method used to improve the stability of pharmaceutical and bio-pharmaceutical products, as well as bacterial cultures and analytical chemical moieties (Hunek *et al.*, 2007; Kamath, 2006). Hunek *et al* (2007) explained that industry experts have recorded a double digit growth in global cGMP lyophilisation equipment sales, reaching approximately $250 million per year, as a result of the increase in lyophilisation capacity. This is an indication that the lyophilisation process continues to grow in demand and continues to be a method of interest to scientists in many fields of interest. It is worthy of note that Nova Laboratories has "the world's only fully validated aseptic spray-drying facility". Nova Laboratories state that the pharma industry is looking for other ways of drug delivery, which are more efficient and cost-effective than lyophilization, and stated that aseptic spray drying may offer these. This new development will see clinical trials concluded and allow the technology to be available proven this may lead to companies turning

from lyophilisation to the more economical spray drying (Hunek *et al*, 2007). Future chapters will highlight the lyophilisation process for protein therapeutics and key changes or developments there has been in the last decade. The principles behind the lyophilisation process will be discussed followed by the effects processing has on proteins.

1.1.   The Lyophilisation Process

Lyophilisation, also known as, freeze-drying is a process widely used for preparing and improving the stability of pharmaceutical products (Wang, 2000; Abdelwaheed *et al*., 2006). The development of lyophilisation as an industrial process was greatly influenced by the high demand for bulk preparations of human blood plasma during World War II (Franks, 1998; Matejtschuk, 2007). Although considered to be time consuming and expensive, in recent years lyophilisation has become the method of choice for improvements in the storage of proteins as the demand for medicinal product grade protein therapeutics has been made.

Historically lyophilisation is the preferred method for dehydrating proteins (Matejtschuk, 2007; Maltesen & van de Weert, 2008). Adams (2007) argues that the term "lyophilisation" is less descriptive than the term "freeze-drying" and made mention of the fact that many definitions of the process though applicable to ideal systems, do not completely define the process for typical systems, which "form an amorphous matrix or glass when cooled". Of all the papers reviewed, only Adams (2007) provided definitions as may be required.

Lyophilisation occurs in three process stages:

- **controlled freezing** during which the protein solution is cooled until an amorphous crystalline or combined amorphous-crystalline solid or matrix is formed (Maltesen & van de Weert, 2008),

- **primary drying** at lower temperatures under vacuum, which involves sublimation of frozen water from the formed solid or matrix and results in the formation of a porous plug (Matejtschuk, 2007; Maltesen & van de Weert, 2008),

- **secondary drying** at slightly elevated temperatures and high vacuum, which involves the removal of unfrozen bound water again by moisture desorption (Jameel & Sugunakar, 2005; Hunek *et al*. 2007; Maltesen & van de Weert, 2008)

In a typical lyophilisation process, an aqueous solution containing the active pharmaceutical ingredient (API) and various excipients is filled into glass vials, and the vials loaded onto the temperature-controlled shelves of the freeze dryer. The shelf temperature is reduced, typically in several stages, to a temperature of about $40^{\circ}C$, thereby converting nearly all the water into ice (Pikal, 2007). Some excipients, such as buffer salts and mannitol, may partially crystallise during freezing, but most APIs particularly proteins, remain amorphous. The API and excipients are usually converted into an amorphous glass also containing large amounts of unfrozen water (15–30%) dissolved in the solid amorphous phase (Pikal, 2007). After all water and solutes have been converted into solids, the entire system is evacuated by the vacuum pumps to the desired control pressure, the shelf temperature is increased to supply energy for sublimation, and primary drying begins. Since primary drying requires a large heat flow, the product temperature runs much lower than the shelf temperature. The removal of ice crystals by sublimation creates an open network of pores which create pathways for the water vapour from the product to pass through (Franks, 2007; Pikal, 2007). As primary drying proceeds, the boundary between frozen and dried regions typically moves from the top of the product towards the bottom of the vial. The start of secondary drying is usually defined as the end of primary drying, even though some secondary drying occurs

during primary drying. Due to vial-to-vial variation, some vials enter secondary drying while other vials are in the last stages of primary drying. The final stages of secondary drying are normally carried out at shelf temperatures in the range of 25–50°C for several hours. Because the demand for heat is low at this point, the shelf temperature and the product temperature are nearly identical (Franks, 2007; Pikal, 2007).

1.1.1. The Phase Diagram for Water

The lyophilisation process involves three states of matter, liquid to solid, and then solid to vapour. As a result, the theory and consequently the practice of lyophilisation cannot be properly understood without understanding and applying the phase diagram for water.
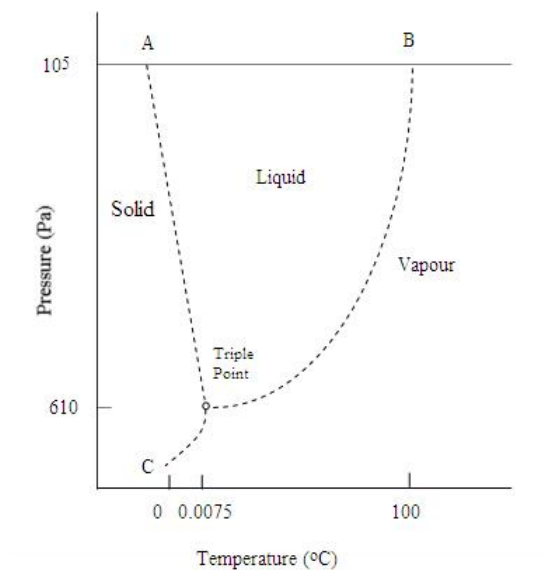
Figure 1.The phase diagram of water (not to scale). Adapted from Pharmaceutics: The Science of Dosage Form Design. Aulton, M. E (2002)

In Figure 1, three separate areas represent the phases of water; solid, liquid or vapour. Under the conditions of temperature and pressure defined by any point along each line, two phases coexist (Aulton, 2002). The point where all three phases are joined is the only unique point where all three phases can coexist; this is known as the triple point

27

with coordinates of 610 Pa pressure and a temperature of 0.0075^{o}C. BO is the vapour pressure curve, indicating the boiling point of water as it is lowered by a reduction in the external pressure above it; along this curve vapour and liquid can coexist in equilibrium. AO is the melting point curve, where liquid and solid coexist in equilibrium. AO has a negative slope, which indicates that the freezing point of water decreases as external pressure increases. CO is the sublimation curve, along which vapour and solid can coexist in equilibrium and indicates the reduction of vapour pressure by ice on reduction of temperature (Aulton, 2002).

It is well established that at constant atmospheric pressure, ice will melt as temperature steadily rises to 0°C (Aulton, 2002). With all parameters constantly maintained, ice will gradually change to water and eventually to water vapour as temperature reaches 100°C. However, at a constant pressure below the triple point, solid ice will sublime, and be converted directly to water vapour without passing through a liquid phase at a temperature lower than 0°C. For this to occur, pressure must be maintained below the triple point pressure by immediately removing any vapour released (Aulton, 2002; Sinko, 2006).

When a solute is dissolved in liquid water at the triple point, the vapour pressure of the liquid water is lowered below that of the pure solid ice. Therefore in order for the system to re-establish equilibrium between the liquid and solid, the temperature within the system must be lowered, causing a depression of the freezing point, and also causing a shift in the phase diagram. The lyophilisation process involves processing of liquids containing various solutes and as such, the freezing point depression phenomenon is a normal occurrence. Hence, solutions processed by lyophilisation must be cooled to temperatures well below the normal freezing point of water to cause initial freezing.

1.1.2. The Freezing Step

The main purpose of freezing is to ensure the removal of most of the water from a formulation by formation of ice, and to convert all solutes into solids, be it crystalline solids or glass (Pikal, 2007). Sun *et al* (2006) defined freezing as the process of removing sensible and latent heat in order to lower product temperature to -18°C or lower. The freezing process consists of two successive processes: nucleation (formation of ice crystals) and the subsequent crystal growth (Zaritzky, 2006). Hottot *et al* (2004) stated that for a given formulation, based on observation, the cooling rate, supercooling degree and the ice nucleation temperature are the three interdependent factors, which control the freezing process.

1.1.2.1. Cooling rate, supercooling, ice nucleation and ice crystal growth

Freezing of a liquid sample begins with chilling of the sample. When the liquid is chilled below its standard freezing point without solidification, it begins to supercool until a *seed crystal* or *nucleus* is formed; this event is termed as *nucleation* and formation of a crystal in a solution containing no existing crystals is known as *primary nucleation*. Following primary nucleation, *secondary nucleation* occurs involving the production of new crystals in the liquid sample, this continues to occur and ice crystals continue to grow until the entire liquid volume is encompassed (Chow *et al*, 2005). The onset of nucleation results in a sharp rise in temperature as bond energies are released as a result of latent heat of crystallization (Sinko, 2006). This temperature rise holds steady as ice crystals grow, and then steadily decreases as solidification of the nucleated volume occurs; further chilling of the resulting frozen ice will cause the sample temperature to equilibrate with the temperature of the chilling surface. The ice nucleation temperature is not under direct control as it is spontaneous, indeterminate and indefinite in nature (Patel *et al.*, 2009). Nucleation could be homogeneous or heterogeneous. Homogeneous nucleation occurs in extremely pure water, free from impurities, and in which a seed crystal is formed by

random orientation and combination of water molecules (Sun *et al.*, 2006; Zaritzky, 2006). Heterogeneous nucleation takes place in typical preparations or formulations to be freeze dried and occurs when water molecules aggregate in a crystalline arrangement on nucleating agents such as walls of containers or particles in the formulation (Sun *et al.*, 2006; Patel *et al.*, 2009). The temperature at which nucleation occurs determines the number of ice nuclei formed during the freezing process, a factor which plays an important role in the eventual drying time of the formulation (Patel *et al.*, 2009)

During the freezing process, water crystallises to ice such that all solutes are concentrated between the ice crystals formed (Patel & Pikal, 2009). An important parameter to note during this step is the degree of supercooling. Patel & Pikal (2009) defined supercooling as "the difference between the ice nucleation temperature and the equilibrium freezing point" of the solution being processed by lyophilisation. The supercooling degree during the freezing step is essential as it determines the number of nuclei and subsequently the number of crystals formed in a sample therefore having a great impact on product resistance and consequently, product temperature and drying time. When the supercooling degree is high, crystallisation of the liquid occurs rapidly resulting in smaller ice crystals and small pore sizes in the dried layer, leading to a high resistance to water vapour transport during primary drying and consequently, longer primary drying times (Pikal, 2007; Patel & Pikal, 2009). Small ice crystals do however mean a high specific surface area in the dried product, which allows for a reduced secondary drying time (Pikal, 2007). A low supercooling degree on the other hand results in slower crystallisation, which generates larger ice crystals and consequently large pores in the dried layer; these ensure faster primary drying times but cause an increased secondary drying time due to a small specific surface area in the dried product (Andrieu *et al.*, 2011).

The overall success of the lyophilisation process hinges greatly on the freezing stage. This is because the main characteristics, such as pore size distribution, pore shape, and pore connectivity of the dried layer formed during the primary drying stage depend on the ice crystals, which are formed during the freezing stage (Boss *et al.*, 2004; Jameel & Sugunakar, 2005; Abdelwaheed *et al.*, 2006; Matejtschuk, 2007). Large crystals allow for the creation of large pores, which in turn allows rapid water sublimation during the primary drying step.

1.1.3. Primary drying

Primary drying involves sublimation of ice from the frozen solution as long as latent heat of sublimation is supplied. The heat generated by the shelf of the freeze-dryer is transferred to the frozen solution through the vial it is contained in. As the ice sublimes, water vapour is formed; this is prevented from returning to the product thanks to the presence of a condenser upon which the vapour condenses (Mellor, 1978; Abdelwaheed *et al.*, 2006). Completion of the primary drying process sees the emergence of a porous solid having pores which correspond to the spaces previously occupied by ice crystals, and a small amount of moisture remaining within the solid (Aulton, 2002; Abdelwaheed *et al.*, 2006).

Heat transfer during the primary drying process is of the essence as insufficient heat results in a longer primary drying time, for a process which on the whole is generally lengthy, whilst excess heat will cause product collapse or melting (Wang, 2000; Aulton, 2002). In order to maintain product elegance and minimise degradation, primary drying must be carried out at product temperatures below the collapse temperature (T_c[1]). The collapse temperature and the glass transition temperature of the maximally concentrated

---

[1]Collapse temperature in freeze drying is the critical temperature above which the frozen sample will flow and lose the microstructure created by freezing when the supporting structure of ice crystals is removed (Boylan *et al.*, 2009).

freeze concentrate ($T'_g{}^2$) are closely related, although the collapse temperature is usually several degrees higher than T'_g (Pikal, 2007). Since all vials do not freeze at exactly the same temperature, the target product temperature must be several degrees below the collapse temperature in order to have a safety margin (Pikal, 2007). The product temperature is generally the most important factor in determining the rate of primary drying; however, product resistance is also an important parameter. As the dry layer of the sample increases in thickness, product resistance also increases, as such, resistance increases as primary drying progresses (Pikal, 2007).

Aston University

Illustration removed for copyright restrictions

Figure 2. Resistance to vapour flow during primary drying. Taken from Pikal (1985)

Figure 2 is a schematic of different resistances to vapour flow through the dried product. The sublimation front proceeds horizontally from the top of the vial towards the bottom. Water vapour created by the sublimation of ice must pass through the dried layer that was formed by the removal of ice (Rambhatla & Pikal, 2004). Mass transfer within the dried layer occurs by bulk flow of material in the direction of a pressure gradient or by diffusive flow, which occurs by the relative movement of molecules as a result of differences in concentration, mole fraction, and partial pressure (Gatlin & Nail, 1994).

---

[2] Glass transition temperature of the frozen sample (T'_g) is the temperature below which the frozen sample exists as a rigid glass and above which the frozen sample becomes a viscous liquid (Boylan *et al*., 2009).

1.1.4. Secondary drying

The secondary drying stage involves the removal of residual moisture from the porous solid and commences when the last ice crystal stops subliming allowing moisture desorption to occur (Mellor, 1978; Abdelwaheed *et al.*, 2006). According to Tang & Pikal (2004), the main objective of secondary drying is to reduce the remaining moisture content to an optimal stability level, typically less than 1%. Secondary drying is typically carried out at much higher temperatures, as high as 60°C in order for desorption of moisture to occur at a practical rate (Aulton, 2002; Tang & Pikal, 2004).

1.1.5. Perspectives on the lyophilisation process

After many years and well over a decade of studying and using the lyophilisation process, it is thought that lyophilisation remains the most expensive of all drying methods and is particularly applied for products with high added value (Brulls & Rasmuson, 2002; Xiang *et al.*, 2004; Abdelwaheed *et al.*, 2006; Hunek *et al.*, 2007; Barresi *et al.*, 2009). Brulls & Rasmuson (2002) expressed this view by stating that the lyophilisation process is "the most expensive of all drying operations both in capital investment and in operating expense". Abdelwaheed *et al.* (2006) again buttressed this point by mentioning that the lyophilisation process is not only slow but "expensive and applies to products which have high added value". Xiang *et al.* (2004) attested to this by pointing out that the process is expensive and by suggesting that for an economical lyophilisation process to be developed, minimising process time, particularly that of primary drying is crucial. In the opinion of Barresi *et al.* (2009), lyophilisation is used only for valuable goods due to high investment and operating costs, amongst other factors. These opinions are a clear indication that more work is still required in order to make the

lyophilisation process cost-effective by improving on primary drying time and consequently reducing cycle length.

The lyophilisation process is generally time-consuming owing to lengthy primary drying times as noted by Xiang *et al.* (2004) and Abdelwaheed *et al.* (2006). Xiang *et al.* (2004) discuss this in-depth and stated that the sublimation of ice in the primary drying stage of the process is usually the longest. Further studies showed the effects of four important freeze drying factors on the rate of sublimation of ice by making use of a custom built freeze-drying microbalance, as it was put forward that the process time during primary drying needs to be minimized in order to develop an economical freeze-drying cycle. The four factors studied include, freezing rate, chamber temperature, chamber pressure and inclusion of an annealing step during freezing. The study concluded that the chamber temperature had the greatest effect on sublimation rate such that an increase in chamber temperature can greatly increase sublimation rate. Xiang *et al.* (2004) further went on to state that the freeze-drying microbalance can provide quantitative evaluation of the effects of freeze-drying variables during a freeze-drying process, thereby optimizing the freeze-drying cycle. Similar work was carried out fairly recently by Daoussi *et al.* (2009) by studying the effect of five freeze-drying parameters including chamber temperature. The findings from this study corroborate findings from the study by Xiang *et al.* (2004).

1.2.   Lyophilisation and its Effects on Proteins

Although lyophilisation is a popular and the preferred method to improve the stability of proteins, it comes with its disadvantages. Lyophilisation of protein systems have been shown to suffer significant dehydration stress. Each stage of the lyophilisation process presents a different form of stress to the material being processed consequently causing

possible damage. The freezing stage of lyophilisation is believed to be the main source of stress during lyophilisation (Adams, 2007; Maltesen & van de Weert, 2008).

Protein stability is greatly affected due to ice formation and increased solute concentration as well as an increase in ionic strength during the freezing process (Adams, 2007; Matejtschuk, 2007; Maltesen & van de Weert, 2008). Denaturation and aggregation can also occur due to a number of factors (Matejtschuk, 2007; Maltesen & van de Weert, 2008; Kadoya *et al.*, 2010). Matejtschuk (2007) stated that because the excluded excipient salts in the ice crystals formed during the freezing process concentrate to local concentrations which are higher than what was in the original liquid state, the protein may become destabilised and denatured due to a change in ionic strength. Matejtschuk (2007) further mentions that denaturation can lead to the exposure of normally buried residues and an increase in aggregation. According to Maltesen & van de Weert (2008), when the supercooling rate during the freezing process is rapid, small crystals with a higher specific surface area are formed; this results in larger protein interface adsorption and consequently, increased protein denaturation and aggregation. It was also mentioned by Maltesen & van de Weert (2008) that a slow supercooling rate can enhance phase separation between proteins and added excipients, which can lead to protein destabilisation.

These challenges with lyophilisation and its effect on proteins remain the same as it was in previous decades, and it appears that not much has changed given the considerable amount of studies that have been carried out relating to lyophilisation and the number of reviews and papers written (Matejtschuk, 2007; Maltesen & van de Weert, 2008). Similarly, the use of lyoprotectants and cryoprotectants remain just as important as it was in previous decades and it appears that the same sub-groups of protectors, such as polymers, surfactants, amino acids, and even protein itself, are being used although the use of sugars seem to have gained more popularity.

1.3. Protection of proteins during lyophilisation

Since lyophilisation generates a number of stresses and since it has been established that proteins are delicate and sensitive, the addition of excipients which will protect the protein product during the lyophilisation process is imperative. These excipients either protect the product from stress brought about by the freezing stage and are therefore known as cryoprotectant, or protect the product from the stress brought about by the drying stage and are known as lyoprotectant. Table 1 provides a list of some cryoprotectants and lyoprotectants.

Table 1. A list of some cryoprotectants and lyoprotectants used in freeze drying. * denotes stabilisers which can function as both.

Cryoprotectant	Lyoprotectant
Sucrose (sugar)*	Polyvinylpyrrolidone (polymer)
Lactose (sugar)*	Pluronic F127 (surfactant)
Mannitol (polyol)*	Proline (amino acid)
Tween 80 (surfactant)	Sodium Glutamate (amino acid)
Bovine Serum Albumin (polymer)*	Dextran (polymer)*
Gelatin (polymer)	Glycerol (polyol)*

Many stabilisers which are effective cryoprotectants do not stabilize proteins during drying and it is typical for a formulation prepared for freeze drying to have more than one stabilizer. In order for stabilisers to sufficiently protect a protein, they must be at an optimum concentration to do so, in other words, the effectiveness of stabilisers during freeze-drying is concentration-dependent. For example, a minimum concentration of 0.3

M has been suggested in order for sugars and polyols to achieve any significant stabilisation (Wang, 2000). However, care must be taken since at high initial concentrations, sugars in particular can crystallise during freeze drying, affording no protection to the protein. Getting the balance of the concentration of cryoprotectants and lyoprotectants right in order for the protein or API in a formulation to be protected during the freeze drying process and storage can therefore be rather tricky since a stabilizer (or a combination of stabilisers) that works for protein A may not work protein B. For example, at 30 mg/ml, Trehalose was more effective in inhibiting IL-6 aggregation during freeze drying compared with sucrose at the same concentration. On the other hand, Sucrose was a much better stabilizer than Trehalose in protecting *Humicola lanuginose* lipase during freeze drying (Arakawa et al., 2001; Wang, 2000).

1.4. Tonicity and Osmolality

When a solute is dissolved in a solvent, the resulting solution has a number of properties, which are different from that of the pure solvent. The solution possesses colligative properties, which depend on the number of solute particles on solution, regardless of the presence of molecules or ions, or their sizes (Gupta, 2013). The colligative properties of a solution are osmotic pressure, vapour pressure lowering, boiling point elevation and freezing point depression. All four properties are related; however, osmotic pressure has the greatest direct importance in pharmaceutical science as to a great extent, it helps determine the physiological acceptability of a range of therapeutic solutions and formulations (Shah, 2007; Gupta, 2013). Body fluids, such as blood and tears exhibit osmotic pressure due the number of solutes dissolved in them and according to Ingham and Poon (2013), have an osmotic pressure that is often said to correspond to that of 0.9%w/v solution of sodium chloride. If for example normal saline solution (0.9%w/v sodium chloride) is infused into a patient's vein, the red blood cells in the blood remain intact and they retain their normal size and shape. Since

the sodium chloride solution maintained the tone of the membrane of the red blood cells, it is considered to be *isotonic*. If a patient is infused with a 1.8%w/v solution of sodium chloride, which is said to be *hypertonic*, the solution will cause the red blood cells to shrink and become wrinkled as their content gets sucked out. The reason for this reaction is because there is a lower concentration of dissolved substances inside the red blood cells compared with the concentration of dissolved substances in solution in solution in the vein surrounding the red blood cells. As a result, the water inside the red blood cells will diffuse through the cell membrane to dilute the surrounding salt solution in the vein in order to equalise the osmotic pressure across the membrane. A 0.2% or 0.45%w/v sodium chloride solution will produce an exact opposite event if injected into a patient. The solution is said to be *hypotonic* and as such has a lower concentration of dissolved substances compared to those inside the red blood cells. As such, water from the surrounding salt solution will enter into the cells, causing hemolysis[3] (Brown, 2009; Shah, 2007). Tonicity is an important factor especially in small and large volume injectables, ophthalmic products, as well as tissue irrigation products, as these come into direct contact with blood, muscle, eyes, nose and delicate tissues respectively. Hypertonic and hypotonic solutions have the tendency to cause tissue irritation, pain on injection or when applied to mucous membranes of the eyes, ears, nose, and so on. In order to adjust a formulation to isotonicity, its tonicity must be measured.

Similarly, the 0.9%w/v sodium chloride solution can be said to be iso-osmotic with physiological fluids. According to Ingham and Poon (2013), isotonic and iso-osmotic are commonly used interchangeably in medicine; however, this should not be the case. The term iso-osmotic is a physical term, which compares osmotic pressure or freezing point depression of two fluids, which may not be physiological or may be physiological under certain circumstances. On the other hand, the terms relating to tonicity must only be

---

[3] Haemolysis is the destruction of red blood cells, which occurs by swelling and finally bursting with the liberation of haemoglobin.

used with reference to physiological fluids (Ingham and Poon, 2013). For example, a 2% boric acid solution is iso-osmotic with erythrocyte cell contents and lacrimal fluid; however, it is isotonic with only lacrimal fluid as it causes haemolysis of red blood cells as molecules of boric acid can move freely across the erythrocyte membrane (Shah, 2007; Ingham and Poon, 2013).

Osmolality has been defined as a measure of the total number of osmotically active particles in a solution, which is equal to the sum of the molalities of all the solutes present in the solution (Ribeiro, 2012). Tonicity on the other hand has been defined as the effective osmolality, which is equal to the sum of the concentrations of the solutes that are able to exert an osmotic force across a specific cell membrane (Arroyo and Schweickert, 2013). Tonicity, much like osmolality, is a way of expressing solute concentration; however, it only includes solutes that cannot cross a specific cell membrane. In other words, osmolality is all encompassing as it includes all osmotically active particles in a solution whilst tonicity exempts solutes, which are ineffective, that is, solutes that can cross a specific cell membrane.

1.5.   Measurement of osmolality

The two most popular methods of measuring osmolality are the vapour pressure depression method and the freezing-point depression method. Vapour pressure osmometers measure the osmolality of a solution by determining the temperature at the point of equilibrium between vaporisation and condensation (also known as dew point) of the solution. The lower the dew point of a solution is, the higher its osmolality and vice versa. Although considered to be easy, rapid and convenient, vapour pressure osmometers are not considered to be as precise as freezing-point osmometers. Vapour pressure osmometers also have a disadvantage in that the presence of volatile substances such as ethanol in a solution are not detected as they work with the

assumption that only water is present in the vapour phase (Shah, 2007; Weiser, 2012; Ingham and Poon, 2013). Freezing-point osmometers are the most common and widely used instruments for measuring osmolality due to their reliability, simplicity and ease of use (Shah, 2007). Determination of osmolality through this method is based on the principle that there is a relationship between freezing point depression and osmolality. According to freezing-point osmometers such as the Löser Micro-Osmometer, freezing point depression and osmolality are related by the following:

$$\xi = \frac{\Delta T \ [°C] \ \times \ 1000 \ [mosm]}{1.858 \ [°C]} \quad \text{(Eq. 1)}$$

and

$$\Delta T \ [°C] = \frac{\xi}{1000 \ [mosm]} \ \times \ 1.858 \ [°C] \quad \text{(Eq. 2)}$$

Where ξ = osmolality and ΔT = freezing point depression

(Equations taken from Löser Micro-Osmometer Type 6. Manual and Operating Instructions)

The freezing point of an aqueous solution is the unique temperature, at atmospheric pressure (commonly 1 atm), when solid and liquid phases co-exist in equilibrium. When a solute is added to an aqueous solution, the freezing point of the solvent is lowered resulting in freezing point depression (Figure 3). In comparison to water, freezing point depression is a direct measure of osmolality. In an ideal solution and provided dissociation does not occur, 1 mol of a substance dissolved in 1 kg of water produces a solution with an osmolality of 1 osmol / kg of water. Pure water freezes at $0°C$; however, an aqueous solution, which has an osmolality of 1 osmol / kg of water, freezes at – $1.858°C$ (Sinko, 2006; Gupta, 2013). This measuring principle explains the equations given above.

Figure 3. Vapour-pressure-temperature diagram for water and an aqueous solution, showing elevation of boiling point and lowering of freezing point of the aqueous solution (Taken from Gupta, P. K. 2013. Solutions and Phase Equilibria. In Rx Remington

1.5.1.   Cooling Mode of the Löser Micro-Osmometer

The Löser Micro-Osmometer makes use of the Peltier effect, a temperature difference created by applying an electric current between two electrodes connected to a sample of semiconductor material. The electrodes are usually made with a metal having excellent electrical conductivity. The semiconductor material between the electrodes creates two junctions, which in turn creates a pair of thermocouple. When voltage is applied, the electrodes force electrical current through the semiconductor, allowing thermal energy to flow in the direct of the electric current. This causes heat to be generated from one junction and then absorbed on the other junction depending on the flow of electric current.

Peltier cooling, using Peltier elements, allows for the cooling and freezing of small samples of liquid. These elements can become warm on one of its side and cool on the other. In the Löser Micro-Osmometer, the cold side of the Peltier element is in contact

with a metal block containing the cooling apertures of the unit, whilst the warm side is mounted on a heat sink. In order to keep the temperature in the cooling apertures constant, the charging of the Peltier element, provided by electric power supply, is controlled by a thermistor.

1.5.2. Osmolality Measurements Using the Löser Micro-Osmometer

Consider the diagram of the inner workings of the Löser Micro-Osmometer (figure 4).

Figure 4. Measuring Principle of the Löser Micro-Osmometer (Löser Micro-Osmometer Type 6. Manual and Operating Instructions)

A sample tube containing about 100 µl of the sample to be measured is attached to the measuring head; this allows insertion of the thermistor into the sample. The thermistor helps to keep track of the temperature of the solution in the sample tube as it cools and subsequently freezes. The measuring head is pushed down, allowing the sample tube to be inserted into the cooling aperture. The sample begins to cool immediately, indicated by decreasing temperature values shown on the osmometer's digital display. ***When a clean aqueous solution is continuously cooled, its temperature can be lowered below its freezing point without it becoming solid; this phenomenon is known as***

supercooling. Whilst the sample is in the supercooled state, freezing is triggered by inserting a freezing needle with ice crystals on it into the sample. The Löser Micro-Osmometer has a defined supercooling point of -6.2^{o}C at which freezing is triggered; once -6.2^{o}C is reached, a buzzer sounds continuously until freezing of the sample occurs. It is thought that this defined supercooling point has been set at -6.2^{o}C in order to allow for uniformity of results for any sample. If for example each sample has its own supercooling point at which freezing is triggered, the authenticity of result comparison can be questioned.

When pure water freezes, the heat of fusion resulting from the freezing process causes a rise in temperature to a plateau which is usually prolonged, indicating crystal formation. Solutions on the other hand have a turning point where ice/water equilibrium is maintained. The sample remains at this temperature for a few seconds during which the osmometer uses the thermistor to sense the sample temperature, control the degree of supercooling and freeze induction, and then measure the freezing point of the sample.

Figure 5. Typical cooling curves of water and aqueous solutions (Löser Micro-Osmometer Type 6. Manual and Operating Instructions)

As can be noted in figure 4, the thermistor is arranged to form two legs of a Wheatstone bridge circuit. The output signal from the Wheatstone bridge circuit corresponds to differential electrical resistance in the thermistor caused by the changes in temperature within the sample as it freezes (Shugar & Ballinger, 1996). The linear correlation between osmolality and freezing point depression allows the measurement values to be displayed in milliosmol/kg H_2O and not ^{o}C. It is thought that the Löser Micro-Osmometer has incorporated a system, which takes into consideration the equations previously provided in order for osmolality to be calculated.

CHAPTER 2: EFFECT OF ULTRASOUND ON FREEZING EVENTS OF IONIC SYSTEMS

2.1   RESEARCH BACKGROUND

The freezing step during lyophilisation is of paramount importance as it dictates ice crystal morphology as well as pore sizes of both the ice and product phases (Searles, 2004). The freezing of a liquid sample begins with chilling of the sample. When the liquid is chilled below its standard freezing point without solidification, it begins to supercool until a *seed crystal* or *nucleus* is formed; this event is termed *nucleation*.

2.1.1.   Primary and secondary nucleation

Nucleation in a clean, homogeneous solution resulting solely from the coming together of molecular clusters is referred to as *primary homogeneous nucleation*. When the kinetics of nucleation is catalysed by the presence of an existing surface such as an impurity or undissolved solute, *primary heterogeneous nucleation* occurs (Garside *et al*, 2002).

In the case where the surface is the crystallizing material itself, *secondary nucleation* occurs, following induction by prior presence of crystals of the material being crystallised (Garside *et al*, 2002).. With secondary nucleation, the production of new crystals continues to occur and ice crystals continue to grow until the entire liquid volume is encompassed (Garside *et al*, 2002; Chow *et al*, 2005). The onset of nucleation results in a sharp rise in temperature as bond energies are released as a result of latent heat of crystallisation (Sinko, 2006). This temperature rise holds steady as ice crystals grow, and then steadily decreases as solidification of the nucleated volume occurs; further chilling of the resulting frozen ice will cause the sample

temperature to equilibrate with the temperature of the chilling surface. Ice crystal growth is controlled by latent heat release as well as the cooling rate the sample is exposed to.

The number of ice nuclei formed, rate of ice growth, and ice crystal size depend on the degree of supercooling. According to Pikal (2007), "the degree of supercooling is the difference between the equilibrium freezing point and the temperature at which ice crystals first form in the sample". The degree of supercooling determines the number of nuclei and consequently, the number of ice crystals formed in the sample (Pikal, 2007). The higher the degree of supercooling, the higher the rate of nucleation and the faster the effective rate of freezing; the result is a high number of small ice crystals. A lower degree of supercooling results in a lower number of large ice crystals

Figure 6 shows a typical freezing thermogram, as illustrated by Searles *et al.* (2001), for solutions frozen in a vial on a lyophilizer shelf as the shelf temperature is reduced.

Aston University

Illustration removed for copyright restrictions

Figure 6. Typical freezing thermogram showing sample (thin trace) and shelf temperatures (thick trace) during shelf freezing. Sample has been cooled at a rate parallel to that of the shelf. The trace identifies A) chilling and subsequent supercooling of the sample, B) onset of nucleation, C) completion of nucleation and onset of ice crystal growth. The trace shows that nucleation temperature of the sample occurs at $-14^{o}C$ with a sharp increase in temperature to approximately $-1^{o}C$. Taken from Searles, J. A., Carpenter, J. F., Randolph, T. W. 2001. The ice nucleation temperature determines the primary drying rate of lyophilisation for samples frozen on a temperature-controlled shelf. Journal of Pharmaceutical Sciences, 90(7), pp 860-871

In general, ice nucleation is a stochastically event and will vary from vial-to-vial, resulting in sample disparity, with some vials having heterogeneous crystal growth and some having homogeneous crystal growth during freezing (Kasper & Friess, 2011).

2.1.2.   Freezing mechanisms: global supercooling and directional solidification

Following secondary nucleation, solidification of the sample is completed relatively slowly as the heat of crystallisation is transferred from the solidification interface through the layer of sample that has solidified and the vial bottom to the shelf (Searles, 2004). This mechanism of freezing occurs by global supercooling, where the entire liquid volume achieves the same level of supercooling. For this mechanism, the secondary nucleation zone encompasses the entire liquid sample, allowing solidification to progress through the already nucleated sample (Searles *et al.*, 2001). Directional solidification happens when a small portion of the sample is supercooled to the point of primary and secondary nucleation. In this case, the nucleation and solidification fronts are in close proximity in space and time, with the front gradually moving into non-nucleated liquid (Searles, 2004).

2.1.3.   The phenomena of freezing point depression

The normal freezing point of a pure compound has been defined by Sinko (2006) as "the temperature at which the solid and liquid phases are in equilibrium under a pressure of 1 atm". Equilibrium in this case refers to the fact that the tendency for the solid to pass into the liquid phase is equal to the tendency of the liquid to pass into the solid phase. When a solute is added to a pure solvent, the vapour pressure of the resulting solution is lowered relative to the pure solvent; therefore when the solution is

chilled, freezing does not occur at the freezing point of the pure solvent since the equilibrium of the solid and liquid phases has been destabilized (Shah, 2006; Sinko, 2006). Further cooling of the solution below the freezing point (supercooling) of the pure solvent causes a reduction in the vapour pressure of the pure solid phase, even lower than that of the liquid phase. Equilibration of the vapour pressure of the two phases causes freezing of the pure solvent (Shah, 2006).

The freezing point depression of a solvent is a colligative property and therefore a function of the number of particles in a solution, and not the physicochemical properties of the solute (Kotz *et al.*, 2009). Ionic salts such as investigated in this work dissociate when in solution; therefore, when 1 mol of sodium chloride dissolves in a solvent (in this case water), two moles of ions form (Na^+ and Cl^-) per solvent particle (particularly in very dilute solutions). This therefore means that the effect on the freezing point of water would be nearly twice as large as that expected if the 1 mole of sodium chloride does not typically dissociate.

The change in freezing point depression of a solution (ΔT_f) relative to the pure solvent can be calculated using the following equation:

$$\Delta T_f = K_f \, i \, m$$

Where K_f is the freezing point depression constant for the solvent (in this investigation, the solvent is water and its K_f is 1.86°C·kg/mol), **m** is the number of moles of solute in solution per kilogram of solvent (molality), and *i* is the number of ions present per formula unit. This formula gives an approximate value for ΔT_f and works well for low solute concentrations as used for this investigation; for high solute concentrations, different assumptions apply (Sinko, 2006; Kotz *et al.*, 2009). Table 2 shows the calculated ΔT_f **for** sodium chloride, calcium chloride, sodium chloride and calcium chloride combinations, and sodium phosphate monobasic of comparable molarity.

Table 2. Calculated freezing point depressions of some ionic solutions showing that an increase in ions per solvent particle increases freezing point depression

Molarity (mM)	Molality (m)	Calculated ΔT_f relative to water (^{o}C)			
		NaCl (2 ions)	CaCl$_2$ (3 ions)	NaCl + CaCl$_2$ (5 ions)	NaH$_2$PO$_4$ (6 ions)
86	0.086	-0.32	-0.48	-0.80	-0.96
154	0.154	-0.57	-0.86	-1.43	-1.72
342	0.342	-1.27	-1.91	-3.18	-3.82
684	0.684	-2.54	-3.82	-6.36	-7.63

2.1.4.   Controlled nucleation

Since the ice nucleation temperature of a sample defines the size, number and morphology of the ice crystals formed during freezing, the random, non-deterministic and spontaneous manner in which nucleation typically occurs poses a major challenge for process control during lyophilisation (Kasper & Friess, 2001). Various methods have been developed to help control and optimise the freezing process. Some of these methods work by influencing ice nucleation by modifying the cooling rate and some statistically increase the mean nucleation temperature. These methods include,

- shelf-ramped freezing
- pre-cooled shelf method
- annealing
- quench freezing
- directional freezing
- addition of nucleating agents
- vial pre-treatment by scoring, scratching, or roughening

Some methods have also been developed, which allow a true control of nucleation at the desired nucleation temperature (Kasper & Friess, 2001). Once of such methods is the **Ice fog technique**, which involves cooling sample vials to the desired nucleation temperature on the freeze dryer shelf and then releasing a flow of cold nitrogen into the chamber. The high humidity of the chamber generates an ice fog, which is a vapour suspension of small ice particles. These ice particles penetrate the vials, where they initiate nucleation at the solution surface (Kasper & Friess, 2001). In 2004, Rambhatla *et al.* investigated the effect of nucleation temperature on the primary drying process using ice-fog induced nucleation to control the nucleation process. The study observed that the specific surface area of the freeze dried cake increased as nucleation temperature decreased. The morphology of the dried cake proved to be well correlated with the degree of supercooling and with the subsequent nucleation temperatures. However, this method has its drawbacks in that the distribution of the small ice crystals can be non-uniform, leading to inter-vial heterogeneity.

Electrofreezing (EF) has also been used as a method to control nucleation. This method uses high voltage pulse to generate an ice nucleus on a platinum electrode, which initiates ice crystallisation. EF is an external freezing method in which samples are first cooled to the desired temperature and then ice nucleation is triggered by electrofreezing (Kasper & Friess, 2001). Petersen *et al.* (2006) were able to demonstrate that EF is a reliable method to induce nucleation; however, the success of EF depends on the sample composition as the study found that a high concentration of additives hindered direct application of electric field induced nucleation inside the sample.

Ultrasonication is another method that has been used to control the nucleation temperature of samples. It is the use of high-intensity acoustic energy to process materials and was first applied in food science (for example, in the manufacture of ice cream) [Guiseppi-Elie *et al.*, 2009]. Nakagawa *et al.* (2006) introduced ultrasound-

controlled nucleation for lyophilisation of pharmaceutical proteins. The contraption used by Nakagawa *et al.* (2006) consisted of an ultrasound transducer connected to an ultrasound generator, which was attached to an aluminium plate that was combined with a cooling stage to cool the vials placed on it (figure 7). Ice nucleation was triggered with an ultrasound wave once the vials reached a desired temperature. The samples were then continually cooled down to the final temperature to allow for complete solidification. Nakagawa *et al.* (2006) observed that larger and directional ice crystals of the dendrite type were found when the sample was nucleated at higher temperatures, while smaller and heterogeneous ice crystals were formed at lower nucleation temperatures.

Figure 7. Cooling device with sonication system used by Nakagawa et al. (2006)

Nakagawa *et al.* (2006) were able to confirm that the mechanisms of ice crystal growth in samples nucleated by ultrasound were equivalent to the mechanisms of ice crystal growth in samples that nucleated spontaneously. This demonstrated that the morphological parameters of ice crystals of frozen formulations in freeze drying are strongly related to nucleation temperatures.

Hottot *et al.* (2008) researched on the effect of ultrasound-controlled nucleation on structural and morphological properties of freeze-dried mannitol solutions. They found that a compromise is necessary between nucleation temperature level and ultrasound pulse power in order to get the most stable mannitol polymorph with a highly permeable cake structure.

2.1.5.   Mechanism of ultrasonication

The sound ranges used by ultrasonication can be classified into two fields: high frequency low energy diagnostic ultrasound in the MHz range, and low frequency high-energy power ultrasound in the kHz range. The application of power ultrasound has gained popularity in the food industry over the years (Li & Sun, 2002; Zheng & Sun, 2006; Delgado *et al.*, 2009; Kiani *et al.*, 2011; Kiani & Sun, 2011). Its use in freeze drying of pharmaceutical products is also promising (Chow *et al.*, 2003; Nakagawa *et al.*, 2006; Saclier *et al.*, 2010).

The beneficial effects of power ultrasound are evident through the mechanical and physical effects that it generates upon the medium through which it transmits (Sun & Li, 2006). Of all the effects generated by power ultrasound, acoustic cavitation is perhaps the most significant. Transmission of sound waves through a supercooled sample can cause the occurrence of cavitation if its amplitude exceeds specific levels (Sun & Li, 2003). The compression and rarefaction of the sound waves cause

a fracture in the liquid sample, leading to the formation of bubbles or cavities which will continue to grow and act as nucleating agents to promote nucleation (figure 8).

Aston University

Illustration removed for copyright restrictions

Figure 8. Motions of bubbles during cavitation. Taken from Zheng et al., 2006

Another significant acoustic phenomenon associated with cavitation is microstreaming, which occurs when the oscillating bubbles produce vigorous circulatory motions. The violent agitation produced by ultrasound results in increasing heat and mass transfer, which can consequently accelerate the freezing process (Sun & Zheng, 2006).

Owing to these acoustic effects, power ultrasound has been used to initiate ice nucleation (Li & Sun, 2002; Chow *et al.*, 2003; Nakagawa *et al.*, 2006; Zheng & Sun, 2006; Delgado *et al.*, 2009; Saclier *et al.*, 2010; Kiani *et al.*, 2011; Kiani & Sun, 2011). Li & Sun (2002, 2003) discovered that the ability of power ultrasound to accelerate the freezing process of a sample is dependent on the level of acoustic power applied to the sample, as well as the duration of the acoustic treatment.

2.1.6.   **Research Aims**

- To investigate the effect of an increase in solute concentration on nucleation events of solutions of selected ionic salts.

- To study the effect of sonication on nucleation events and how this impacts on the freezing process.

2.2   MATERIALS AND METHODS

2.2.1   Sample preparation

Ionic salts selected for the purpose of this investigation include: Sodium Chloride (NaCl), Calcium Chloride ($CaCl_2$) and Magnesium Chloride ($MgCl_2$). Buffering agents, Sodium Phosphate monobasic (NaH_2PO_4) and Potassium Phosphate monobasic (KH_2PO_4), typically used in freeze-drying for protein stabilisation were also selected. All salts were obtained from Sigma-Aldrich. Sodium Chloride 0.9%w/v was used as a reference point as this concentration is typically used for fluid replenishment for intravenous administration. Varying concentrations of these salts were prepared in distilled water based on percentage weight and solute osmolarity[4], as shown in Table 3.

Table 3. Concentrations of salts prepared based on percentage weight and solute osmolarity. Salt combinations consisting of NaCl and CaCl2, were also prepared.

%w/v	0.5	0.9	2.0	4.0
Osmolarity (mOsmol/L)	171	308	684	1369

2.2.2   Solution loading

0.2ml of ionic salt solution was pipetted into 4 x 0.25ml French mini straws (figure 9). French mini straws were used because they are popularly used in animal science for storage of semen embryos, and have been shown to preserve semen potency and

---

[4] Osmolarity is a measure of the osmotic pressure of a solution expressed in osmoles or milliosmoles per litre (Osmol/L or mOsmol/L) of the solution. It is a colligative property and is therefore dependent on the number of particles in a solution and not the nature of the particles (Mosby's, 2002; Sinko, 2006).

embryo survival after cryopreservation as observed by Avenell (1982) and El-Gayar *et al.* (2001) respectively.

The changes in temperature of the solutions were recorded by fitting each straw with k-type thermocouple probes inserted comfortably in the salt solution and connected to a data acquisition system (Madgetech, Dorset, UK). The k-type thermocouples are applied due to a wide temperature range with high resolution for low temperature ranges. Straws were placed on a pre-chilled surface, inside an aluminium bowl (figure 10) specially built with a connection to an ultrasound transducer. The surface was chilled to ~70°C using the shelf of a freeze dryer. A metal block was placed on top of the straws to ensure contact was made with the pre-chilled surface. Temperature changes were monitored until evidence of nucleation and solidification were observed.
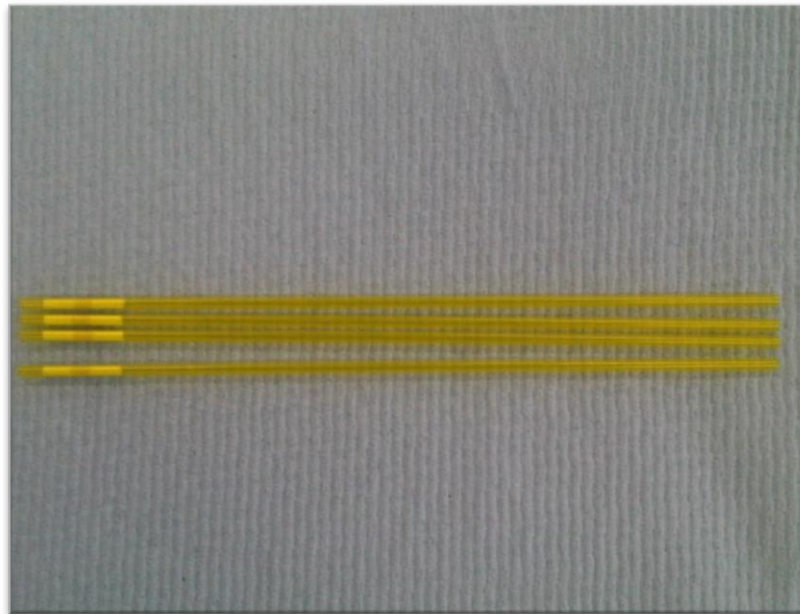
Figure 9. French mini straws. 0.2ml of ionic salt solution was pipetted into 4 x 0.25ml for each concentration of solution.

Figure 10. Straws were placed on a pre-chilled surface, inside an aluminium bowl specially built with a connection to an ultrasound transducer.

2.2.3 Ultrasonication

0.2ml of ionic salt solution was again pippetted into 4 x 0.25ml French mini straws and the straws placed on a pre-chilled surface. A 30W ultrasound transducer, with an operation frequency of 42kHz, was applied every 5s with 4s intervals. This was applied within 5 to 10s of placing the straws on the pre-chilled surface. The application of ultrasound was done this way following observations of freezing patterns for unsonicated samples.

2.2.4 Analysis

Temperature means (n = 4) and standard deviations were calculated. To determine statistically significant differences in nucleation temperatures between sonicated and unsonicated samples, means of nucleation temperatures were analysed by paired sample t-test. Significance level was set at 5%.

2.2.4.1   Hypothesis

Null*: The means of the sonicated and unsonicated samples are equal. Therefore there is no statistically significant difference between both sets of samples.*

Alternative*: The means of the sonicated and unsonicated samples are not equal; there is therefore a statistically significant difference between both sets of samples.*

2.3   RESULTS

Figure 11 shows an example of the freezing thermogram for sonicated and unsonicated samples of 0.5% w/v Sodium Chloride. Please refer to Appendix 1 for thermograms of other concentrations of Sodium Chloride, Calcium Chloride, Magnesium Chloride, Sodium Phosphate monobasic and Potassium Phosphate monobasic (Figure 51-68).

Sodium Chloride
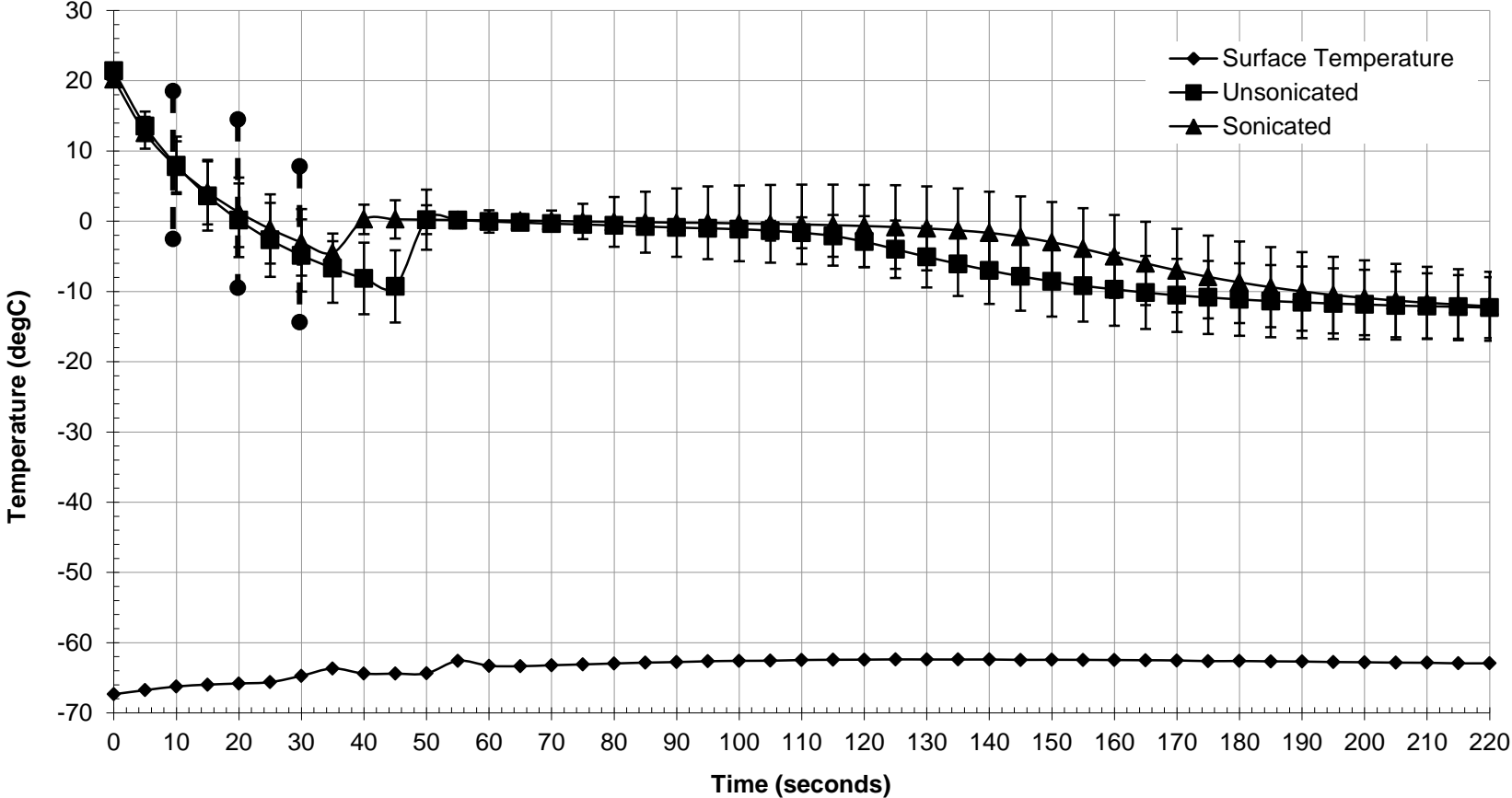
Figure 11. Temperature trace for 0.5%w/v Sodium Chloride unsonicated and sonicated showing +/-SD, n=4. Vertical dotted lines indicate sonication times.

Table 4 and figure 12 provide a summary of nucleation temperatures and graphical representations of these values respectively for sodium chloride. Kindly refer to appendix 2 for tables and graphs for other individual salt samples. Graphs for nucleation temperature against freezing point were not plotted as they have similar trends to graphs of nucleation temperature against osmolarity.

Sodium Chloride

Table 4. Mean nucleation temperatures for percentage weight and solute osmolarity concentrations of Sodium Chloride showing +/-SD values, n=4, * denotes statistical significance at P < 0.05.

Concentration (%w/v)	Osmolarity (mOsmol/L)	Nucleation Temperature (degC, n=4)	
		Control	Sonicated
0.5	171	-5.62 ± 3.62	-5.29 ± 1.48
0.9	308	-7.1 ± 2.45	-5.5 ± 1.85
2	684	-7.7 ± 4.23	-5.03 ± 3.38
4	1369	-9.6 ± 1.86	-8.3 ± 3.33
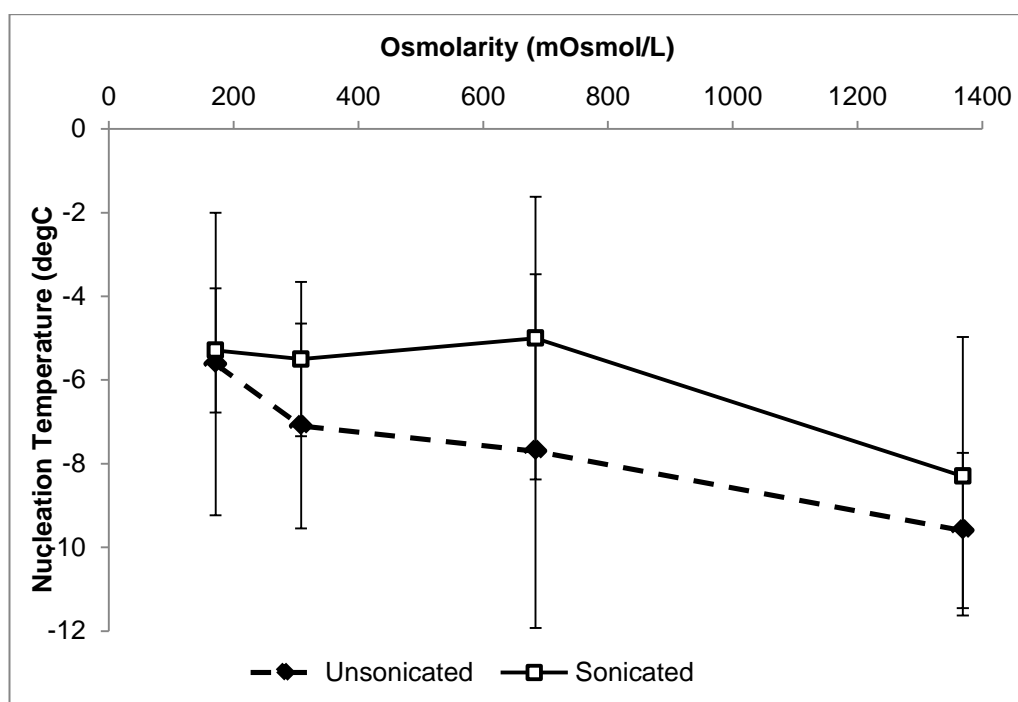
Figure 12. Graph showing mean nucleation temperatures for varying concentrations of Sodium Chloride showing +/-SD values.

2.3 1.   Freezing observations of individual salt samples

It was observed that an increase in solute concentration resulted in increased supercooling and subsequently lower freezing point for each salt. This was expected since freezing point depression increases with increase in solute concentration; in view of this, it was also expected that nucleation temperatures will decrease with increase in solute concentration. However, only sodium chloride (table 4) and magnesium chloride [percentage weight concentrations, table 11 (appendix 2)] followed this consecutive trend.

2.3.2.   Nucleation temperatures of individual salt samples

Primary and secondary nucleations were not distinctly apparent as they took place in rapid succession; in each case, primary nucleation would have occurred as the starting point of secondary nucleation.

Differences in nucleation temperatures were expected when comparing salts due to their different eutectic temperatures. It was thought that salts with lower eutectic temperatures would exhibit lower nucleation temperatures. This appeared to be the case; however, there was no consistency or pattern. For example, sodium chloride has a eutectic temperature of -21.2^{o}C whilst calcium chloride has a eutectic temperature of -51°C; in 0.5%w/v solution, nucleation occurred at -5.62^{o}C and -7.27^{o}C respectively. However, in 0.9%w/v solution for the same salts, nucleation occurred at -7.10^{o}C and -5.59^{o}C respectively. Solutions of magnesium chloride with a eutectic temperature of -33°C nucleated earlier than solutions of sodium chloride with a higher eutectic temperature. Sodium phosphate and potassium phosphate monobasic with much higher eutectic temperatures, -9.7^{o}C and -2.7^{o}C respectively showed no consistency as regards what was expected from the freezing patterns of the salts. For example, nucleation temperatures for percentage weight concentrations of sodium phosphate monobasic increased with increase in concentration, with nucleation occurring at -4.38^{o}C for 0.5%w/v and at -2.44^{o}C for 4%w/v. No clearly distinct trend was observed whilst comparing freezing patterns between percentage weight concentrations and osmolarity concentrations for each of the salts.

2.3.3. Effect of ultrasound on individual salt samples

Triggering of ultrasound allowed nucleation to occur at temperatures higher than they would ordinarily occur and in most cases earlier (an average of 5 to 10s earlier). However, statistical t-test carried out showed that the difference in nucleation temperatures were statistically significant for 19% of the individual salt samples. This is low as it was expected, before this work began, that at least 90% of the individual salt samples would be statistically significant barring any experimental errors.

Ultrasonication caused an increase in crystal growth time, with sonicated samples of 0.5%w/v solutions of calcium chloride, magnesium chloride and sodium phosphate monobasic having a growth time of 95 seconds, 40 seconds, and 75 seconds respectively compared with crystal growth time for equivalent unsonicated samples of 45 seconds, 15 seconds and 45 seconds respectively. This pattern occurred in up to 90% of the individual salt samples.

Figures 13-20 show the freezing thermogram for sonicated and unsonicated samples of salt combinations consisting of NaCl and $CaCl_2$ (percentage weight concentrations).

Sodium Chloride & Calcium Chloride Combinations
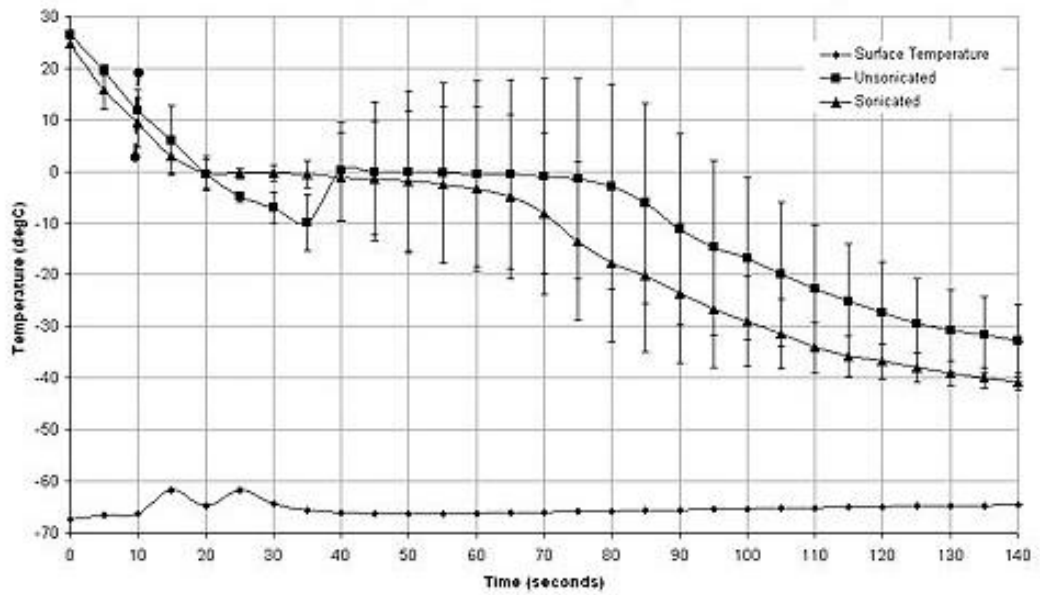
Figure 13. Temperature trace for equivalent concentrations of 0.5%w/v Sodium Chloride & Calcium Chloride combinations, unsonicated and sonicated. Vertical dotted lines indicate sonication times.
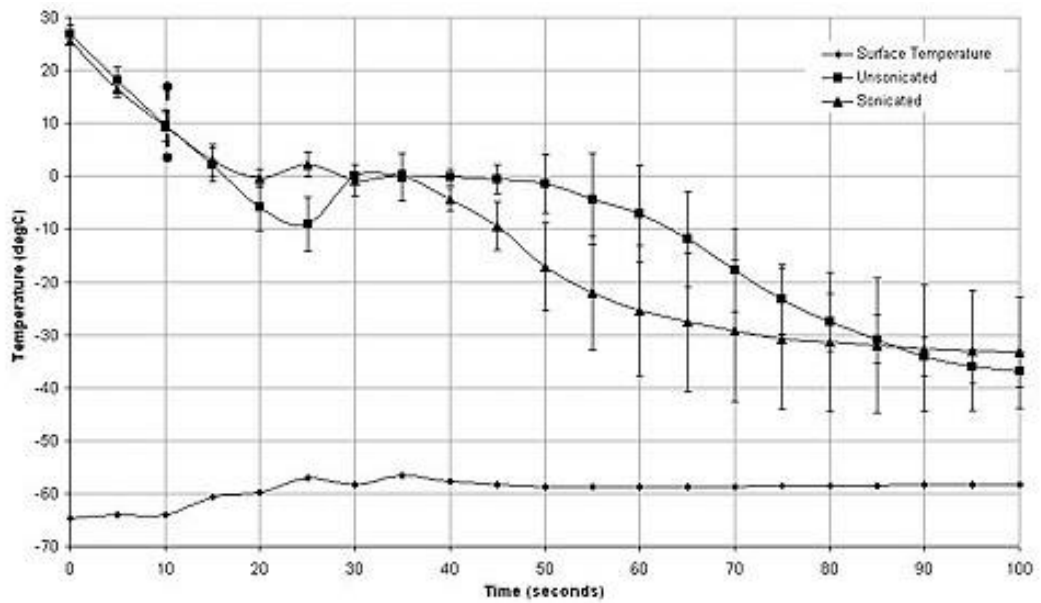
Figure 14. Temperature trace for equivalent concentrations of 0.9%w/v Sodium Chloride & Calcium Chloride combinations, unsonicated and sonicated. Vertical dotted lines indicate sonication times.
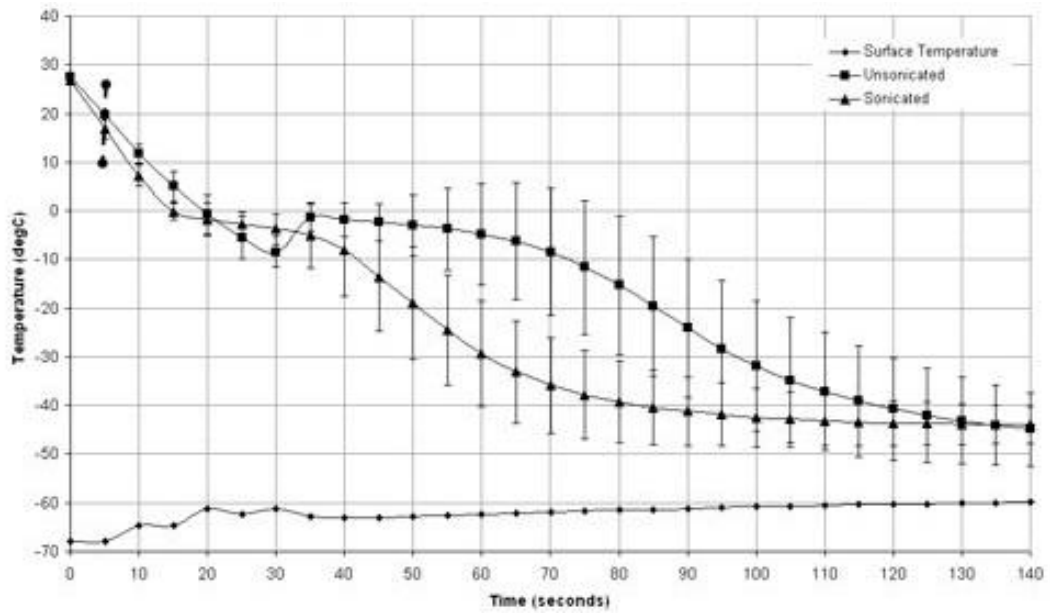
Figure 15. Temperature trace for equivalent concentrations of 2%w/v Sodium Chloride & Calcium Chloride combinations, unsonicated and sonicated. Vertical dotted lines indicate sonication times.
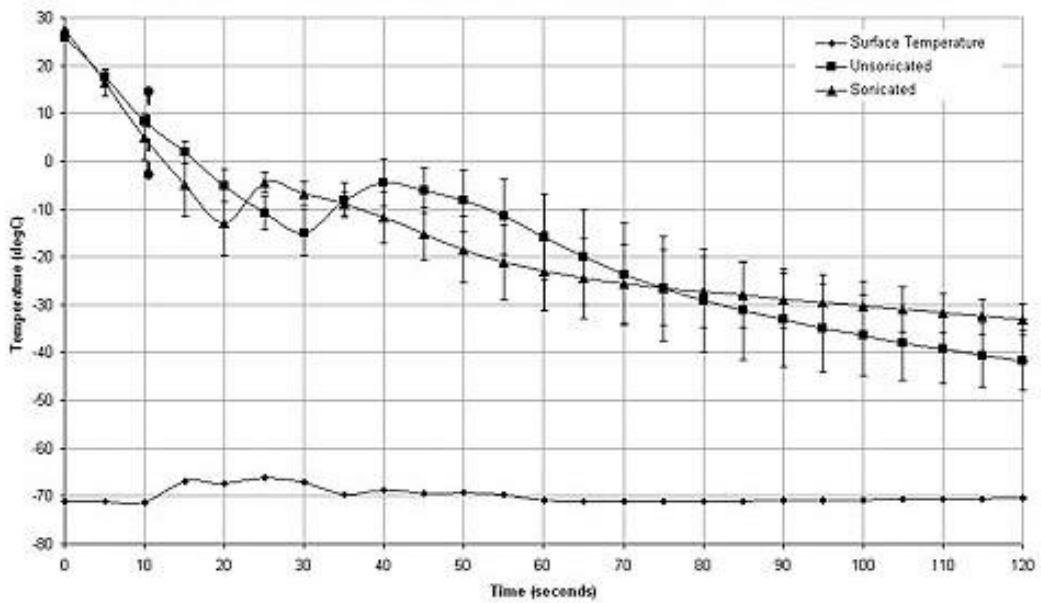
Figure 16. Temperature trace for equivalent concentrations of 4%w/v Sodium Chloride & Calcium Chloride combinations, unsonicated and sonicated. Vertical dotted lines indicate sonication times.
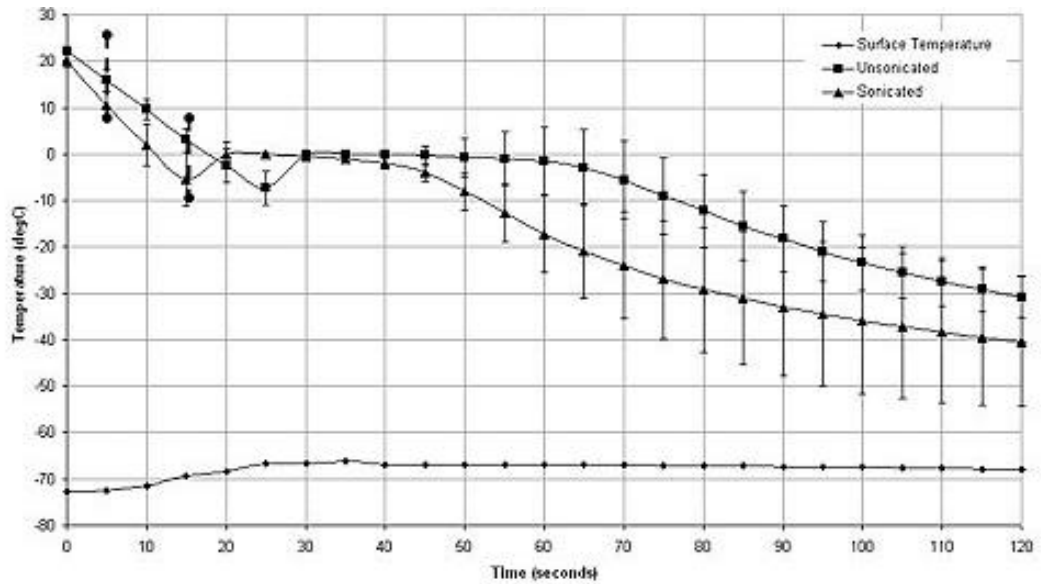
Figure 17. Temperature trace for 171mOsmol/L Sodium Chloride & Calcium Chloride combinations, unsonicated and sonicated. Vertical dotted lines indicate sonication times.
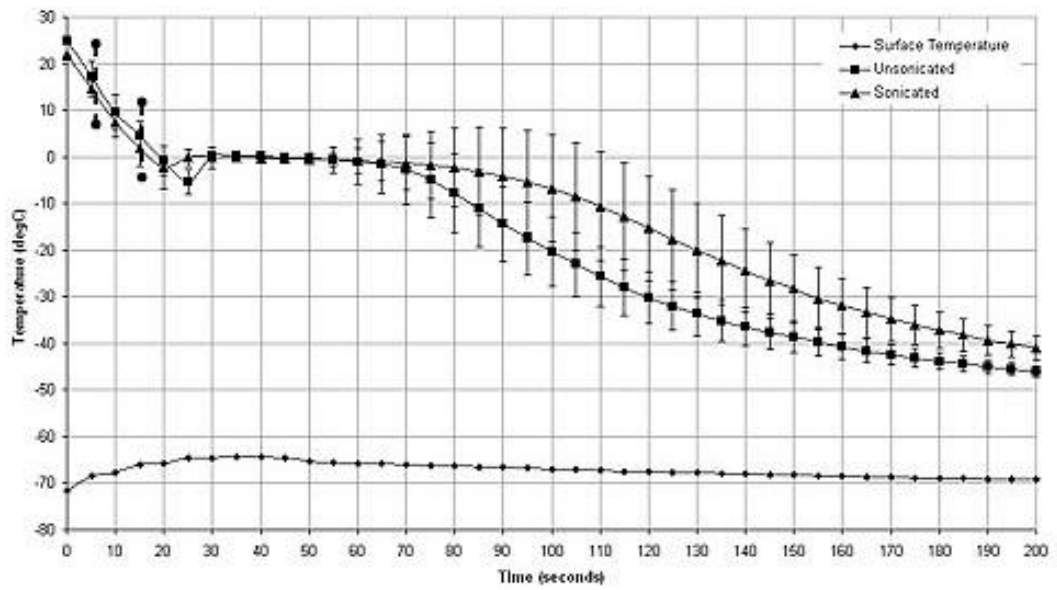
Figure 18. Temperature trace for 308mOsmol/L Sodium Chloride & Calcium Chloride combinations, unsonicated and sonicated. Vertical dotted lines indicate sonication times.
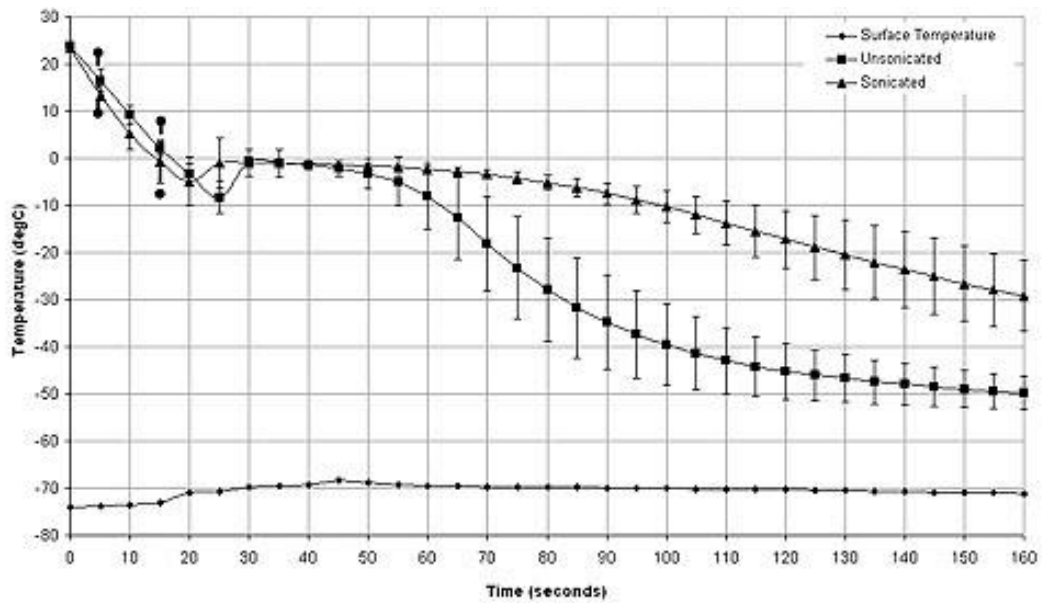
Figure 19. Temperature trace for 684mOsmol/L Sodium Chloride & Calcium Chloride combinations, unsonicated and sonicated. Vertical dotted lines indicate sonication times.
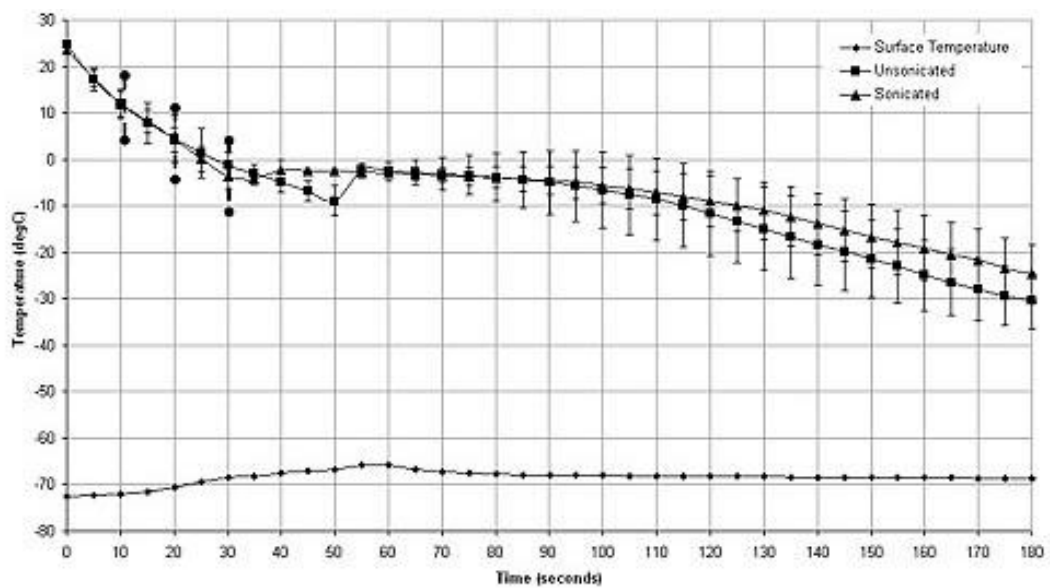
Figure 20. Temperature trace for 1369mOsmol/L Sodium Chloride & Calcium Chloride combinations, unsonicated and sonicated. Vertical dotted lines indicate sonication times.

Tables 5 & 6, and figures 21 & 22 provide a summary of nucleation temperatures and graphical representations of these values, respectively for the NaCl and CaCl$_2$ combinations.

Sodium Chloride – Calcium Chloride combinations - % weight concentrations

Table 5. Mean nucleation temperatures for equivalent percentage weight concentrations of Sodium Chloride & Calcium Chloride combinations showing +/-SD values, n=4, * denotes statistical significance at P < 0.05.

Concentration (%w/v)	Osmolarity (mOsmol/L)	Nucleation Temperature (degC, n=4)	
		Control	Sonicated
0.5	154	-6.82 ± 2.33	-1.45 ± 2.77
0.9	276	-6.90 ± 2.66	-5.72 ± 3.78
2	612	-8.15 ± 0.55	-4.46 ± 4.30
4	1224	-11.8 ± 2.93	-14.0 ± 1.76
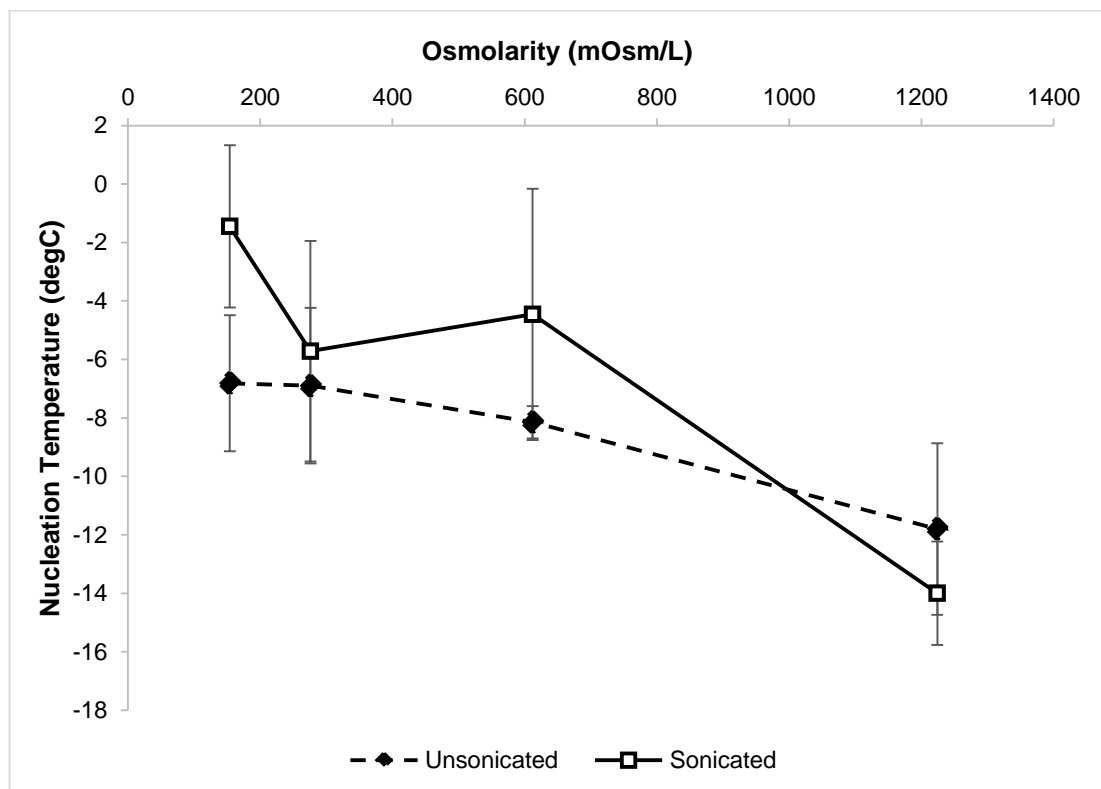
Figure 21. Graph showing mean nucleation temperatures for equivalent percentage weight concentrations of Sodium Chloride & Calcium Chloride combinations showing +/-SD values, n=4

Sodium Chloride – Calcium Chloride combinations - osmolarity concentrations

Table 6. Mean nucleation temperatures for equivalent solute osmolarity concentrations of Sodium Chloride & Calcium Chloride combinations showing +/-SD values, n=4, * denotes statistical significance at P < 0.05.

Concentration (%w/v)	Osmolarity (mOsmol/L)	Nucleation Temperature (degC, n=4)	
		Control	Sonicated
0.6	171	-4.95 ± 3.90	-2.56 ± 1.94
1.1	308	-4.15 ± 1.04	-3.46 ± 1.56
2.3	684	-5.11 ± 2.13	-3.76 ± 2.01
4.6	1369	-7.04 ± 1.76	-5.90 ± 1.66
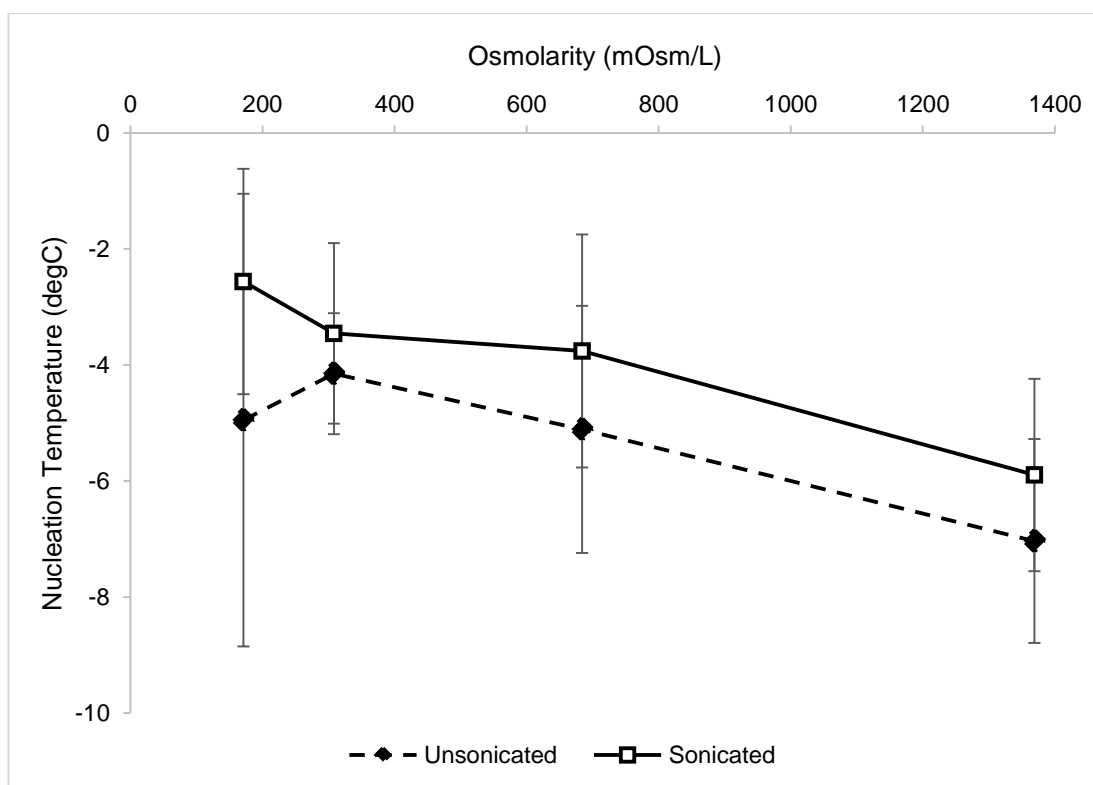
Figure 22. Graph showing mean nucleation temperatures for equivalent solute osmolarity concentrations of Sodium Chloride & Calcium Chloride combinations showing +/-SD values, n=4

2.3.4. Freezing observations and nucleation temperatures of combined salts

Response of the combined salts was no different from that of the individual salts as nucleation temperatures decreased with increase in solute concentration. What was interesting to note is that the freezing point and consequently the nucleation temperatures of the mixtures are very nearly within the range of values that may have been postulated had these been calculated on the basis of each salt component producing a freezing point depression proportional to its concentration and to the number of particles into which its solute dissociates, when it is alone in a solution of the same total salt concentration. For example, the postulated nucleation temperature for a 0.9%w/v combination of sodium chloride and calcium chloride would be between $-5.41^{o}C$ and $-6.34^{o}C$, taking into consideration its concentration and the number of particles the solution dissociates into. The actual nucleation temperatures obtained for the 0.9%w/v salt combination ranged between $-4.24^{o}C$ and $-9.56^{o}C$ ($-6.90^{o}C \pm 2.66$).

2.3.5. Effect of ultrasound on combined salt samples

Similar to individual salts, triggering of ultrasound allowed nucleation to occur at temperatures higher than they would ordinarily occur and in most cases earlier with an average of 5 to 10s earlier. However, statistical t-test showed that the difference in nucleation temperatures were statistically significant for just one out of eight samples ($\cong$ 12%).

As expected, ultrasonication caused an increase in crystal growth time, with the sonicated sample of 684mOsmol/L combination solution having a growth time of 65 seconds compared with crystal growth time for the equivalent unsonicated sample of 25 seconds.

2.4 DISCUSSION

2.4.1 Randomness of nucleation

The nucleation of ice from a supercooled aqueous solution typically occurs in a random, non-deterministic and spontaneous manner, often related to material and process parameters which are normally difficult to control; these parameters include impurities, use of thermocouples which can serve as nucleation sites, surface roughness, and so on (Wilson, 2003; Nakagawa *et al.*, 2006). This therefore accounts for the inconsistencies observed for the nucleation temperatures of the unsonicated ionic salts, which in most cases did not follow expected patterns.

2.4.2 The effect of ultrasound on nucleation

Although triggering of ultrasound caused nucleation to occur at temperatures higher than it would typically occur and in most cases an average of 5 to 10 seconds earlier, the differences in nucleation temperature between unsonicated and sonicated samples were only significant for 19% of the samples for individual salts and approximately 12% for the salt mixtures. These low percentages may be due to the inability of ultrasound waves to efficiently propagate through the entire volume of solution in the French mini straws, thereby allowing nucleation to occur naturally or triggering of nucleation to occur at temperatures that are not significantly different from nucleation temperatures obtained when the samples were not sonicated. It is however important to note that ultrasonication typically increases the freezing rate of a sample. This is due to the presence of small crystals, which result from ice crystal fracturing due to the application of sound waves.

72

Of great importance is the observation of ultrasonication causing an increase in crystal growth time. Sonicated samples of 0.5%w/v solutions of calcium chloride, magnesium chloride and sodium phosphate monobasic had a growth time of 95 seconds, 40 seconds, and 75 seconds respectively compared with crystal growth time for equivalent unsonicated samples of 45 seconds, 15 seconds and 45 seconds respectively. With this pattern occurring in up to 90% of the individual salt samples, this is worthy of note. Since ultrasonication makes use of acoustic cavitation, it is believed that this phenomenon ensures that small ice crystals are rapidly formed throughout the product. At higher degrees of supercooling, nucleation is dominant while at lower degrees of supercooling, crystal growth is the dominant factor. Since ultrasound was applied when the solutions were in relatively low degree of supercooling, only a few nuclei would have been formed, which would have been able to grow extensively.

It is also worthy to note that application of ultrasound generates heat within the system it is being used and if not applied intermittently can raise the temperature of the chilling surface and/or the temperature of the samples; this is due to the fact that as more ultrasound is applied to the system, more acoustic energy is converted to heat and absorbed by the system. According to Li *et al* (2002), although the heat produced by ultrasound is much less than the latent heat typically required to lower sample temperatures, if the cooling system is not capable of immediately removing the heat produced by the effects of ultrasound (especially high powered ultrasound systems), the amount of heat generated would be large enough to raise the temperature of the chilling medium, leading to a retardation in the heat transfer of the freezing process. It is therefore necessary to choose an ultrasound transducer with a power level that is not too high such that its thermal effect would hinder the triggering of nucleation or hinder heat transfer. It is not known whether this was the case in this investigation as an ultrasonic transducer with a lower power level was

not tested to observe whether there would be improvement on triggering of nucleation.   74

Nevertheless, the use of ultrasound to trigger and accelerate ice nucleation offers several advantages compared with other methods such as the use of chemicals including silver iodide, amino acids, and ice nucleating bacteria (e.g. *Pseudomonas syringae*). Unlike nucleating agents, ultrasound does not require direct contact with formulations and is not chemically invasive, making it unlikely to face legislative difficulties. Ultrasound is also a very efficient process as if executed properly only requires one or two pulses to fulfil nucleation requirements (Zheng *et al*., 2006).

2.5 CONCLUSION AND FUTURE WORK

2.5.1 Conclusion

This work set out to investigate the effect of an increase in solute concentration on nucleation events of solutions of selected ionic salts and to study the effect sonication has on nucleation events. Results obtained confirmed that an increase in solute concentration increases freezing point depression and consequently lowers nucleation temperature. Compared to non-ionic compounds, ionic compounds cause even further freezing point depression due to the fact that they dissociate in solution to form even more particles per solvent particle, and the higher the number of dissociated ions, the more freezing point depression occurs.

Although knowing the eutectic temperatures of the ionic solutions used can provide some insight into what range the nucleation temperatures of these salts would fall within, the fact that the nucleation of ice occurs in random and spontaneous patterns overrides any insight that may exist. This has been confirmed in this work given the many inconsistencies observed for the nucleation temperatures of the unsonicated ionic salts as they did not follow expected patterns. It is therefore difficult to predict what the ice nucleation temperature of a solution would be.

Ultrasonication is able to improve nucleation temperatures and allow nucleation to take place earlier than it naturally would. Its advantages far outweigh other modes of accelerating ice nucleation and it affords the opportunity of being able to dictate the initial nucleation temperature of a solution. However, it is highly important to choose an ultrasound transducer with a power level that is not too high such that its thermal effect would hinder the triggering of nucleation or hinder heat transfer.

Based on the sonication results obtained thus far, the null hypothesis is partially accepted owing to the fact that some statistical significance difference was found

between unsonicated and sonicated samples of the ionic solutions, and these showed that it is indeed possible to use ultrasound to accelerate the ice nucleation of solutions. The conclusion thus far is that the use of ultrasound to aid the freezing process of formulations is indeed promising, and further research in this area is required to prove this.

2.5.2 Future work

→ Thermal transition studies using Differential Scanning Calorimetry (DSC) and Modulated Differential Scanning Calorimetry (MDSC). This is needed to observe differences in thermal transition, if any, between sonicated and unsonicated ionic samples, and any other forms of formulations prepared thereafter.

→ Incorporation of enzymes such as beta-galactosidase and asparaginase in single salt solutions to observe nucleation events in these systems and the effect of sonication on these systems.

→ Enzyme activity assays to investigate whether ionic salts still maintain the ability to protect enzymes even upon sonication. Being able to prove that enzymes remain well protected following sonication would be of great benefit particularly in terms of storage of enzyme formulations in the frozen state and in freeze drying.

→ Morphological studies of freeze dried cakes of sonicated and unsonicated formulations using scanning electron microscopy (SEM); as well as examination of the physical state of cake powders by wide angle x-ray diffraction (WAXD).

CHAPTER 3: SHOULD FORMULATION OSMOLALITY BE CONSIDERED PRIOR TO FREEZE DRYING?

3.1   RESEARCH BACKGROUND

The lyophilisation (freeze drying) process can generate a number of stresses, which can destabilise an unprotected protein, cause unfolding or denaturation (Wang, 2000). It is for this reason (as mentioned in the general introduction) that cryoprotection (protection during freezing) and lyoprotection (protection during drying/dehydration) of the protein or active pharmaceutical ingredient by stabilisers are important. As previously mentioned, the effectiveness of stabilisers at protecting a protein during freeze-drying and beyond is concentration-dependent. More importantly, getting the balance right in term of cryoprotectant and lyoprotectant concentration is of the utmost importance.

Cryopreservation of animal sperm is an important aspect of breeding in animal science especially for endangered species. In order for sperm cryopreservation to be successful, cryoprotectants as well as semen extenders[5] are used. According to Orfão *et al.* (2011), an optimum preservation medium should prevent initiation of sperm motility during storage. One of the factors allowing a semen preservation medium to be optimum is the osmolality of the semen extenders used. Woelders *et al.* (1997) carried out a study investigating the influence of the osmolality of the freezing medium (amongst other factors) on the success of cryopreservation of bull sperm by freezing bull semen at different cooling rates varying from 40 to 300°C/min in standard Tis-egg yolk medium and in hyperosmotic or isosmotic media containing 0.2 M trehalose or sucrose. It was found that at the highest cooling rate, the presence of the sugars and the high osmolality of the hyperosmotic media conferred significant protection of the sperm against fast cooling damage. Similarly, Zeng et al. (2001) investigated the effects of different

---

[5] Semen extenders are liquid diluents added to sperm for preservation during freezing. Extenders are nutrient medium, frequently containing an antibiotic. Extenders help elongate the efficient life of the sperm, with the antibiotic acting to destroy any infective organism present (Equine Reproduction)

osmolalities of freezing diluents on boar sperm cryosurvival and observed that moderately hyperosmotic diluents are favourable for the cryopreservation of boar spermatozoa.

Although preservation of animal sperm has no relation with freeze drying of pharmaceuticals, it is being used in this thesis to make a case for how it may be necessary to take the osmolality of a formulation being prepared for freeze drying into consideration as a factor for conferring protein protection against the stresses of freeze drying. In other words, could it be possible that there is an optimum medium osmolality within which a protein or Active Pharmaceutical Ingredient (API) would be protected throughout the rigours of freeze drying and through storage? It is thought that knowledge of this and consequently creation of a database of favourable osmolalities for popular proteins and API's may benefit the world of freeze drying in the long run.

3.1.1 Research Aims

- To carry out preliminary investigation on the osmolality and osmotic coefficients of common solutes and their trends.
- To investigate whether or not osmolality should be an important factor to consider for protein/API protection during freeze drying.

3.2 MATERIALS AND METHODS

3.2.1 Sample preparation

A few solutes commonly were selected for osmolality measurements: Sucrose, Trehalose, Glucose, Raffinose, Galactose, Lactose, Mannitol, Urea and Sodium

Chloride. All solutes were obtained from ACROS Organics. Molal concentrations from 0.1m to 1.2m were prepared in distilled water.

3.2.2 Osmolality measurement

A Löser Micro-Osmometer Type 6 was used to make all measurements. A sample containing about 100 µl of the sample to be measured is attached to a measuring head, which allows insertion of a thermistor into the sample. The measuring head is pushed down, allowing the sample tube to be inserted into a cooling aperture, which uses a Peltier cooling effect. The sample begins to cool immediately, indicated by decreasing temperature values shown on the osmometer digital display. The Löser Micro-Osmometer has a defined supercooling point of -6.2°C at which the freezing process must be triggered by dipping a needle with ice crystals into the sample tube. The linear correlation between osmolality and freezing point allows for the determination of osmolality by freezing point measurement. Osmolality values are displayed by the Löser Micro-Osmometer as mosm/kg H_2O.

3.2.3 Analysis

Osmolality measurements were carried out in four replicates for each solute and osmotic coefficient was calculated using the following equation:

$$\frac{\text{Actual Osmolality}}{\text{Ideal Osmolality}}$$

Mean and standard deviation values of osmolality and osmotic coefficient values were calculated. Graphs of osmolality (mOsm/kg) against molality (mol/kg) as well as osmotic coefficient against molality (mol/kg) were plotted. To determine statistically significant

differences between means of both osmolality values and osmotic coefficients of the solutes, a one-way ANOVA test was carried out. Bartlett's test for equal variance was used to verify the outcome of the one-way ANOVA. Significance levels were set at 5%. Where one-way ANOVA indicates statistical significance, a post hoc test was also carried out using the Tukey Multiple Comparison Test to determine which means amongst the set of means analysed differ from the rest.

Individual graphs of osmolality against molality were plotted for each solute, and linear regression analysis was performed to evaluate the relationship between osmolality and molality. From the resulting linear regression analysis, a factor was derived using the slope of the line resulting from the linear regression analysis.

3.2.3.1 Hypothesis

<u>One-Way ANOVA</u>

Null: The means of all solutes are equal. Therefore there is no statistically significant difference between all means.

Alternative: At least one solute mean is different; there is therefore a statistically significant difference between some solute means.

<u>Bartlett's Test</u>

Null: Batch variances are all equal and therefore there is no statistically significant difference between variances.

Alternative: At least one batch variance is different from the others and as such there is a statistically significant difference between variances.

All graphs and statistical analysis were done with GraphPad Prism.

3.3 RESULTS

3.3.1 Correlation between molality and osmolality

Figure 23 shows a graph representing the osmolality data for some common solutes. These data indicate a linear relationship of osmolality with the total solute concentration, expressed in molality (mol/kg) as osmolality is directly proportional to molality. This relationship depends on the number of particles into which a molecule of the solute dissociates.
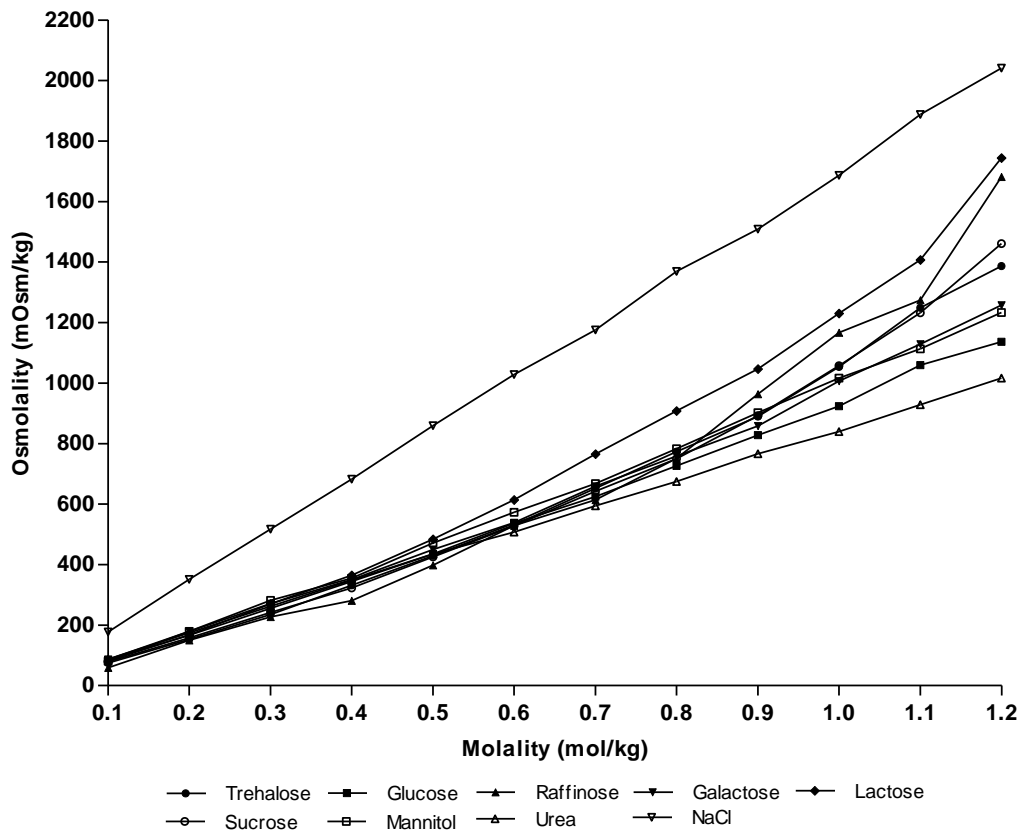
Figure 23. Osmolality data for some common solutes. Each solute was prepared in water and 100μl of each was measured using a Löser Messtechnik Type 6 Osmometer. Individual data points represent mean ± SD, n=4. (Ref: Sinko, P.J. 2006. Martin's Physical Pharmacy and Pharmaceutical Sciences, Fifth Edition. Baltimore: Lippincott Williams & Wilkins)

According to the one-way ANOVA test [$F_{(8, 99)} = 1.639$, $P = 0.1234$], differences between osmolality means were not statistically significant. This was verified by Bartlett's test for equal variance ($P = 0.4128$) with both significance levels set at 5%.

Figures 24-28 show regression line graphs for each solute. Regression analysis was used to calculate the equation of the line for each graph.
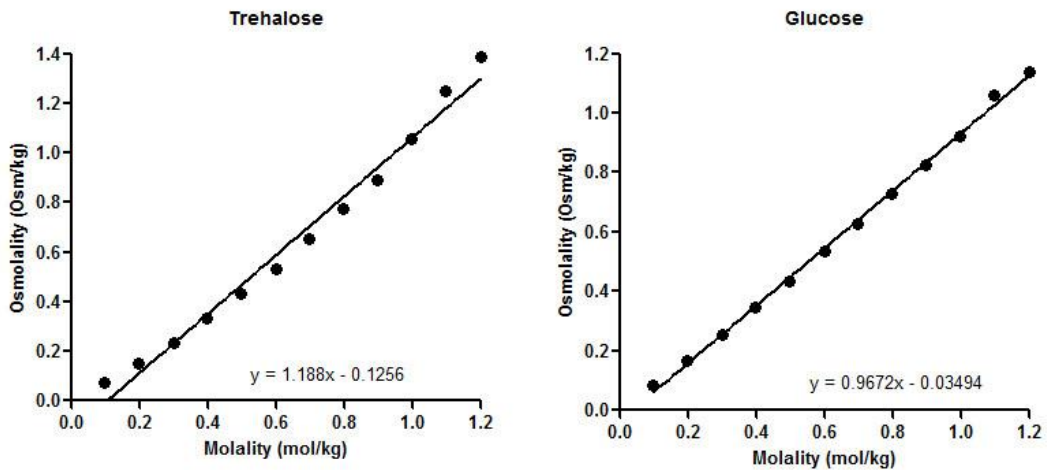
Figure 24. Regression analysis of osmolality (osm/kg) and molality of Trehalose and Glucose. Osmolality measurements were carried out using a Löser Messtechnik Type 6 Osmometer. Each solute was prepared in water and 100µl of each was measured. Individual data points represent mean ± SD, n=4.
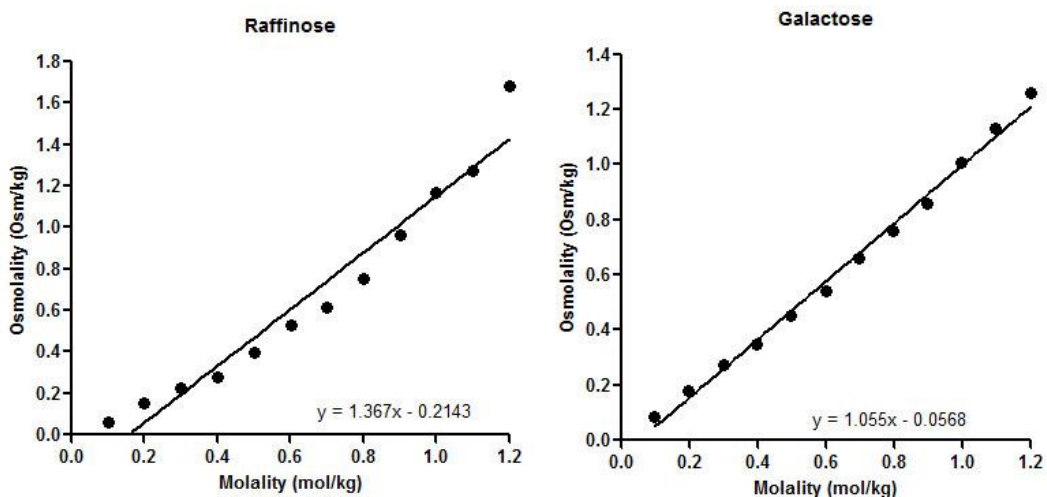
Figure 25. Regression analysis of osmolality (osm/kg) and molality of Raffinose and Galactose. Osmolality measurements were carried out using a Löser Messtechnik Type 6 Osmometer. Each solute was prepared in water and 100µl of each was measured. Individual data points represent mean ± SD, n=4.
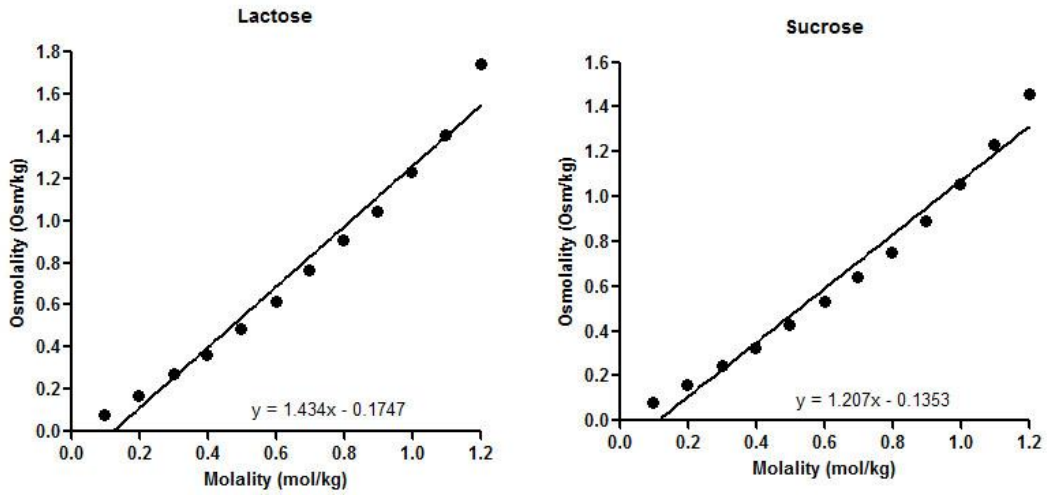
Figure 26. Regression analysis of osmolality (osm/kg) and molality of Lactose and Sucrose. Osmolality measurements were carried out using a Löser Messtechnik Type 6 Osmometer. Each solute was prepared in water and 100µl of each was measured. Individual data points represent mean ± SD, n=4.
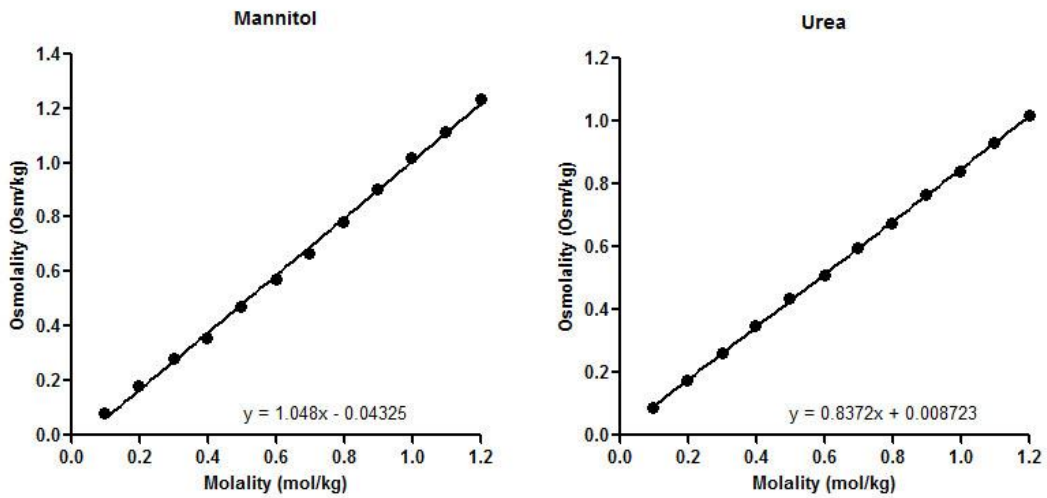
Figure 27. Regression analysis of osmolality (osm/kg) and molality of Mannitol and Urea. Osmolality measurements were carried out using a Löser Messtechnik Type 6 Osmometer. Each solute was prepared in water and 100µl of each was measured. Individual data points represent mean ± SD, n=4.
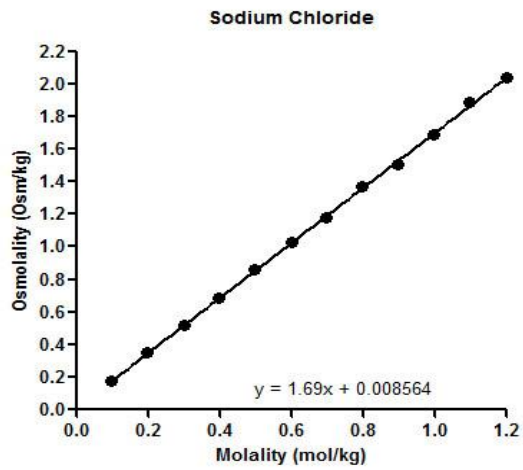
Figure 28. Regression analysis of osmolality (osm/kg) and molality of Sodium Chloride. Osmolality measurements were carried out using a Löser Messtechnik Type 6 Osmometer. Each solute was prepared in water and 100µl of each was measured. Individual data points represent mean ± SD, n=4.

The slope of the line, which describes the relationship between the molality and osmolality of each solute, gives a factor (n). Table 7 provides details of n-value for each solute.

Table 7. Details of i values for each solute. i values were determined from the slope of the line, which describes the relationship between osmolality and molality for each solute. * denotes i values less than 1.

Solute	Slope of Line - Factor (n)
Trehalose	1.188
Glucose	0.967*
Raffinose	1.367
Galactose	1.055
Lactose	1.434
Sucrose	1.207
Mannitol	1.048
Urea	0.837*
Sodium Chloride	1.69

The factor, n, accounts for the number of particles into which the solute dissociates. Therefore a factor of 1.188 can be applied to Trehalose to account for the number of particles in solution.

The slope of the line that describes the relationship between Sodium Chloride (NaCl) molality and osmolality was given as 1.69; however, generally n=2 for NaCl, accounting for the fact that NaCl dissociates into two ions in solution.

3.3.2 Osmotic Coefficient Trends

Figure 29 shows a graph representing osmotic coefficient trends for the same solutes.
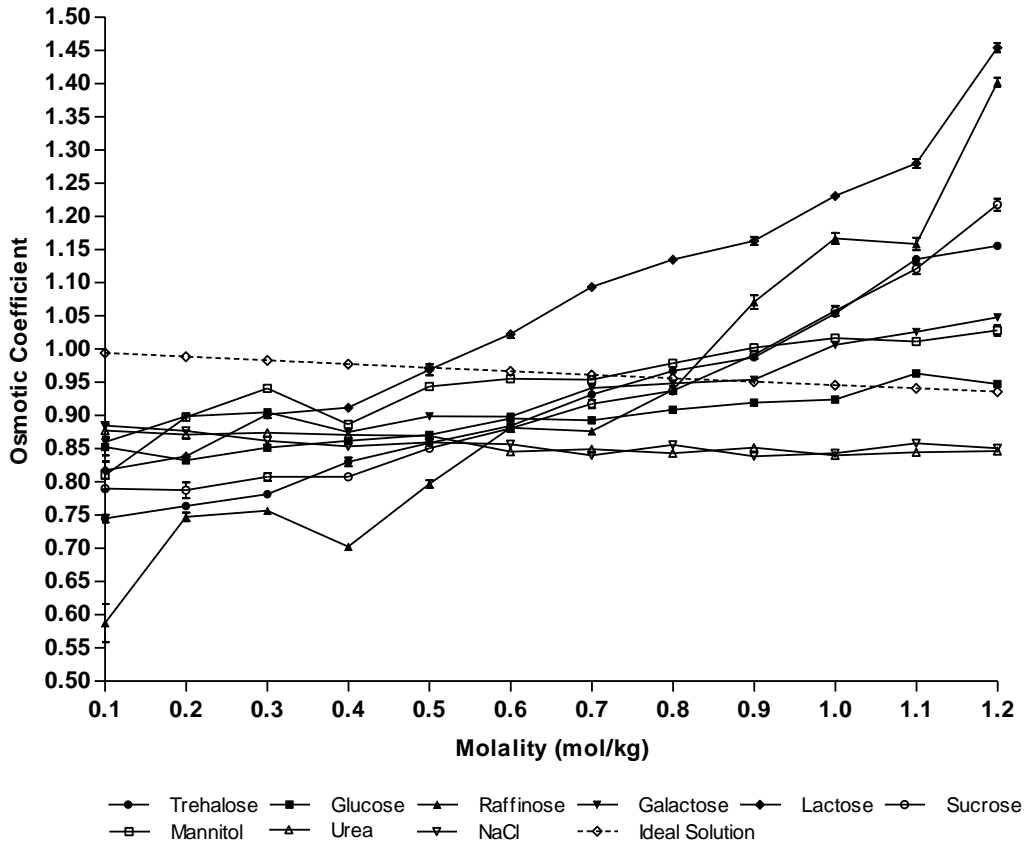
Figure 29. Osmotic coefficient for some common solutes. Osmolality values of samples were obtained using the freezing depression method and osmotic coefficient was calculated using the measured osmolality values and calculated osmolality values. Each solute was prepared in water and 100µl of each was measured using a Löser Messtechnik Type 6 Osmometer. Individual data points represent mean ± SD, n=4. (Ref: Sinko, P.J. 2006. Martin's Physical Pharmacy and Pharmaceutical Sciences, Fifth Edition. Baltimore: Lippincott Williams & Wilkins)

There was a statistically significant difference between groups as determined by one-way ANOVA [$F_{(9, 110)}$ = 3.091, P = 0.0024]. This was also verified by Bartlett's test for equal variance (P < 0.0001) with both significance levels set at 5%. Tukey's Multiple Comparison Test revealed that Lactose vs Glucose, Lactose vs

NaCl and Lactose vs Urea were the statistically significant groups at P < 0.05. There were no statistically significant differences between other groups.

Figure 30 is a graph showing the close-up comparison of the statistically significant mean osmotic coefficient groups as analysed by one-way ANOVA.
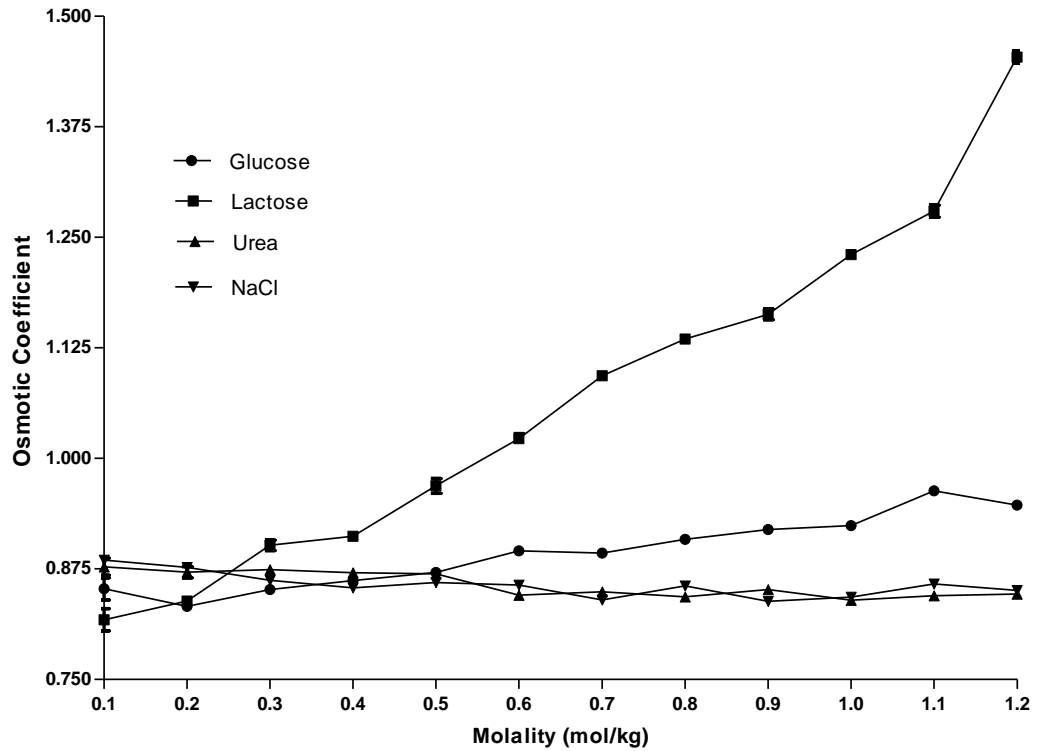
Figure 30. A close up comparison of the statistically significant osmotic coefficient mean groups - Glucose vs Lactose, Lactose vs Urea, Lactose vs NaCl. Lactose is the common denominator of all three statistically significant mean groups as indicated by Tukey's Multiple Comparison Test.

The graph clearly shows a difference in trend between Lactose and Glucose, Urea, and NaCl, with Glucose being the only sugar of all the sugars to have a mean value statistically different from Lactose

Figure 31 is a graph showing close up comparison of the osmotic coefficient trends for Lactose and Raffinose.
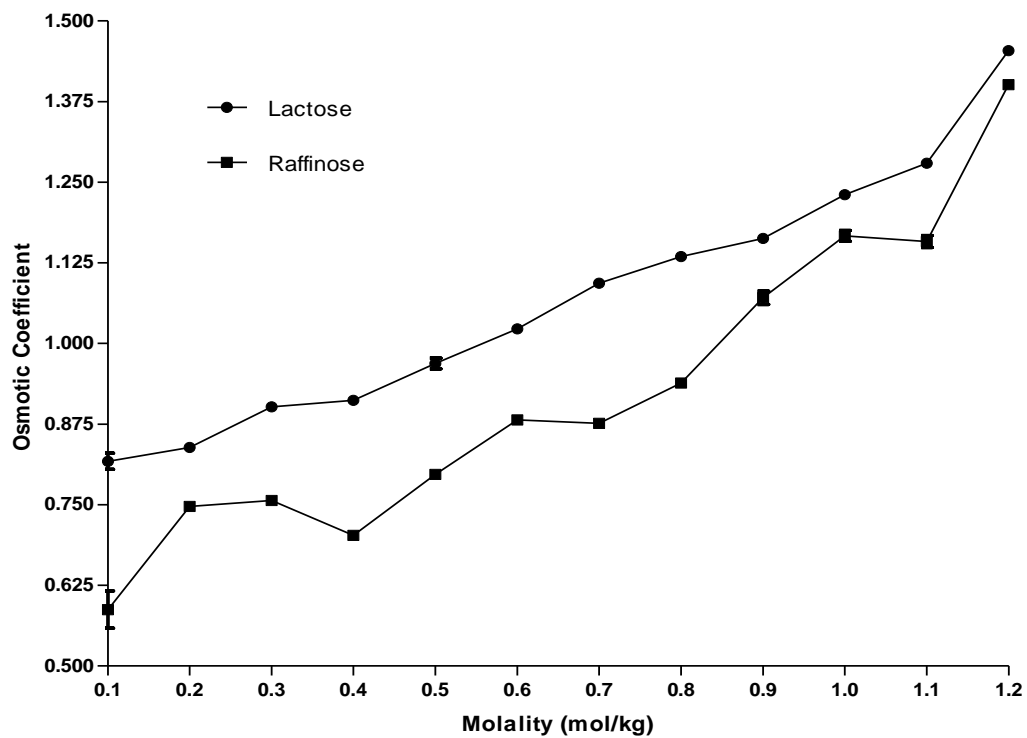
Figure 31. A close up comparison of osmotic coefficient of Lactose and Raffinose. No statistical significance between means of both sugars according to t-test analysis.

Figure 31 shows that Lactose and Raffinose have a similar osmotic coefficient trend. T-test analysis [t (22) = 1.643, p = 0.1146] show that there is no statistically significant difference between the means of both solutes, substantiating the fact that there is a similarity in trend to a degree.

3.4   DISCUSSION

3.4.1   Molality and osmolality

Figure 23 shows what was already expected, a linear relationship between molality and osmolality. Both molality and osmolality are measures of concentrations of solute in solvent; however, where molality concerns molecular concentration, osmolality is related to particle concentration (Bevan, 1978). According to Ingham and Poon (2013), "a solution has an osmolal concentration of 1 when it contains 1 osmol of solute/kg of water". Essentially, osmolality measures the total number of particles dissolved in 1kg of water, expressed as osmols/kg, and depends on the electrolytic nature of the solute (Sinko, 2006).

For an electrolyte like sodium chloride, 1 osmol is approximately 0.5 mol of sodium chloride and as such, a 1 osmolal solution of sodium chloride is said to be equivalent to 0.5 molal solution. For a nonelectrolyte like glucose, 1 osmol is approximately 1 mol of glucose and therefore, 1 osmolal solution of glucose is said to equivalent to 1 molal solution (Ingham and Poon, 2013). It is worthy to note here that a 1 osmolal solution of glucose or sodium chloride will each contain the same concentration of particles given by Avogadro's number 6.02×10^{23}. Whereas in the glucose solution there will be 6.02×10^{23} molecules/kg of water, in the sodium chloride solution, there will also be a total of 6.02×10^{23} ions/kg of water; however, one-half of this total amount of ions are sodium ions and the other half are chloride ions (Bevan, 1978; Ingham and Poon, 2013). Sinko (2006) states that when an ionic specie (or electrolyte) is dissolved in water, it will dissociate to form ions or 'particles', which tend to associate due to their ionic interactions. The extent of these interactions plays an important role in determining the number of 'particles' in

solution as measured by an osmometer. In the case of non-electrolytes, ionic interactions is thought to be insignificant.

When a molecule in solution dissociates into two or three ions or 'particles', its osmolality is doubled or tripled respectively (Bevan, 1978). This can be observed for sodium chloride, compared with other solutes in Figure 23 since it is believed that sodium chloride dissociates into two ions when in solution. Since other solutes represented in Figure 23 are nonelectrolytes, they appear to have similar osmolalities as molality increases, compared with sodium chloride, which stands alone. Although the osmolalities of sodium chloride at different molalities was nearly double that of the other solutes, there was no statistically significant difference between osmolality means as analysed by one-way ANOVA; however, this does not mean that the difference does not exist.

3.4.2 Number of ions formed per molecule (i)

According to Sinko (2006), "for an electrolyte that dissociates into ions in a dilute solution, osmolality or milliosmolality can be calculated from the following",

---

Milliosmolality (mOsm/kg) = i x mm

where, i is approximately the number of ions formed per molecule

mm is the millimolal concentration (mmol/kg)

Where no ionic interactions occur in a sodium chloride solution, i would be 2; however for a 1:1 electrolyte like sodium chloride in dilute solution, and due to ionic interactions between Na+ and Cl- ions, i is approximately 1.86 (Sinko, 2006).

Khajuria and Krahn (2005) carried out some work on deriving and validating the best method for calculated osmolality. According to Khajuria and Krahn (2005), the slope

of the line describing the relationship between osmolality gap and the common osmotically active constituents of serum (sodium, potassium, glucose, and urea) was believed to provide a factor, which must be applied to each constituent to account completely for its contribution to osmolality. Following in this similar path, and bearing in mind the formulae for milliosmolality as stated above, the slope of the line for each solute as represented in figures 24-28 describes the relationship between the molalities of each solute and their corresponding osmolalities, and provides a factor, which is thought to represent i.

According to Sinko (2006), Jacobus van't Hoff upon expressing the equation for osmotic pressure Π of dilute solutions of nonelectrolytes as $\Pi = RT_c$, where R is the gas constant, T is the absolute temperature and c is the concentration in moles/liter, found that solutions of electrolytes, depending on the electrolyte investigated, actually gave osmotic pressures which were about two, three, and more times larger than what was expected from the equation. As a result, a correction factor i, which accounts for the irrational behaviour of ionic solutions was introduced allowing the formulae to be rewritten as $\Pi = iRT_c$. Using this formulae, van't Hoff observed that i approached the number of ions into which a molecule dissociates as the solution was made increasingly dilute. Figure 32 [taken from Sinko (2006)] shows a graph of the i factor plotted against the molal concentration of both electrolytes and nonelectrolytes, as can be observed, for a nonelectrolyte like sucrose, i approaches unity as the solution becomes more dilute whilst for strong electrolytes, i tends towards the number of ions formed when they dissociate.

Figure 32. van't Hoff *i* factor of sample electrolytes and nonelectrolytes. Taken from Sinko, P.J. 2006. Martin's Physical Pharmacy and Pharmaceutical Sciences, Fifth Edition. Baltimore: Lippincott Williams & Wilkins

Typically, since trehalose is a nonelectrolyte, it would be assumed that *i* is 1; however, the slope obtained for trehalose was 1.188 (Figure 24). A similar assumption of $i = 1$ goes for Raffinose, Lactose and Sucrose; however the slope of the line obtained for these are 1.367, 1.434, and 1.207 respectively. These values are an indication that molecule interactions do occur when nonelectrolytes are in solution even though these interactions may not be at an ionic level. They are also a confirmation of van't Hoff's observation as are the slope of the line for Glucose and Urea, which are given by 0.967 and 0.837 respectively.

3.4.3   The osmotic coefficient

The osmotic coefficient is the ratio between observed and theoretical osmolalities, and can be used to correct for deviations of real (nonideal) solutions. Although less than unity for electrolyte solutions (particularly at physiological concentrations), it can be greater than unity for more concentrated ionic and nonelectrolyte solutions,

as well as protein solutions (Friedman, 2008). The real osmolality of a solute can be calculated by multiplying its ideal osmolality by the osmotic coefficient (Silbernagl and Despopoulos, 2009). Therefore, the formulae previously provided for milliosmolality as obtained from Sinko (2006) can be re-written as,

---

Milliosmolality (mOsm/kg) = *i* x *mm* x φ

where, *i* is approximately the number of ions formed per molecule

mm is the millimolal concentration (mmol/kg)

φ is the osmotic coefficient of the solute

Generally, measured osmotic coefficients increase with increase in concentration (Zhang et al., 2002). This was observed for all solutes in Figure 26 except Sodium Chloride and Urea, which exhibit dips in osmotic coefficients at certain points as concentration increased. For example, the osmotic coefficient for Urea at 0.1 mol/kg was calculated to be 0.8775; however, the osmotic coefficient at 0.2 mol/kg was calculated to be 0.87125, whilst at 0.3 mol/kg, it went up to 0.874167.

It can also be noted from Figure 29 that Urea and Sodium Chloride exhibit trends fairly similar to that of an Ideal Solution. Figure 33 shows a close up comparison of the osmotic coefficients for an ideal solution, urea and sodium chloride.
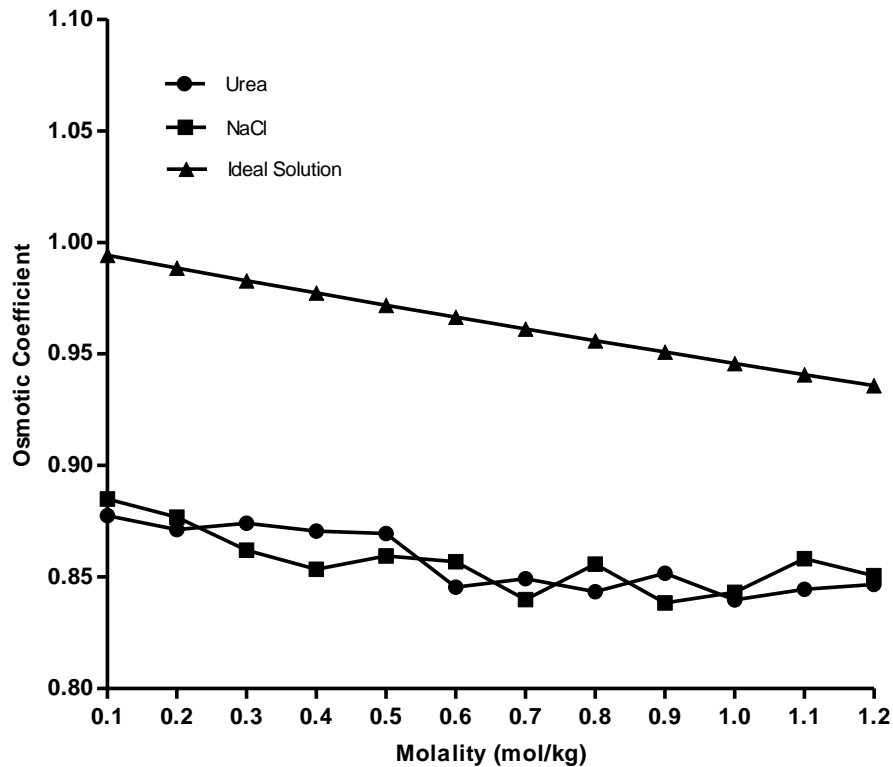
Figure 33. A close up comparison of osmotic coefficients for an ideal solution vs sodium chloride and urea showing a similarity in trend between osmotic coefficients of an ideal solution, sodium chloride and urea.

Although it appears that the osmotic coefficient of Sodium Chloride between 0.1 mol/kg and 1.2 mol/kg has a similar trend with that of an ideal solution, this is not actually the case as shown in Figure 34. Scatchard et al. (1938) calculated and plotted osmotic coefficients of some common solutes in order to compare chemical potential (activity) of water in their aqueous solutions. It can be noted from Figure 34, that the osmotic coefficient of sodium chloride begins to increase steadily (and veers off the trend as that of an ideal solution) from about 0.6 mol/kg. Urea on the other hand maintains a trend that can be said to be similar to that of an ideal solution. According to Paul *et al* (2012), the almost ideal behaviour of urea, prepared in water, may be as a result of the similar average interaction energies between water molecules and urea and water molecules with a smaller average urea self-interaction energy.

94

Figure 34. Osmotic coefficient for some common solutes. Taken from G. Scatchard, W. Hamer, and S. Wood, J. Am. Chem. Soc. 60, 3061, 1938.

Lactose and Raffinose have osmotic coefficient trends, which look significantly different from the other solutes (figures 29 and figure 31). It was thought that lactose has such an osmotic coefficient trend as shown due to its ability to undergo mutarotation when dissolved in water. Lactose can form two structures (α and β), which can change into one another continuously. Both forms differ in molecular structure and as a result, properties of lactose such as crystallisation behaviour, crystal morphology, solid state properties and solubility are affected. Although this was thought to be the reason for lactose, a similar explanation could not be provided for the osmotic trend of Raffinose as Raffinose does not undergo mutarotation. In the same vein, Glucose and Galactose, which also have the ability to undergo mutarotation like Lactose do not have similar osmotic coefficient trends like Lactose. As such, the argument for mutarotation cannot be set in stone as a reason for the osmotic trends of Lactose and Raffinose.

It was also thought that perhaps the reasons for such behaviour by Lactose and Raffinose may be due to the presence of multiple carbohydrates, with Lactose being a disaccharide and Raffinose being a trisaccharide. Looking closely at figure 29, it

can be observed that Sucrose and Trehalose (both disaccharides) follow Lactose and Raffinose closely trend-wise, whilst the monosaccharides, Galactose and Glucose lag behind. Indeed, the osmotic coefficient trends observed for the solutes investigated shows the need for further studies to be carried out with osmolality and how it may be of importance to protein or API protection during freeze drying processes.

3.5   CONCLUSION AND FUTURE WORK

3.5.1   Conclusion

The aim of this work was to begin preliminary investigation on the osmolality and osmotic coefficients of common solutes in the bid to investigate whether or not osmolality should be an important factor to consider for the protection of proteins/APIs during freeze drying. Results obtained show a linear relationship between molality and osmolality as these two are directly proportional to each other. It has also been shown that by doing a regression analysis of the osmolality vs molality graph for solutes, it is possible to obtain a factor, n, which accounts for the number particles in a solution.

The osmotic coefficient trends of some common solutes were also investigated. These provided an insight into how solutes actually deviate from what is expected theoretically. In essence, solutes behave differently from how they are theoretically expected to behave when in solution. Interesting trends were observed for most of the solutes investigated and these observations give an early indication that formulation osmolality is an intriguing factor that may need to be considered prior to freeze drying in terms of protein/API protection against the stresses of freeze drying.

This investigation is only a preliminary investigation into what could be a very important aspect of freeze drying.

3.5.2   Future Work

→ Osmolality measurements and osmotic coefficient determination for more solutes, particularly those used frequently in freeze drying – sugars, polyols, buffering agents, surfactants, amines, amino acids, e.t.c

→ Measurements of osmolality within wider concentration ranges, particularly concentrations used in freeze drying

→ Osmolality measurements of formulations including proteins such as beta-galactosidase

→ Freeze thaw and freeze drying experiments to determine optimum osmolalities which will protect protein during freeze thaw and freeze drying

→ Osmolality measurements for excipient combinations to determine optimum osmolalities that will protect protein during freeze thaw and freeze drying

→ Creation of a go-to database of optimum osmolalities for common proteins/APIs

CHAPTER 4: METHOD OPTIMISATION - USING DIFFERENTIAL SCANNING CALORIMETRY (DSC) AS A TOOL FOR MEASURING FREEZING POINT DEPRESSION

4.1 RESEARCH BACKGROUND

The Differential Scanning Calorimetry (DSC) is a well-known method of thermal analysis typically used in the study of crystalline and amorphous materials. In pharmaceutical sciences in particular, it is a technique that is used to characterise physical and chemical events using changes in enthalpy and/ or heat capacity of a sample (Coleman and Craig, 1996). It is an excellent tool for measuring reaction and decomposition kinetics, detection of polymorphism, studying glass transition temperatures, and purity determination among other benefits (Rades *et al.*, 2013). One of the many advantages of DSC is the fact that only small samples (typically 2-6 mg) of the material to be investigated is required and this is usually in solid form.

Solute osmolalities are typically measured in the laboratory using an osmometer. An osmometer provides an easy and quick way in which osmolalities can be obtained for solutes. During the process of investigating solute osmolalities, it was observed that the osmometer being used had a limit to which it could measure solute osmolalities. The osmometer available could not measure beyond 2500 mOsm/kg. This therefore meant that many highly concentrated solutions could not be measured using the osmometer. Although osmometers with higher measuring capacity are available, it was thought that a device which was already available in the laboratory and can cool and subsequently freeze solutions could be used to determine freezing point depression and consequently, osmolality can be calculated.

The DSC was an excellent choice of equipment to use since DSC's can cool down to sub-zero temperatures with some DSC's able to go as low as -150°C and a range of cooling rates can be used. In addition, for most DSC's, a trace of the process can

be observed whilst the sample is being processed. This therefore formed the basis of this investigation.

4.1.1   Research Aims

- To develop and optimise a method that can be used to measure the freezing point of solutes

- To develop the best method that can be used to analyse traces obtained in order to determine freezing point of solutes.

4.2   MATERIALS AND METHODS

4.2.1   Sample preparation

Samples of Sodium Chloride with concentrations between 0.1 molal and 2.0 molal were initially prepared. Sodium Chloride was picked as it has initially been used in freezing experiments and was thought to be an easy and cheap compound to use for initial method optimisation before moving on to more expensive compounds.

4.2.2   Instruments and materials used

- 50 µl Perkin Elmer Autosample Alumium Sample Pans

- DSC TA Q200

- Iron filings

- Ferrite C5 Magnet Rectangular Blocks 100x20x10mm

4.2.3   Method Optimisation

Several DSC runs were carried out in order to determine the best method for measuring freezing point depression. These involved volume changes, temperature ramp rate changes as well as DSC sequence changes.

4.2.3.1   *Method 1*

Distilled water was first used before Sodium Chloride in order to check that the measurement of the freezing point of water will yield $0^{o}C$ as expected. 30 µl of water was sealed in aluminium pans and cooled in the DSC from $35^{o}C$ to $-30^{o}C$ at the rate of $20^{o}C$/min. A rate of $10^{o}C$/min and $5^{o}C$/min were also used.

4.2.3.2   Method 2

Method 2 is an extension of method 1. 30 µl of Sodium Chloride sample (concentrations from 0.1 mol/kg to 2.0 mol/kg) was sealed in an aluminium pan and cooled in the DSC from 35^oC to -30^oC at the rate of 5^oC/min. 2.0 mol/kg sodium chloride samples were cooled to -40^oC at the same rate, since it is known that due to its higher solute concentration, nucleation will occur at a lower temperature. Measurements were carried out in four replicates.

Following observations from method 2, a decision was made to limit number of replicates to a maximum of two if required otherwise, one measurement would suffice until a working method was established.

4.2.3.3   Method 3

Volume of sample solutions (water and 0.1 mol/kg to 2.0 mol/kg of sodium chloride) was increased to 100 µl and 0.3g of iron filings added to each pan before sealing. The following DSC recipe was used,

- Ramp 100^oC/min from 35^oC to 5^oC
- Ramp 2^oC/min from 5^oC to -30^oC

Similar to method 2, 2.0 mol/kg sodium chloride samples were cooled to -40^oC.

4.2.3.4   Method 4

Volume of sample solutions (water and 0.3 mol/kg of sodium chloride) was kept at 100 µl. The following DSC recipes were used after each pan was sealed,

4.2.3.4(a)   Water

- Ramp 100^oC/min from 35^oC to 5^oC

- Ramp 2°C/min to -4°C

- Isothermal hold for 5 minutes

- Ramp 2°C/min to -20°C

4.2.3.4(b)   0.3 mol/kg Sodium Chloride

- Ramp 100°C/min from 35°C to 5°C

- Ramp 2°C/min to -10°C

- Isothermal hold for 10 minutes

- Ramp 2°C/min to -30°C

The above recipe was repeated with iron filings and also repeated with isothermal hold at -6, -8, -12, and -14 (only with iron filings).

4.2.3.4(c)   0.3 mol/kg Sodium Chloride

The following recipe was attempted as a trial.

- Ramp 100°C/min from 35°C to 5°C

- Ramp 2°C/min to -8°C

- Isothermal hold for 10 minutes during which magnet was applied

- Ramp 2°C/min to -30°C

4.2.3.4(d)   Water

The following recipe was used with iron filings.

- Ramp 100°C/min from 35°C to 5°C

- Ramp 2°C/min to -3°C

- Isothermal hold for 1 hour

- Ramp 2°C/min to -20°C

4.2.3.4(e)   0.3 mol/kg Sodium Chloride

The following recipe was used with iron filings.

- Ramp 100°C/min from 35°C to 5°C

- Ramp 2°C/min to -3°C

- Isothermal hold for 1 hour

- Ramp 2°C/min to -30°C

4.2.3.5   Method 5

0.3g of iron filings was placed in an aluminium pan and 150 µl of water added to the pan. The pan was not sealed. The following DSC recipe was used.

- Ramp 100°C/min from 35°C to 5°C

- Ramp 2°C/min to -3°C

- Isothermal hold for 1 hour

- Ramp 2°C/min to -20°C

The above was repeated and a magnet applied intermittently during the isothermal hold.

4.2.3.6   Method 6

40 µl of water was sealed in an aluminium pan. The following DSC recipe was used after each pan was sealed,

- Ramp 10°C/min from 35°C to -30°C

This was repeated for 0.1 mol/kg sodium chloride solution.

4.2.3.7   Method 7

50 µl of water was sealed in an aluminium pan. The following DSC recipe was used after each pan was sealed,

- Ramp 2°C/min from 35°C to -30°C

This was repeated for 0.1 to 0.3 mol/kg sodium chloride solution, followed by 1.6 mol/kg to 2.0 mol/kg.

4.2.4   DSC Trace Analysis

DSC traces obtained from methods one and two were analysed by reading off the temperature at which there was a sudden increase in heat flow, this is also known as the nucleation temperature.

Following a few revisions and considerations, temperatures were read off at the highest temperature achieved by each solution during the freezing process. This was believed to be the freezing point. However, upon obtaining literature with similar methods to the method being used for this work, it was discovered that by transforming the axis of the DSC traces from heat flow (mW) vs temperature (^{o}C) to heat flow (mW) vs time (minutes) and drawing a tangential line which is extrapolated backwards to intersect with the baseline of the trace, the freezing point of the solution would be obtained.

4.4 RESULTS

DSC traces were initially analysed by reading off the temperature at which a sharp increase in heat flow occurred.

4.4.1 Method 1 – DSC Trace

Figure 35 shows an example of a DSC trace using method 1. Please refer to appendix 2 for all other traces for method 1.

Pure Water
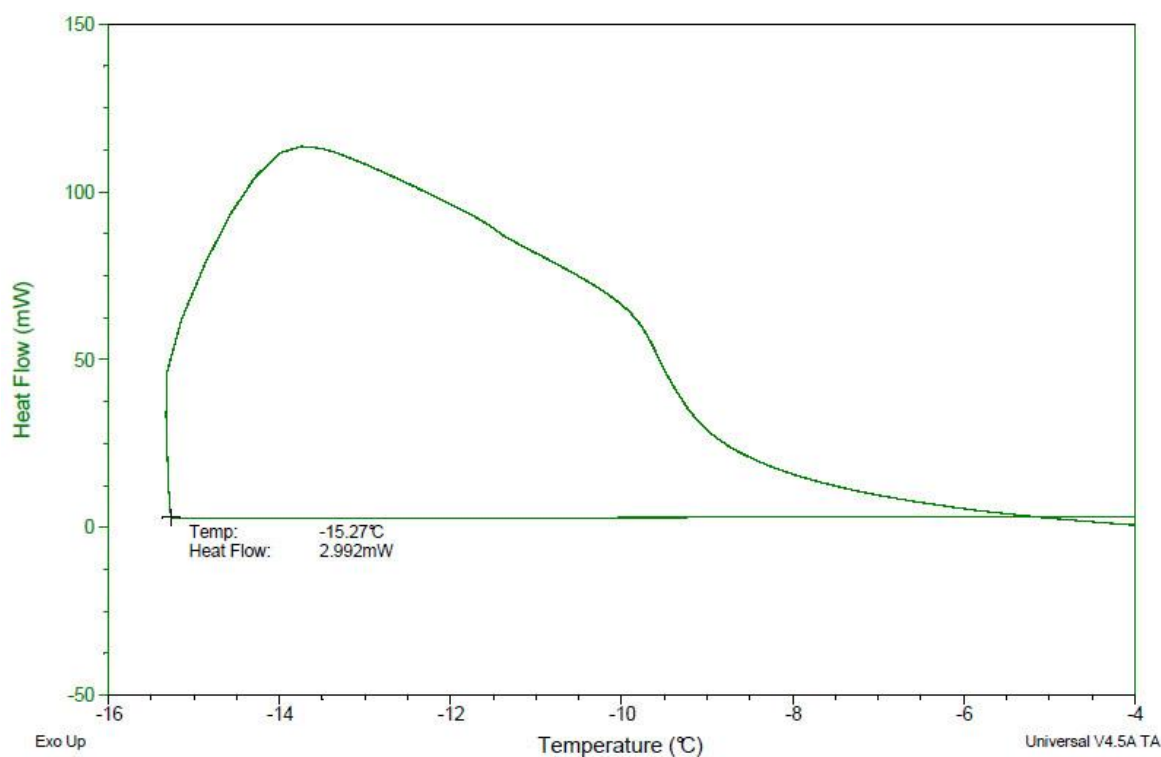
Figure 35. Freezing profile for 30 µl of pure water sealed in an aluminium pan and cooled from 35°C to -30°C at a rate of 20°C/min. Heat flow (mW) is plotted against temperature (^{o}C). Analysis was carried out by reading off temperature at which a sharp rise in heat flow occurred.

4.4.2 Method 2 – DSC Traces

Figure 36 shows an example of a DSC trace using method 2. Please refer to appendix 2 for all other traces for method 2.

0.1 mol/kg Sodium Chloride Solution
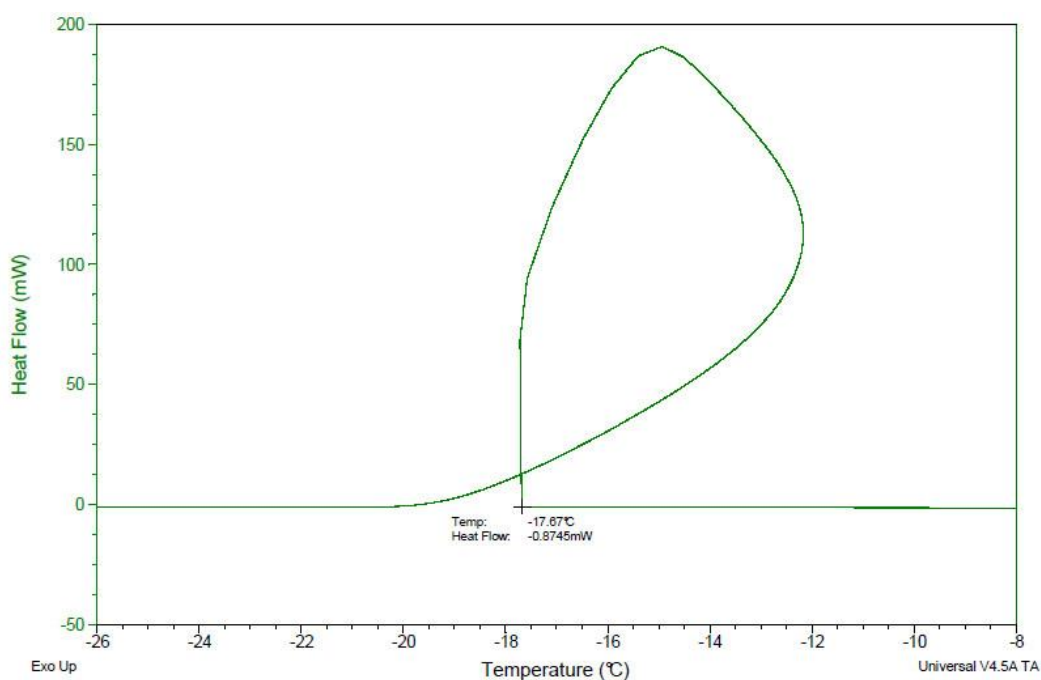
Figure 36. Freezing profile for 30 µl of 0.1 mol/kg Sodium Chloride sealed in an aluminium pan and cooled from 35°C to -30°C at a rate of 5°C/min. Heat flow (mW) is plotted against temperature (°C). Analysis was carried out by reading off temperature at which a sharp rise in heat flow occurred.

As previously mentioned, after a few revisions and considerations, temperatures were read off at the highest temperature achieved by each solution during the freezing process. All traces collected at this point were re-analysed. Please refer to appendix 2 for the reanalysed traces.

.

4.4.3 Method 3 DSC Traces

Figure 37 shows an example of a DSC trace using method 3. Please refer to appendix 2 for all other traces for method 3.

Pure Water
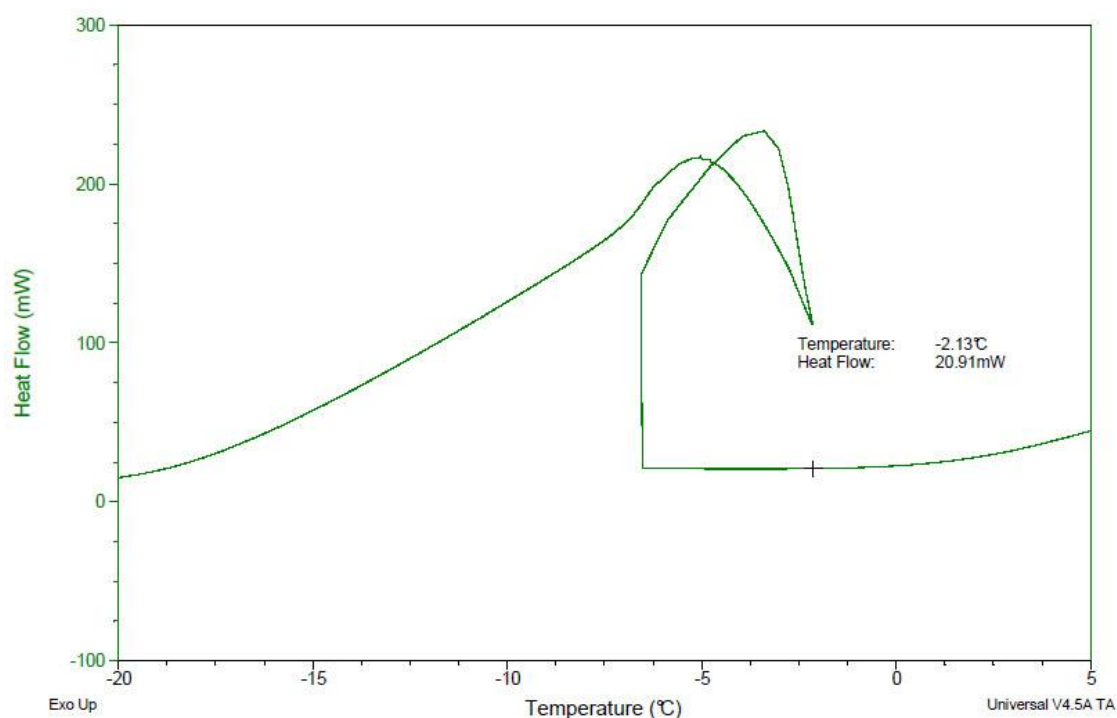
Figure 37. Freezing profile for 100 µl of Pure Water sealed in an aluminium pan with 0.3g of iron filings. Temperature was ramped from 35°C to 5°C at a rate of 100°C/min and then ramped from 5°C to -30°C at a rate of 2°C/min. Heat flow (mW) is plotted against temperature (°C). Analysis was carried out by reading off temperature at the highest temperature achieved by the solution during the freezing process.

DSC traces for methods 4 to 6 can be found in appendix 2.

Following the discovery of a patent application made by Nakamura (2009), for an invention based on freezing point temperature measurements using the DSC. Changes were made to how the DSC traces were analysed. According to Nakamura (2009), the axis of the DSC traces can be transformed from heat flow (mW) vs

temperature (^{o}C) to heat flow (mW) vs time (minutes). This would allow for a tangential line to be drawn; this line is then extrapolated backwards to intersect with the baseline of the trace as shown in Figure 38. The temperature value read off the baseline is the freezing point of the solution (Nakamura, 2009).

Figure 38. DSC trace of freezing indium. Heat flow (mW) is plotted against time (minutes). Analysis was carried out by drawing a tangential line which is extrapolated backwards to intersect with the baseline of the trace [Taken from Nakamura, T. (2009). Freezing Point Temperature Measuring Method and Temperature Calibrating Method in Differential Scanning Calorimetry (Chiba)].

This method of analysis appeared to work for pure water; however, this was not the case for sodium chloride solutions.

Nakamura (2009) illustrated a different method of analysis in which freezing point can be determined without changing the axis of the DSC trace. In other words, the DSC trace can remain as heat flow (mW) vs temperature (^{o}C); however, the tangential line is extrapolated forward to intersect with the baseline of the trace as shown in Figure 39.

Figure 39. DSC trace of freezing indium. Heat flow (mW) is plotted against temperature (^{o}C). Analysis was carried out by drawing a tangential line which is extrapolated forward to intersect with the baseline of the trace [Taken from Nakamura, T. (2009). Freezing Point Temperature Measuring Method and Temperature Calibrating Method in Differential Scanning Calorimetry (Chiba)].

This method of analysis was therefore adopted and adapted for use with the traces obtained in this investigation.

4.5 DISCUSSION

Although obtaining the optimum method for use in the DSC to determine the freezing point of solution is of immense importance, the success of the procedure actually lies in the analysis of the freezing traces produced by the DSC. As can be noted from the methods section, a number of parameters were tried in order to obtain the best method to measure freezing point using the DSC. For example, volumes of solutions were varied from 30 µl to 150 µl, and so far 50 µl appears to be the best volume to work with. Ramp rates were also varied to obtain the best possible ramp rate, that is, slow cooling (e. g 2°C/min) or fast cooling (e. g 100°C/min). It was discovered that since the sample size used is small, slow cooling particularly 2°C/min produced better results compared with fast rates of cooling.

As previously stated, DSC traces obtained were initially analysed by reading off the temperature at which there was a sudden increase in heat flow (latent heat), this temperature is also known as the nucleation temperature. However, the temperatures were lower than expected for the freezing points of the solutions analysed. For example, figure 35 shows the DSC trace for water and the temperature was read as -15.27^{o}C; however, the freezing point of water is ~0°C.

It was decided that perhaps the temperature obtained for water should be used as a baseline; therefore, the temperature obtained for water would be subtracted from those obtained from other solutions to get their freezing point. By doing this, table 8 was created. Osmolality values were also calculated since osmolality is directly related to freezing point depression.

Table 8. Determination of freezing point depression using DSC. Temperatures were read off at the temperature at which there was a sudden increase in heat flow (latent heat), Temperatures obtained for water was subtracted from those obtained for Sodium Chloride solutions (n = 4). Osmolality was also calculated using freezing point depression values

Molality (mol/kg)	Freezing Point (°C)						Freezing Point Depression	Osmolality (Osm/kg)	Osmolality (mOsm/kg)
	Run 1	Run 2	Run 3	Run 4	Average	St. Dev			
0 (Water)	15.22	15.38	16.28	16.17	15.7625	0.5399			
0.1	18.04	19.04	17.67	12.2	16.7375	3.079853	0.975	0.26209677	262.096774
0.154	17.6	15.68	20.34	18.72	18.085	1.958528	2.3225	0.62432796	624.327957
0.2	20.97	19.88	16.7	15.64	18.2975	2.533829	2.535	0.68145161	681.451613
0.3	18.01	18.48	19.59	18.01	18.5225	0.745358	2.76	0.74193548	741.935484
0.4	20.53	19.16	16.96	23.68	20.0825	2.813259	4.32	1.16129032	1161.29032
0.5	22.53	19.3	20.85	18.16	20.21	1.899351	4.4475	1.19556452	1195.56452
0.6	23.73	20.72	19.93	20.13	21.1275	1.767114	5.365	1.4422043	1442.2043
0.7	23.08	23.08	20.54	20.07	21.6925	1.613596	5.93	1.59408602	1594.08602
0.8	22.19	25.67	22.22	23.71	23.4475	1.64281	7.685	2.06586022	2065.86022
0.9	20.6	20.65	21.43	21.09	20.9425	0.392545	5.18	1.39247312	1392.47312
1	25.31	23.53	26.26	23.44	24.635	1.383871	8.8725	2.38508065	2385.08065
1.2	21.59	20.11	22.99	23.57	22.065	1.545779	6.3025	1.69422043	1694.22043
1.4	21.53	25.28	22.99	24.97	23.6925	1.76277	7.93	2.13172043	2131.72043
1.6	28.22	24.09	22.02	22.91	24.31	2.741083	8.5475	2.29771505	2297.71505
1.8	25.85	25.96	26.24	24.93	25.745	0.567597	9.9825	2.68346774	2683.46774
2	29.43	26.5	29.64	27.77	28.335	1.481947	12.5725	3.3797043	3379.7043

However, this method of analysis was incorrect as the nucleation temperature of a solution is not the freezing point of the solution. After reviewing the data already obtained, a decision was made to read off the temperature for each solution at the highest temperature achieved by each solution during the freezing process. Although this method of analysis yielded improved temperatures, the temperatures obtained were nowhere near what was expected.

As stated in the results section, Nakamura (2009), applied for a patent for an invention based on freezing point temperature measurements using the DSC. According to Nakamura (2009), the axis of the DSC traces can be transformed from heat flow (mW) vs temperature (^{o}C) to heat flow (mW) vs time (minutes), allowing for a tangential line to be drawn; this line is then extrapolated backwards to intersect with the baseline of the trace (shown in Figure 4.62). The temperature value read off the baseline is the freezing point of the solution (Nakamura, 2009). The tangential line is tracked from a region where the temperature of the chilled sample is constant in the freezing process and where the DSC trace shows a constant inclination. This method of analysis worked for pure water; however, this was not the case for the sodium chloride solutions.

Nakamura (2009) provided another method of analysis by which freezing point can be determined without changing the axis of the DSC trace. The DSC trace can remain as heat flow (mW) vs temperature (^{o}C); however, the tangential line is extrapolated forward to intersect with the baseline of the trace as shown in Figure 39. The reasoning behind extrapolating to obtain the freezing point is that the method is not influenced by the latent heat of the sample since the temperature of the sample is constant at the point where the tangential line is drawn.

4.6   CONCLUSION AND FUTURE WORK

4.6.1   Conclusion

This investigation set out to begin preliminary work on method optimisation for a method that is not typically used in science laboratory – using the DSC to determine the freezing point of a solution. Although the investigation is still far from being called a success, it is a promising area and certainly a method, when well established, can save money for laboratories that already have a DSC machine and require freezing point measurements or osmolality measurements since osmolality can be calculated from freezing point depression values. It is believed that if more time is spent with this investigation, an optimised method will be obtained.

4.6.2   Future work

- $\rightarrow$ Further investigation into method optimisation and trace analysis
- $\rightarrow$ Incorporating osmotic coefficients obtained from experiments in Chapter 3 to calculate osmolality
- $\rightarrow$ Once method has been optimised, introduction of different solutes

CHAPTER 5: NOVEL SYSTEM FOR INCREASING PRIMARY FREEZE DRYING RATE OF FORMULATIONS

5.1 RESEARCH BACKGROUND

Primary drying is usually the longest part of the freeze drying process, and primary drying times lasting days or even weeks are not uncommon; however, longer primary drying time leads to longer freeze drying cycles, and consequently increased production costs (Pikal, 2007).

Increasing the shelf temperature for a primary drying cycle can increase primary drying rate and reduce primary drying time; however, this would result in product collapse (which would affect product stability) and loss of cake structure, brought about by viscous flow (Liu *et al.*, 2004; Patel *et al.*, 2009). In order to preserve cake structure and prevent product collapse, the shelf temperature of the cycle and more importantly, product temperature must be below a critical temperature (Yang *et al.*, 2010). The three critical temperatures regularly used in freeze drying are: *glass transition temperature* (T'_g) for amorphous systems, *eutectic temperature*[6] (T_{eu}) for crystalline systems, and *collapse temperature*, which is closely related to T'_g and is normally a few degrees higher (Pikal, 2007). An example of product collapse is shown in Figure 40.

---

[6] Eutectic temperature of a crystalline system is the temperature at which all areas of concentrated solute are frozen, above this temperature, the frozen sample will begin to melt.
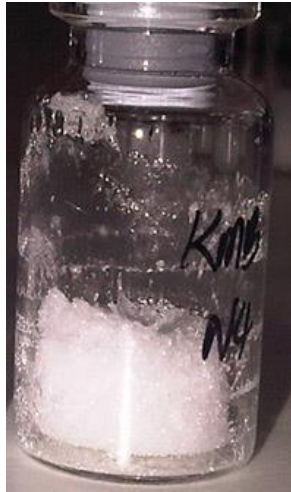
Figure 40. Product collapse in freeze drying can range from a slight shrinkage of the dried cake, for example in this instance where the cake has pulled away from the vial wall, to complete loss of cake structure

Annealing[7] has also been used as a process to improve primary drying rates and is often used to enhance crystallization of active ingredients and bulking agents in a formulation, as well as having an effect on particle size distribution of resulting ice crystals (Searles *et al.*, 2001). The process is carried out after freezing but before primary drying commences and is such that frozen samples are kept, for a specified length of time, at a temperature above T′$_g$ but below the freezing point of the solution (Randolph *et al.*, 2002). Investigations carried out by Searles *et al.* (2001) using formulations containing sucrose and hydroxyethyl starch (HES) showed that annealing brought about an increase in primary drying rates up to 3.5 times of samples which did not undergo annealing. The annealing process does have its drawbacks; one of such is that it results in slower reconstitution due to the morphological changes that occur during the process. Searles *et al.* (2001) reported that annealed samples of HES were completely dissolved in slightly shorter times than samples which did not undergo annealing.

In view of these, an appropriate way to improve on primary freeze drying rates without causing any damage to the formulation is essential since a reduction in primary drying

---

[7] Annealing as defined by Searles *et al.* (2001) is a "process step in which samples are maintained at a specified subfreezing temperature for a period of time.

time will have a significant economic impact on the development and commercialisation of freeze dried products (Liu *et al.*, 2004).

5.1.1 Research Aim

- To increase the primary freeze drying rate of formulations, and consequently reduce primary drying time, without product damage, using a novel system to increase the surface area of the formulation.

-

5.2   MATERIALS AND METHODS

5.2.1   Sample preparation

Formulations of mannitol, inositol, sucrose and lactose (all obtained from ACROS Organics) were prepared in the following concentrations: 50mM, 200mM, 400mM, and 500mM. These were kept in ice to chill until required.

5.2.2   Preparation of drying wall

2ml of water was first added to a 10ml vial (vials were obtained from Adelphi UK) after which the vial was tilted on its side to lay perpendicular to upright and then frozen at a temperature of $\cong$-65°C. Once frozen in place, the vial was stood upright having solid ice on its side; this solid ice is referred to as the drying wall. 5ml of the pre-chilled formulation was added to the vial and frozen at $\cong$-65°C for 3 hours, resulting in the formation of a vial system. Figure 41 provides a pictorial description of how the vial system was made.
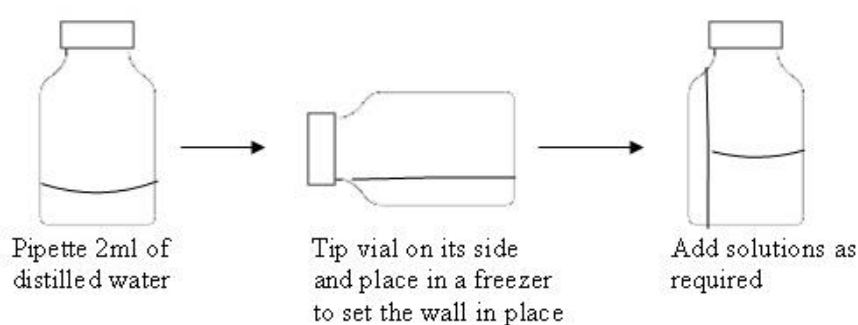
Figure 41. Pictorial representation of the preparation of a drying wall and the resulting vial system

For each formulation concentration prepared, four vials with the drying wall, and four vials without the drying wall were prepared. Prior to freeze drying, each vial was weighed individually.

5.2.3 Freeze drying cycle

Primary drying parameters were set at the following - *Shelf Temperature: +20°C; Condenser: -70°C; Vacuum: 200 mTorr*. A Virtis Wizard 2.0 Control System freeze dryer was used.

Primary drying was carried out for 14 hours and then 24 hours to begin with. After the stipulated duration, vials were pulled out from the freeze dryer and re-weighed. Percentage loss of water after primary drying was calculated.

5.2.4 Analysis

To determine statistically significant differences in primary drying rate between samples with or without the drying wall, mean values were analysed by paired sample t-test. Significance level was set at 5%.

5.2.4.1   *Hypothesis*

Null: *The means of the primary drying rate of vials with drying walls and without drying walls are equal. Therefore there is no statistically significant difference between both sets of samples.*

Alternative: *The means of the primary drying rate of vials with drying walls and without drying walls are not equal; there is therefore a statistically significant difference between both sets of samples.*

5.3   RESULTS

Figure 42 shows a photograph of resulting cakes of vials with and without a drying wall.
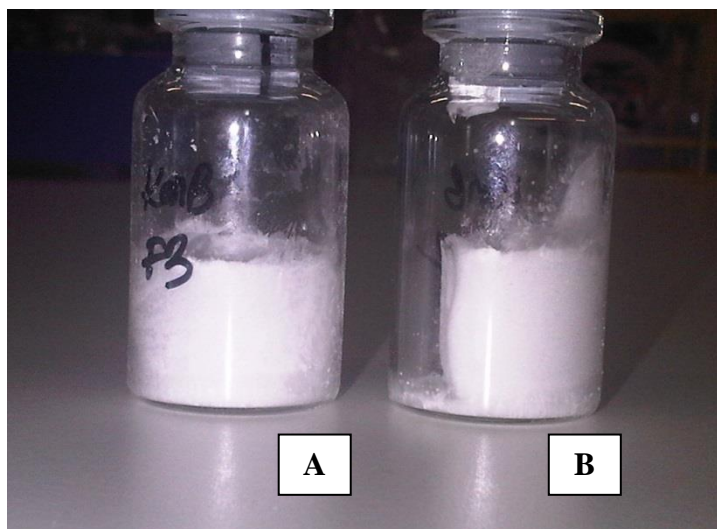
Figure 42. Freeze dried cakes of 5ml Mannitol obtained after 14hrs of primary drying. (A) shows vial which contained mannitol solution without the drying wall whilst (B) shows vial which contained mannitol solution with the drying wall.

5.3.1   Percentage loss of water

Figures 43 to 46 show graphs representing percentage loss of water after 14hrs and 24hrs of primary drying of mannitol, inositol, sucrose and lactose respectively.
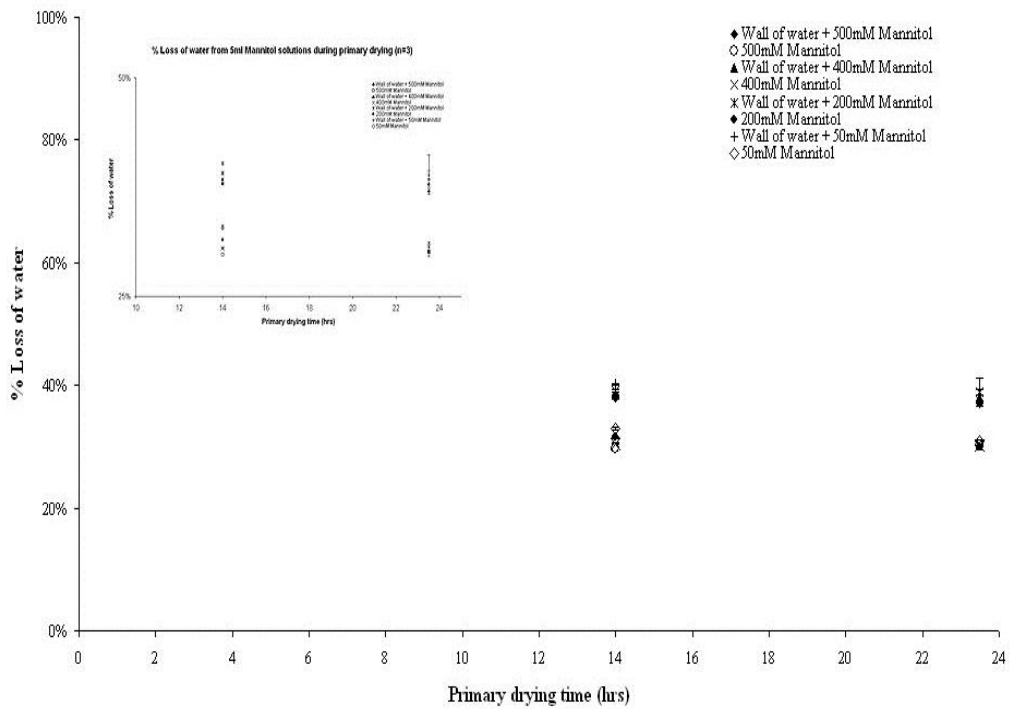
Figure 43. Percentage loss of water following 14 hours and 24 hours of primary drying of 5ml mannitol solutions. Each data point represents mean ±SD, n=3. Zoomed version of graph inset.
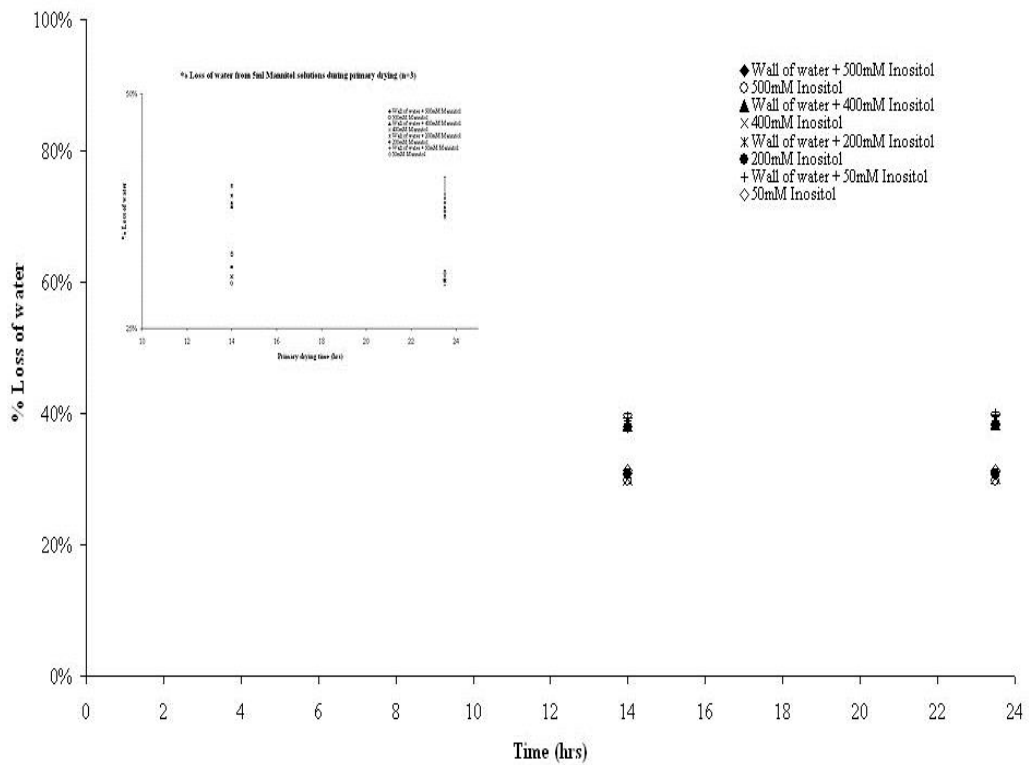
Figure 44. Percentage loss of water following 14 hours and 24 hours of primary drying of 5ml inositol solutions. Each data point represents mean ±SD, n=3. Zoomed version of graph inset.
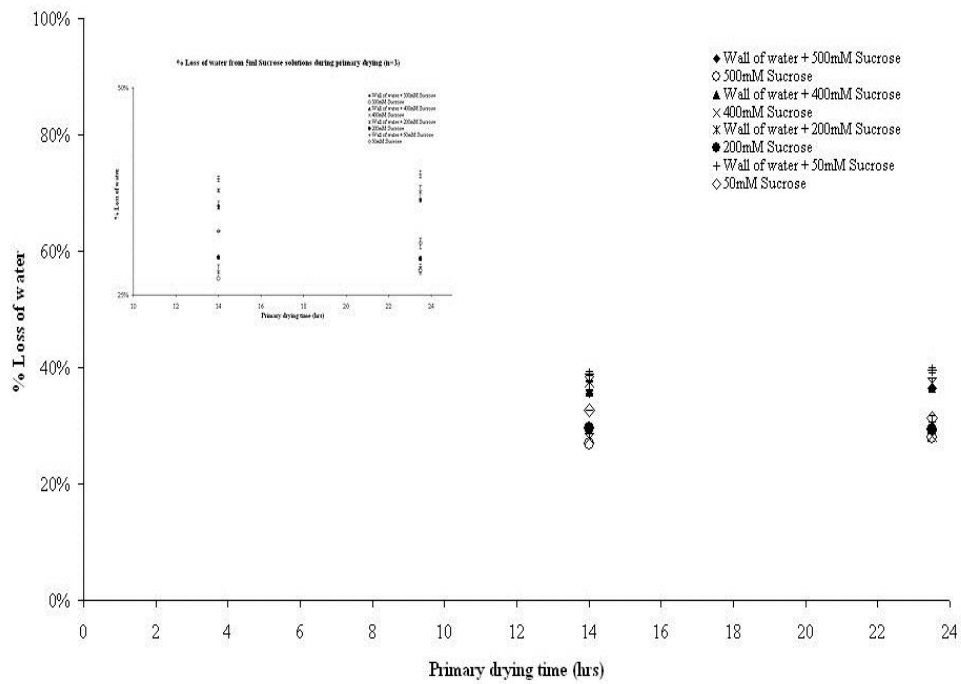
Figure 45. Percentage loss of water following 14 hours and 24 hours of primary drying of 5ml sucrose solutions. Each data point represents mean ±SD, n=3. Zoomed version of graph inset.
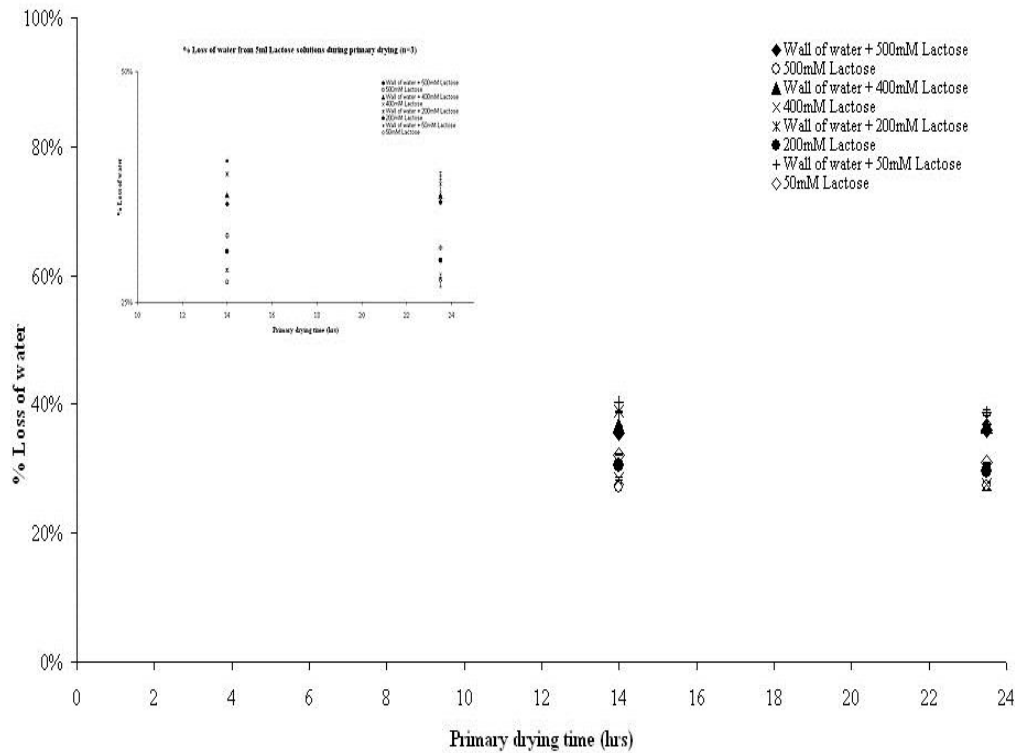
Figure 46. Percentage loss of water following 14 hours and 24 hours of primary drying of 5ml lactose solutions. Each data point represents mean ±SD, n=3. Zoomed version of graph inset.

The set of points towards the bottom of the graphs indicate percentage loss of water in vials without the drying wall, whilst those at the top indicate percentage loss of water in vials with the drying wall. The results obtained suggest that the presence of a drying wall helps increase loss of water during primary drying. After 14 hours of primary drying, the differences in percentage loss of water between vials with the drying wall and vials without the drying wall, for 5ml mannitol ranged from 7.3% to 8.13%; for inositol, sucrose and lactose, the range was from 8.15% to 8.3%, 6.3% to 8.72% and 8.1% to 8.43% respectively. Differences in percentage loss of water after 24 hours followed the same order as observed after 14 hours of primary drying. Statistical t-test showed that the difference in percentage loss of water between vials with and without the drying wall were statistically significant for all formulations. Significance was at P<0.05 and, in all but one set of sample, at P<0.01.

5.3.2 Primary drying rates

Figures 47 to 50 show bar graphs representing primary drying rate for mannitol, inositol, sucrose and lactose respectively.
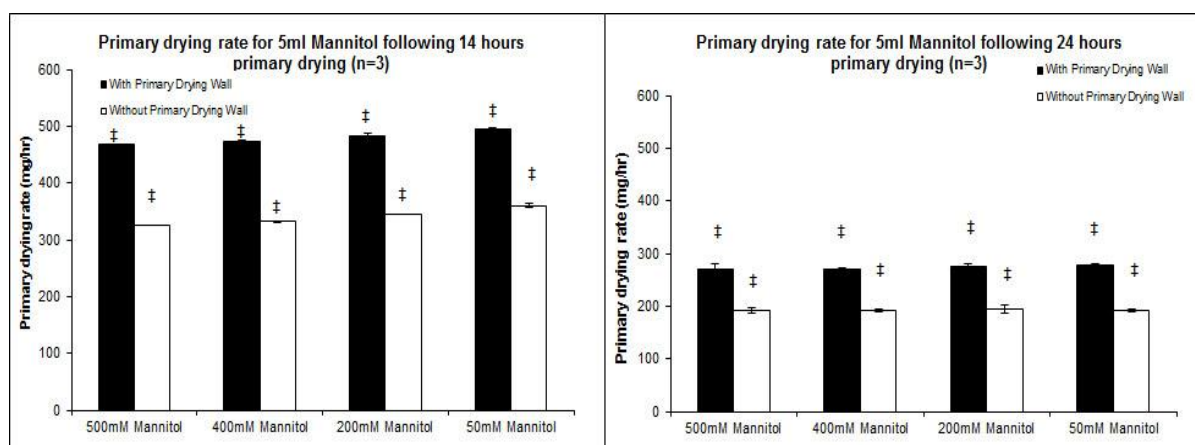
Figure 47. Primary drying rate for 5ml Mannitol after 14 hours and 24 hours primary drying. Each bar represents mean ±SD, n=3. ‡ denotes statistical significance at P < 0.05
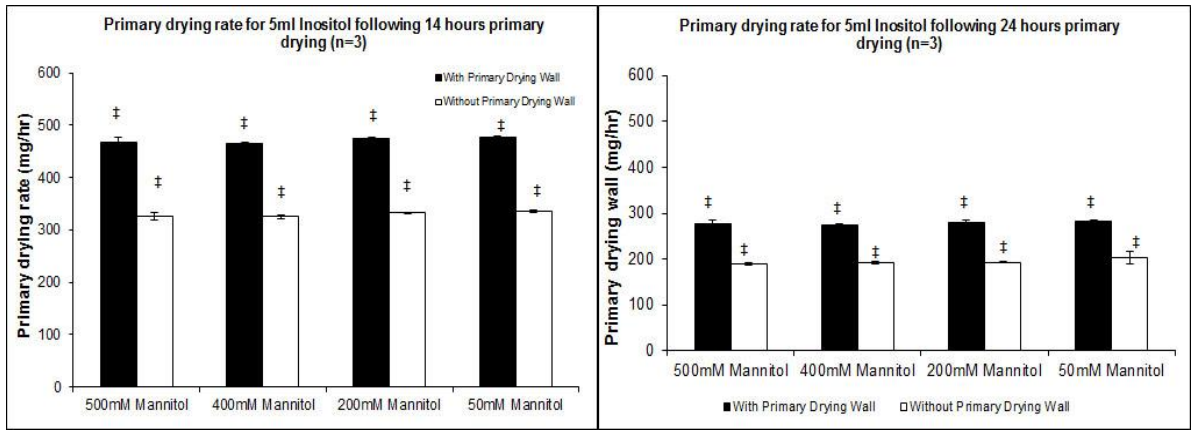
Figure 48. Primary drying rate for 5ml Inositol after 14 hours and 24 hours primary drying. Each bar represents mean ±SD, n=3. ‡ denotes statistical significance at P < 0.05
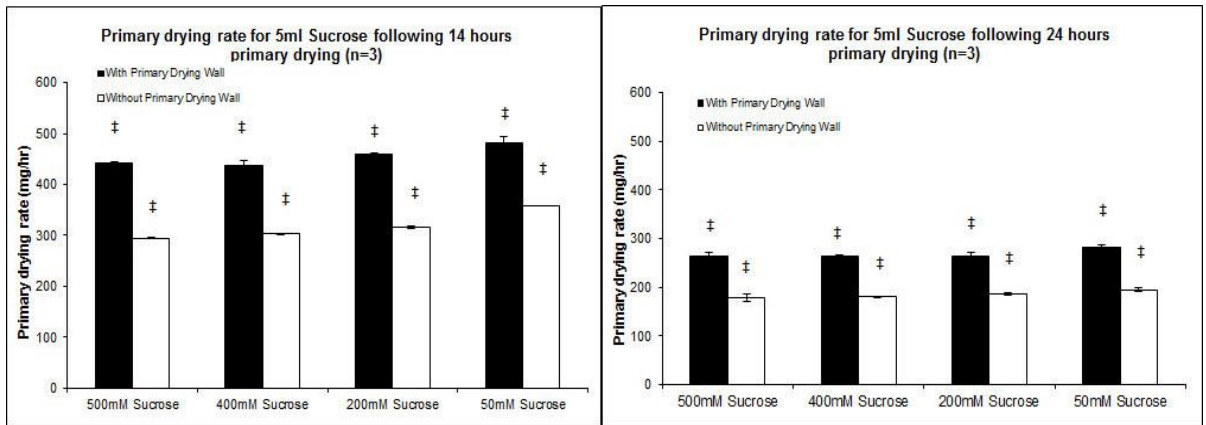
Figure 49. Primary drying rate for 5ml Sucrose after 14 hours and 24 hours primary drying. Each bar represents mean ±SD, n=3. ‡ denotes statistical significance at P < 0.05
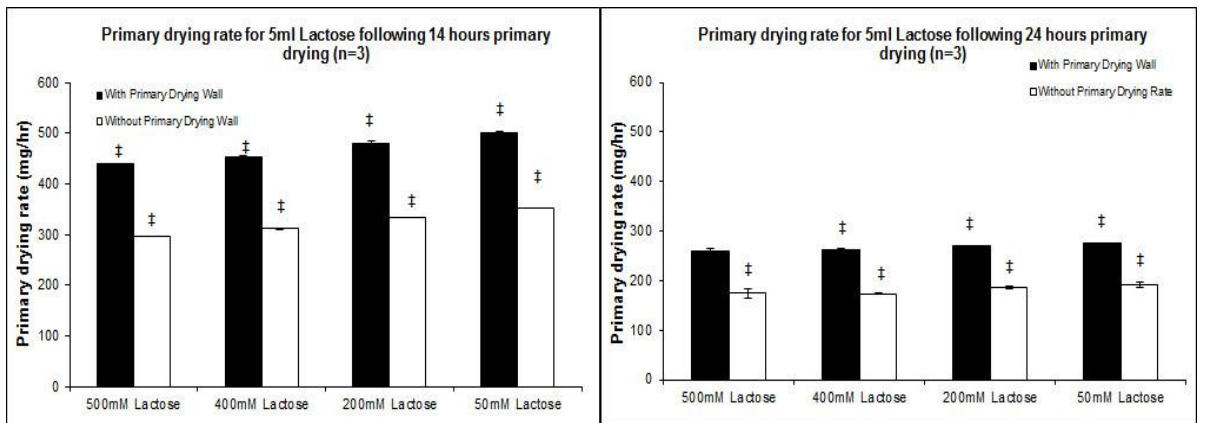
Figure 50. Primary drying rate for 5ml Lactose after 14 hours and 24 hours primary drying. Each bar represents mean ±SD, n=3. ‡ denotes statistical significance at P < 0.05

Since the presence of a drying wall helps increase loss of water from formulations during primary drying, it follows that the rate of primary drying would be higher in vials with a drying wall. This was clearly the case as shown in figures 47 to 50. Presence of the drying wall allowed an increment in primary drying rate between 25% and 33% across all samples. Statistical t-test showed that the primary drying rate in vials with and without the drying wall were significantly different for all formulations. Significance was at $P<0.05$ and at $P<0.01$.

5.4   DISCUSSION

A novel system, which involves creating a void between the formulation and the inside wall of a vial was used in order to improve primary drying rates during a freeze drying cycle. By measuring water loss during primary drying, percentage loss of water and primary drying rates were calculated.

The drying wall, built with water, is shown to disappear at the early stage of primary drying, leaving behind a void between the formulation and the wall of the vial. Sublimation, during primary drying, from the frozen matrix typically follows a top-down direction, that is, from the top of the matrix to the bottom. However, the presence of a void caused by the drying wall, allows for a change in direction of the sublimation front. In essence, as one sublimation front moves in the conventional manner, from the top of the vial to the bottom, another moves perpendicular to this, allowing the primary drying rate to increase and consequently drying time to reduce. Since statistical t-test analysis indicated significant difference between primary drying rate in vials with and without the drying wall, the null hypothesis is rejected.

This work is however nowhere near complete, and as can be noted from the depth of work carried out so far, is still at a somewhat preliminary stages. Following the first set of experiments reported, a decision was made to change the parameters of the freeze drying cycle since the shelf temperature first used was $+20^{o}C$, which limited the number of formulations that could be investigated as collapse of resulting cakes will occur. Using this temperature also made freeze drying of sucrose and lactose fairly difficult as these both have a collapse temperature of $-32^{o}C$ compared with mannitol, which has a eutectic temperature of $-1.5^{o}C$. Therefore to allow for adequate sample comparison and the ability to use compounds or materials with varied collapse and eutectic temperatures, a shelf temperature of $-40^{o}C$ is to be used.

The eutectic temperature of inositol could not be found from any literature, as such, a decision has been made to determine the eutectic temperature of inositol and other compounds of interest; this now forms part of the future work to be done.

5.5   CONCLUSION AND FUTURE WORK

5.5.1   Conclusion

The aim of this work was to increase the primary freeze drying rate of formulations without product damage by using a novel system to increase the surface area of the formulation. This novel system involves formation of a frozen vial system which results in the creation of a void between the formulation and the inside wall of a vial.

Although the work is not yet complete, results obtained thus far shows that it is indeed possible to improve and increase the primary drying rate of formulations without making any modifications to existing formulations, changing storage vials, or increasing the surface area of freeze dryer shelves.

5.5.2   Potential future work

$\rightarrow$ Primary drying cycles of mannitol, inositol, sucrose and lactose at -40°C, running for 12, 24, 48, 72 hours and so on until primary drying is complete.

$\rightarrow$ Increasing fill volumes up to 30ml or higher to ensure that the system still works even at higher fill volumes. This is very crucial and if found to work would be highly beneficial in industry.

$\rightarrow$ Varying the size of the drying wall to determine whether or not an increase in size of the drying wall will equate to even higher primary drying rates.

$\rightarrow$ Incorporation of an enzyme or protein and preparation of a complete formulation (including excipients and stabilisers) is the main destination point for this work. It is hoped that viable results would be obtained to confirm that the drying wall system works for any form of formulation.

$\rightarrow$ Carrying out of activity assays to,

- determine the enzyme activity in formulations freeze dried with the drying wall in place

- determine whether the enzyme activity differs from that found in formulations without the drying wall. It is highly important to prove that enzyme activity remains the same in formulations with the drying wall when compared with those in formulations without a drying wall. This would help show that no damage to the enzyme is caused by the presence of a drying wall.

→ Carrying out accelerated stability and thermal stability tests to ensure that the resulting freeze dried cakes of enzyme formulations with the drying wall have characteristics which are no different from those without the drying wall.

CHAPTER 6: SUMMARY & CONCLUSION

The body of work presented in this thesis are in three main parts: [1] the effect of ultrasound on freezing events of ionic systems, [2] the importance of formulation osmolality in freeze drying, and [3] a novel system for increasing primary freeze drying rate. Chapter 4 briefly presents the work on method optimisation, which is still very much in its infancy.

Aspects of freezing such as nucleation and ice crystal growth are strongly related with ice crystal morphology; however, the ice nucleation process typically occurs in a random, non-deterministic and spontaneous manner. In depth literature review revealed the different methods that have been developed to help control and optimise the freezing process. Some of these methods work by influencing ice nucleation by modifying the cooling rate and some statistically increase the mean nucleation temperature. Other methods developed allow a true control of nucleation at the desired nucleation temperature (Kasper & Friess, 2001). Ultrasonication, an emerging application in pharmaceutical sciences, has been applied to aid in the acceleration of nucleation, and to shorten the freezing process. Ultrasonication uses high-intensity acoustic energy to process materials and has gained popularity in the food industry over the years (Li & Sun, 2002; Zheng & Sun, 2006; Delgado *et al.*, 2009; Kiani *et al.*, 2011; Kiani & Sun, 2011).

The research presented in this thesis aimed to study the effect of sonication on nucleation events in ionic solutions, and more importantly how sonication impacts on the freezing process. Sodium Chloride (NaCl), Calcium Chloride (CaCl$_2$) and Magnesium Chloride (MgCl$_2$), as well as Sodium Phosphate monobasic (NaH$_2$PO$_4$) and Potassium Phosphate monobasic (KH$_2$PO$_4$) were investigated. In order to successfully study these effects, a contraption was built with an aluminium pan, which could be directly connected to an ultrasound transducer. Solutions of varying

concentrations were prepared based on percentage weight and solute osmolarity. These were loaded into French mini straws. The surface of the aluminium pan was chilled to ~70°C using the shelf of a freeze dryer. A metal block was placed on top of the straws to ensure contact was made with the pre-chilled surface. Temperature changes were monitored until evidence of nucleation and solidification were observed.

This work showed that triggering of ultrasound allowed nucleation to occur at temperatures higher than they would occur if there was no external control of nucleation. However, these observations were not statistically significant. This may have been due in part to the inability of ultrasound waves to efficiently propagate through the entire volume of solution in the French mini straws, allowing nucleation to occur naturally or triggering of nucleation to occur at temperatures that are not significantly different from nucleation temperatures obtained when the samples were not sonicated. It was also shown that ultrasonication can cause an increase in crystal growth time. This may have been due to the fact that ultrasound was applied when the solutions were in relatively low degree of supercooling, meaning only a few nuclei would have been formed, which would have been able to grow extensively. It is believed that at higher degrees of supercooling, nucleation is dominant while at lower degrees of supercooling, crystal growth is the dominant factor (Zheng & Sun, 2006).

Cryopreservation of animal sperm is an important aspect of breeding in animal science especially for endangered species. In order for sperm cryopreservation to be successful, cryoprotectants as well as semen extenders are used. One of the factors allowing semen preservation media to be optimum is the osmolality of the semen extenders used. Although preservation of animal sperm has no relation with freeze drying of pharmaceuticals, it was used in this thesis to make a case for considering the

osmolality of a formulation (prepared for freeze drying) as a factor for conferring protein protection against the stresses of freeze drying.

The osmolalities of some common solutes (mostly sugars) used in freeze drying (Sucrose, Trehalose, Glucose, Raffinose, Galactose, Lactose, Mannitol, Urea and Sodium Chloride.) were determined (molal concentration from 0.1m to 1.2m). Preliminary investigation on the osmolality and osmotic coefficients of common solutes were carried out. It was observed that the osmotic coefficient trend for the sugars analysed could be grouped based on the types of sugar they are or based on whether or not these sugars are able to undergo mutarotation. The trends observed show the need for further studies to be carried out with osmolality and to determine how it may be of importance to protein or API protection during freeze drying processes.

During the process of investigating solute osmolalities, the osmometer available for use could not measure beyond 2500 mOsm/kg. This meant that many highly concentrated solutions could not be measured using the osmometer. Although osmometers with higher measuring capacity are available, it was thought that a device which was already available in the laboratory and can cool and subsequently freeze solutions could be used to determine freezing point depression and consequently, osmolality can be calculated. A decision was made to use the since Differential Scanning Calorimetry (DSC), which can cool down to sub-zero temperatures with some DSC's able to go as low as -150°C and a range of cooling rates can be used. In addition, for most DSC's, a trace of the process can be observed whilst the sample is being processed. This therefore formed the basis of the preliminary work on the method optimisation of ways in which the DSC can be used as a tool for measuring freezing point depression. The work set out to develop and optimise a method that can be used to measure the freezing point of solutes, as well as the best method that can be used to analyse traces obtained in order to

determine the freezing point of solutes. Sodium Chloride was used as it had previously been used in freezing experiments and was thought to be an easy and cheap compound to use for initial method optimisation before moving on to more expensive compounds. Several DSC runs were carried to determine the best method for measuring freezing point depression.

DSC traces were initially analysed by reading off the temperature at which there was a sudden increase in heat flow, known as the nucleation temperature. However, after a few revisions and considerations, temperatures were read off at the highest temperature achieved by each solution during the freezing process - this was believed to be the freezing point. Upon further search for literature similar to this area of work, it was discovered that by transforming the axis of the DSC traces from heat flow (mW) vs temperature (^{o}C) to heat flow (mW) vs time (minutes) and drawing a tangential line which is extrapolated backwards to intersect with the baseline of the trace, the freezing point of the solution would be obtained. This investigation is still far from being called a success; however, it is a promising area and certainly a method, when well established, can save money for laboratories that already have a DSC machine and require freezing point measurements or osmolality measurements since osmolality can be calculated from freezing point depression values.

Primary drying is usually the longest part of the freeze drying process, and primary drying times lasting days or even weeks are not uncommon; however, longer primary drying times lead to longer freeze drying cycles, and consequently increased production costs. Much work has been done previously by others using different processes (such as annealing) in order to improve primary drying times; however, these do not come without drawbacks. A novel system involving the formation of a frozen vial system which results in the creation of a void between the formulation and the inside wall of a

vial has been devised to increase the primary freeze drying rate of formulations without product damage. Although the work is not nearly complete, it has been shown that it is possible to improve and increase the primary drying rate of formulations without making any modifications to existing formulations, changing storage vials, or increasing the surface area of freeze dryer shelves.

In conclusion, this body of work has provided some methods with which the freezing step during lyophilisation can be improved in order for the entire lyophilisation process to be optimised. The use of ultrasound to trigger and accelerate ice nucleation offers several advantages compared with other more invasive methods such as the use of chemicals including silver iodide, amino acids, and ice nucleating bacteria (e.g. *Pseudomonas syringae*). Since stability of APIs during freeze drying is of utmost importance, it may be necessary to delve further into the area of solute osmolalities in order to determine whether or not these hold the key to adequate protection of APIs. Many drug manufacturers are reluctant to change product formulation in the bid to improve on primary drying rates during freeze drying. Part of this body of work has been able to show that it is indeed possible to improve and increase the primary drying rate of formulations without making any modifications to existing formulations, changing storage vials, or increasing the surface area of freeze dryer shelves. A reduction in primary drying time will have a significant economic impact on the development and commercialisation of freeze dried products

REFERENCES

1.   Abdelwaheed, W., Degobert, G., Stainmesse, S., Fessi, H. 2006. Freeze-drying of nanoparticles: Formulation, process and storage considerations. Advanced Drug Delivery Reviews, 58, pp. 1688-1713.

2.   Adams, G. 2007. The principles of freeze-drying. Day, J. G., Stacey, G. N. (eds) In: Methods of Molecular Biology, Vol. 368: Cryopreservation and Freeze-Drying Protocols, Second Edition. Totowa: Humana Press Inc., pp 15-38.

3.   Andrieu, J., Vessot, S. 2011. Characterization and control of physical quality factors during freeze-drying of pharmaceuticals in vials. Tsotsas, E., Mujumdar, A. S. (eds) In: Modern Drying Technology, Vol. 3: Product Quality and Formulation, Weinheim: Wiley-VCH Verlag & Co., pp 51-90.

4.   Arakawa, T., Prestrelski, S.J., Kenney, W.C., and Carpenter, J.F. (2001). Factors affecting short-term and long-term stabilities of proteins. Adv. Drug Deliv. Rev. *46*, 307–326.

5.   Arroyo, J.P., and Schweickert, A.J. (2013). How Fluid Is Distributed in the Body: Cells, Water, Salt, and Solutions. In Back to Basics in Physiology Fluids in the Renal and Cardiovascular Systems, (San Diego: Academic Press), pp. 1–24.

6.   Aulton, M. E. 2002. Dosage form design and manufacture: drying. Aulton, M. E (eds) In: Pharmaceutics, The Science of Dosage Form Design, Second Edition. Philadelphia: Churchill Livingston, pp 390-393

7.   Avenell, J. A. 1982. Freezing of swamp buffalo semen. Animal Production Science, 5(2), pp 141-145.

8.   Barresi, A. A., Pisano, R., Fissore, D., Rasetto, V., Velardi, S. A., Vallan, A., Parvis, M., Galan, M. 2009. Monitoring of the primary drying of a lyophilization process in vials. Chemical Engineering and Processing, 48, pp 408-423.

9. Bevan, D.R. (1978). Osmometry. 1. Terminology and principles of measurement. Anaesthesia *33*, 794–800.

10. Boss, E. A., Filho, R. M., Vasco de Toledo, E. C. 2004. Freeze drying process: real time model and optimization. Chemical Engineering and Processing, 43, pp. 1475-1485.

11. Boylan, J. C., Nail, S. L. 2009. Parenteral products. Florence, A. T., Siepmann, J. (eds) In: Modern Pharmaceutics, Vol. 1: Basic Principles and Systems. New York: Informa Healthcare Inc., Vol. 188, pp 565-609.

12. Brown, D. (2009). Tonicity, pH, Buffer Capacity, and Stability Considerations for Technicians. J. Pharm. Soc. Wis. 17–20.

13. Brulls, M., Rasmuson, A. 2002. Heat transfer in vial lyophilization. International Journal of Pharmaceutics, 246, pp. 1-16.

14. Coleman, N.J., and Craig, D.Q.M. (1996). Modulated temperature differential scanning calorimetry: A novel approach to pharmaceutical thermal analysis. International Journal of Pharmaceutics. *135*, 13–29.

15. Chow, R., Blindt, R., Chivers, R., Povey, M. 2005. A study on the primary and secondary nucleation of ice by power ultrasound. Ultrasonics, 43(4), pp 227-230.

16. Daoussi, R., Vessot, S., Andrieu, J., Monnier, O. 2009. Sublimation kinetics and sublimation end-point times during freeze-drying of pharmaceutical active principle with organic co-solvent formulations. Chemical Engineering Research Design, 87, pp 899-907.

17. Delgado, A. E., Zheng, L., Sun, D. W. 2009. Influence of ultrasound on freezing rate of immersion-frozen apples. Food and Bioprocess Technology, 2, pp 263-270.

18. El-Gayar, M., Holtz, W. 2001. Technical note: Vitrification of goat embryos by the open pulled-straw method. Journal of Animal Science, 79, pp 2436–2438.

19. Equine Reproduction. 1998. FAQ – A.I and T.S. Available from http://equine-reproduction.com/articles/faqai.htm [Accessed 12 Oct 2013].

20. Franks, F. 2007. Freeze-Drying of Pharmaceuticals and Biopharmaceuticals, First Edition. Cambridge: The Royal Society of Chemistry.

21. Friedman, M. H. 2008. Principles and Models of Biological Transport, Second Edition. New York: Springer Science and Business Media.

22. Garside, J., Mersmann, A., Nyvlt, J. 2002. Measurement of Crystal Growth and Nucleation Rates, Second Edition. Bodmin: MPG Books.

23. Gatlin, L.A. and Nail, S.L. 1994. Protein Purification Process Engineering. Freeze-Drying: A Practical Overview. Bioprocess Technology, 18, pp. 317-367

24. Guiseppi-Elie, A., Choi, S., Geckeler, K. E. 2009. Ultrasonic processing of enzymes: Effect on enzymatic activity of glucose oxidase. Journal of Molecular Catalysis: Enzymatic, 58, pp 118-123.

25. Gupta, P. K. 2013. Solutions and Phase Equilibria. In: Rx Remington, Twenty-second edition. London: Pharmaceutical Press, pp 583-603.

26. Hottot, A., Vessot, S., Andrieu, J. 2004. A direct characterization method of the ice morphology. Relationship between mean crystals size and primary drying times of freeze-drying processes. Drying Technology, 22(8), pp 2009-2021.

27. Hottot, A., Nakagawa, K., Andrieu, J. 2008. Effect of ultrasound-controlled nucleation on structural and morphological properties of freeze-dried mannitol solutions, Chemical Engineering. Research and. Design, 86, pp 193–200.

28. Hunek, B., Cheng, A., Capettini, J. 2007. Increasing lyophilization productivity, flexibility, and reliability using liquid nitrogen refrigeration. Available from www.biopharminternational.com [Accessed 4 Feb 2010].

29. Ingham, A., Poon, C. Y. 2013. Tonicity, Osmoticity, Osmolality, Osmolarity. In: Rx Remington, Twenty-second edition. London: Pharmaceutical Press, pp 642-643.

30. Jameel, F., Patro, S. Y. 2005. Impact of formulations for optimizing lyophilization process development. American Pharmaceutical Review, 8 (2), pp. 46-51.

31. Kadoya, S., Fujii, K., Izutsu, K., Yonemochi, E., Terada, K., Yomota, C., Kawanishi. 2010. Freeze-drying of proteins with glass-forming oligosaccharide-derived sugar alcohols. International Journal of Pharmaceutics, doi: 10.1016/j.ijpharm,2010.01.027.

32. Kamath, L. 2006. Practical Technologies for Lyophilization. Genetic Engineering & Biotechnology News, 26 (20).

33. Kasper, J. C., Friess, W. 2011. The freezing step in lyophilization: physic-chemical fundamentals, freezing methods and consequences on process performance and quality attributes of biopharmaceuticals. European Journal of Pharmaceutics and Biopharmaceutics, 78, pp 248-263.

34. Khajuria, A., and Krahn, J. (2005). Osmolality revisited—Deriving and validating the best formula for calculated osmolality. Clinical. Biochemistry. *38*, pp 514-519.

35. Kiani, H., Zhang, Z., Delgado, A., Sun, D. W. 2011. Ultrasound assisted nucleation of some liquid and solid model foods during freezing. Food Research International, 44, pp 2915-2921.

36. Kiani, H., Sun, D. W. 2011. Water crystallization and its importance to freezing of foods: A review. Trends in Food Science & Technology, 22(8), pp 407-426.

37. Kotz, J. C., Treichel, P., Townsend, J. R. 2009. Chemistry and chemical reactivity volume 2, Seventh Edition. Belmont: Thomson Brooks/Cole.

38. Li, B., Sun, D. W. 2002. Effect of power ultrasound on freezing rate during immersion freezing of potatoes, Journal of Food Engineering, 55, pp 277 – 282.

39. Liu, W., Kelkar, A. S., Yeh, P. Y. 2004. Prediction of the optimum primary drying temperature from a stepwise temperature increased lyophilization cycle, American Pharmaceutical Review, 7(6), pp 20-27.

40. Löser Micro-Osmometer Type 6. Manual and Operating Instructions. Revised October 22nd, 2008.

41. Maltesen, M. J., van de Weert, M. 2008. Drying methods for protein pharmaceuticals. Drug Discovery Today: Technologies, doi: 10.1016/j.ddtec.2008.11.001.

42. Matejtschuk, P. 2007. Lyophilization of proteins. Day, J. G., Stacey, G. N. (eds) In: Methods of Molecular Biology, Vol. 368: Cryopreservation and Freeze-Drying Protocols, Second Edition. Totowa: Humana Press Inc., pp 59-71.

43. Mellor, J. D. 1978. Fundamentals of freeze-drying, First Edition. London: Academic Press.

44. Nakagawa, K., Hottot, A., Vessot, S., Andrieu, J. 2006. Influence of controlled nucleation by ultrasounds on ice morphology of frozen formulations for pharmaceutical proteins freeze-drying. Chemical Engineering and Processing, 45, pp 783-791.

45. Nakamura, T. (2009). Freezing Point Temperature Measuring Method and Temperature Calibrating Method in Differential Scanning Calorimetry (Chiba).

46. Orfão, L.H., Nascimento, A.F., Corrêa, F.M., Cosson, J., and Viveiros, A.T.M. (2011). Extender composition, osmolality and cryoprotectant effects on the motility of sperm in the Brazilian endangered species Brycon opalinus (Characiformes). Aquaculture *311*, 241–247.

47. Patel, M., Bhugra, C., Pikal, M. J. 2009. Reduced pressure ice fog technique for controlled ice nucleation during freeze-drying. AAPS Pharmaceutical Science and Technology, 10(4), pp 1406-1411.

48. Patel, S. M., Pikal, M. 2009. Process Analytical Technologies (PAT) in freeze-drying of parenteral products. Pharmaceutical Development and Technology, 14(6), pp. 567–587.

49. Patel, S. M., Doen, T., Pikal, M. J. 2009. Determination of end point of primary drying in freeze-drying process control. AAPS Pharmaceutical Science and Technology, doi: 10.1208/s12249-009-9362-7.

50. Petersen, A., Rau, G., Glasmacher, B., 2006. Reduction of primary freeze-drying time by electric field induced ice nucleus formation. Heat Mass Transfer, 42, pp 929–938.

51. Pikal, M.J. 1985. Use of Laboratory Data in Freeze Drying Process Design: Heat and Mass Transfer Coefficients and the Computer Simulation of Freeze Drying. Journal of Parenteral Science and Technology, 39, pp. 115-139.

52. Pikal, M. J. 2007. Freeze Drying. Swarbrick, J. (eds) In: Encyclopedia of Pharmaceutical Technology, Third Edition. New York: Informa Healthcare Inc., pp 1807-1833.

53.   Rades, T., Gordon, K. C., Graeser, K. 2013. Molecular structure, properties, and states of matter. In: Rx Remington, Twenty-second edition. London: Pharmaceutical Press, pp 541 - 570.

54.   Rambhatla, S. and Pikal. 2004. M.J. Heat and Mass Transfer Issues in Freeze-drying Process Development. In: H.R. Costantino and M.J. Pikal. Lyophilization of Biopharmaceuticals. Arlington VA: AAPS Press, pp. 75-109.

55.   Rambhatla, S., Ramot, R., Bhugra, C., Pikal, M. 2004. Heat and mass transfer scale-up issues during freeze drying: II. Control and characterization of the degree of supercooling, AAPS Pharmaceutical Science and Technology, 5, pp 54–62.

56.   Ribeiro, B. da S. (2012). Metabolic and bioprocess engineering of production cell lines for recombinant protein production (Berlin: Logos Verlag).

57.   Roumeliotis, G. 2006. The challenges of protein formulation. Available from http://www.in-pharmatechnologist.com/Materials-Formulation/The-challenges-of-protein-formulation [Accessed 8 Feb 2010].

58.   Saclier, M., Peczalski, R., Andrieu, J. Effect of ultrasonically induced nucleation on ice crystals' size and shape during freezing in vials, 65(10), 3064-3071.

59.   Sarmento, B. 2008. The oral delivery of therapeutic proteins. Available from http://www.scitopics.com/The_oral_delivery_of_therapeutic_proteins.html [Accessed 8 Feb 2010].

60.   Scatchard, G., Hamer, W.J., and Wood, S.E. (1938). Isotonic Solutions. I. The Chemical Potential of Water in Aqueous Solutions of Sodium Chloride, Potassium Chloride, Sulfuric Acid, Sucrose, Urea and Glycerol at 25°1. J. Am. Chem. Soc. *60*, 3061–3070.

61. Searles, J. A. 2004. Freezing and annealing phenomena in lyophilization. Rey, L., & May, J.C. (eds) In: Freeze-Drying/ Lyophilization of Pharmaceutical and Biological Products. New York: Marcel Dekker Inc., Vol. 96, pp 108-144.

62. Searles, J. A., Carpenter, J. F., Randolph, T. W. 2001. The ice nucleation temperature determines the primary drying rate of lyophilization for samples frozen on a temperature-controlled shelf. Journal of Pharmaceutical Sciences, 90(7), pp 860-871.

63. Shah, J. C. 2006. Tonicity. Swarbrick, J. (eds) In: Encyclopedia of Pharmaceutical Technology, Third Edition. New York: Informa Healthcare Inc., pp 3768-3781.

64. Shugar, G. J., Ballinger, J.T. 1996. Chemical Technicians' Ready Reference Handbook, Fourth Edition. New York: McGraw-Hill Inc.

65. Silbernagl, S., Despopoulos, A. 2009. Colour Atlas of Physiology, Sixth Edition. New York: Thieme Publishing Group.

66. Sinko, P.J. 2006. Martin's Physical Pharmacy and Pharmaceutical Sciences, Fifth Edition. Baltimore: Lippincott Williams & Wilkins.

67. Sun, D. W., Li, B. 2003. Microstructural change of potato tissues frozen by ultrasound-assisted immersion freezing. Journal of Food Engineering, 57, pp 337-345.

68. Sun, D. W., Zheng, L. 2006. Innovations in freezing process. Sun, D. W (eds). In: Handbook of frozen food processing and packaging. Boca Raton: Taylor & Francis Group, pp 58-81.

69. Tang, X.C., Pikal, M. J. 2004. Design of freeze-drying processes for pharmaceuticals: practical advice. Pharmaceutical Research, 21(2), pp 191-200.

70. Wang, W. 2000. Lyophilization and development of solid protein pharmaceuticals. Int. J. Pharm. *203*, 1–60.

71. Weiser, G. 2012. Laboratory Technology for Veterinary Medicine. In Veterinary Hematology and Clinical Chemistry, M.A. Thrall, G. Weiser, R. Allison, and T. Campbell, eds. (John Wiley & Sons, Inc.), pp. 3–33.

72. Wilson, P.W., Heneghan, A. F., Haymet, A. D. J. 2003. Ice nucleation in nature: supercooling point (SCP) measurements and the role of heterogeneous nucleation. Cryobiology, 46, pp 88-98.

73. Woelders, H., Matthijs, A., and Engel, B. 1997. Effects of Trehalose and Sucrose, Osmolality of the Freezing Medium, and Cooling Rate on Viability and Intactness of Bull Sperm after Freezing and Thawing. Cryobiology *35*, 93–105.

74. Xiang, J., Hey, J. M., Liedtke, V., Wang, D. Q. 2004. Investigation of freeze-drying sublimation rates using a freeze-drying microbalance technique. International Journal of Pharmaceutics, 279, pp 95-105.

75. Yang, G., Gilstrap, K., Zhang, A., Xu, L. X., He, X. 2010. Collapse temperature of solutions important for lyopreservation of living cells at ambient temperature, Biotechnology and Bioengineering, 106(2), pp 247-259.

76. Zaritzky, N. 2006. Physical-Chemical principles in freezing. Sun, D. W (eds). In: Handbook of frozen food processing and packaging. Boca Raton: Taylor & Francis Group, pp 4-29.

77. Zeng, W.X., Shimada, M., Isobe, N., and Terada, T. (2001). Survival of boar spermatozoa frozen in diluents of varying osmolality. Theriogenology *56*, 447–458.

78.   Zhang, B., Yu, D., Liu, H.-L., and Hu, Y. (2002). Osmotic coefficients of polyelectrolyte solutions, measurements and correlation. Polymer *43*, 2975–2980.

79.   Zheng, L., Sun, D. W. 2006. Innovative applications of power ultrasound during food freezing processes – a review, Trends in Food Science & Technology, 17, pp 16 – 23.

APPENDICES

APPENDIX 1: SALT THERMOGRAMS

Sodium Chloride
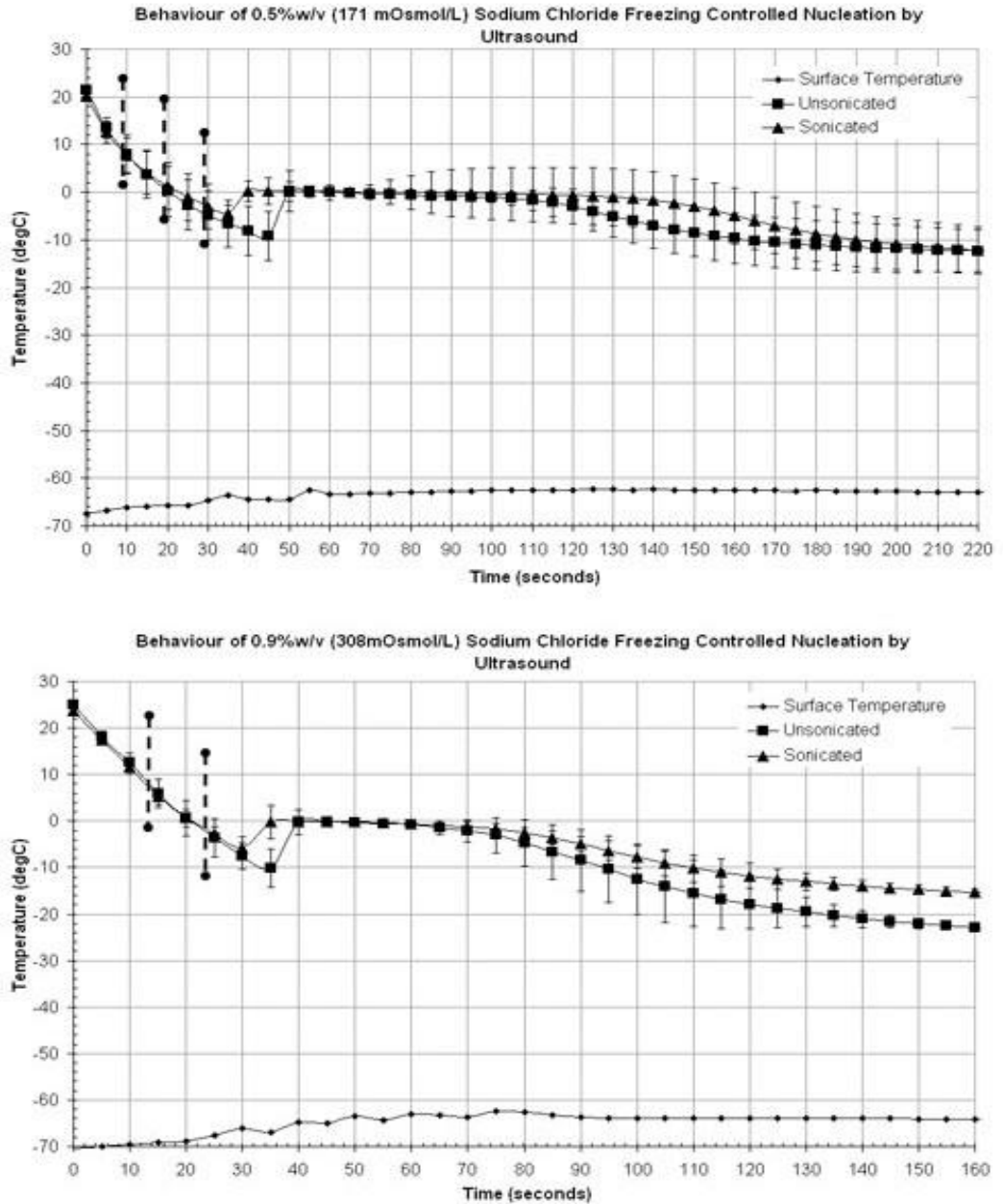
Figure 51. Temperature trace for 0.5%w/v and 0.9%w/v Sodium Chloride unsonicated and sonicated showing +/-SD, n=4. Vertical dotted lines indicate sonication times
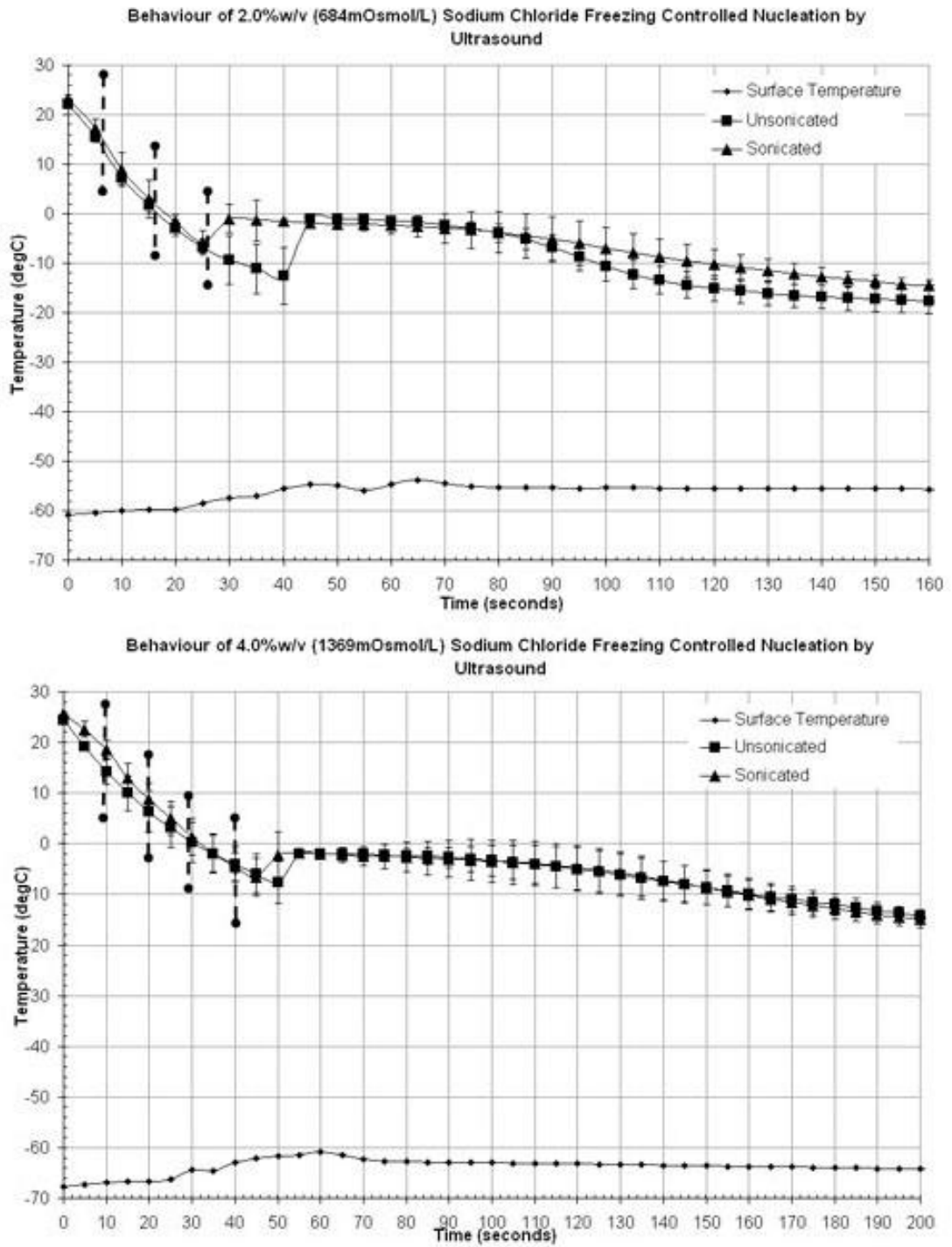
Figure 52. Temperature trace for 2%w/v and 4%w/v Sodium Chloride unsonicated and sonicated showing +/-SD, n=4. Vertical dotted lines indicate sonication times

148

Calcium Chloride

Behaviour of 0.5%w/v (135mOsmol/L) Calcium Chloride Freezing Controlled Nucleation by Ultrasound

Behaviour of 0.9%w/v (243mOsmol/L) Calcium Chloride Freezing Controlled Nucleation by Ultrasound
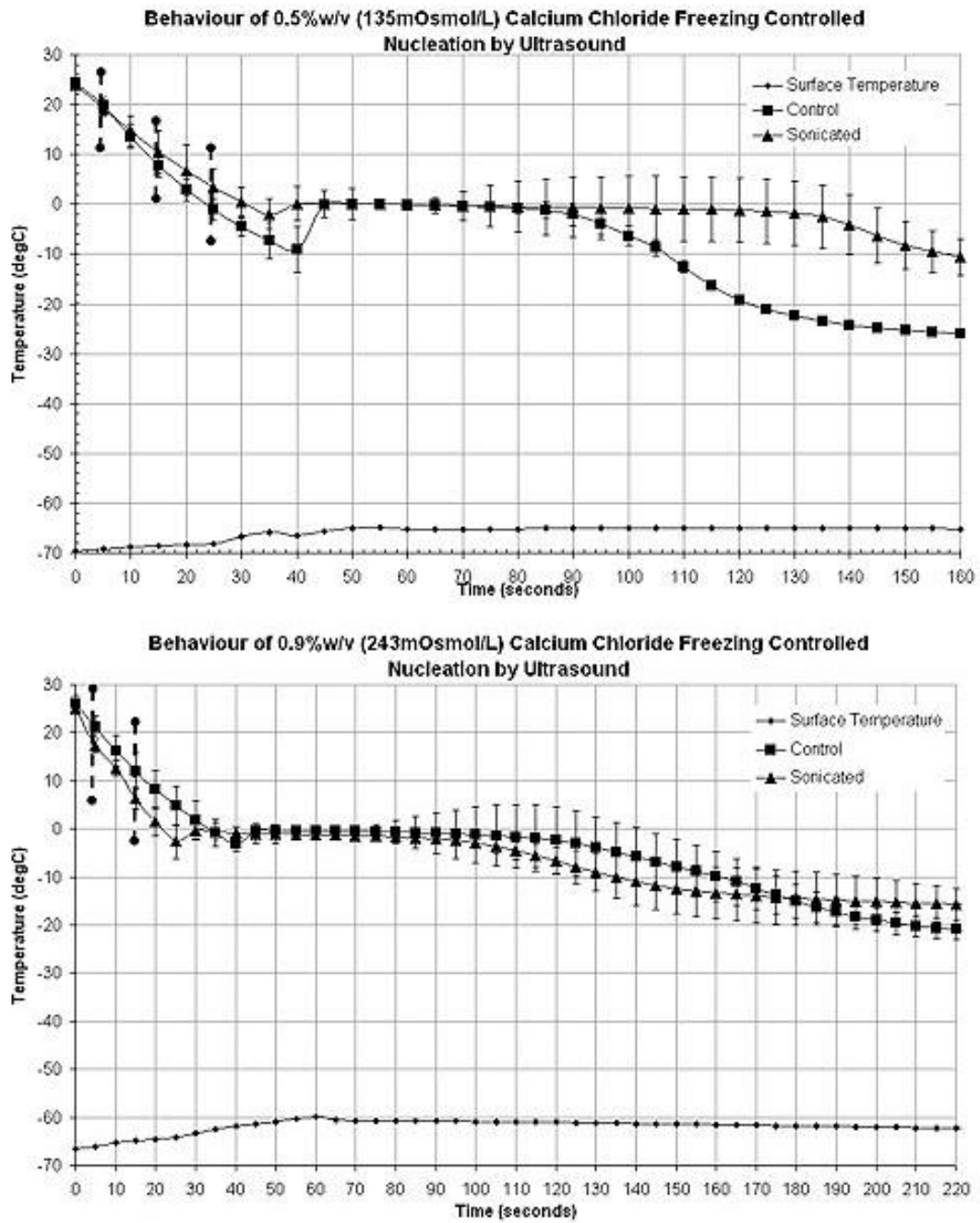
Figure 53. Temperature trace for 0.5%w/v and 0.9%w/v Calcium Chloride unsonicated and sonicated showing +/-SD, n=4. Vertical dotted lines indicate sonication times
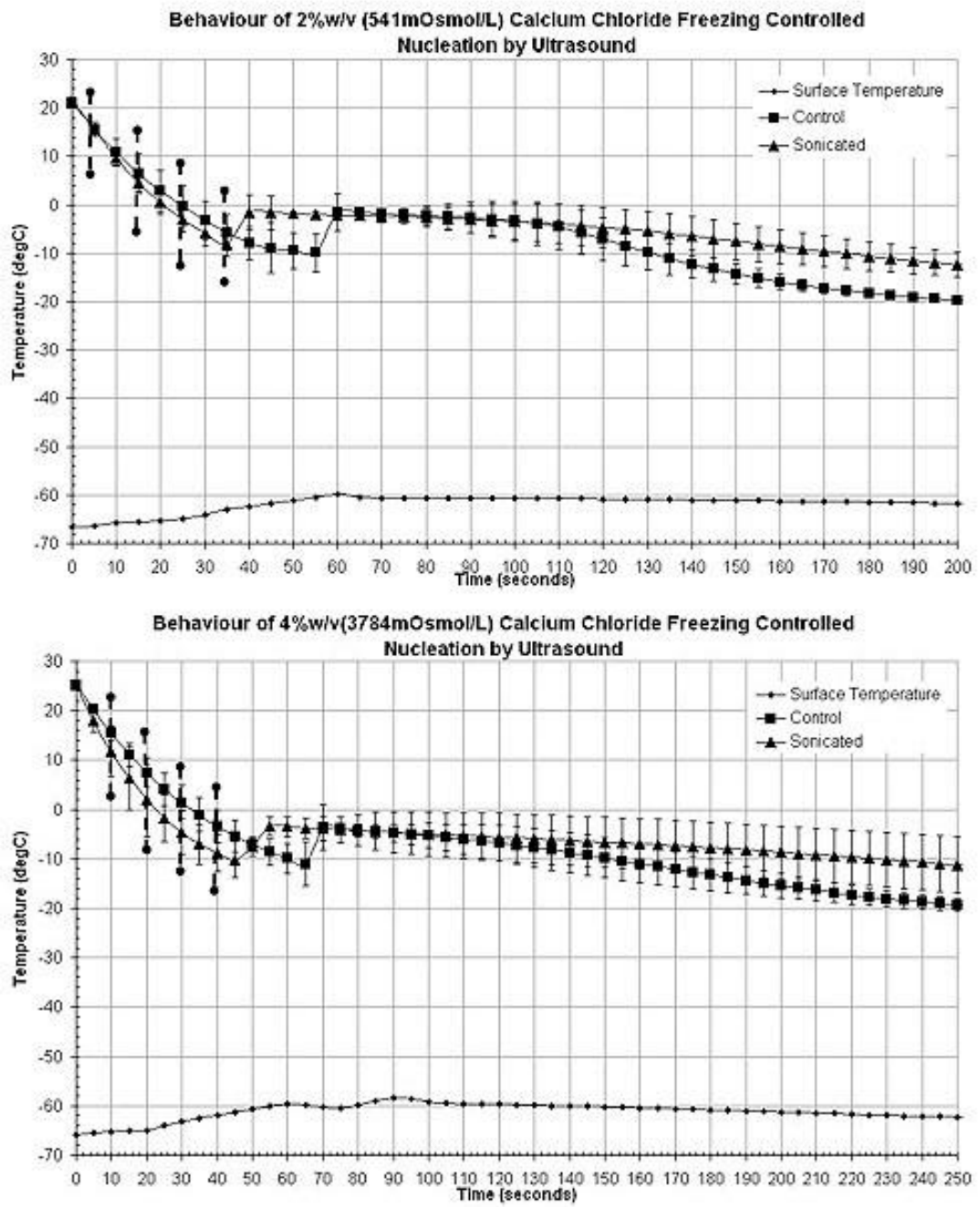
Figure 54. Temperature trace for 2%w/v and 4%w/v Calcium Chloride unsonicated and sonicated showing +/-SD, n=4. Vertical dotted lines indicate sonication times
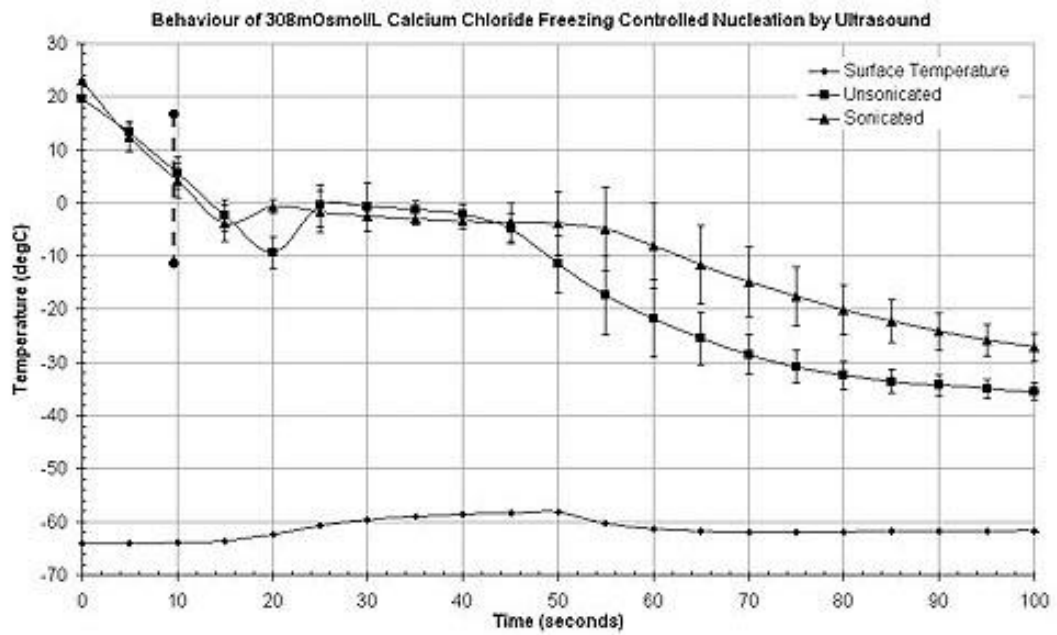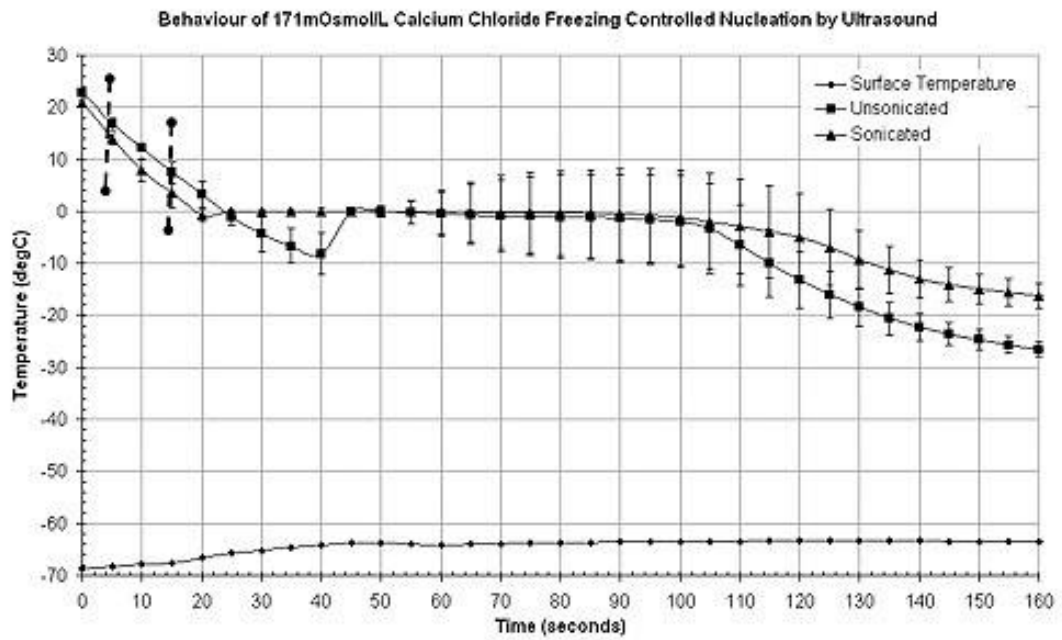
Figure 55. Temperature trace for 171mOsmol/L and 308mOsmol/L Calcium Chloride unsonicated and sonicated showing +/-SD, n=4. Vertical dotted lines indicate sonication times
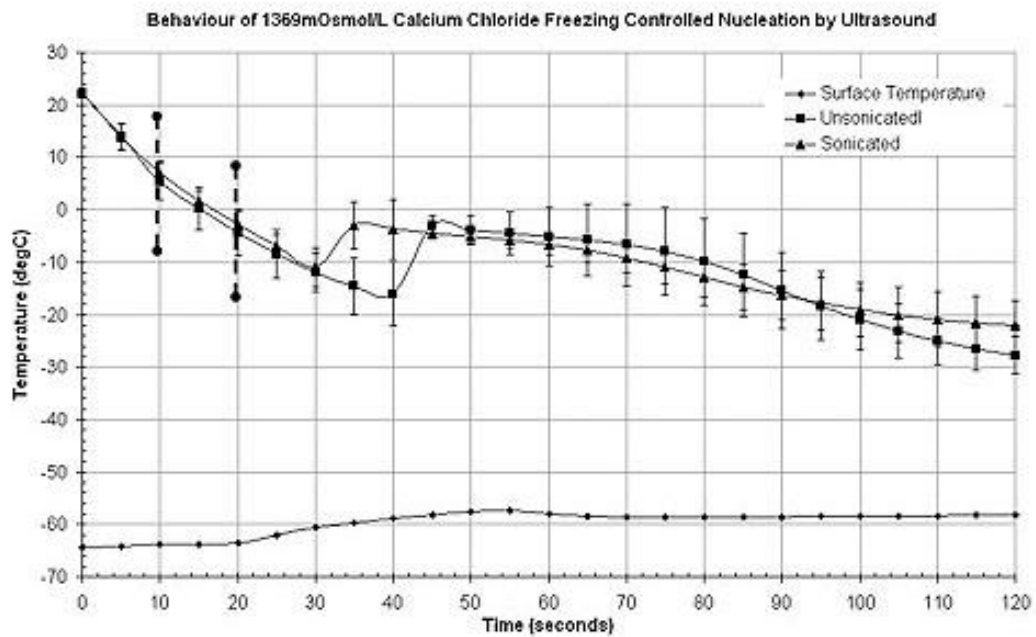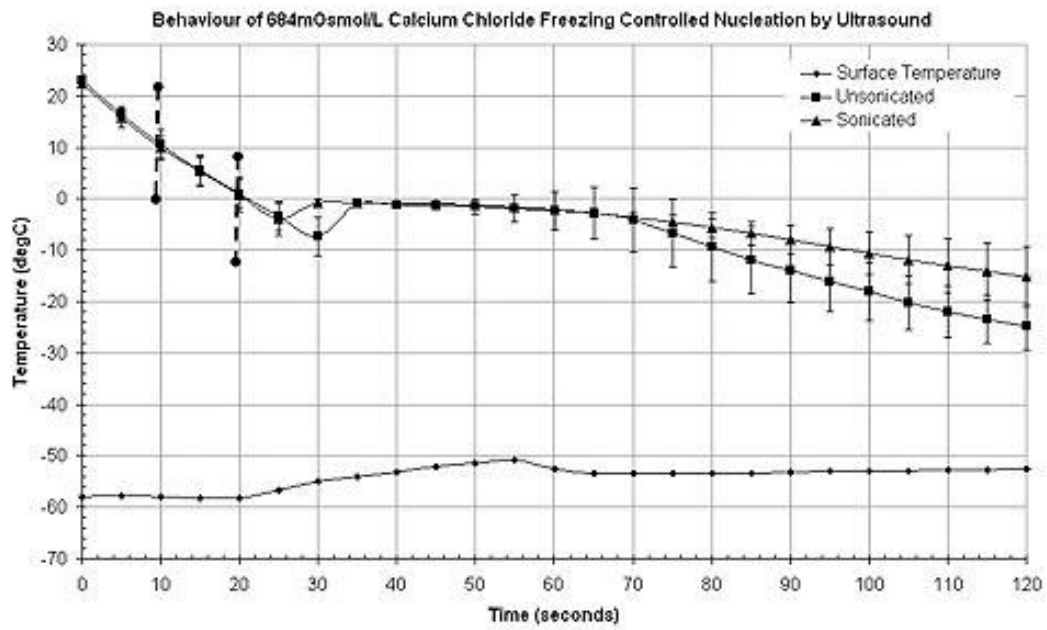
Figure 56. Temperature trace for 684mOsmol/L and 1369mOsmol/L Calcium Chloride unsonicated and sonicated showing +/-SD, n=4. Vertical dotted lines indicate sonication times

Magnesium Chloride

Behaviour of 0.5%w/v (158mOsmol/L) MgCl₂ Freezing Controlled Nucleation by Ultrasound

Behaviour of 0.9%w/v (284mOsmol/L) MgCl₂ Freezing Controlled Nucleation by Ultrasound
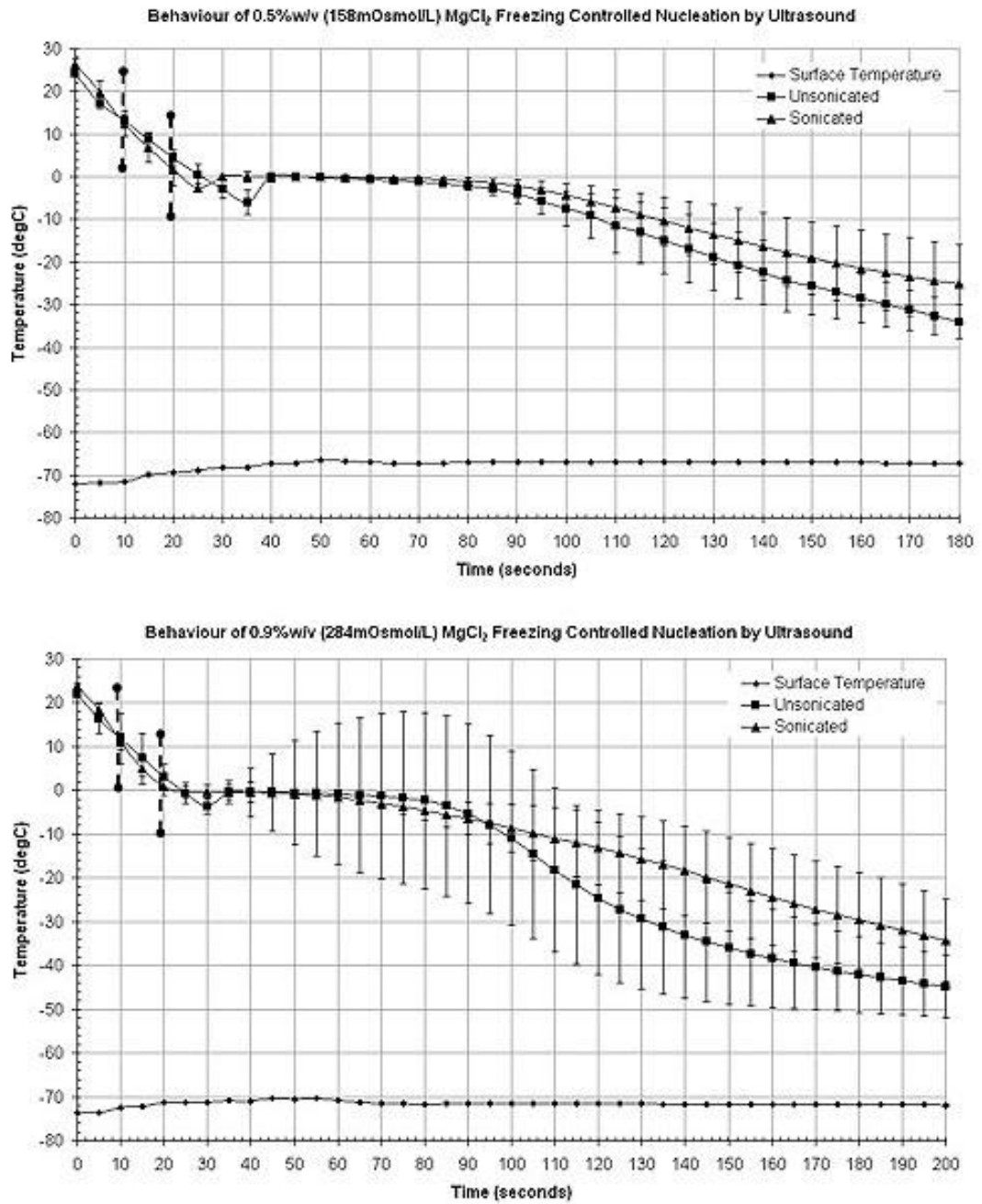
Figure 57. Temperature trace for 0.5%w/v and 0.9%w/v Magnesium Chloride unsonicated and sonicated showing +/-SD, n=4. Vertical dotted lines indicate sonication times

.
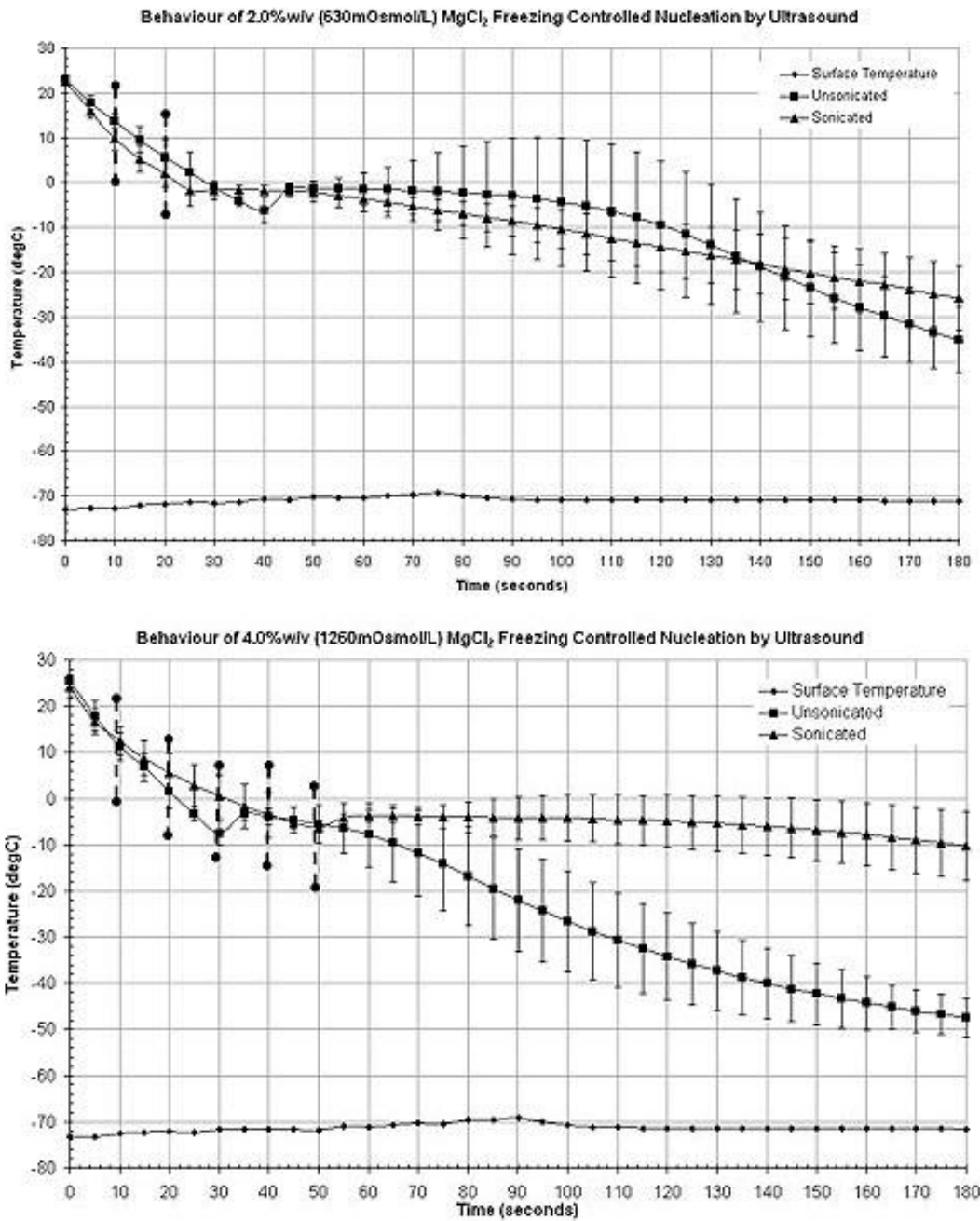
Figure 58. Temperature trace for 2%w/v and 4%w/v Magnesium Chloride unsonicated and sonicated showing +/-SD, n=4. Vertical dotted lines indicate sonication times
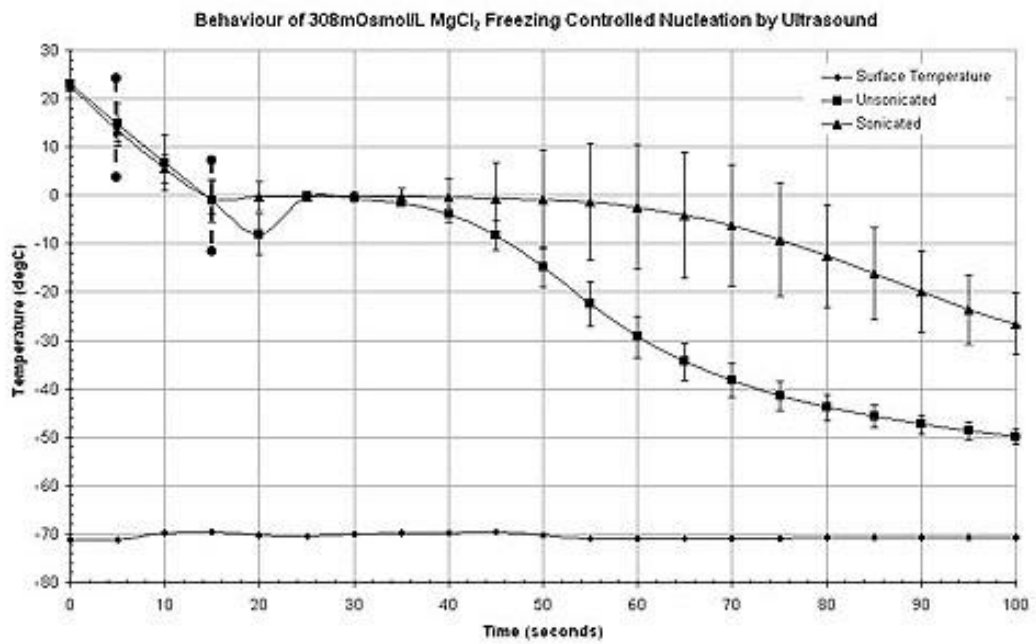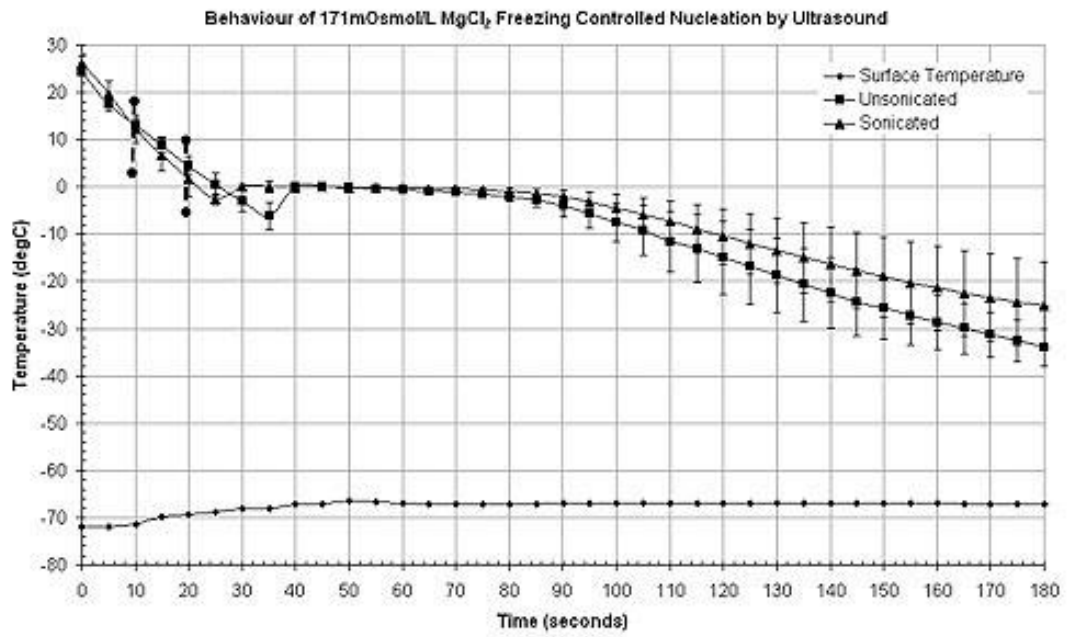
Figure 59. Temperature trace for 171mOsmol/L and 308mOsmol/L Magnesium Chloride unsonicated and sonicated showing +/-SD, n=4. Vertical dotted lines indicate sonication times

155
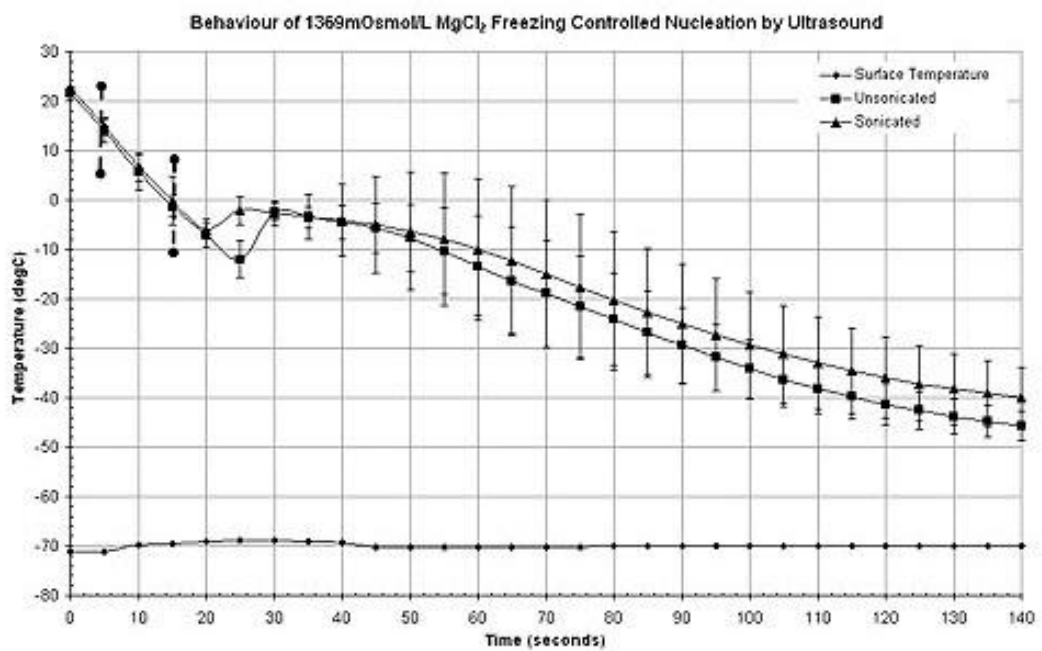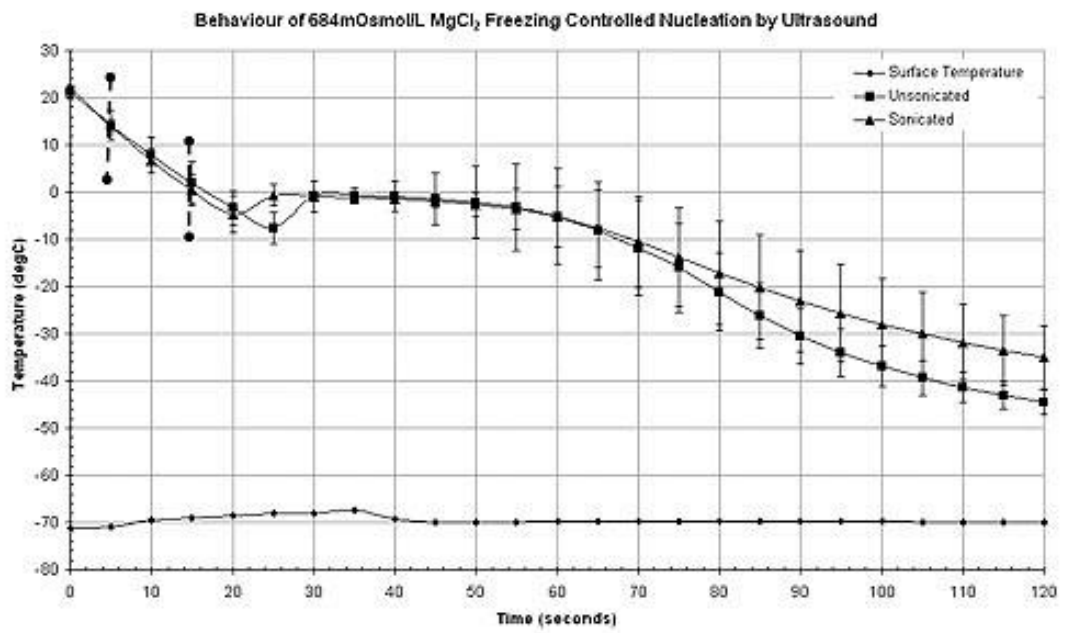
Figure 60. Temperature trace for 684mOsmol/L and 1369mOsmol/L Magnesium Chloride unsonicated and sonicated showing +/-SD, n=4. Vertical dotted lines indicate sonication times

Sodium Phosphate Monobasic
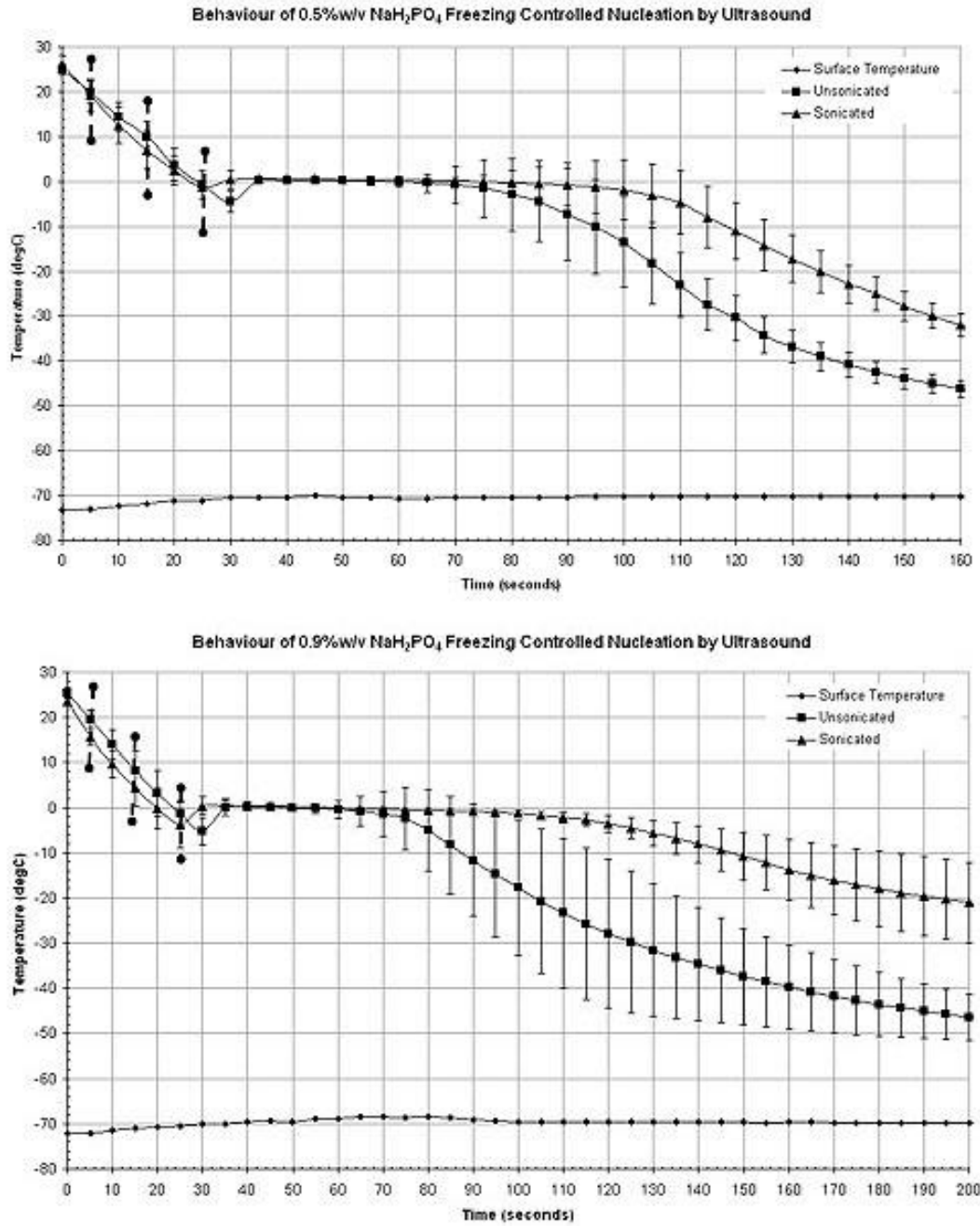
Figure 61. Temperature trace for 0.5%w/v and 0.9%w/v Sodium Phosphate monobasic unsonicated and sonicated showing +/-SD, n=4. Vertical dotted lines indicate sonication times
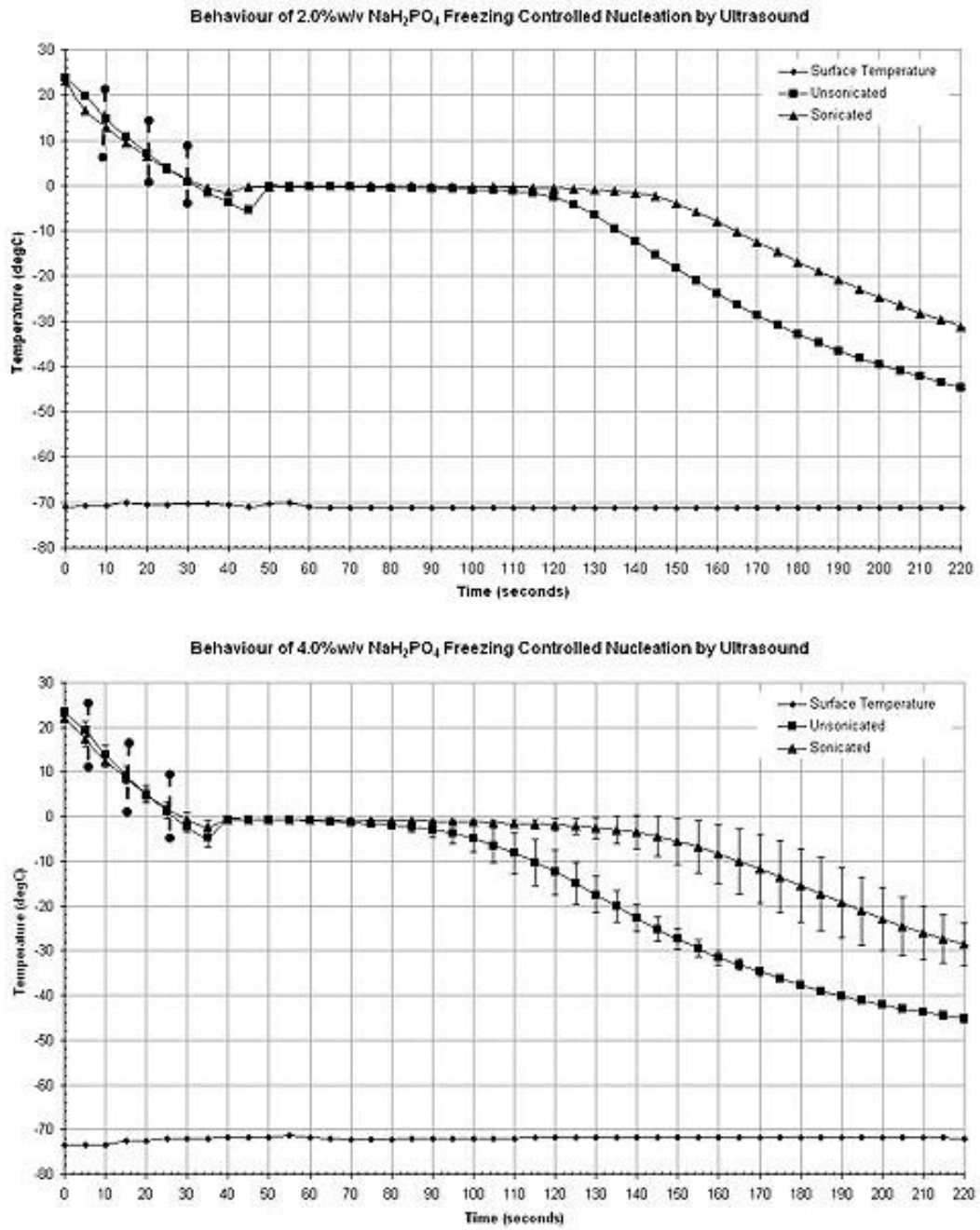
Figure 62. Temperature trace for 2%w/v and 4%w/v Sodium Phosphate monobasic unsonicated and sonicated showing +/-SD, n=4. Vertical dotted lines indicate sonication times

158
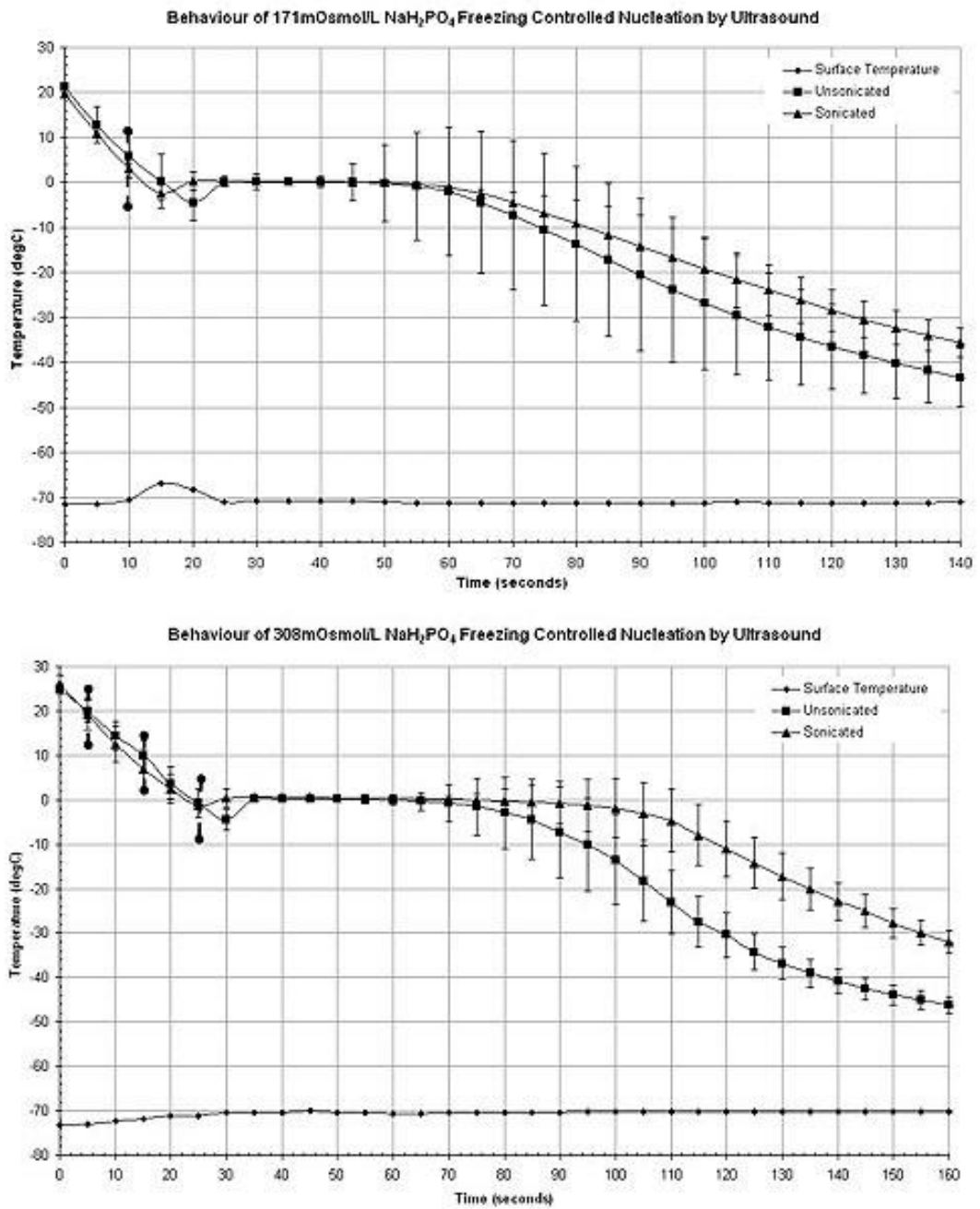
Figure 63. Temperature trace for 171mOsmol/L and 308mOsmol/L Sodium Phosphate monobasic unsonicated and sonicated showing +/-SD, n=4. Vertical dotted lines indicate sonication times
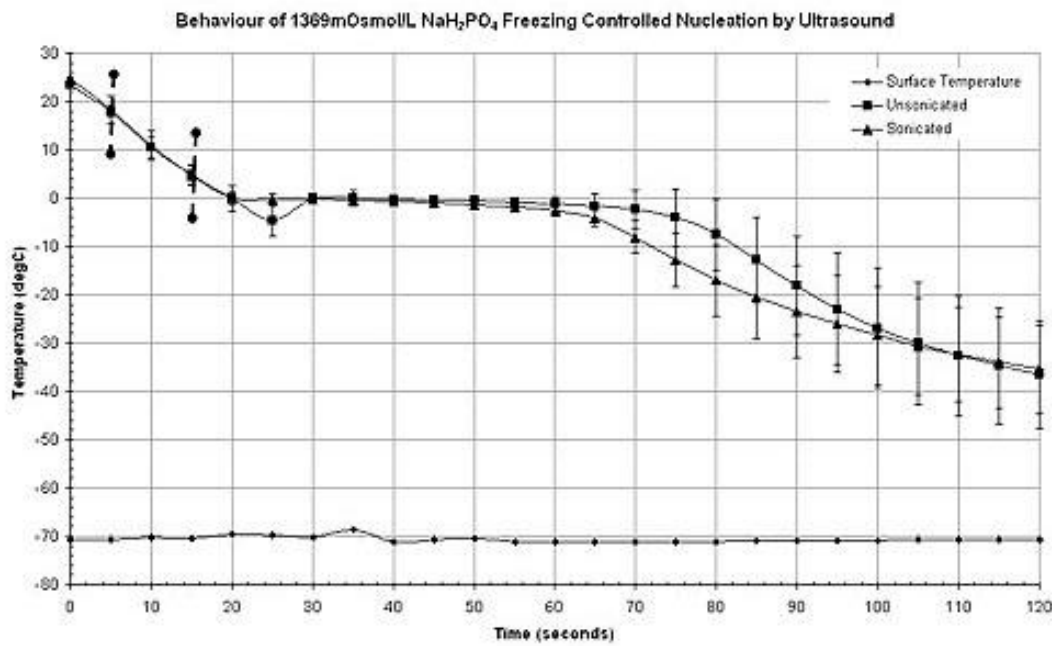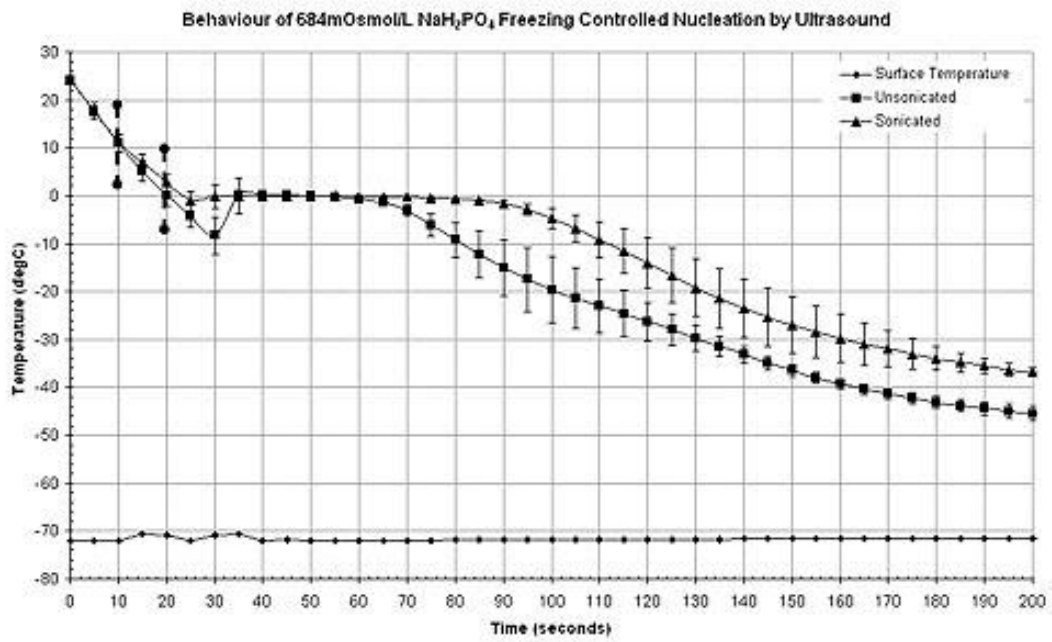
Figure 64. Temperature trace for 684mOsmol/L and 1369mOsmol/L Sodium Phosphate monobasic unsonicated and sonicated showing +/-SD, n=4. Vertical dotted lines indicate sonication times

Potassium Phosphate Monobasic

Behaviour of 0.5%w/v Potassium Phosphate Freezing Controlled Nucleation by Ultrasound

Behaviour of 0.9%w/v Potassium Phosphate Freezing Controlled Nucleation by Ultrasound
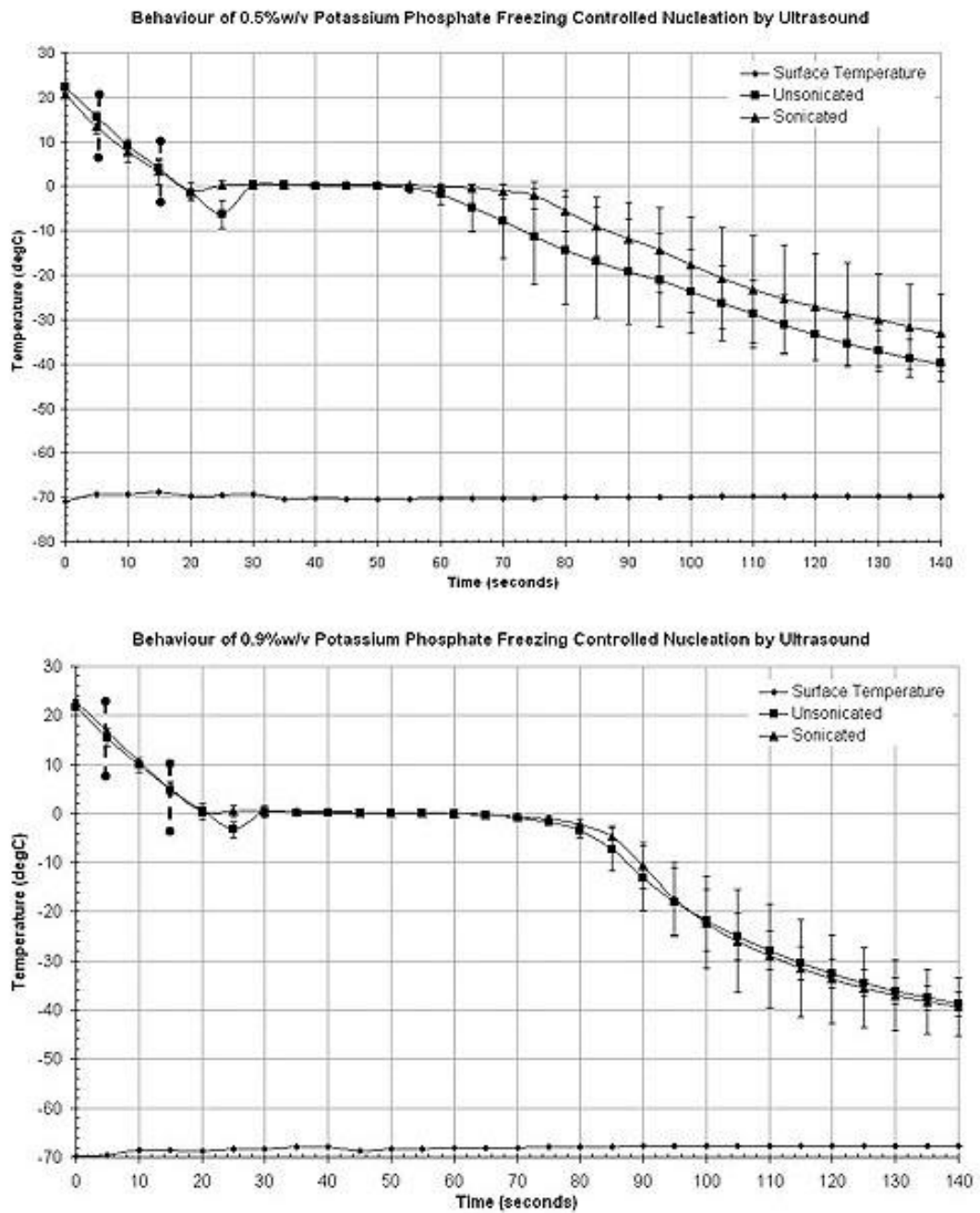
Figure 65. Temperature trace for 0.5%w/v and 0.9%w/v Potassium Phosphate monobasic unsonicated and sonicated showing +/-SD, n=4. Vertical dotted lines indicate sonication times

161
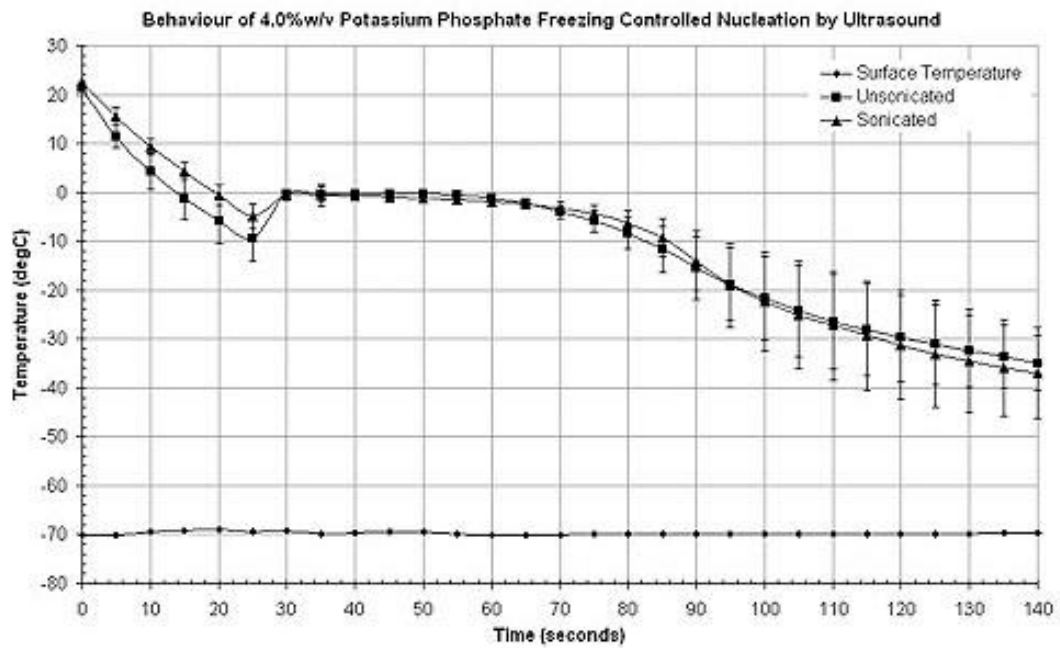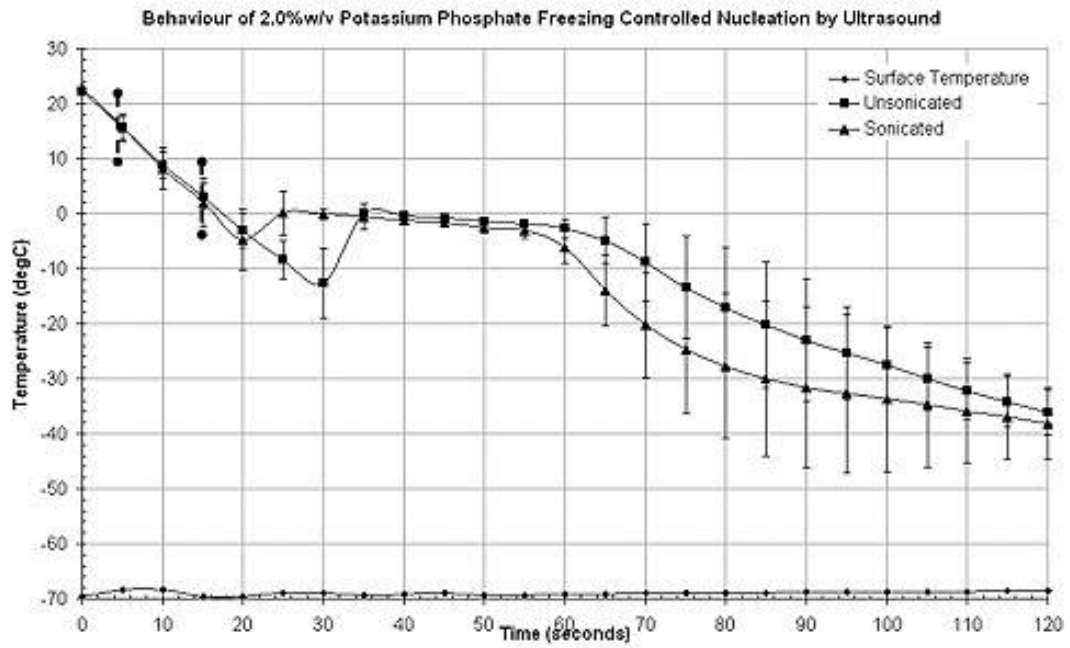
Figure 66. Temperature trace for 2%w/v and 4%w/v Potassium Phosphate monobasic unsonicated and sonicated showing +/-SD, n=4. Vertical dotted lines indicate sonication times
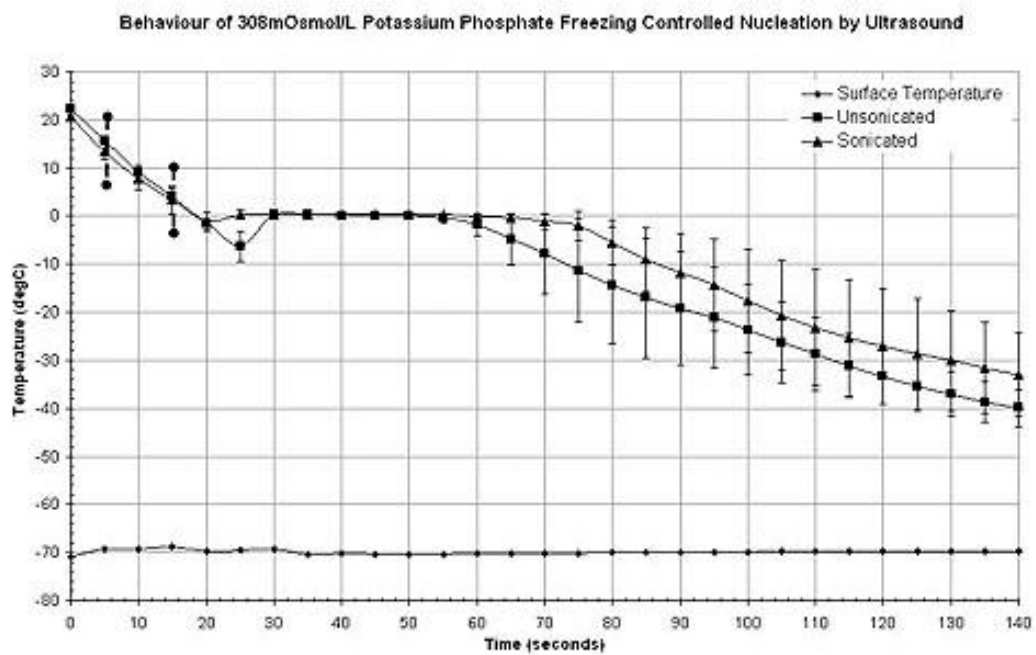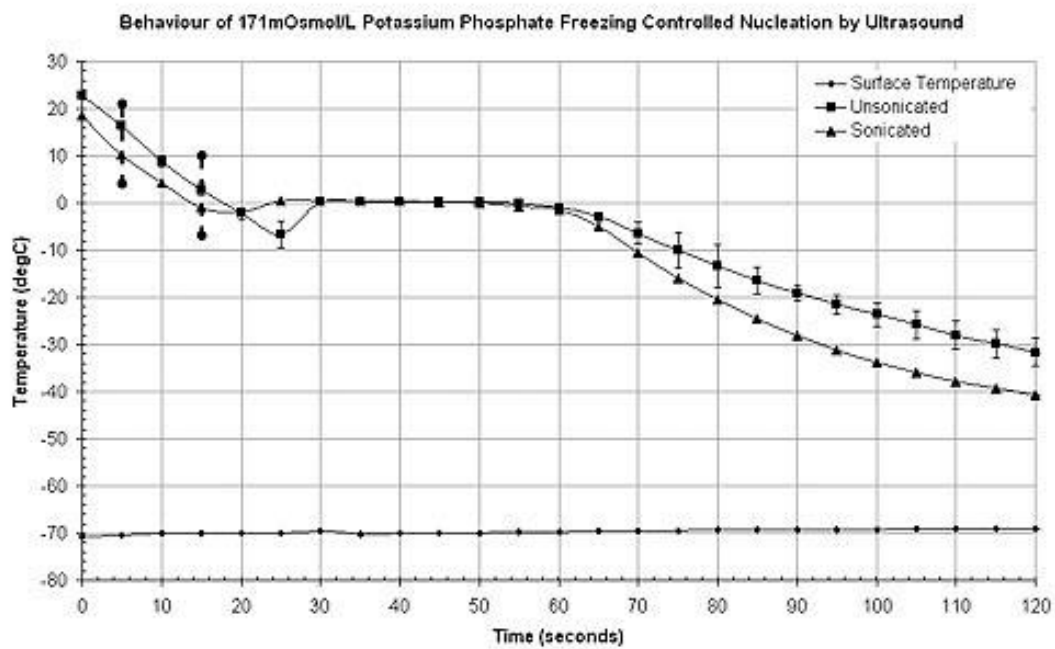
Figure 67. Temperature trace for 171mOsmol/L and 308mOsmol/L Potassium Phosphate monobasic unsonicated and sonicated showing +/-SD, n=4. Vertical dotted lines indicate sonication times
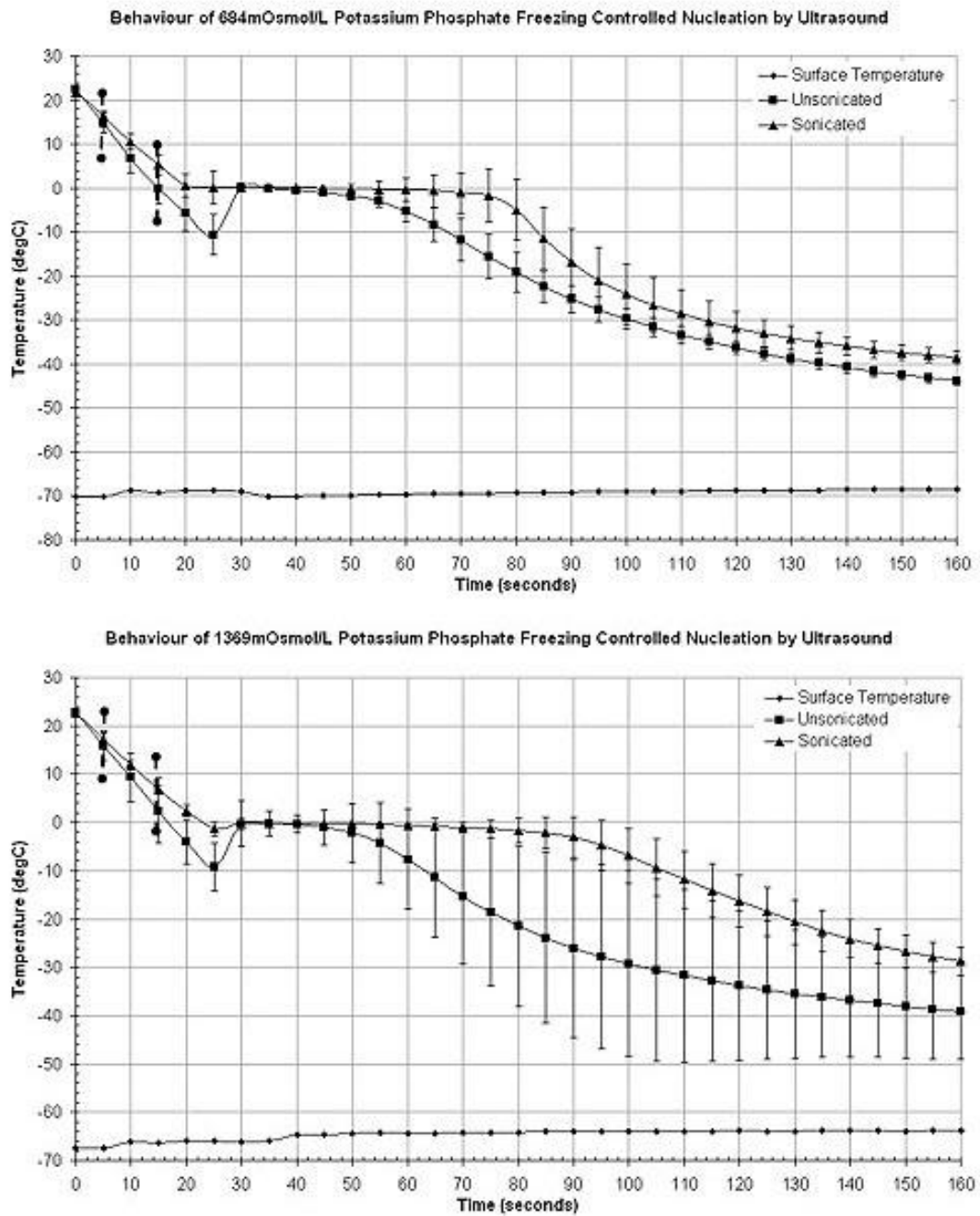
Figure 68. Temperature trace for 684mOsmol/L and 1369mOsmol/L Potassium Phosphate monobasic unsonicated and sonicated showing +/-SD, n=4. Vertical dotted lines indicate sonication times

APPENDIX 2: TABLES AND GRAPHS FOR INDIVIDUAL SALT SAMPLES

Calcium Chloride - % weight concentrations

Table 9. Mean nucleation temperatures for percentage weight concentrations of Calcium Chloride showing +/-SD values, n=4, * denotes statistical significance at P < 0.05.

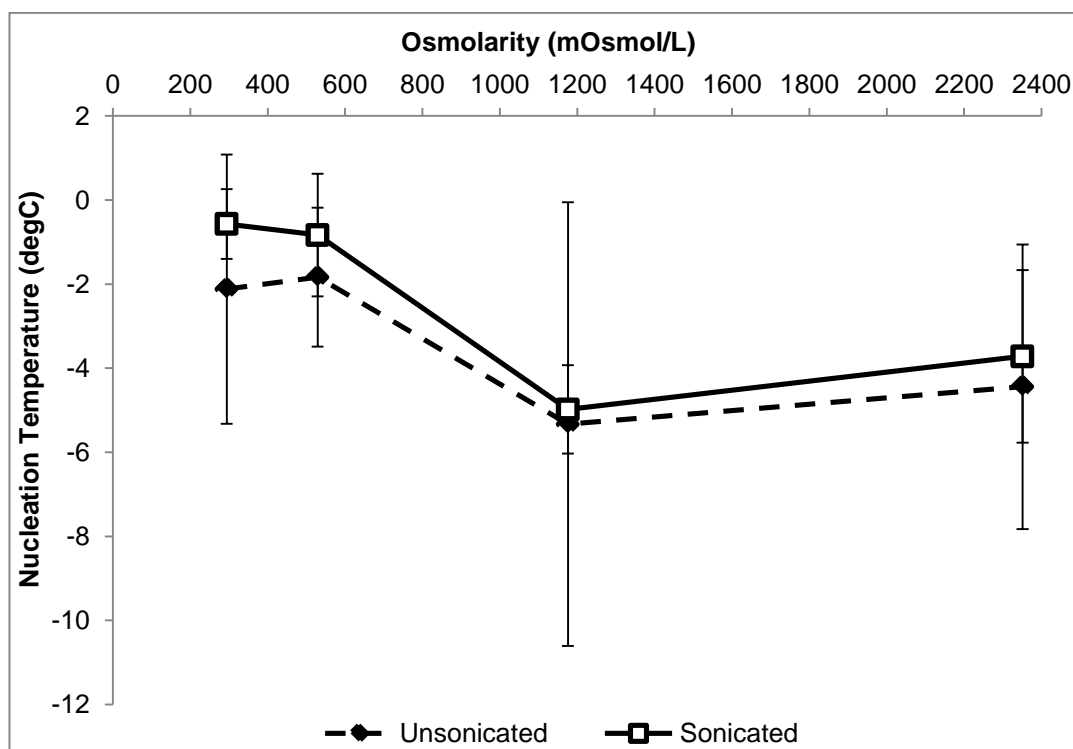| Concentration (%w/v)	Osmolarity (mOsmol/L)	Nucleation Temperature (degC, n=4)	
		Control	Sonicated
0.5	135	-7.27 ± 1.77	-4.13 ± 3.75
0.9	243	-5.59 ± 2.09	-3.68 ± 0.96
2	541	-9.78 ± 3.26	-9.38 ± 1.50
4	1081	-11.1 ± 1.79	-8.12 ± 1.44
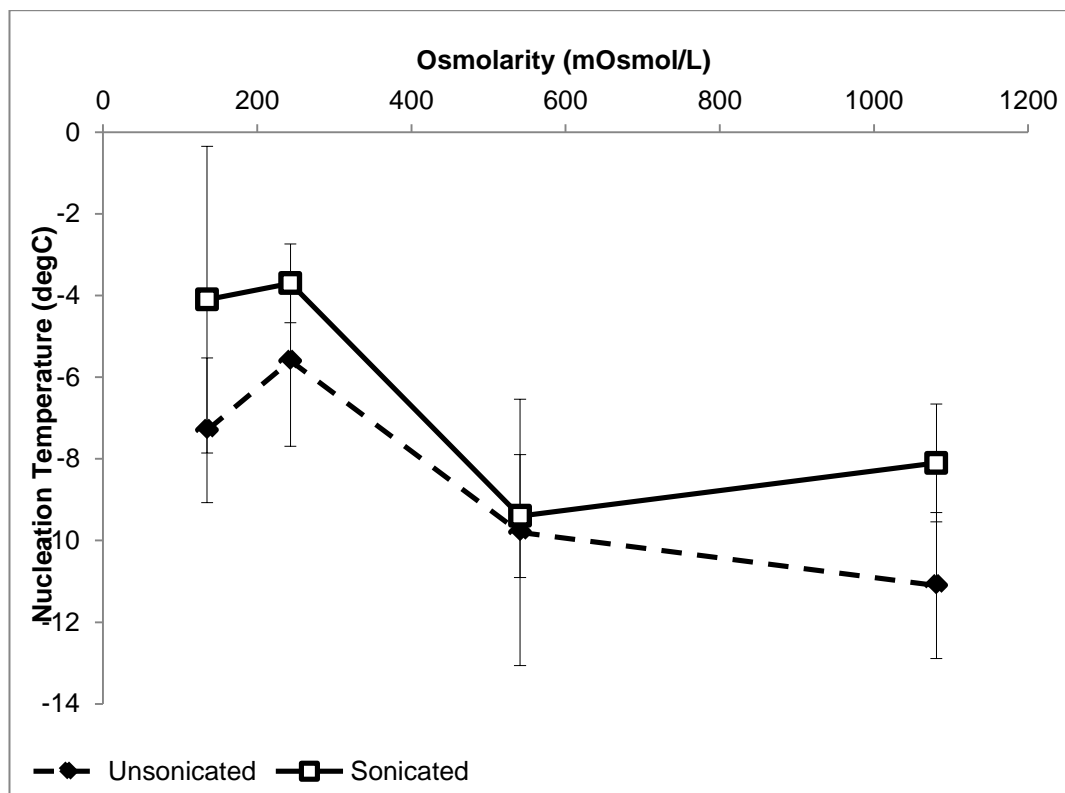
Figure 69. Graph showing mean nucleation temperatures for percentage weight concentrations of Calcium Chloride showing +/-SD values.

Calcium Chloride - osmolarity concentrations

Table 10. Mean nucleation temperatures for solute osmolarity concentrations of Calcium Chloride showing +/-SD values, n=4, * denotes statistical significance at P < 0.05.

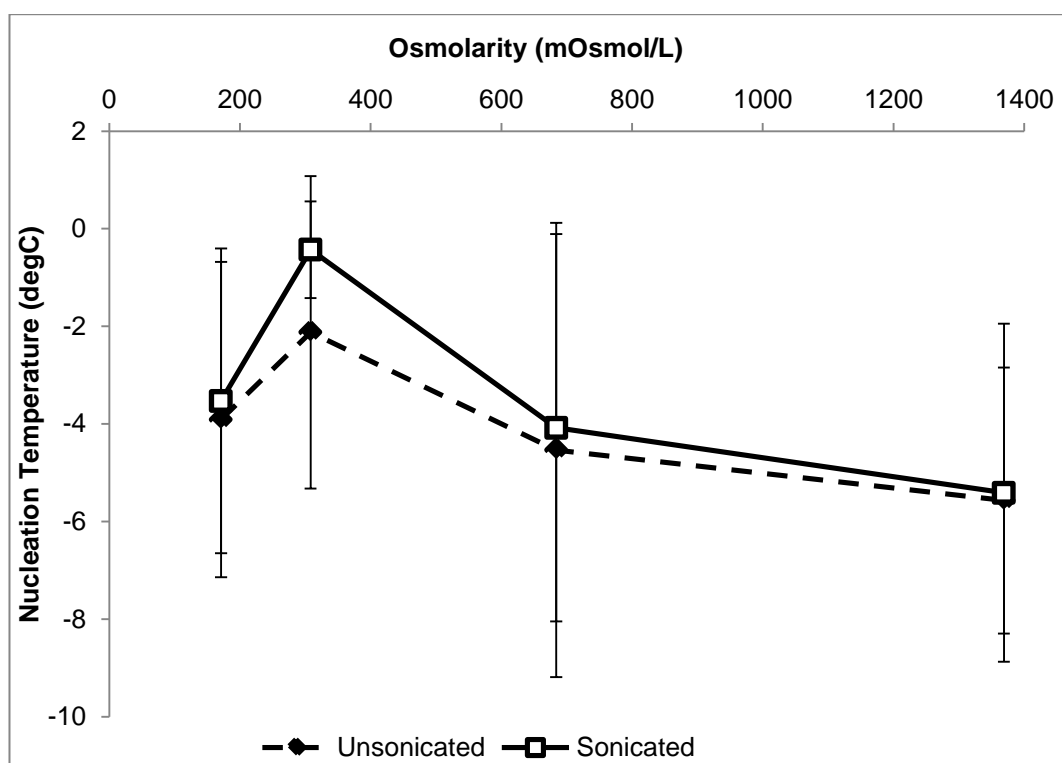| Concentration (%w/v)	Osmolarity (mOsmol/L)	Nucleation Temperature (degC, n=4)	
		Control	Sonicated
0.6	171	-5.39 ± 2.52	-1.23 ± 0.79
1.1	308	-10.5 ± 0.84	-4.17 ± 3.16
2.5	684	-6.51 ± 2.77	-1.90 ± 1.46
5.1	1369	-13.3 ± 2.54	-9.56 ± 4.28
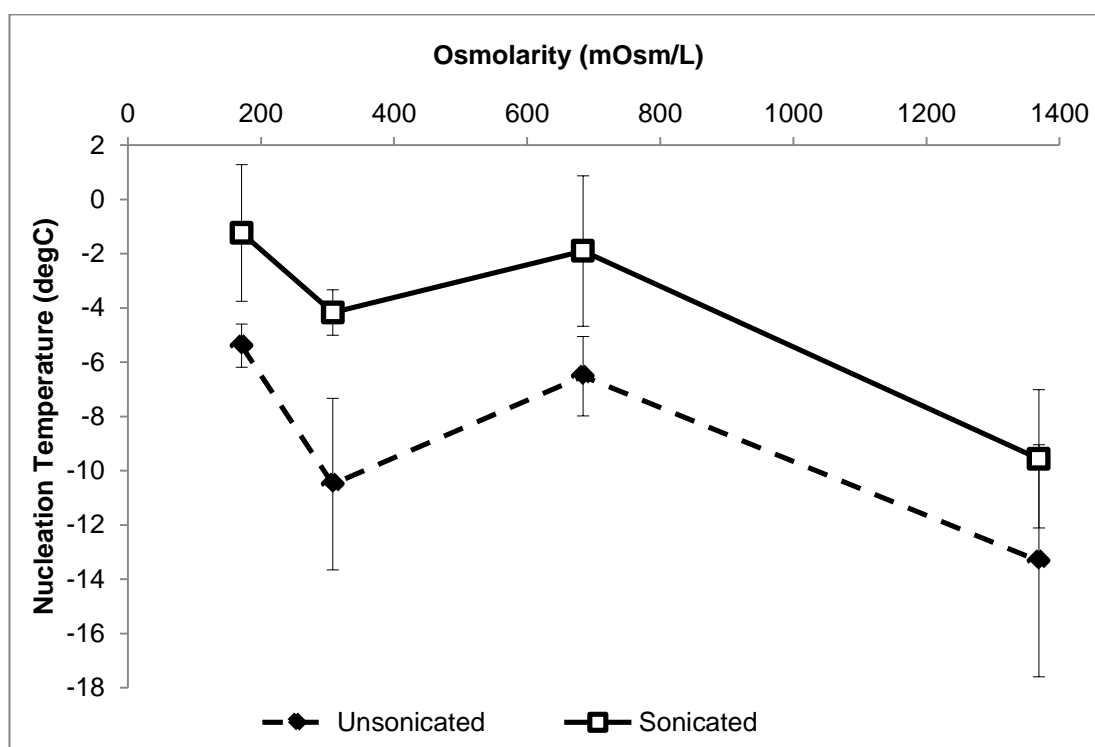
Figure 70. Graph showing mean nucleation temperatures for solute osmolarity concentrations of Calcium Chloride showing +/-SD values.

Magnesium Chloride - % weight concentrations

Table 11. Mean nucleation temperatures for percentage weight concentrations of Magnesium Chloride showing +/-SD values, n=4, * denotes statistical significance at P < 0.05.

Concentration (%w/v)	Osmolarity (mOsmol/L)	Nucleation Temperature (degC, n=4)	
		Control	Sonicated
0.5	158	-3.42 ± 2.00	-1.83 ± 0.98
0.9	284	-3.82 ± 1.09	-2.61 ± 2.13
2	630	-6.18 ± 1.33	-4.54 ± 2.66
4	1260	-8.50 ± 1.63	-7.86 ± 3.05
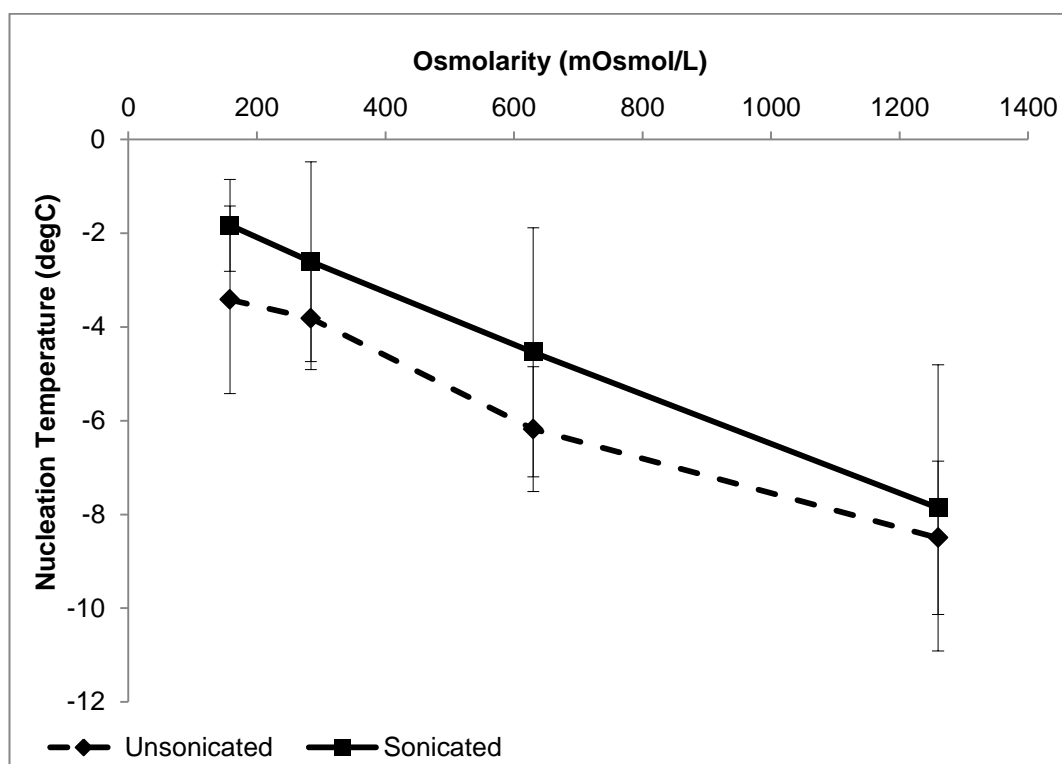
Figure 71. Graph showing mean nucleation temperatures for percentage weight concentrations of Magnesium Chloride showing +/-SD values.

Magnesium Chloride - osmolarity concentrations

Table 12. Mean nucleation temperatures for solute osmolarity concentrations of Magnesium Chloride showing +/-SD values, n=4, * denotes statistical significance at P < 0.05.

Concentration (%w/v)	Osmolarity (mOsmol/L)	Nucleation Temperature (degC, n=4)	
		Control	Sonicated
0.5	171	-3.42 ± 2.00	-1.83 ± 0.98
1.0	308	-4.41 ± 3.27	-4.51 ± 2.70
2.2	684	-7.97 ± 0.37	-6.54 ± 1.98
4.3	1369	-7.46 ± 4.30	-6.07 ± 2.60
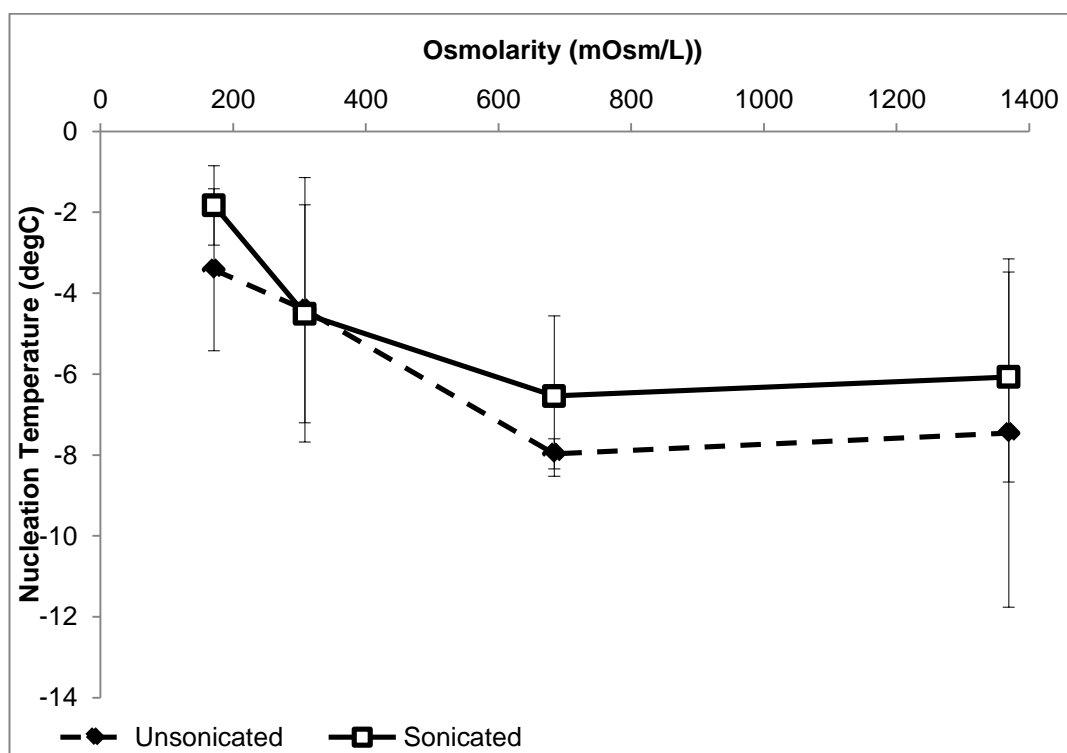
Figure 72. Graph showing mean nucleation temperatures for solute osmolarity concentrations of Magnesium Chloride showing +/-SD values.

Sodium Phosphate Monobasic - % weight concentrations

Table 13. Mean nucleation temperatures for percentage weight concentrations of Sodium Phosphate Monobasic showing +/-SD values, n=4, * denotes statistical significance at P < 0.05.

Concentration (%w/v)	Osmolarity (mOsmol/L)	Nucleation Temperature (degC, n=4)	
		Control	Sonicated
0.5	217	-4.38 ± 1.89	-1.80 ± 2.13
0.9	391	-3.40 ± 1.66	-1.62 ± 1.53
2	870	-3.20 ± 2.18	-0.96 ± 0.41
4	1739	-2.44 ± 1.55	-3.06 ± 0.57
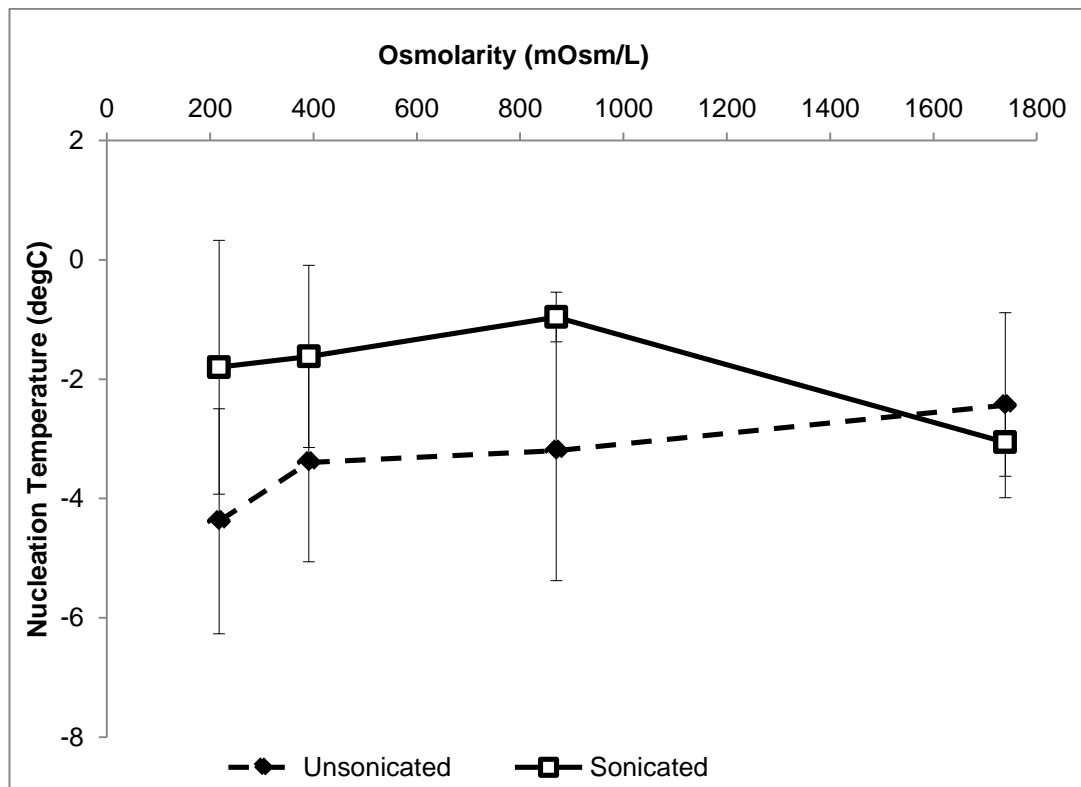
Figure 73. Graph showing mean nucleation temperatures for percentage weight concentrations of Sodium Phosphate Monobasic showing +/-SD values.

Sodium Phosphate Monobasic - osmolarity concentrations

Table 14. Mean nucleation temperatures for solute osmolarity concentrations of Sodium Phosphate Monobasic showing +/-SD values, n=4, * denotes statistical significance at P < 0.05.

Concentration (%w/v)	Osmolarity (mOsmol/L)	Nucleation Temperature (degC, n=4)	
		Control	Sonicated
0.3	171	-3.27 ± 1.19	-1.00 ± 1.35
0.5	308	-4.38 ± 1.89	-1.80 ± 2.13
1.2	684	-4.85 ± 2.43	-4.76 ± 2.60
2.4	1369	-4.07 ± 0.52	-1.33 ± 1.13
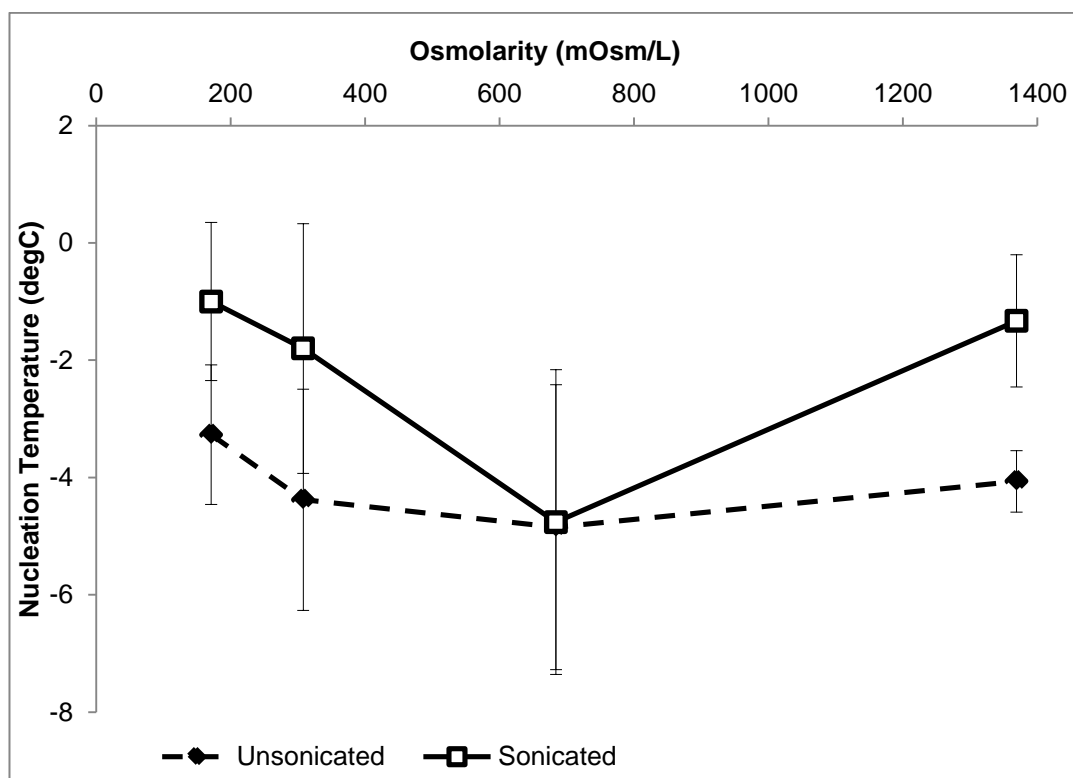
Figure 74. Graph showing mean nucleation temperatures for solute osmolarity concentrations of Magnesium Chloride showing +/-SD values.

171

Potassium Phosphate Monobasic - % weight concentrations

Table 15. Mean nucleation temperatures for percentage weight concentrations of Potassium Phosphate Monobasic showing +/-SD values, n=4, * denotes statistical significance at P < 0.05.

Concentration (%w/v)	Osmolarity (mOsmol/L)	Nucleation Temperature (degC, n=4)	
		Unsonicated	Sonicated
0.5	220	-2.12 ± 0.20	-0.57 ± 0.83
0.9	397	-1.84 ± 1.65	-0.83 ± 1.46
2	882	-5.33 ± 5.28	-4.98 ± 1.05
4	1764	-4.44 ± 3.39	-3.72 ± 2.05

Figure 75. Graph showing mean nucleation temperatures for percentage weight concentrations of Potassium Phosphate Monobasic showing +/-SD values, n=4.

Potassium Phosphate Monobasic - osmolarity concentrations

Table 16. Mean nucleation temperatures for solute osmolarity concentrations of Potassium Phosphate Monobasic showing +/-SD values, n=4, * denotes statistical significance at P < 0.05.

Concentration (%w/v)	Osmolarity (mOsmol/L)	Nucleation Temperature (degC, n=4)	
		Unsonicated	Sonicated
0.3	171	-3.91 ± 3.23	-3.53 ± 3.12
0.5	308	-2.12 ± 3.20	-0.43 ± 0.99
1.2	684	-4.54 ± 4.65	-4.08 ± 3.97
2.3	1369	-5.57 ± 2.73	-5.41 ± 1.06

Figure 76. Graph showing mean nucleation temperatures for solute osmolarity concentrations of Magnesium Chloride showing +/-SD values.

APPENDIX 3: DSC TRACES

174

Method 1 – DSC Traces
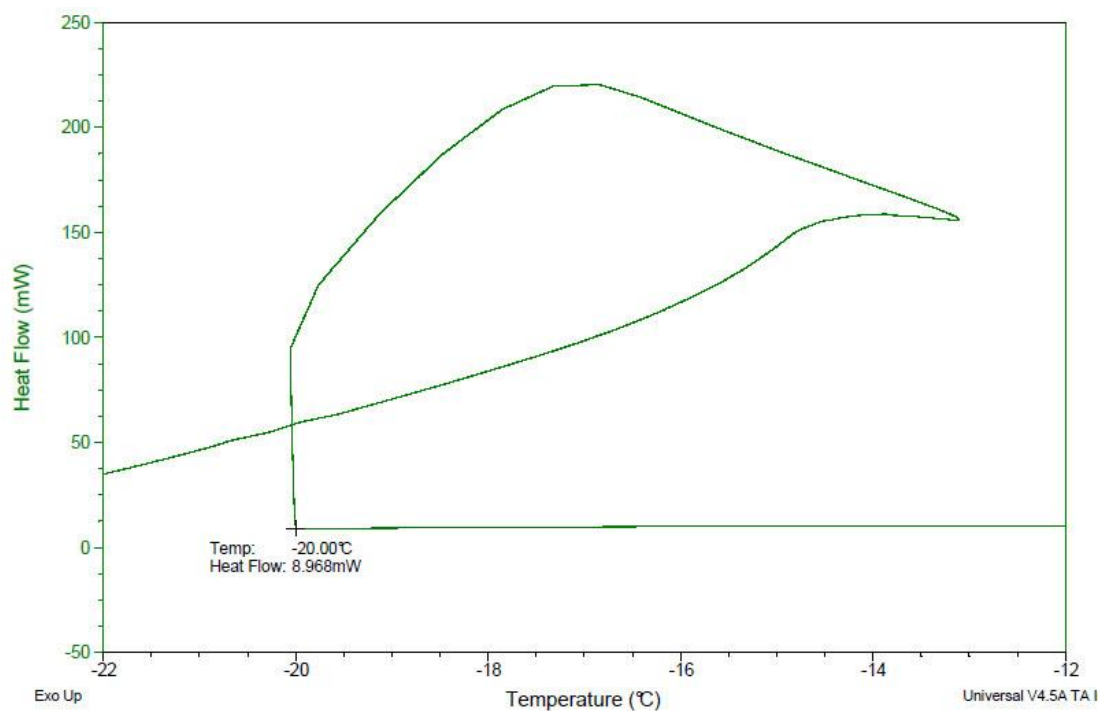
Figure 77. Freezing profile for 30 µl of pure water sealed in an aluminium pan and cooled from 35°C to -30°C at a rate of 10°C/min. Analysis was carried out by reading off temperature at which a sharp rise in heat flow occurred.
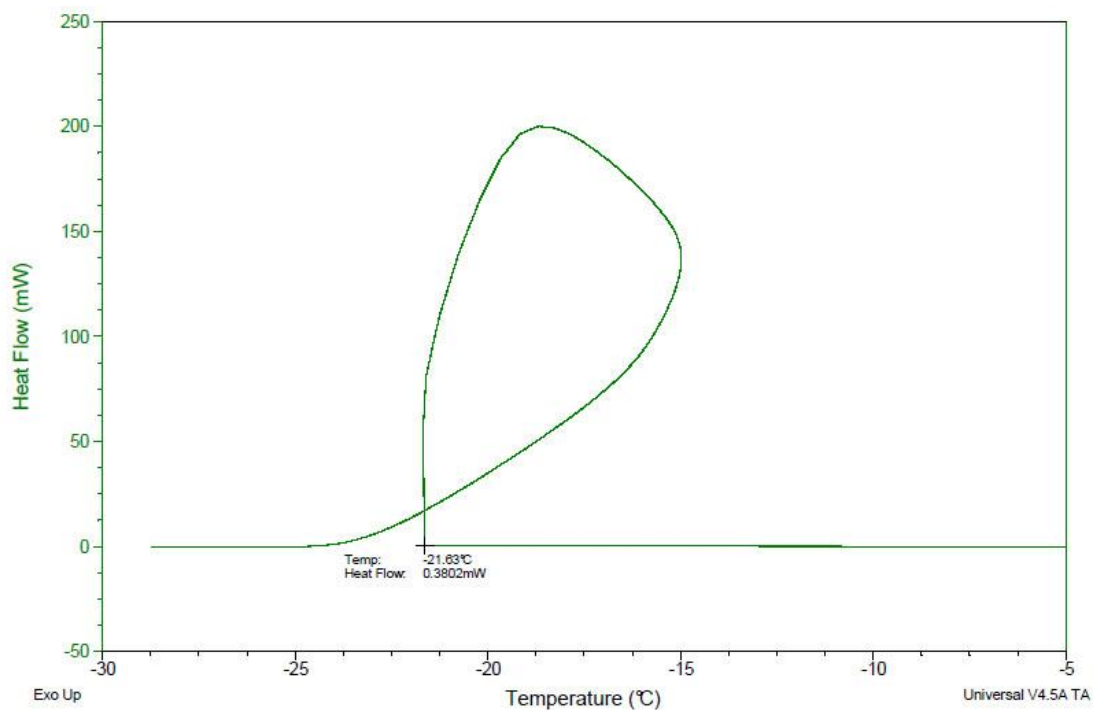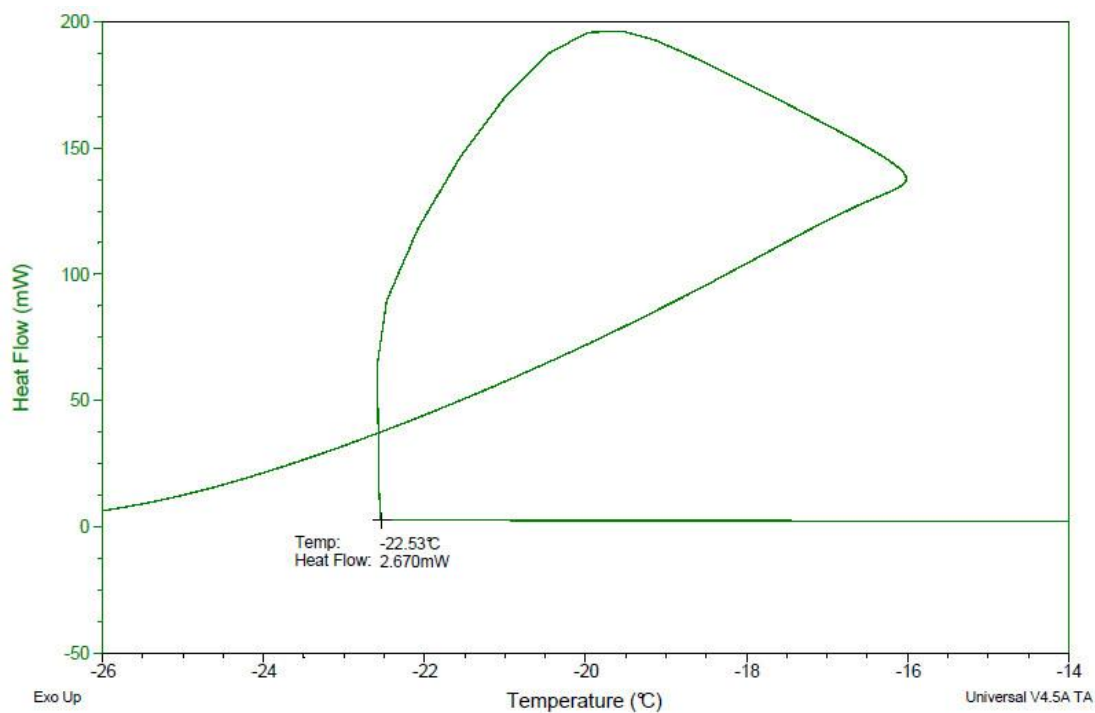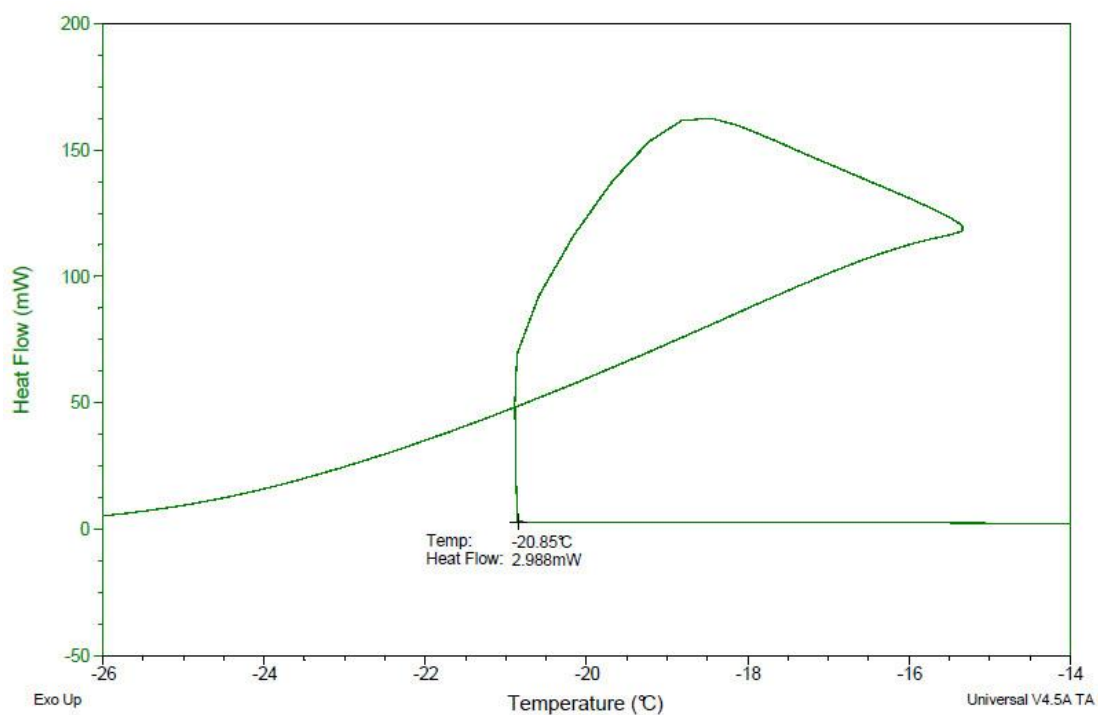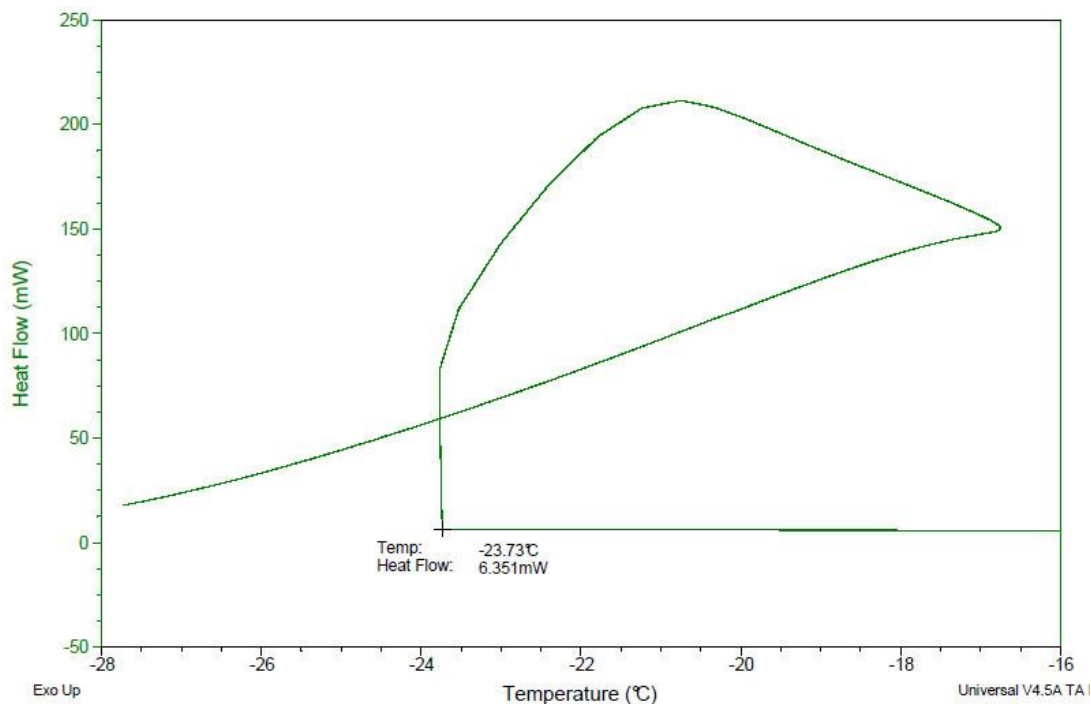

Figure 78. Freezing profile for 30 µl of pure water sealed in an aluminium pan and cooled from 35°C to -30°C at a rate of 5°C/min. Analysis was carried out by reading off temperature at which a sharp rise in heat flow occurred.
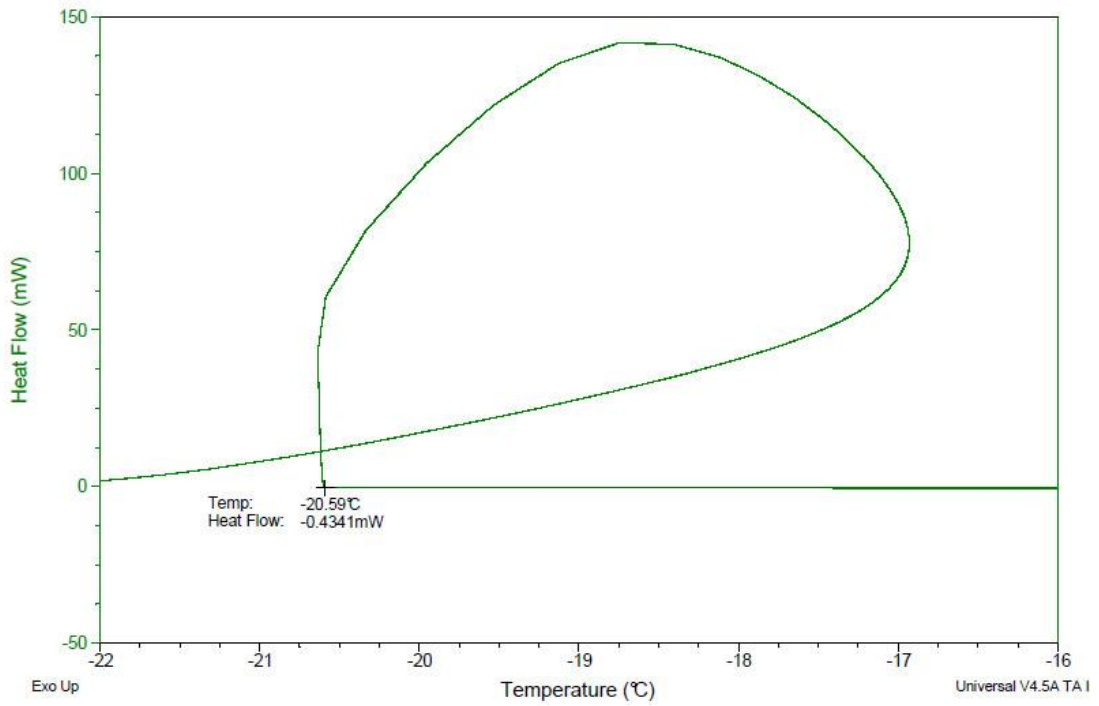
Figure 79. Freezing profile for 30 µl of pure water sealed in an aluminium pan and cooled from 35°C to -30°C at a rate of 5°C/min. Analysis was carried out by reading off temperature at which a sharp rise in heat flow occurred.
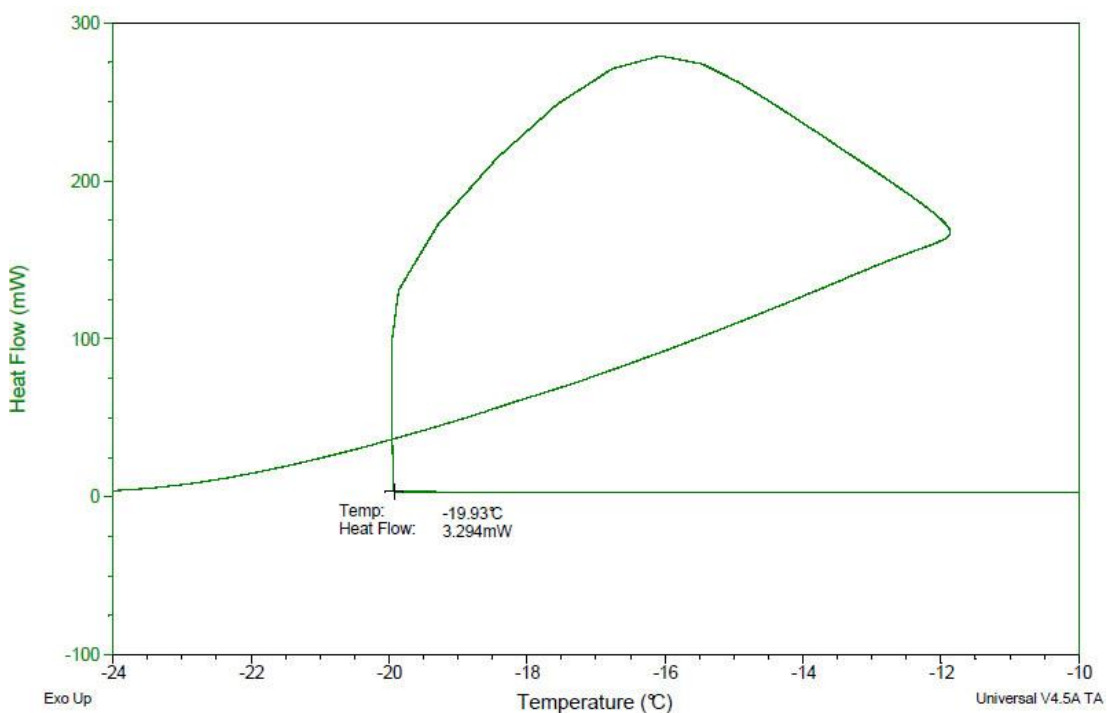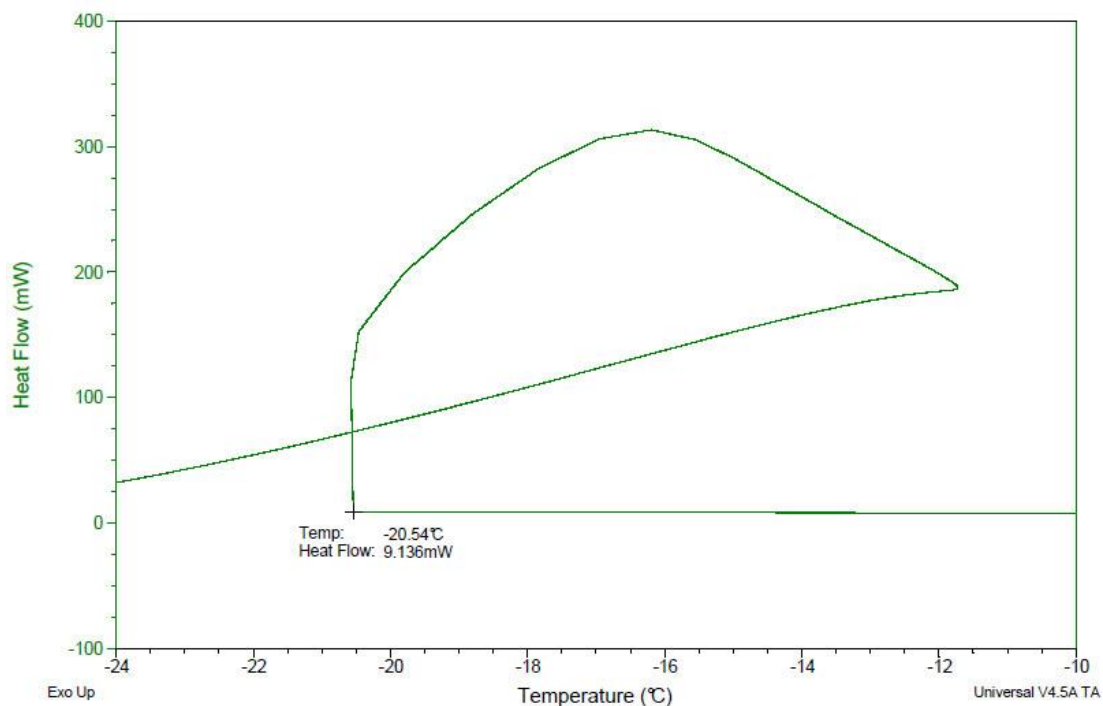

Method 2 – DSC Traces
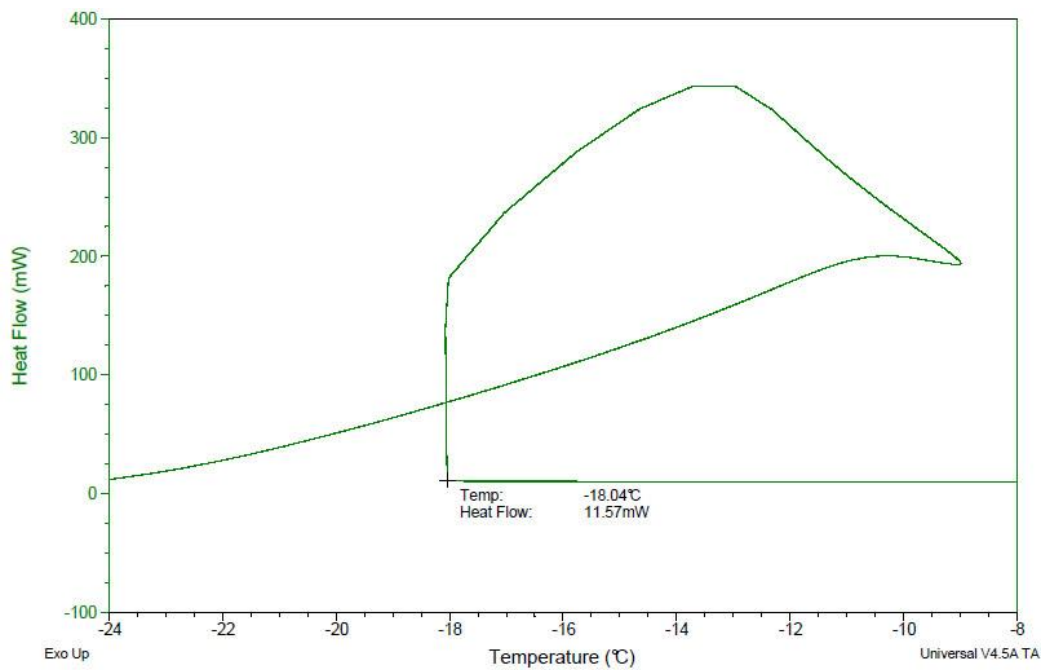
Figure 80. Freezing profile for 30 µl of 0.1 mol/kg Sodium Chloride sealed in an aluminium pan and cooled from 35°C to -30°C at a rate of 5°C/min. Analysis was carried out by reading off temperature at which a sharp rise in heat flow occurred.
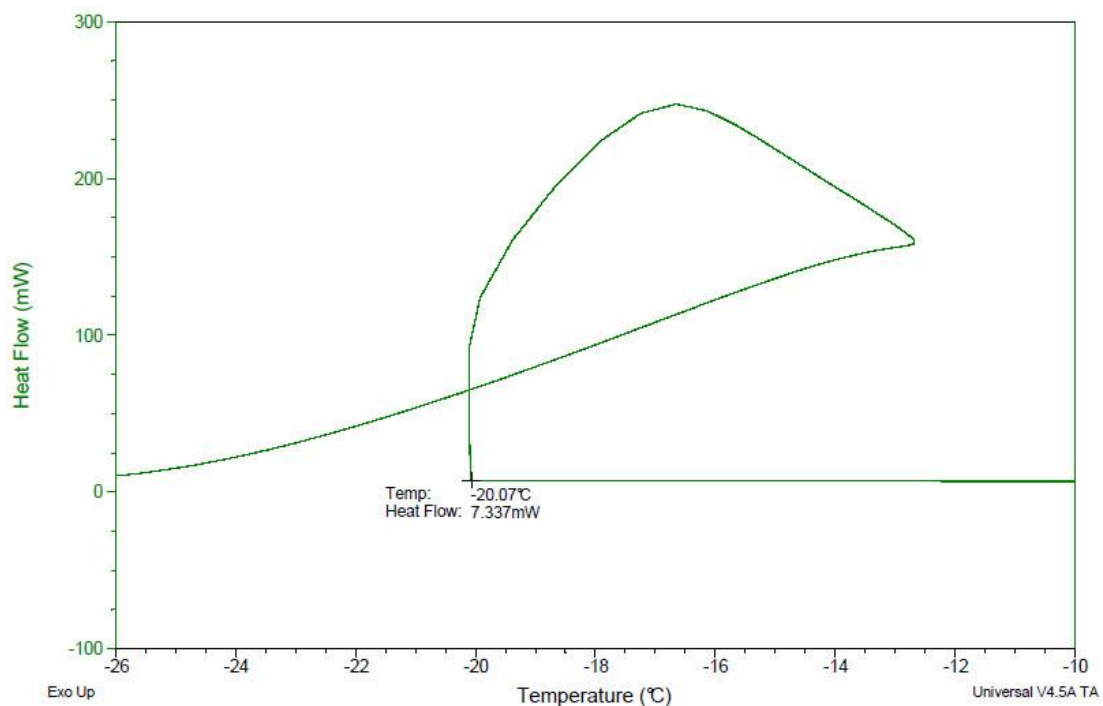
0.154 mol/kg Sodium Chloride Solution
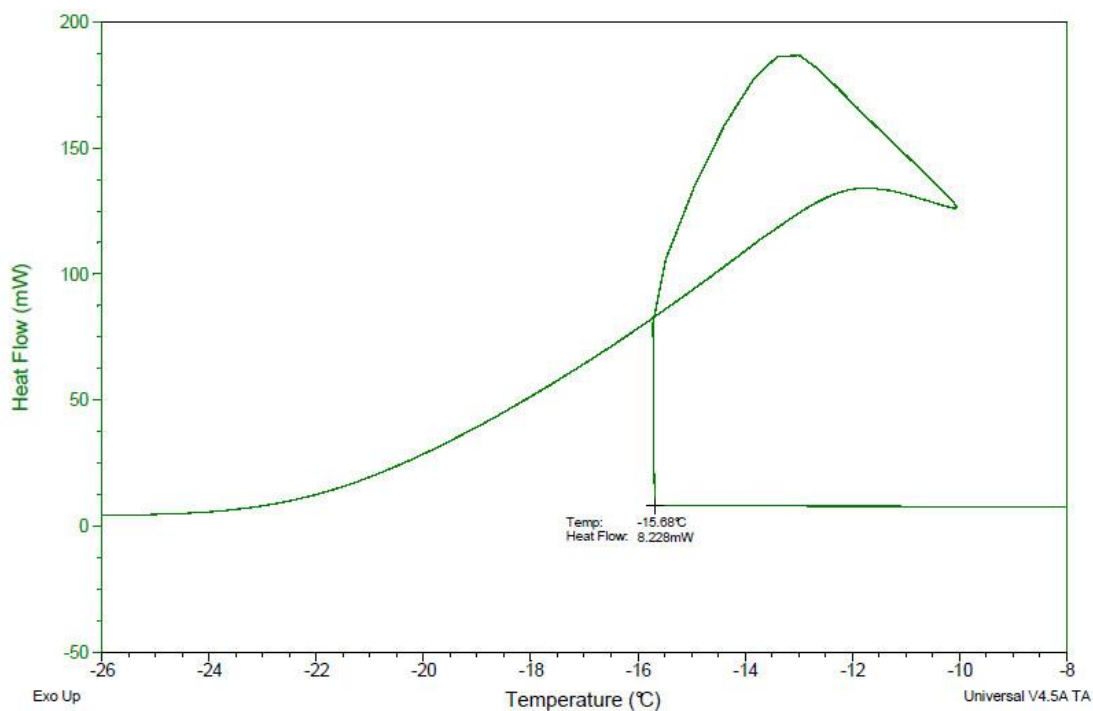
Figure 81. Freezing profile for 30 µl of 0.154 mol/kg Sodium Chloride sealed in an aluminium pan and cooled from 35°C to -30°C at a rate of 5°C/min. Analysis was carried out by reading off temperature at which a sharp rise in heat flow occurred.
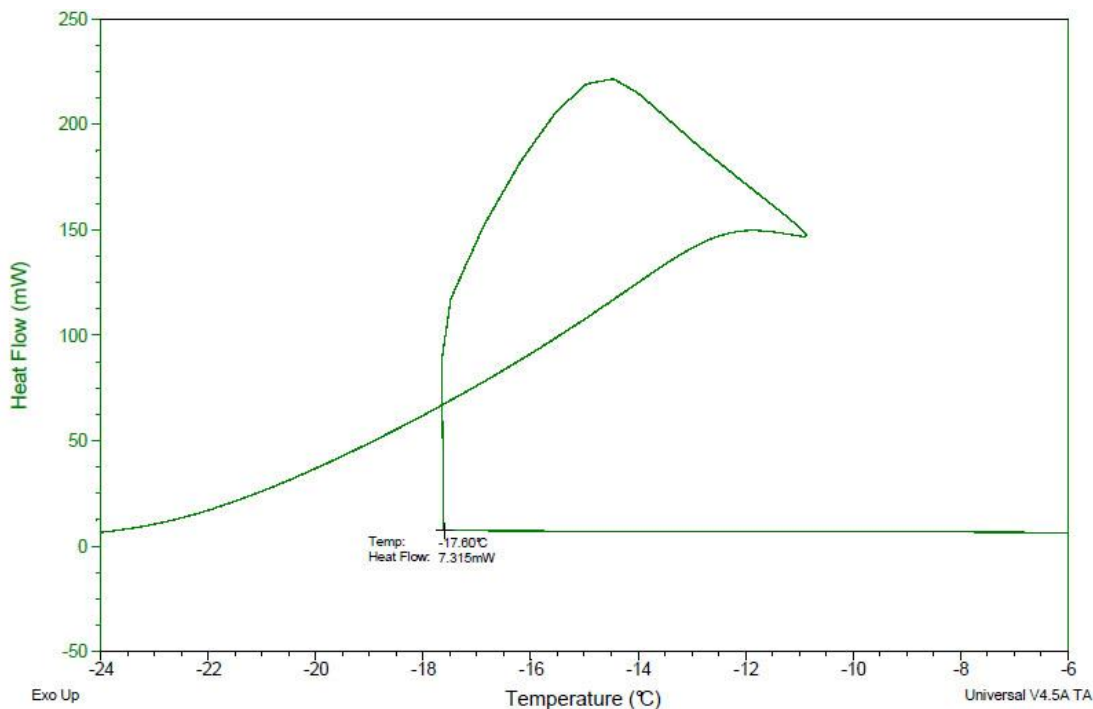
Figure 82. Freezing profile for 30 µl of 0.154 mol/kg Sodium Chloride sealed in an aluminium pan and cooled from 35°C to -30°C at a rate of 5°C/min. Analysis was carried out by reading off temperature at which a sharp rise in heat flow occurred.
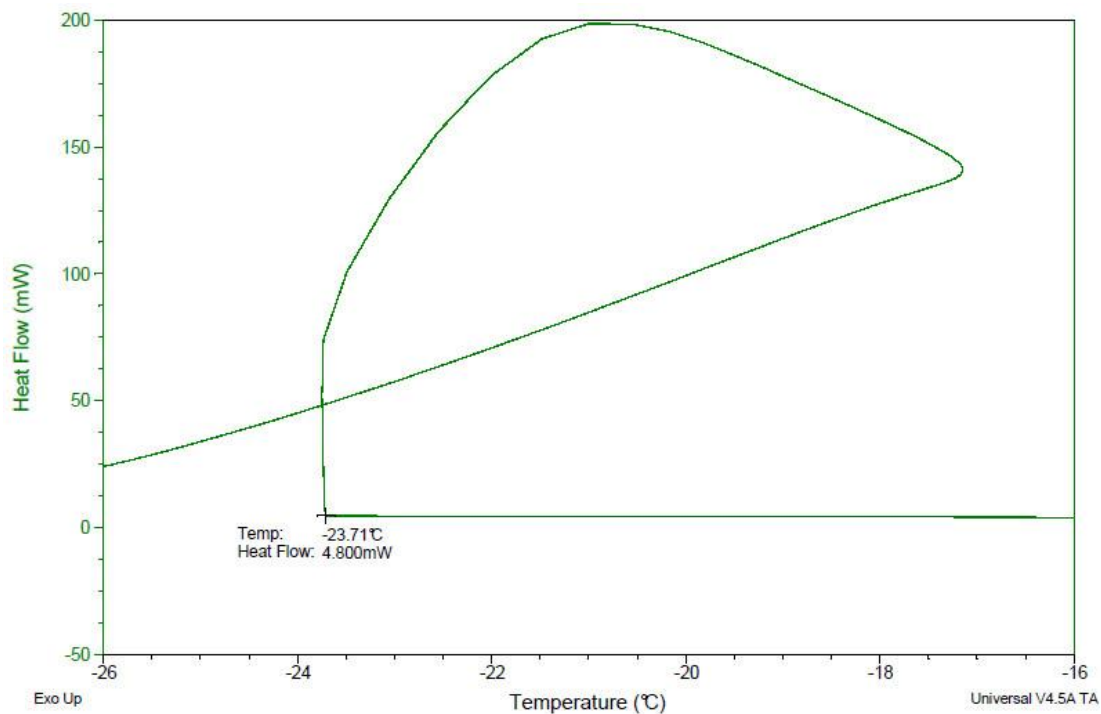
0.2 mol/kg Sodium Chloride Solution
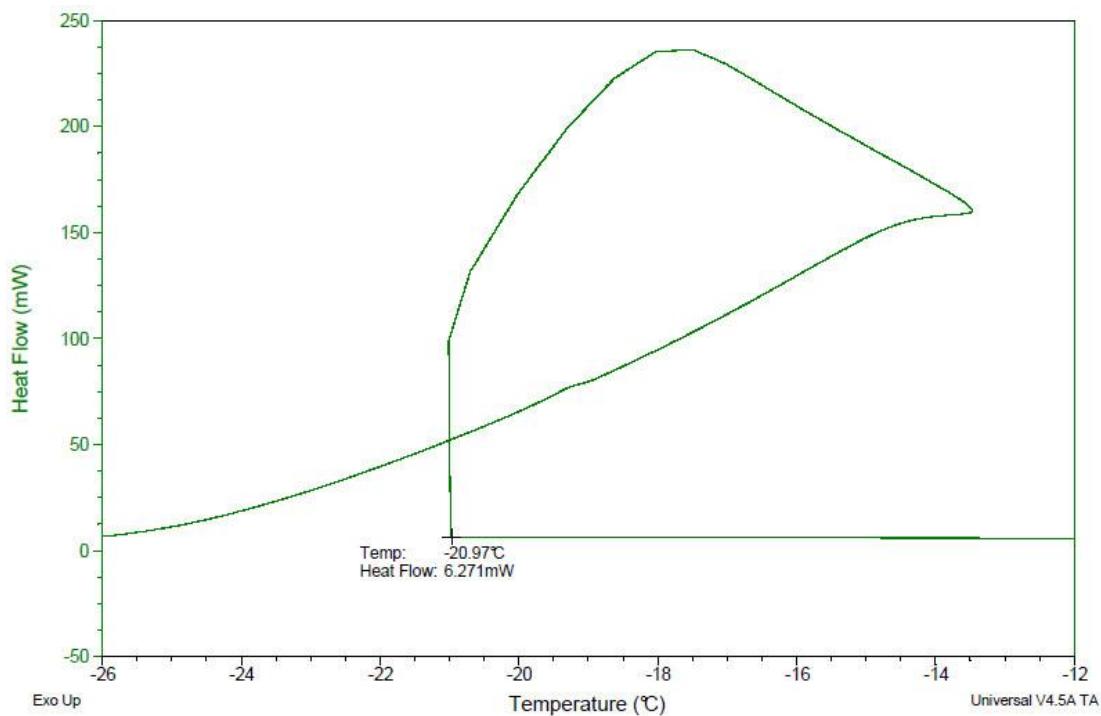
Figure 83. Freezing profile for 30 µl of 0.2 mol/kg Sodium Chloride sealed in an aluminium pan and cooled from 35°C to -30°C at a rate of 5°C/min. Analysis was carried out by reading off temperature at which a sharp rise in heat flow occurred.
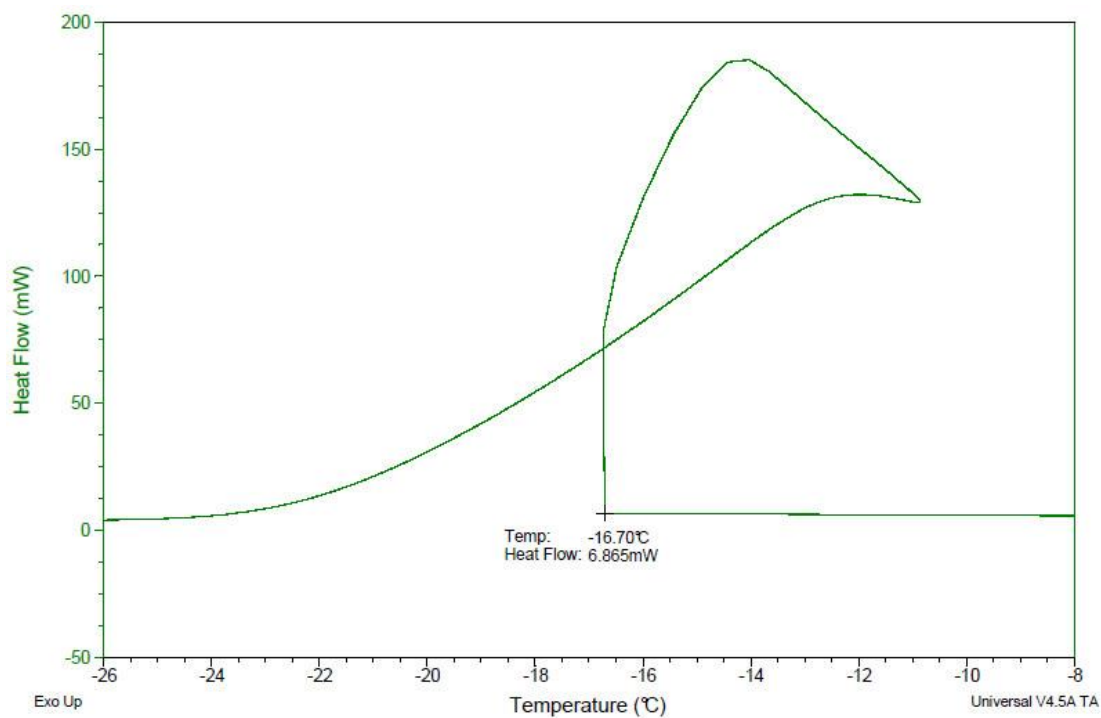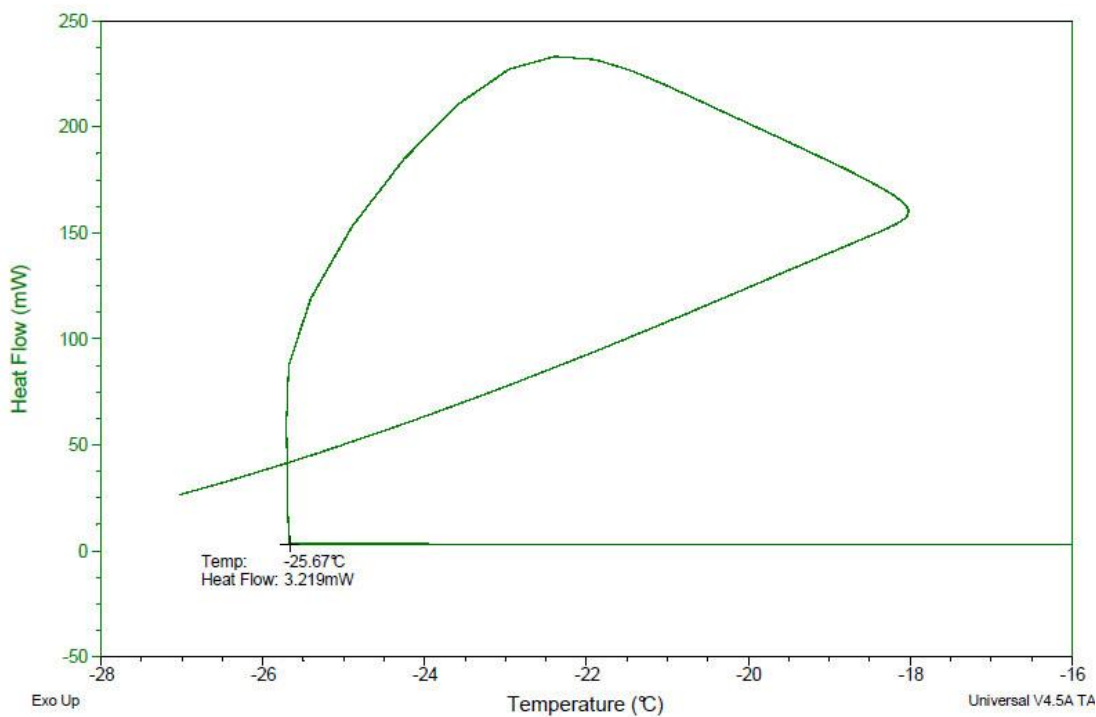

Figure 84. Freezing profile for 30 µl of 0.2 mol/kg Sodium Chloride sealed in an aluminium pan and cooled from 35°C to -30°C at a rate of 5°C/min. Analysis was carried out by reading off temperature at which a sharp rise in heat flow occurred.
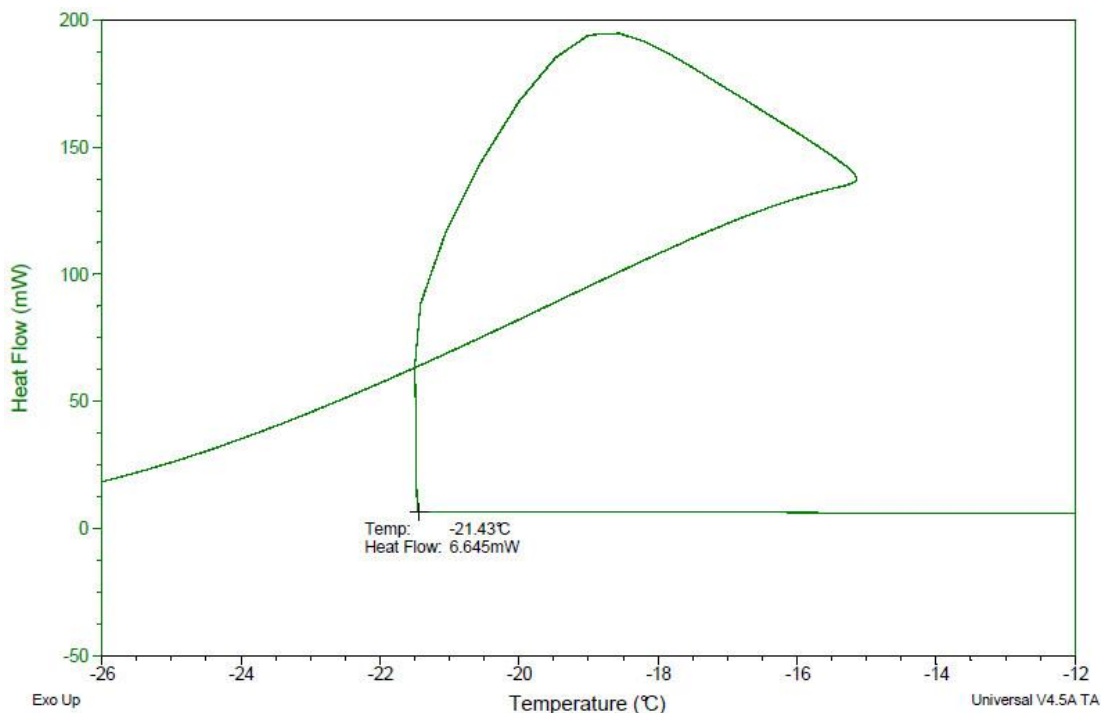
0.3 mol/kg Sodium Chloride Solution
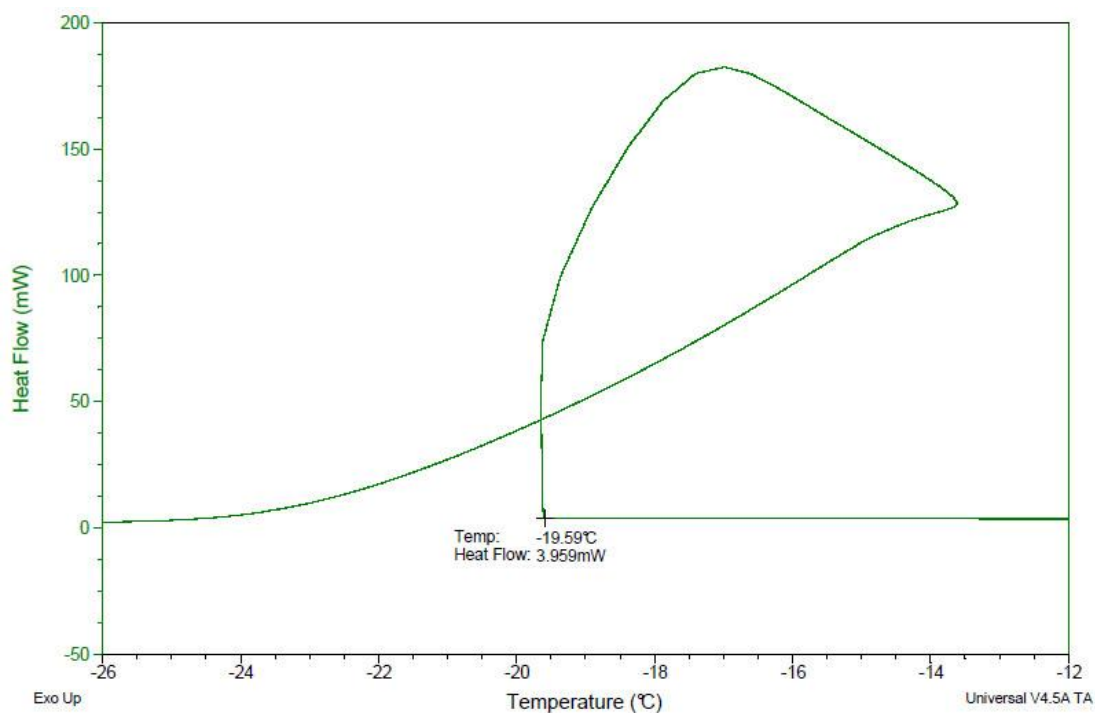
Figure 85. Freezing profile for 30 µl of 0.3 mol/kg Sodium Chloride sealed in an aluminium pan and cooled from 35°C to -30°C at a rate of 5°C/min. Analysis was carried out by reading off temperature at which a sharp rise in heat flow occurred.
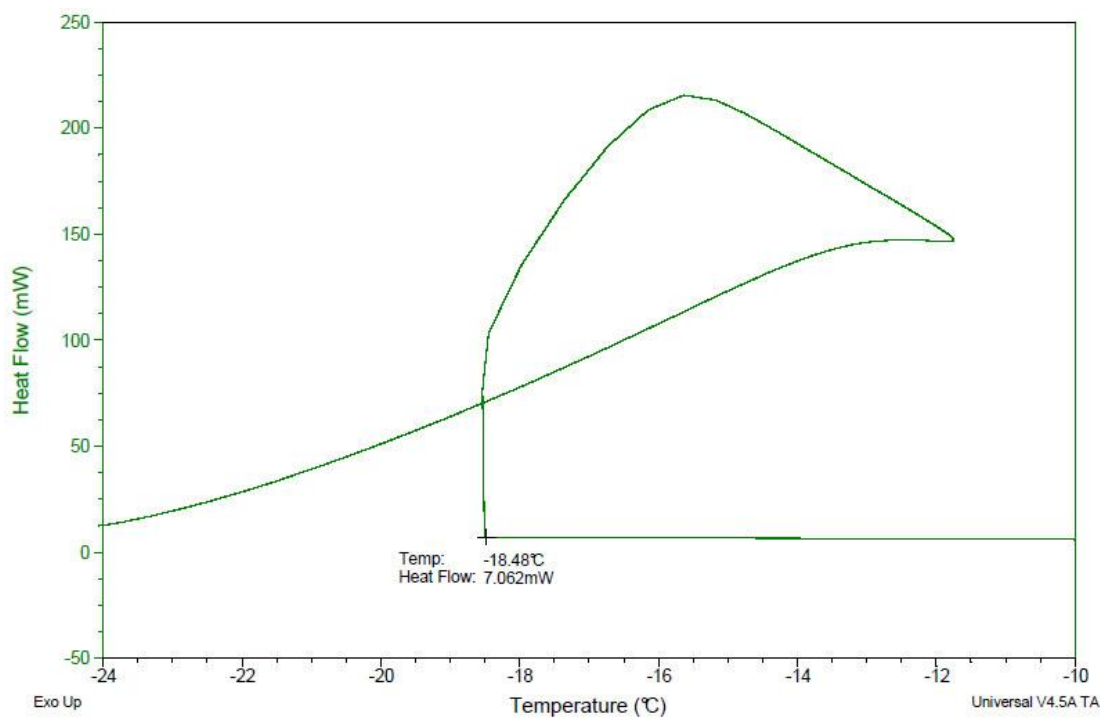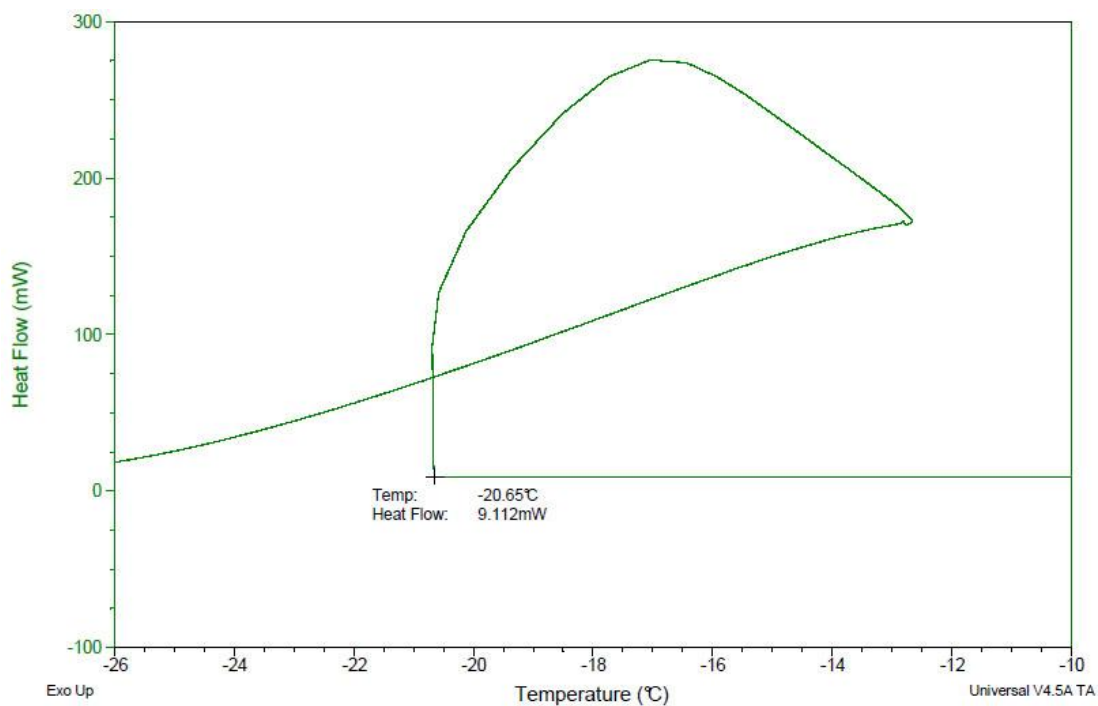

Figure 86. Freezing profile for 30 µl of 0.3 mol/kg Sodium Chloride sealed in an aluminium pan and cooled from 35°C to -30°C at a rate of 5°C/min. Analysis was carried out by reading off temperature at which a sharp rise in heat flow occurred.
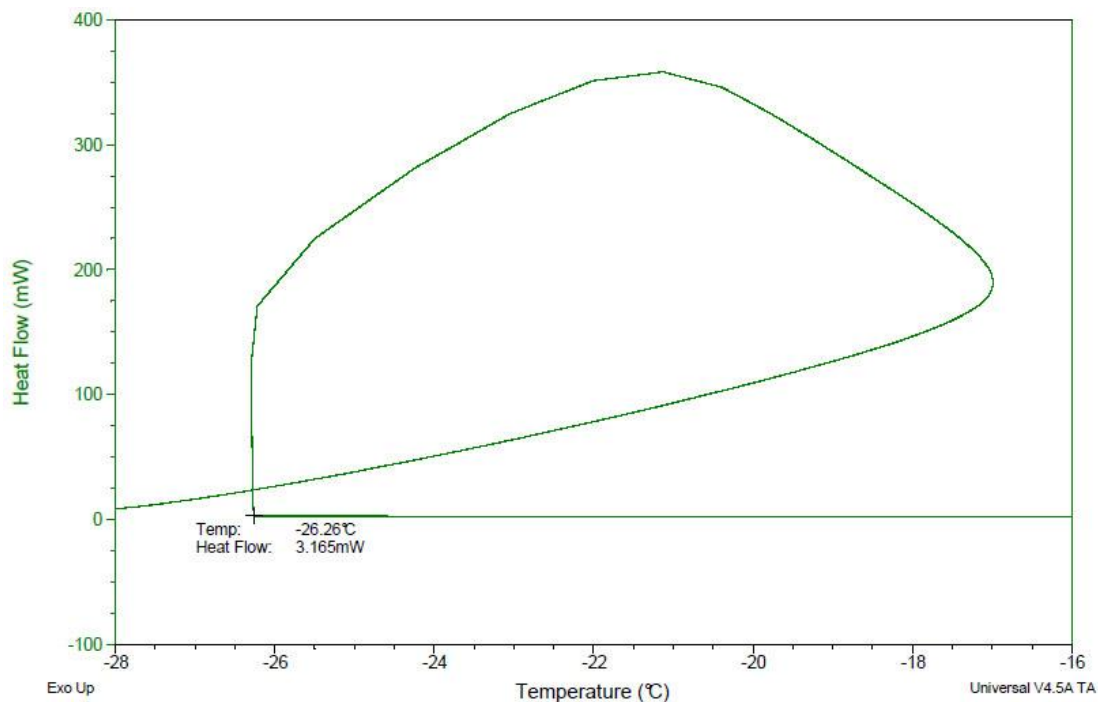
179

0.4 mol/kg Sodium Chloride Solution
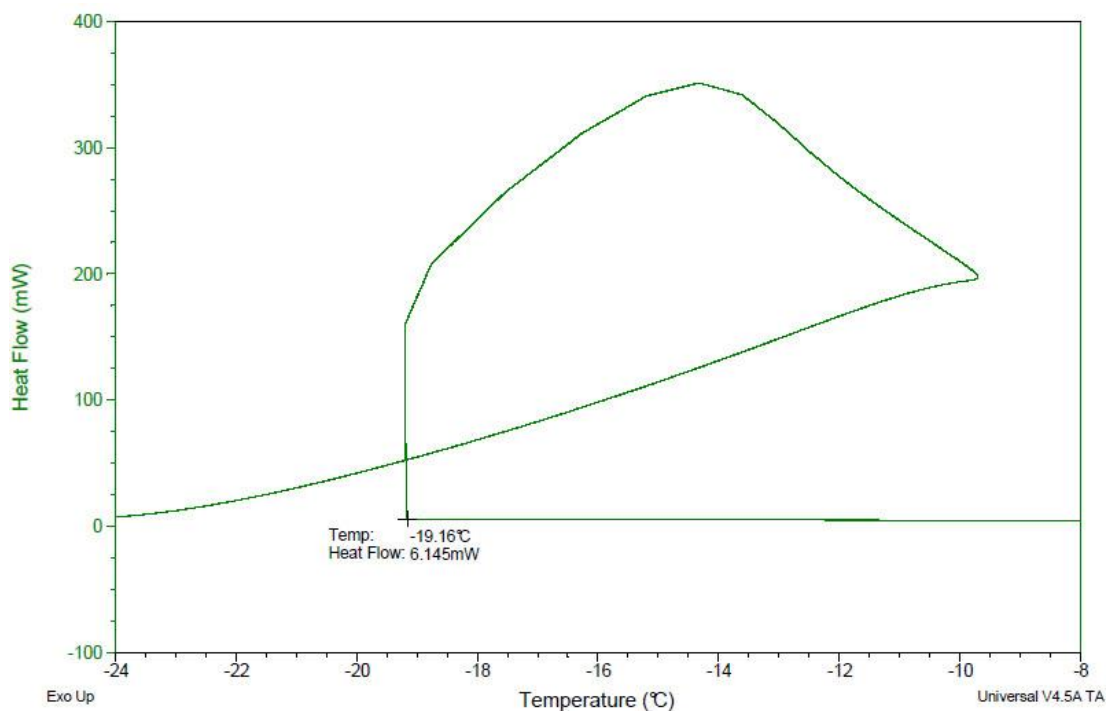
Figure 87. Freezing profile for 30 µl of 0.4 mol/kg Sodium Chloride sealed in an aluminium pan and cooled from 35°C to -30°C at a rate of 5°C/min. Analysis was carried out by reading off temperature at which a sharp rise in heat flow occurred.
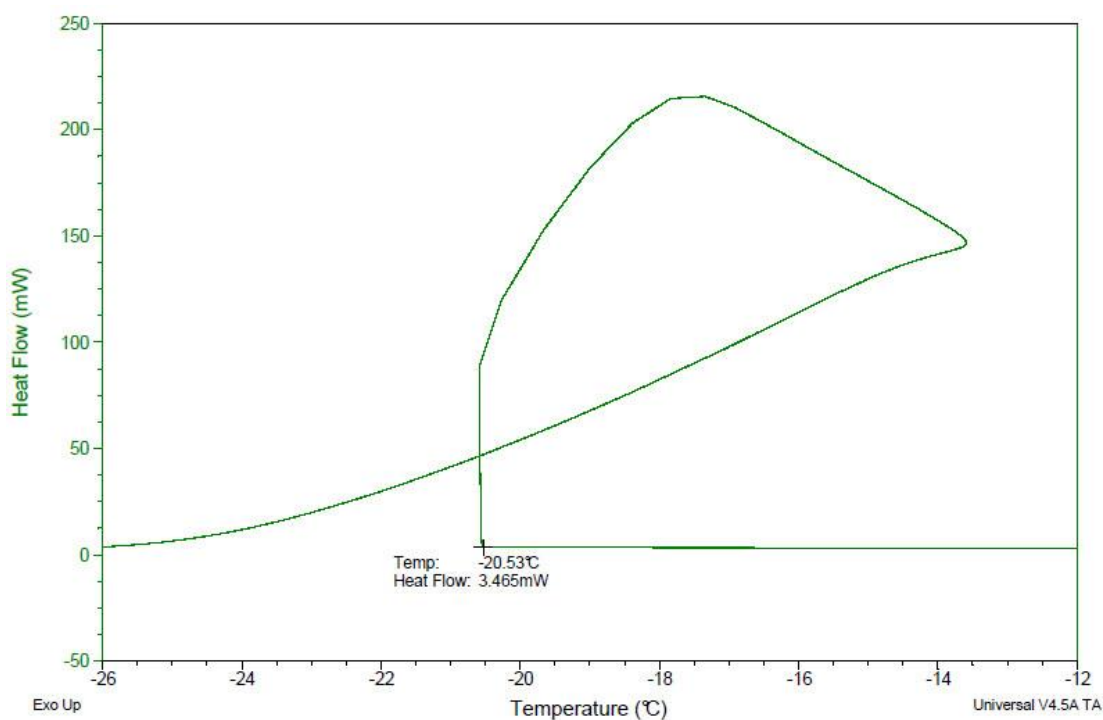
Figure 88. Freezing profile for 30 µl of 0.4 mol/kg Sodium Chloride sealed in an aluminium pan and cooled from 35°C to -30°C at a rate of 5°C/min. Analysis was carried out by reading off temperature at which a sharp rise in heat flow occurred.
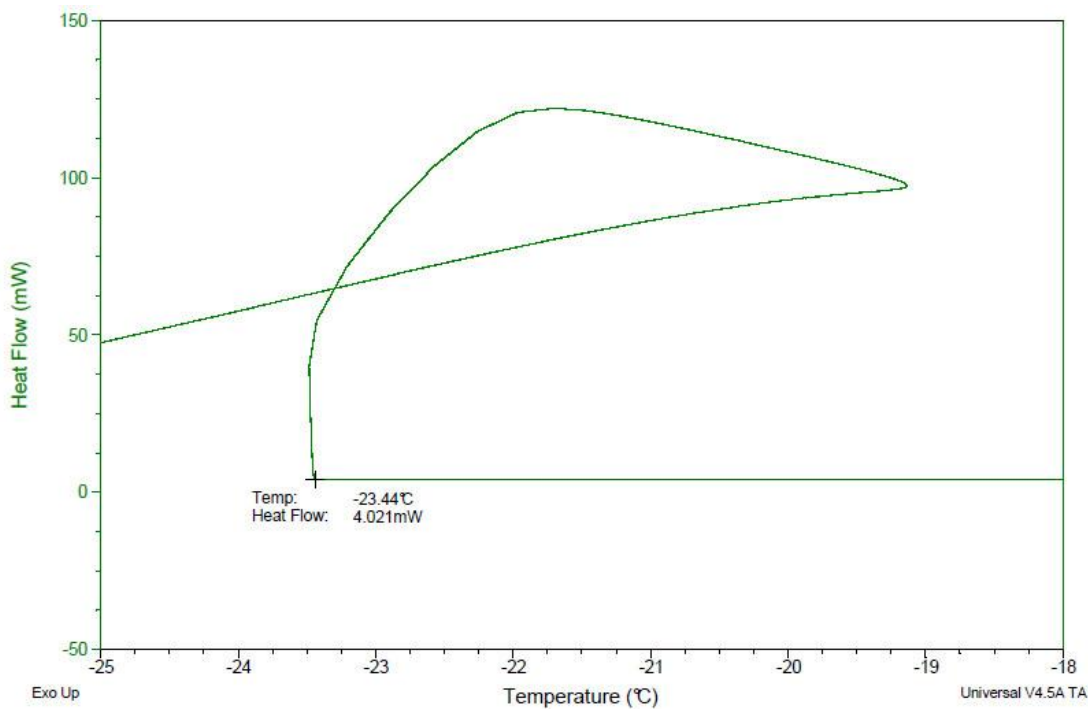
0.5 mol/kg Sodium Chloride Solution

Figure 89. Freezing profile for 30 μl of 0.5 mol/kg Sodium Chloride sealed in an aluminium pan and cooled from 35°C to -30°C at a rate of 5°C/min. Analysis was carried out by reading off temperature at which a sharp rise in heat flow occurred.

Figure 90. Freezing profile for 30 μl of 0.5 mol/kg Sodium Chloride sealed in an aluminium pan and cooled from 35°C to -30°C at a rate of 5°C/min. Analysis was carried out by reading off temperature at which a sharp rise in heat flow occurred.
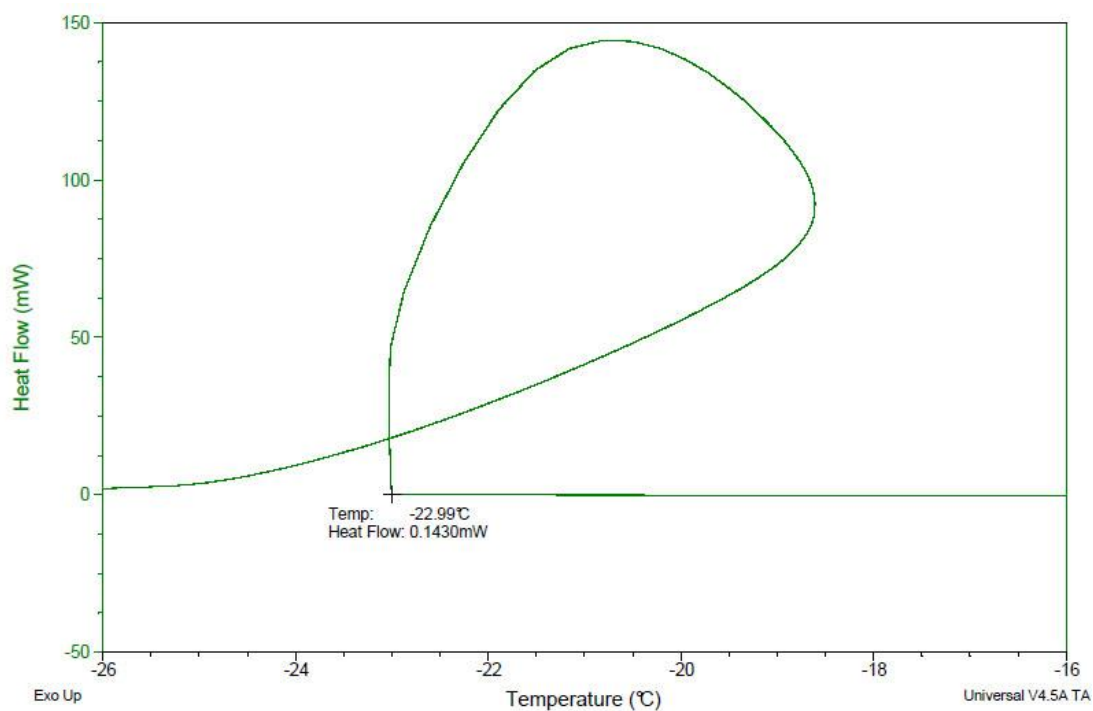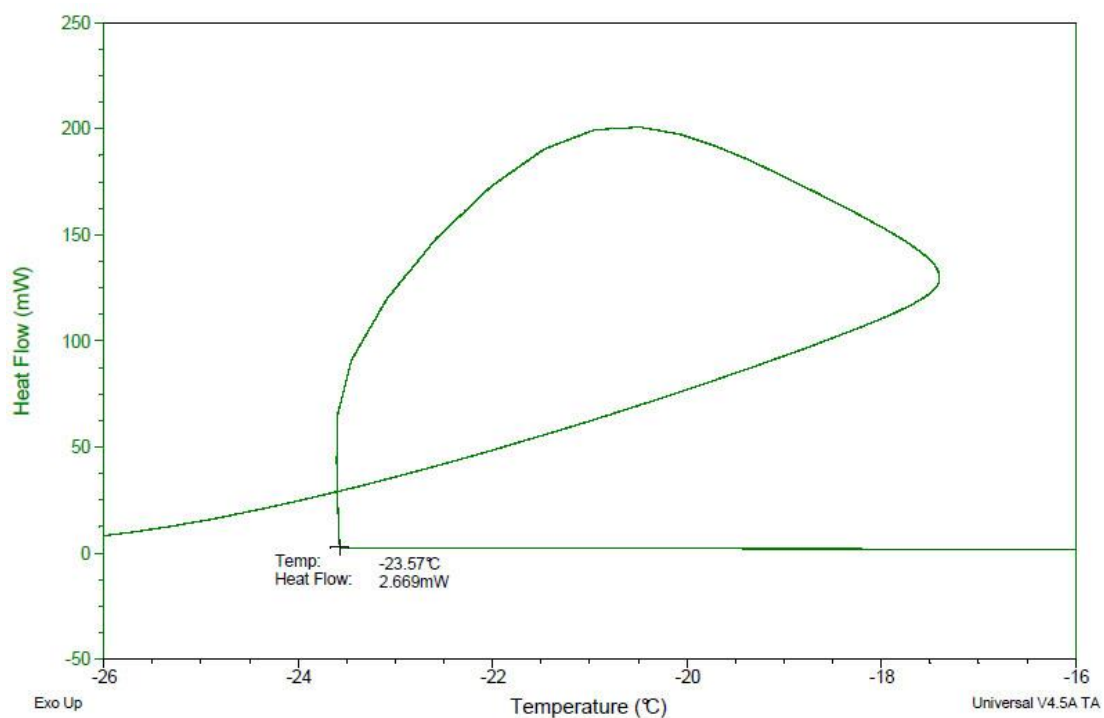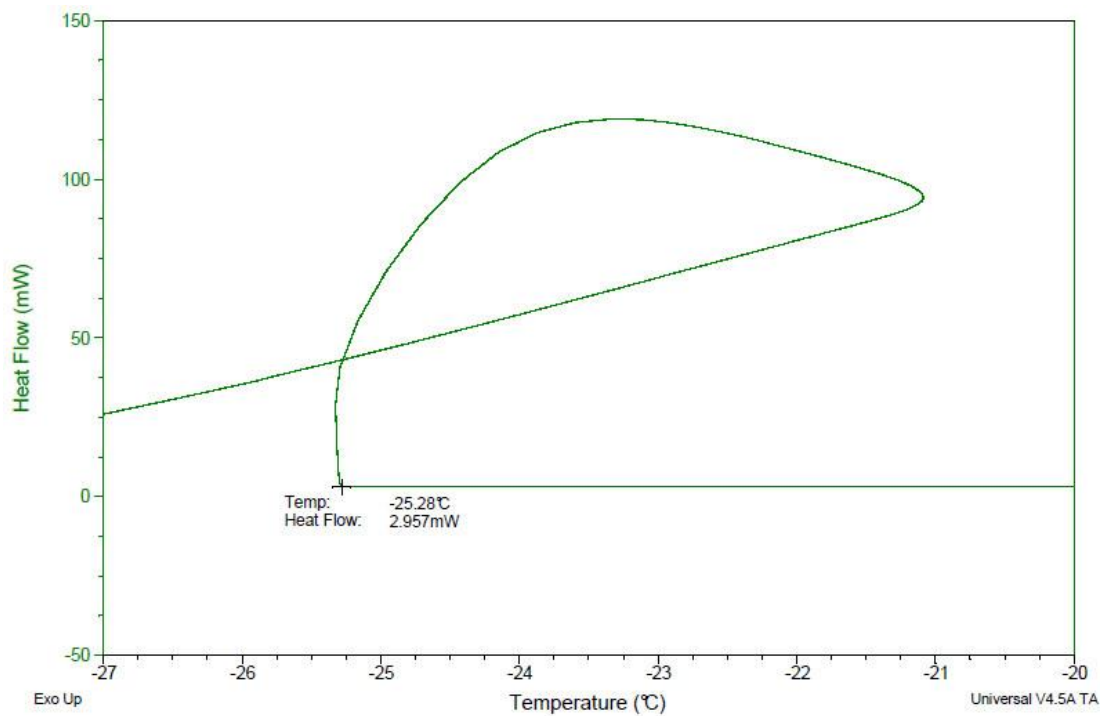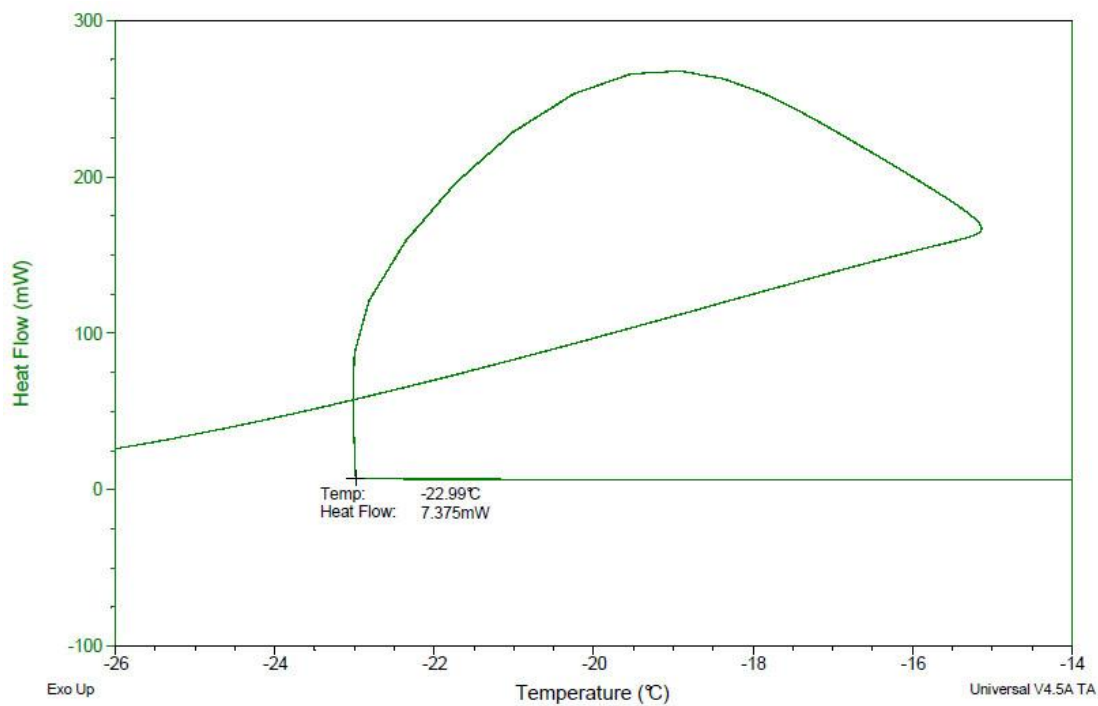
0.6 mol/kg Sodium Chloride Solution

Figure 91. Freezing profile for 30 μl of 0.6 mol/kg Sodium Chloride sealed in an aluminium pan and cooled from 35°C to -30°C at a rate of 5°C/min. Analysis was carried out by reading off temperature at which a sharp rise in heat flow occurred.

Figure 92. Freezing profile for 30 μl of 0.6 mol/kg Sodium Chloride sealed in an aluminium pan and cooled from 35°C to -30°C at a rate of 5°C/min. Analysis was carried out by reading off temperature at which a sharp rise in heat flow occurred.

0.7 mol/kg Sodium Chloride Solution

Figure 93. Freezing profile for 30 µl of 0.7 mol/kg Sodium Chloride sealed in an aluminium pan and cooled from 35°C to -30°C at a rate of 5°C/min. Analysis was carried out by reading off temperature at which a sharp rise in heat flow occurred.

Figure 94. Freezing profile for 30 µl of 0.7 mol/kg Sodium Chloride sealed in an aluminium pan and cooled from 35°C to -30°C at a rate of 5°C/min. Analysis was carried out by reading off temperature at which a sharp rise in heat flow occurred.
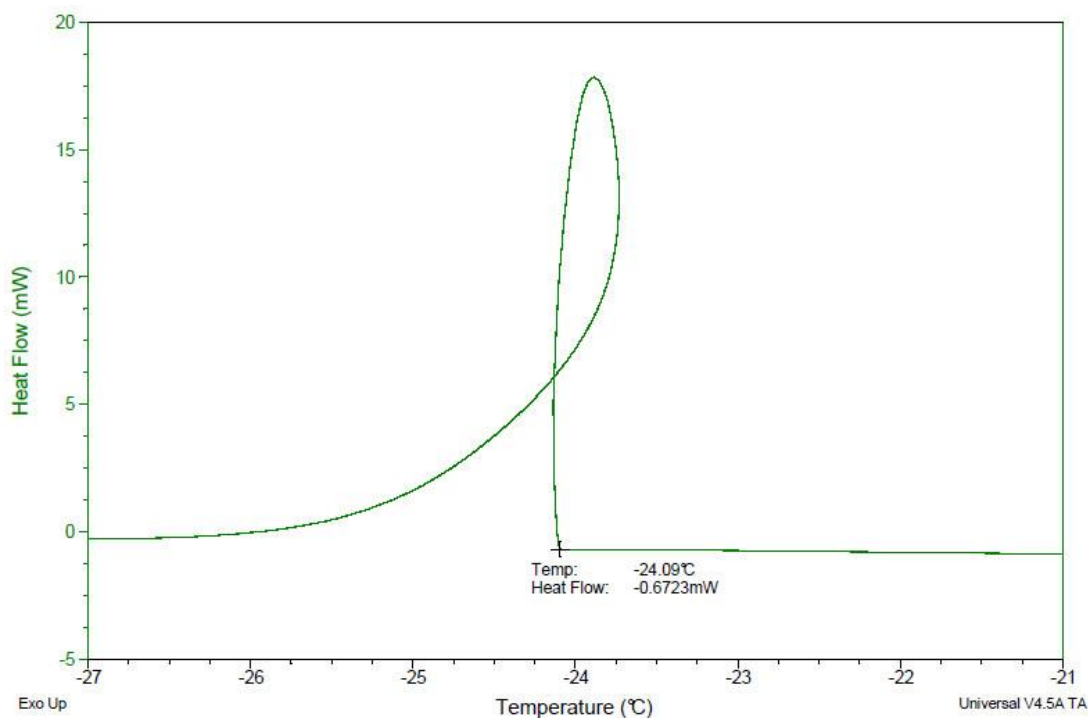
0.8 mol/kg Sodium Chloride Solution

Figure 95. Freezing profile for 30 µl of 0.8 mol/kg Sodium Chloride sealed in an aluminium pan and cooled from 35°C to -30°C at a rate of 5°C/min. Analysis was carried out by reading off temperature at which a sharp rise in heat flow occurred.
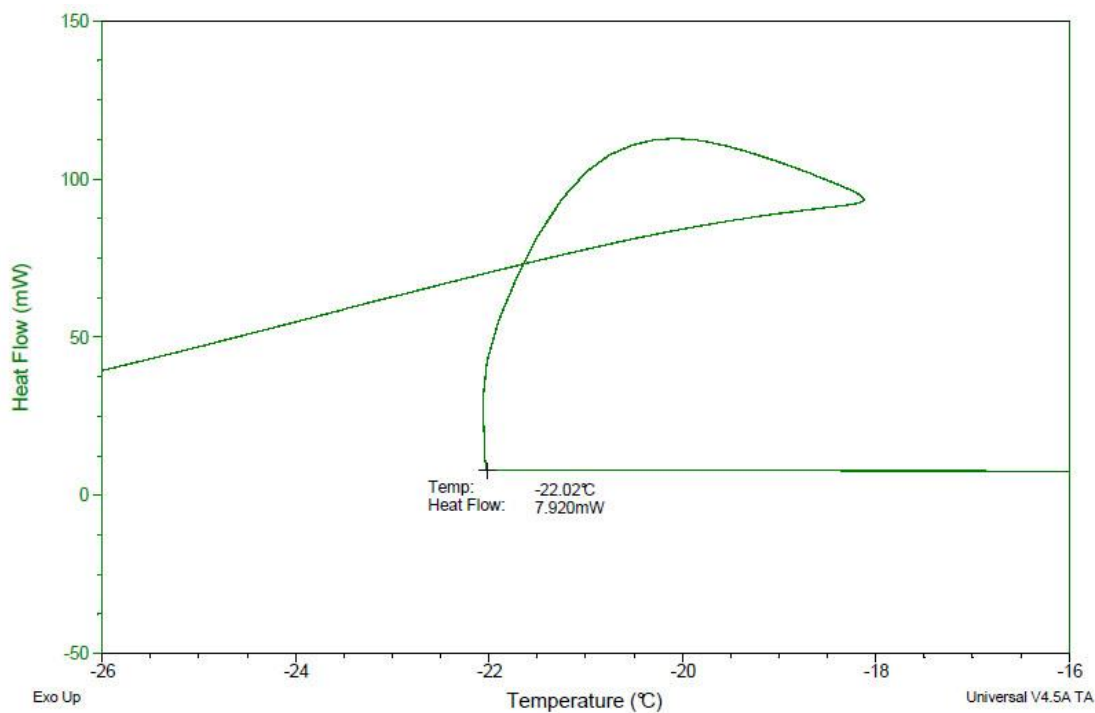

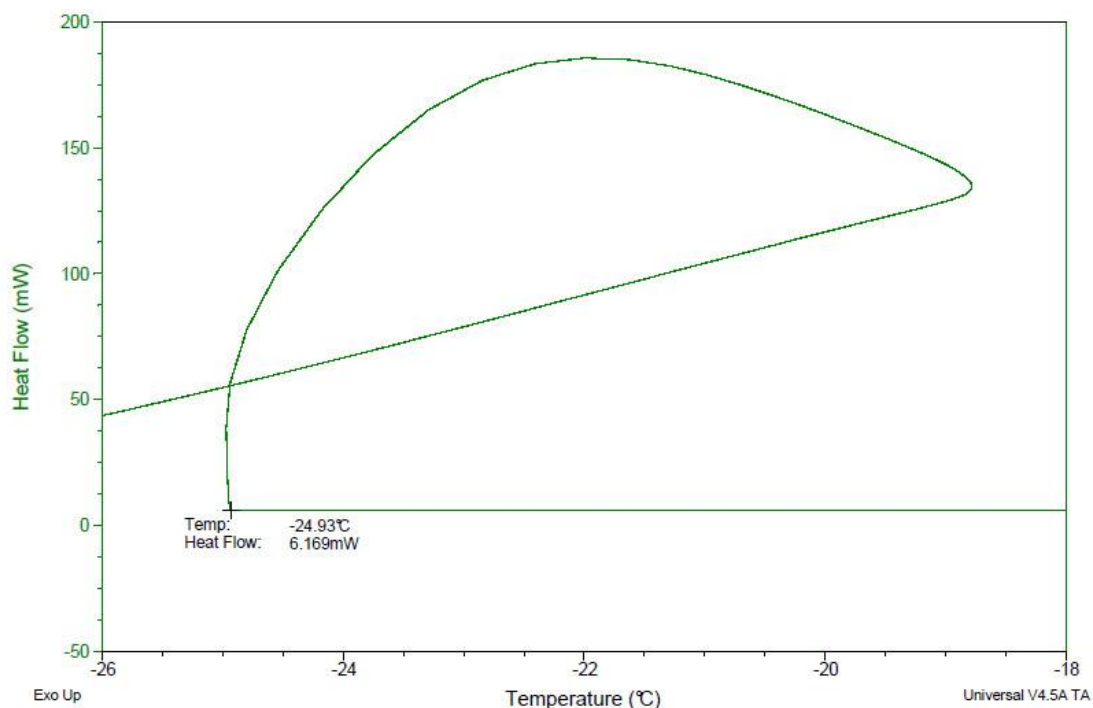Figure 96. Freezing profile for 30 µl of 0.8 mol/kg Sodium Chloride sealed in an aluminium pan and cooled from 35°C to -30°C at a rate of 5°C/min. Analysis was carried out by reading off temperature at which a sharp rise in heat flow occurred.
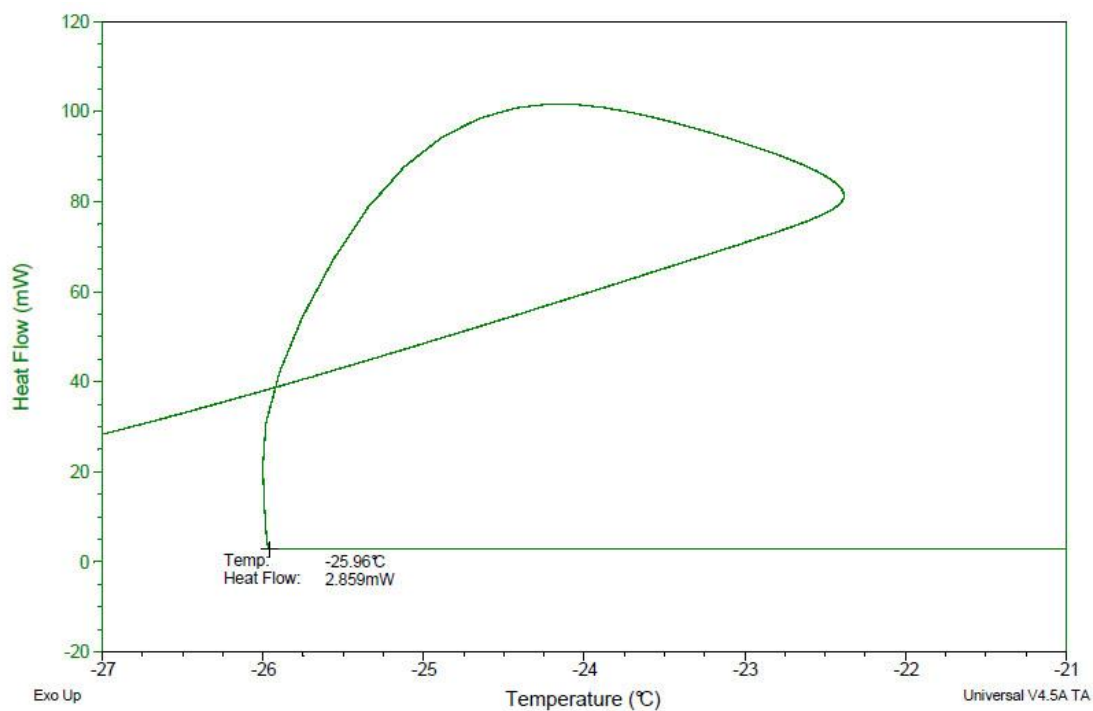
184

0.9 mol/kg Sodium Chloride Solution

Figure 97. Freezing profile for 30 µl of 0.9 mol/kg Sodium Chloride sealed in an aluminium pan and cooled from 35°C to -30°C at a rate of 5°C/min. Analysis was carried out by reading off temperature at which a sharp rise in heat flow occurred.

Figure 98. Freezing profile for 30 µl of 0.9 mol/kg Sodium Chloride sealed in an aluminium pan and cooled from 35°C to -30°C at a rate of 5°C/min. Analysis was carried out by reading off temperature at which a sharp rise in heat flow occurred.
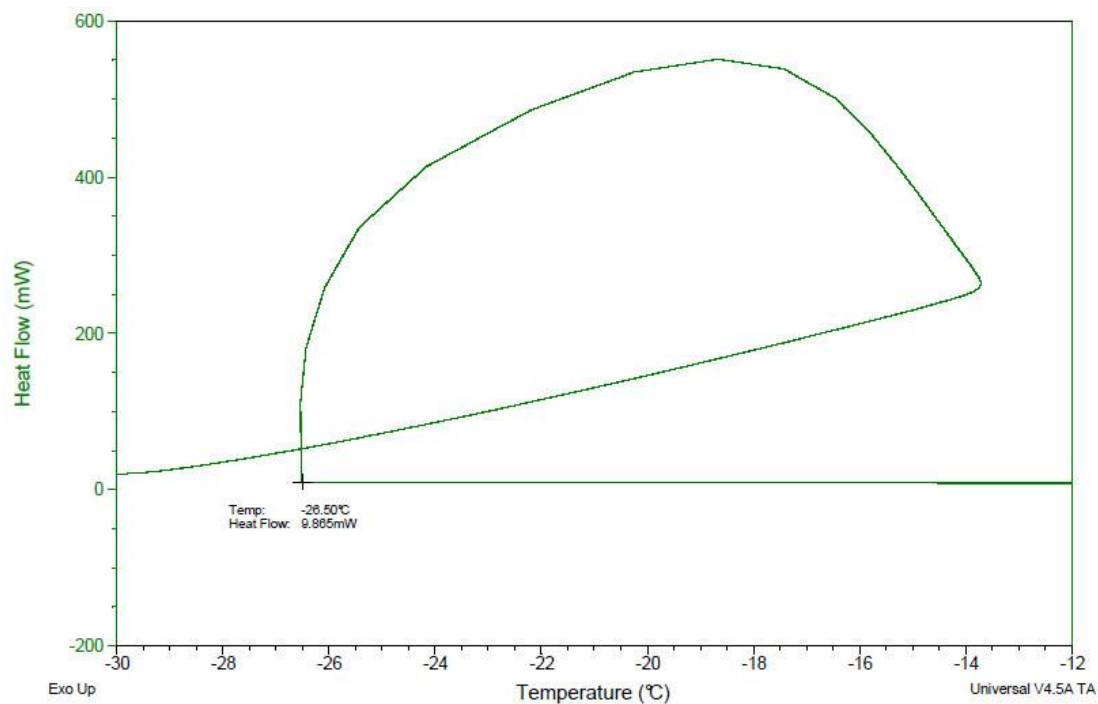
185

1.0 mol/kg Sodium Chloride Solution

Figure 99. Freezing profile for 30 µl of 1.0 mol/kg Sodium Chloride sealed in an aluminium pan and cooled from 35°C to -30°C at a rate of 5°C/min. Analysis was carried out by reading off temperature at which a sharp rise in heat flow occurred.

Figure 100. Freezing profile for 30 µl of 1.0 mol/kg Sodium Chloride sealed in an aluminium pan and cooled from 35°C to -30°C at a rate of 5°C/min. Analysis was carried out by reading off temperature at which a sharp rise in heat flow occurred.
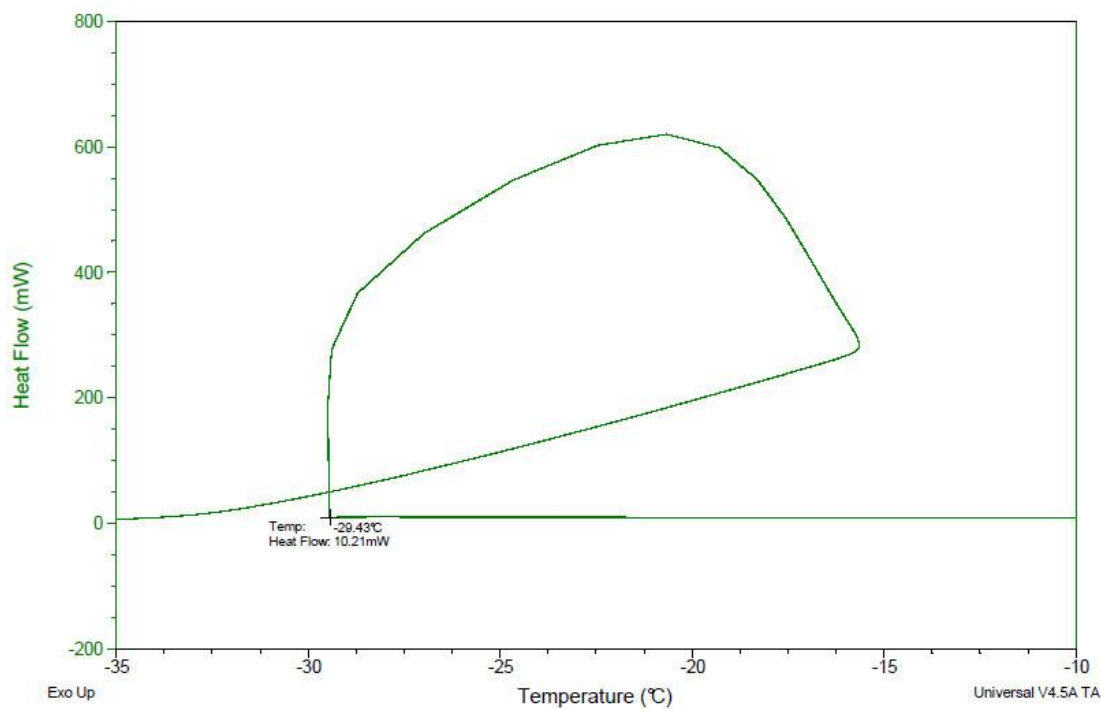
1.2 mol/kg Sodium Chloride Solution

Figure 101. Freezing profile for 30 µl of 1.2 mol/kg Sodium Chloride sealed in an aluminium pan and cooled from 35°C to -30°C at a rate of 5°C/min. Analysis was carried out by reading off temperature at which a sharp rise in heat flow occurred.

Figure 102. Freezing profile for 30 µl of 1.2 mol/kg Sodium Chloride sealed in an aluminium pan and cooled from 35°C to -30°C at a rate of 5°C/min. Analysis was carried out by reading off temperature at which a sharp rise in heat flow occurred.
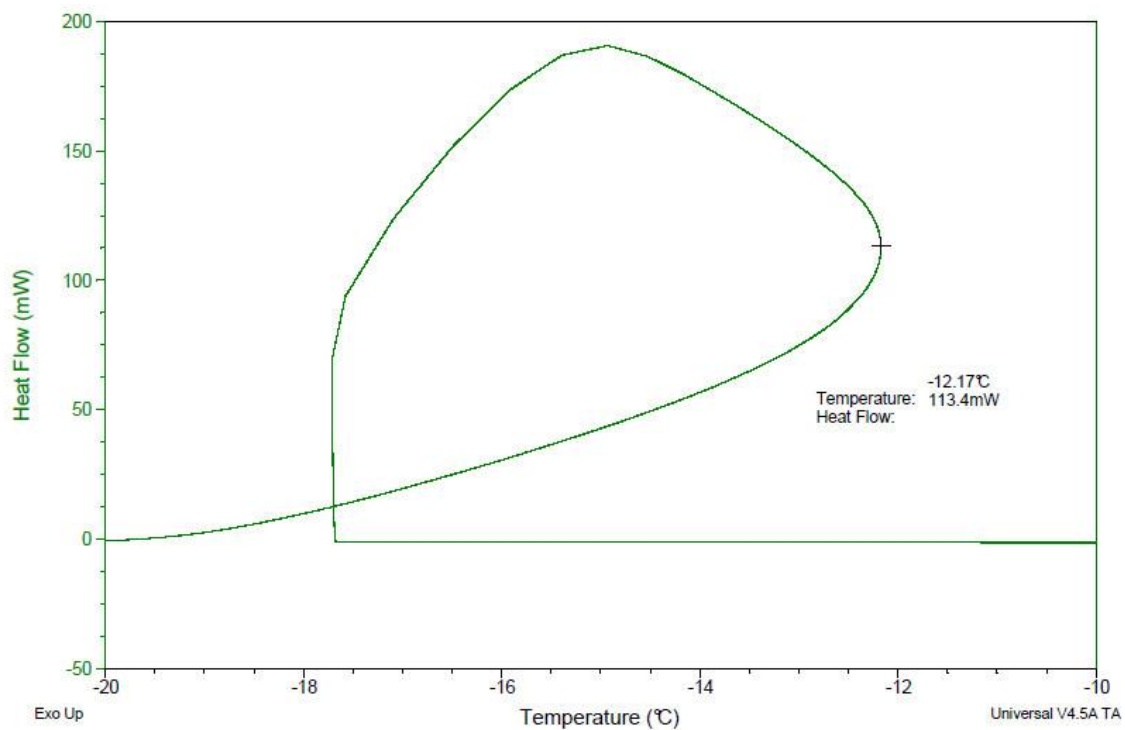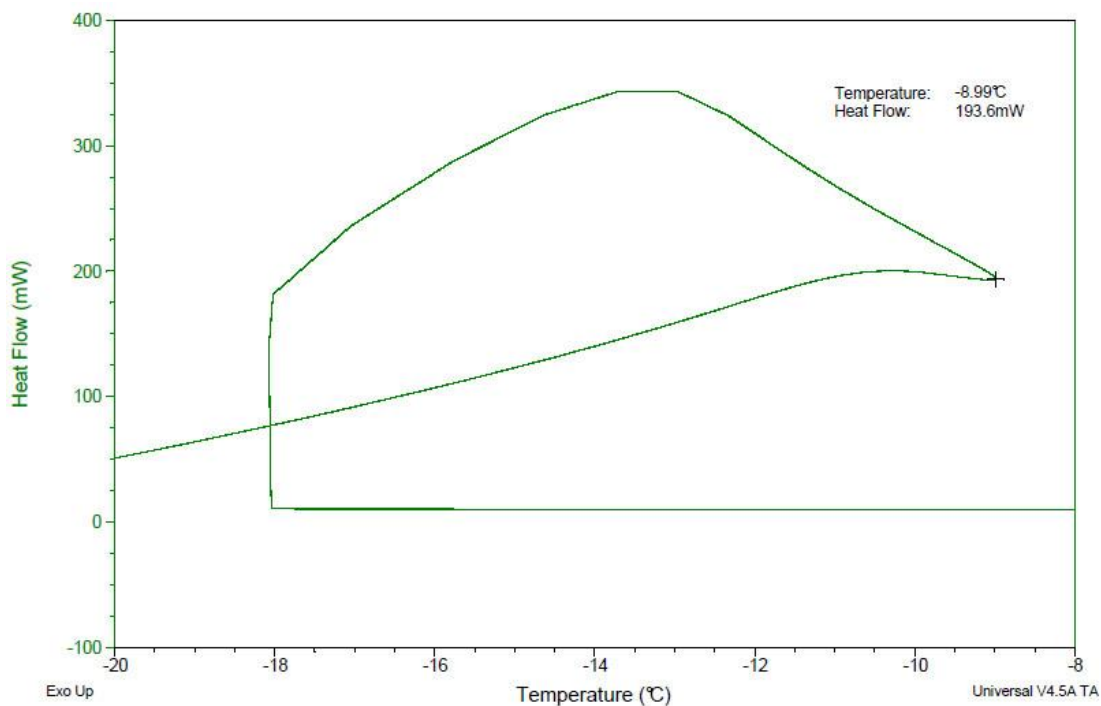
187

1.4 mol/kg Sodium Chloride Solution

Figure 103. Freezing profile for 30 µl of 1.4 mol/kg Sodium Chloride sealed in an aluminium pan and cooled from 35°C to -30°C at a rate of 5°C/min. Analysis was carried out by reading off temperature at which a sharp rise in heat flow occurred.

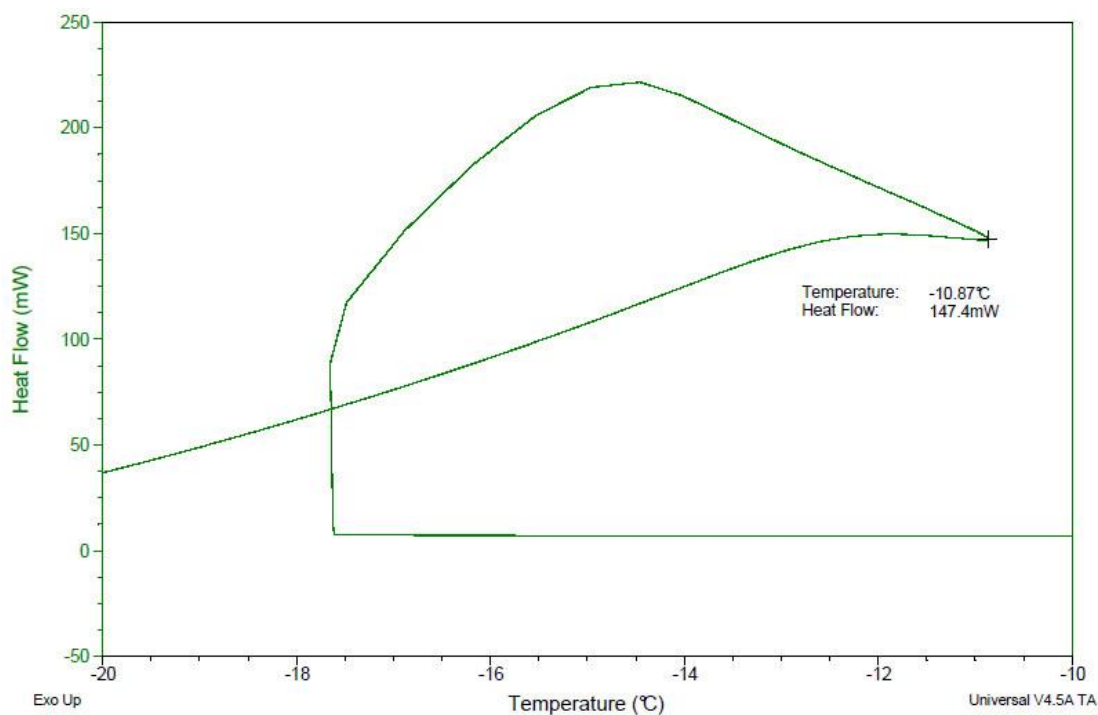Figure 104. Freezing profile for 30 µl of 1.4 mol/kg Sodium Chloride sealed in an aluminium pan and cooled from 35°C to -30°C at a rate of 5°C/min. Analysis was carried out by reading off temperature at which a sharp rise in heat flow occurred.
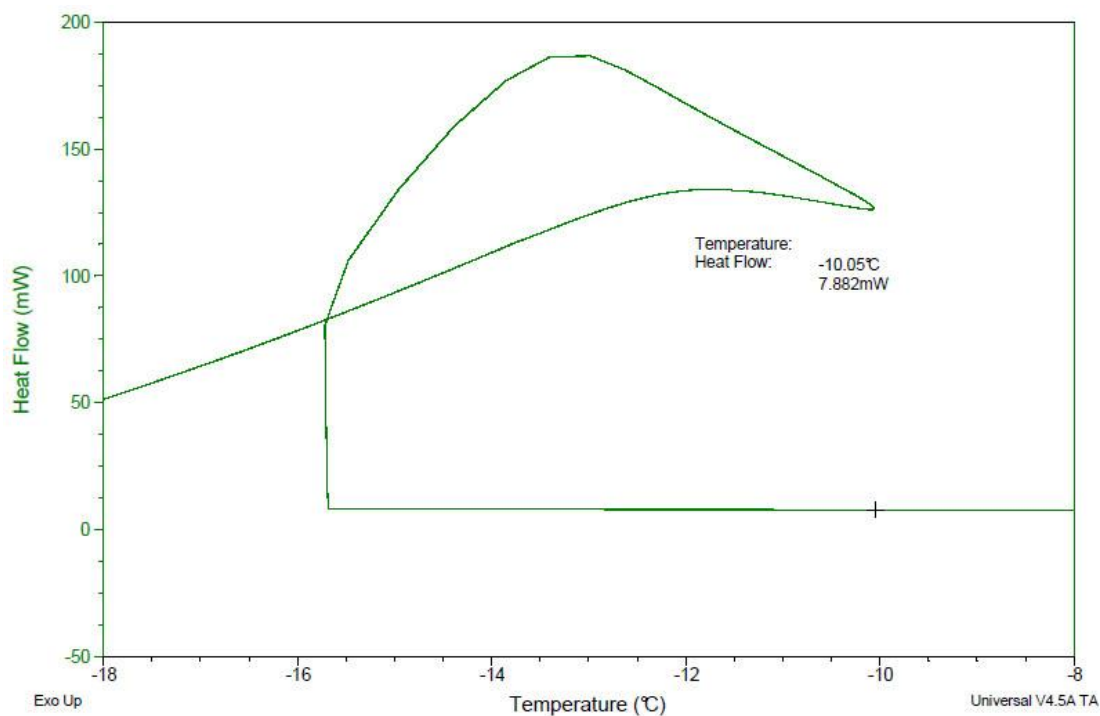
1.6 mol/kg Sodium Chloride Solution

Figure 105. Freezing profile for 30 µl of 1.6 mol/kg Sodium Chloride sealed in an aluminium pan and cooled from 35°C to -30°C at a rate of 5°C/min. Analysis was carried out by reading off temperature at which a sharp rise in heat flow occurred.

Figure 106. Freezing profile for 30 µl of 1.6 mol/kg Sodium Chloride sealed in an aluminium pan and cooled from 35°C to -30°C at a rate of 5°C/min. Analysis was carried out by reading off temperature at which a sharp rise in heat flow occurred.
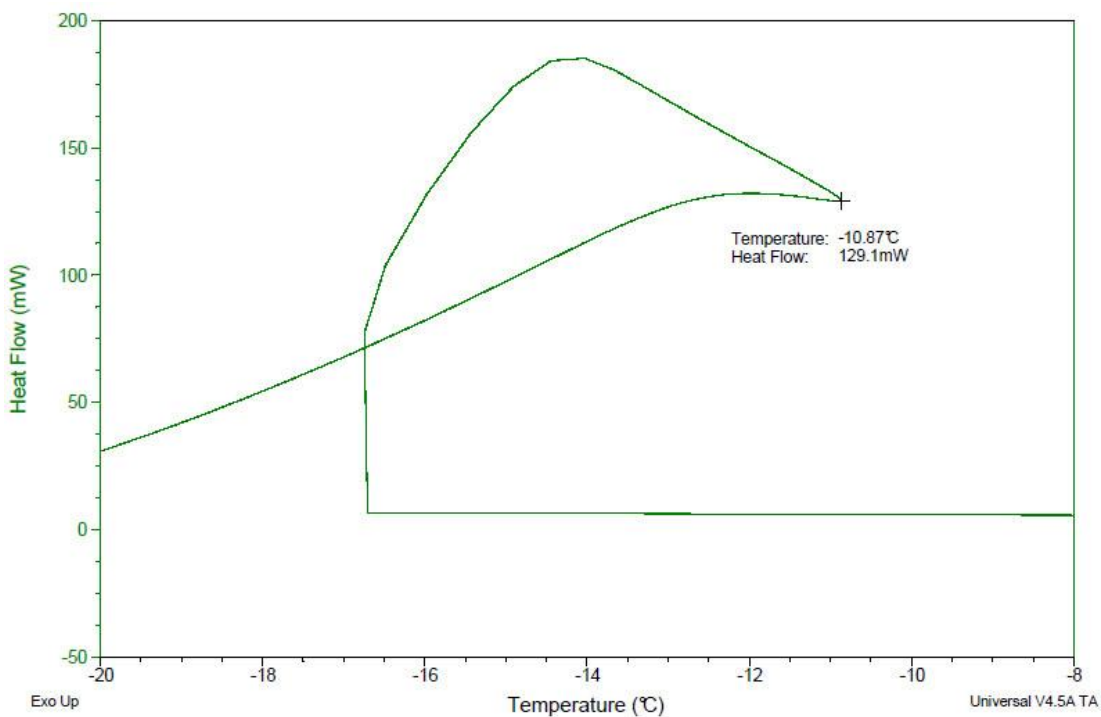
1.8 mol/kg Sodium Chloride Solution

Figure 107. Freezing profile for 30 µl of 1.8 mol/kg Sodium Chloride sealed in an aluminium pan and cooled from 35°C to -30°C at a rate of 5°C/min. Analysis was carried out by reading off temperature at which a sharp rise in heat flow occurred.

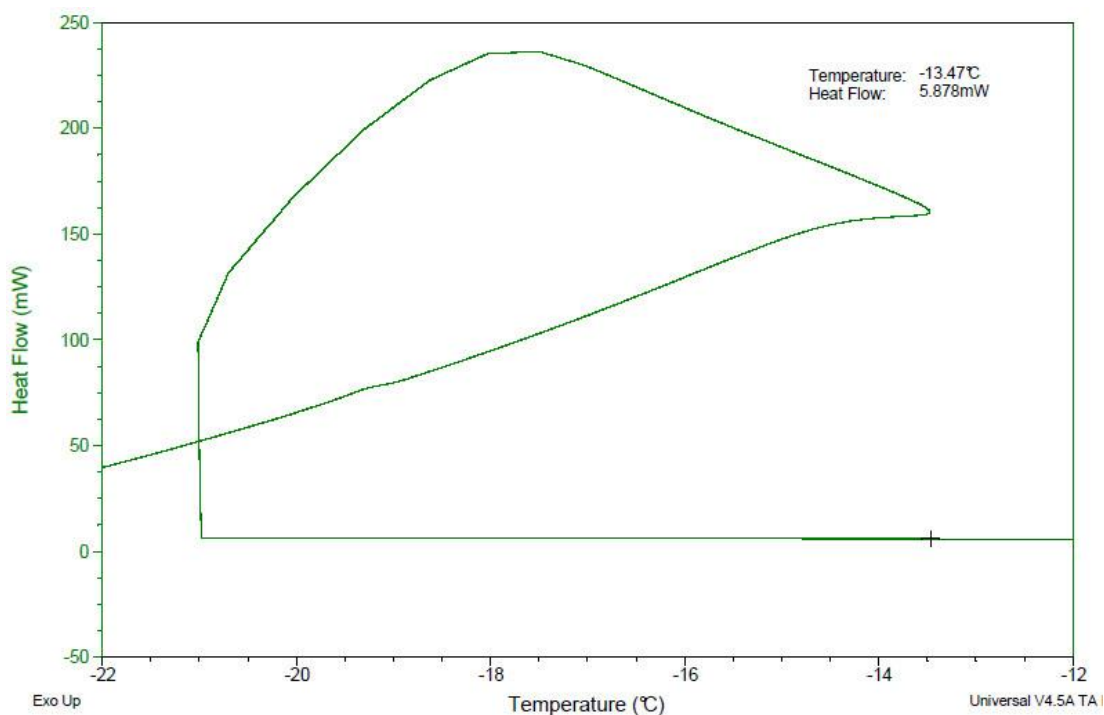Figure 108. Freezing profile for 30 µl of 1.8 mol/kg Sodium Chloride sealed in an aluminium pan and cooled from 35°C to -30°C at a rate of 5°C/min. Analysis was carried out by reading off temperature at which a sharp rise in heat flow occurred.
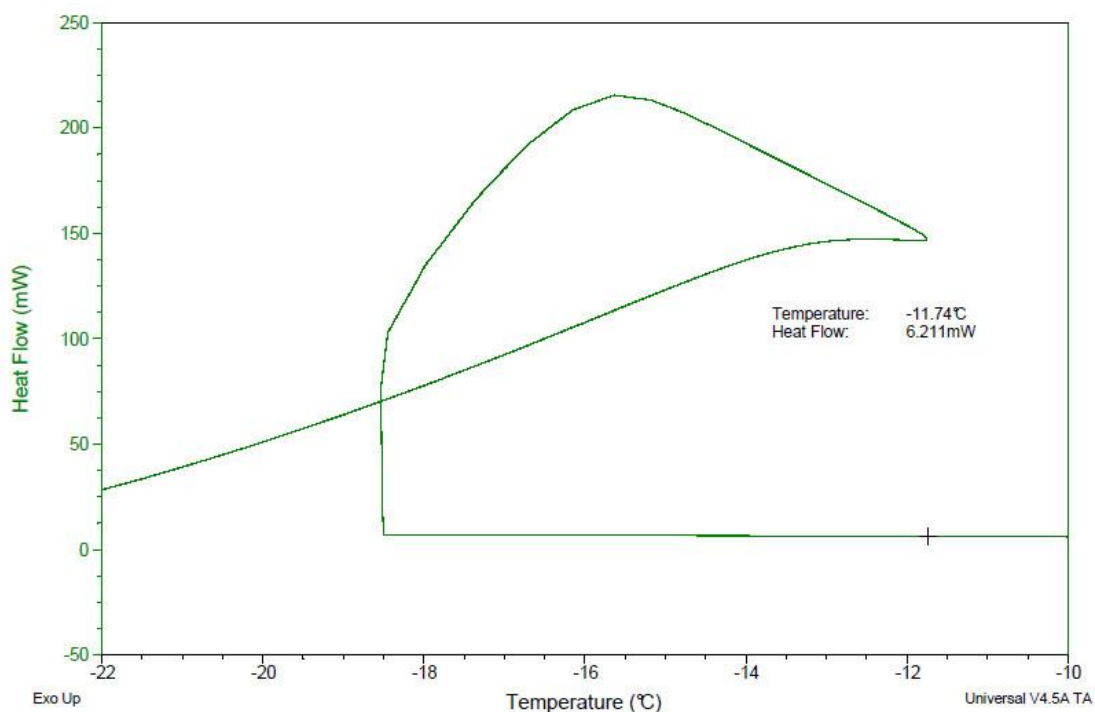
2.0 mol/kg Sodium Chloride Solution

Figure 109. Freezing profile for 30 μl of 2.0 mol/kg Sodium Chloride sealed in an aluminium pan and cooled from 35°C to -30°C at a rate of 5°C/min. Analysis was carried out by reading off temperature at which a sharp rise in heat flow occurred.

Figure 110. Freezing profile for 30 μl of 2.0 mol/kg Sodium Chloride sealed in an aluminium pan and cooled from 35°C to -40°C at a rate of 5°C/min. Analysis was carried out by reading off temperature at which a sharp rise in heat flow occurred.

0.1 mol/kg Sodium Chloride Solution

Figure 111. Freezing profile for 30 µl of 0.1 mol/kg Sodium Chloride sealed in an aluminium pan and cooled from 35°C to -30°C at a rate of 5°C/min. Analysis was carried out by reading off temperature at the highest temperature achieved by the solution during the freezing process.
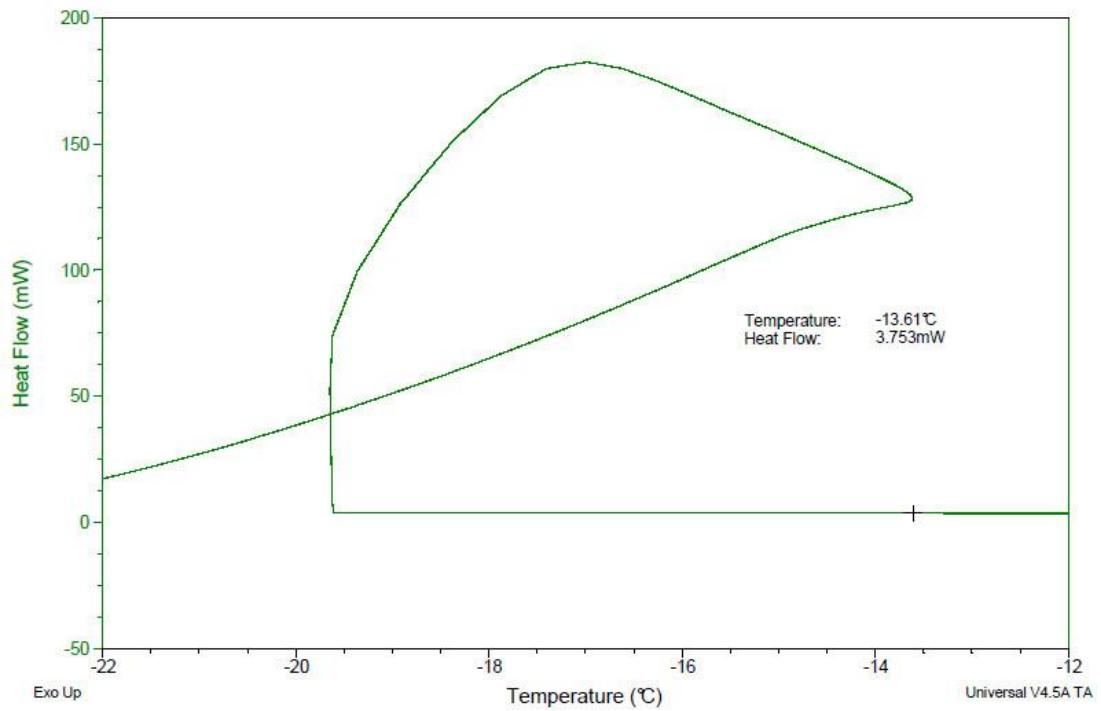
Figure 112. Freezing profile for 30 µl of 0.1 mol/kg Sodium Chloride sealed in an aluminium pan and cooled from 35°C to -30°C at a rate of 5°C/min. Analysis was carried out by reading off temperature at the highest temperature achieved by the solution during the freezing process.
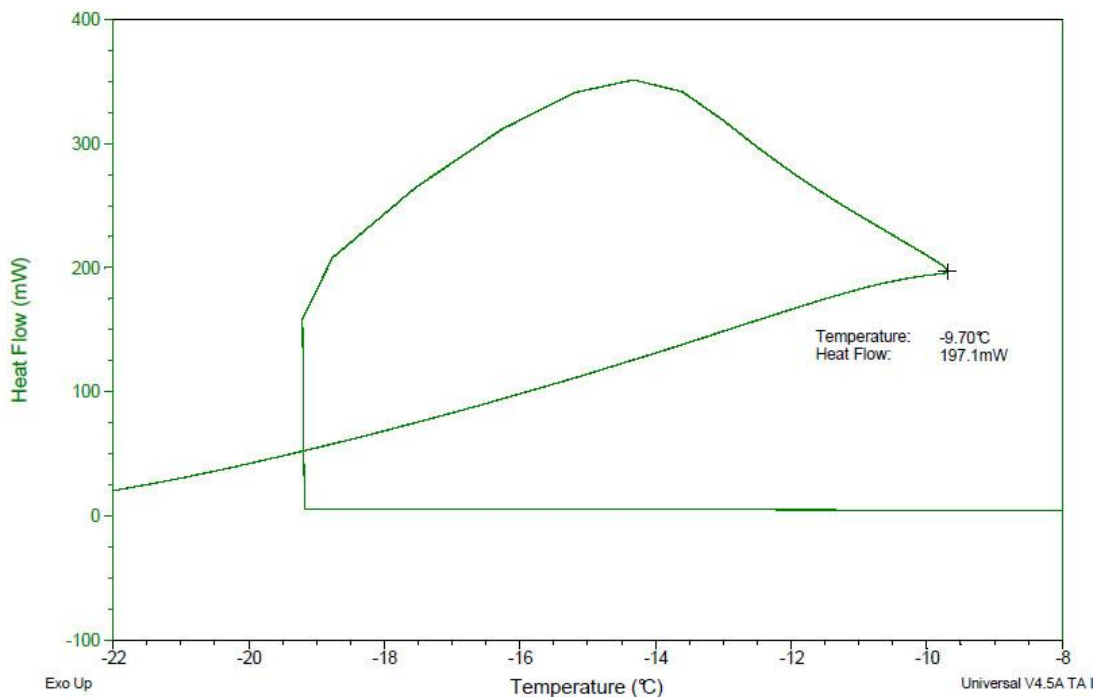
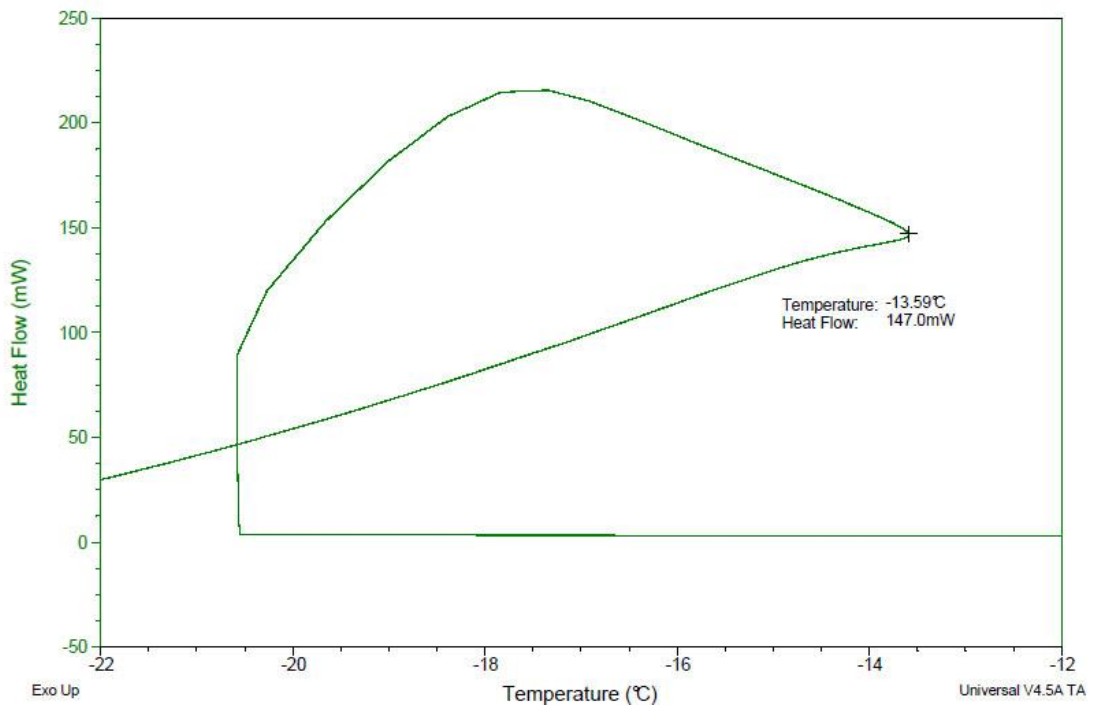## 0.154 mol/kg Sodium Chloride Solution

Figure 113. Freezing profile for 30 µl of 0.154 mol/kg Sodium Chloride sealed in an aluminium pan and cooled from 35°C to -30°C at a rate of 5°C/min. Analysis was carried out by reading off temperature at the highest temperature achieved by the solution during the freezing process.

Figure 114. Freezing profile for 30 µl of 0.154 mol/kg Sodium Chloride sealed in an aluminium pan and cooled from 35°C to -30°C at a rate of 5°C/min. Analysis was carried out by reading off temperature at the highest temperature achieved by the solution during the freezing process.

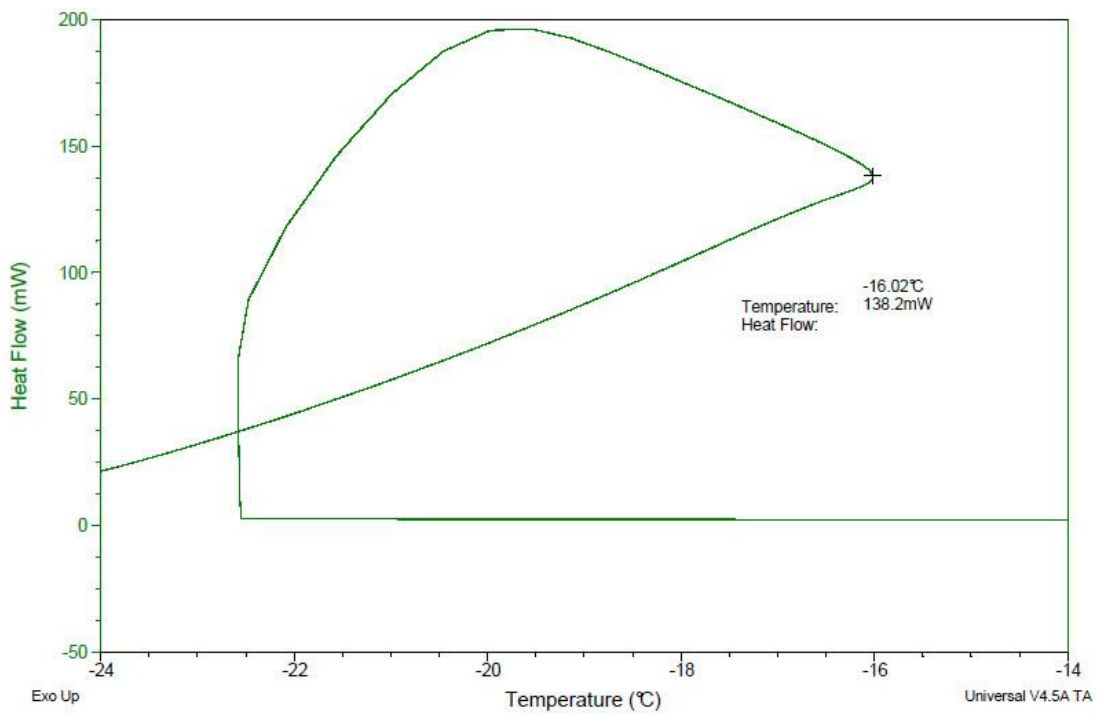## 0.2 mol/kg Sodium Chloride Solution

Figure 115. Freezing profile for 30 µl of 0.2 mol/kg Sodium Chloride sealed in an aluminium pan and cooled from 35°C to -30°C at a rate of 5°C/min. Analysis was carried out by reading off temperature at the highest temperature achieved by the solution during the freezing process.
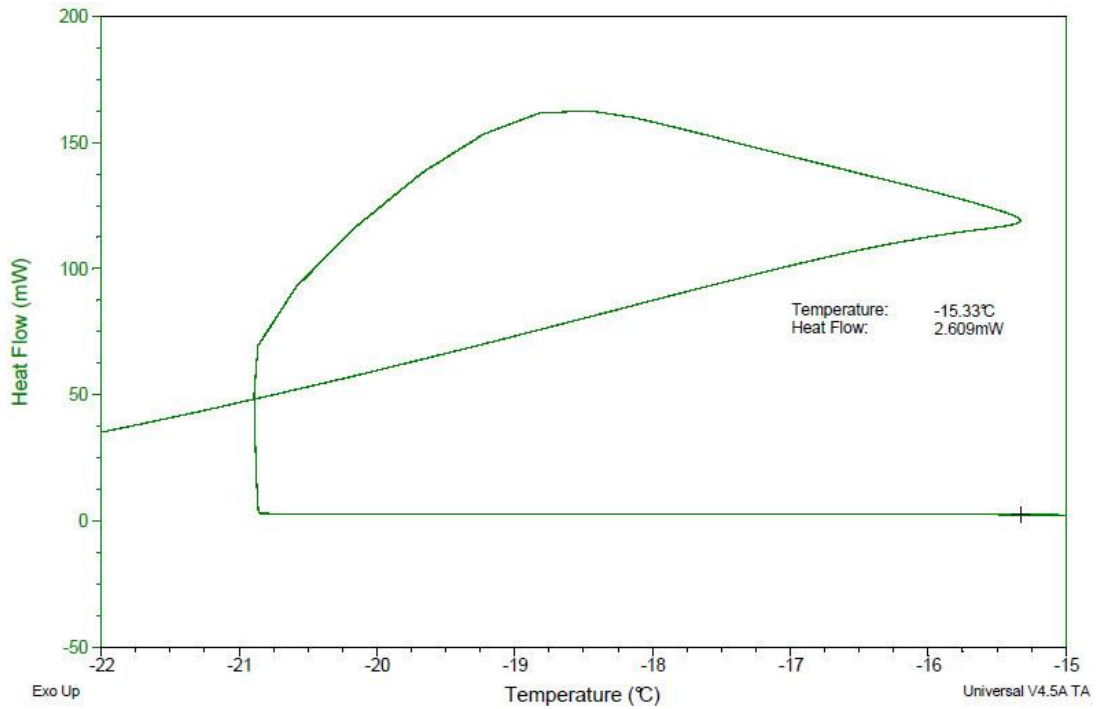
Figure 116. Freezing profile for 30 µl of 0.2 mol/kg Sodium Chloride sealed in an aluminium pan and cooled from 35°C to -30°C at a rate of 5°C/min. Analysis was carried out by reading off temperature at the highest temperature achieved by the solution during the freezing process.

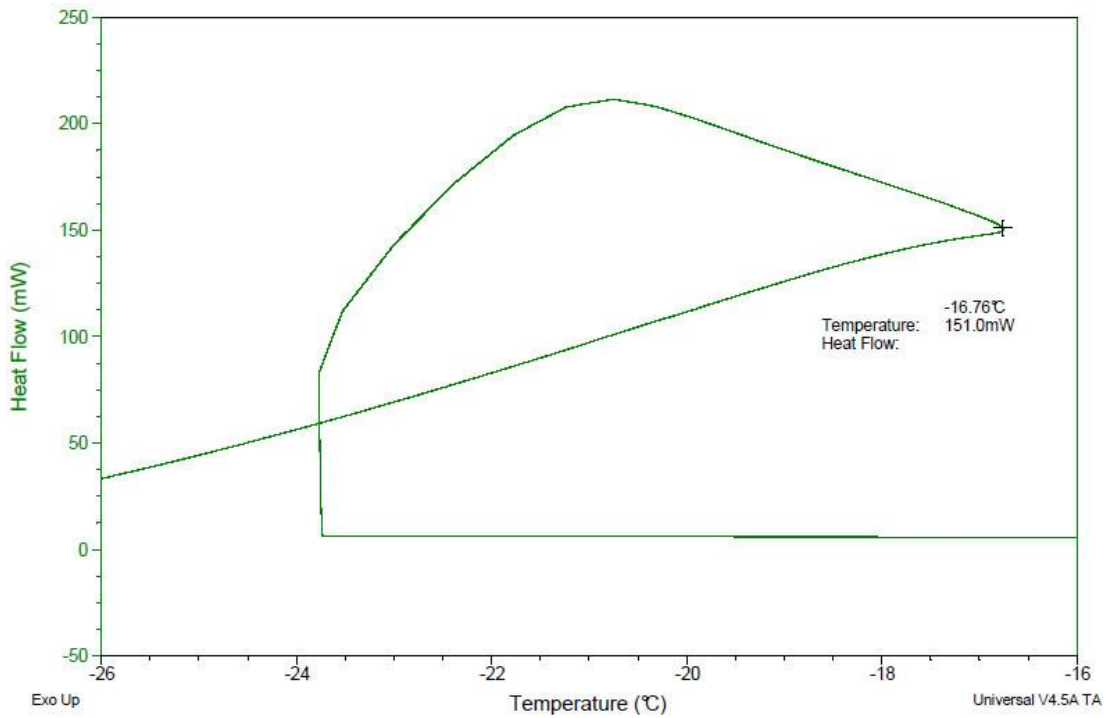## 0.3 mol/kg Sodium Chloride Solution

Figure 117. Freezing profile for 30 µl of 0.3 mol/kg Sodium Chloride sealed in an aluminium pan and cooled from 35°C to -30°C at a rate of 5°C/min. Analysis was carried out by reading off temperature at the highest temperature achieved by the solution during the freezing process.

Figure 118. Freezing profile for 30 µl of 0.3 mol/kg Sodium Chloride sealed in an aluminium pan and cooled from 35°C to -30°C at a rate of 5°C/min. Analysis was carried out by reading off temperature at the highest temperature achieved by the solution during the freezing process.
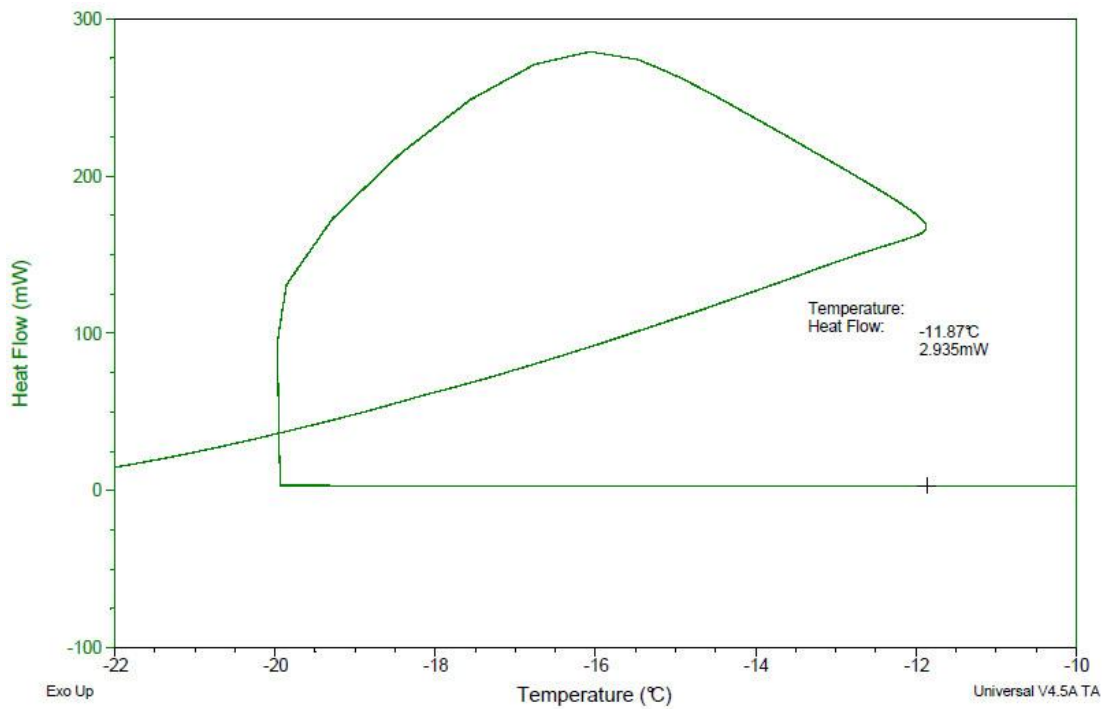
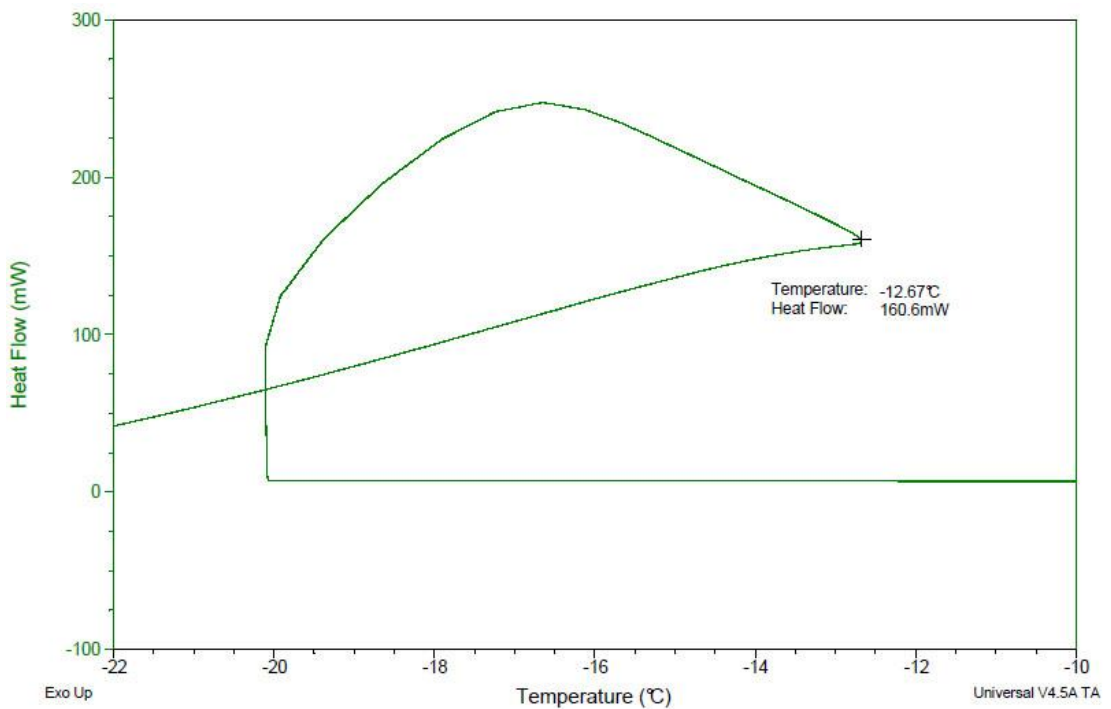## 0.4 mol/kg Sodium Chloride Solution

Figure 119. Freezing profile for 30 µl of 0.4 mol/kg Sodium Chloride sealed in an aluminium pan and cooled from 35°C to -30°C at a rate of 5°C/min. Analysis was carried out by reading off temperature at the highest temperature achieved by the solution during the freezing process.

196

Figure 120. Freezing profile for 30 µl of 0.4 mol/kg Sodium Chloride sealed in an aluminium pan and cooled from 35°C to -30°C at a rate of 5°C/min. Analysis was carried out by reading off temperature at the highest temperature achieved by the solution during the freezing process.
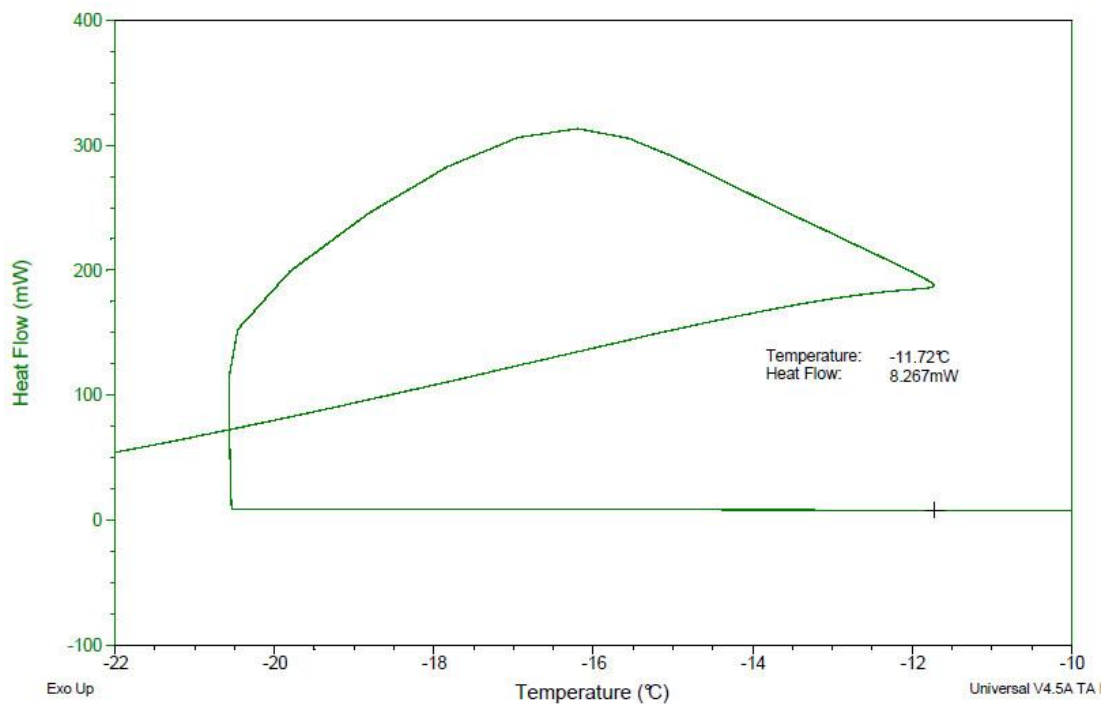
0.5 mol/kg Sodium Chloride Solution

Figure 121. Freezing profile for 30 µl of 0.5 mol/kg Sodium Chloride sealed in an aluminium pan and cooled from 35°C to -30°C at a rate of 5°C/min. Analysis was carried out by reading off temperature at the highest temperature achieved by the solution during the freezing process.
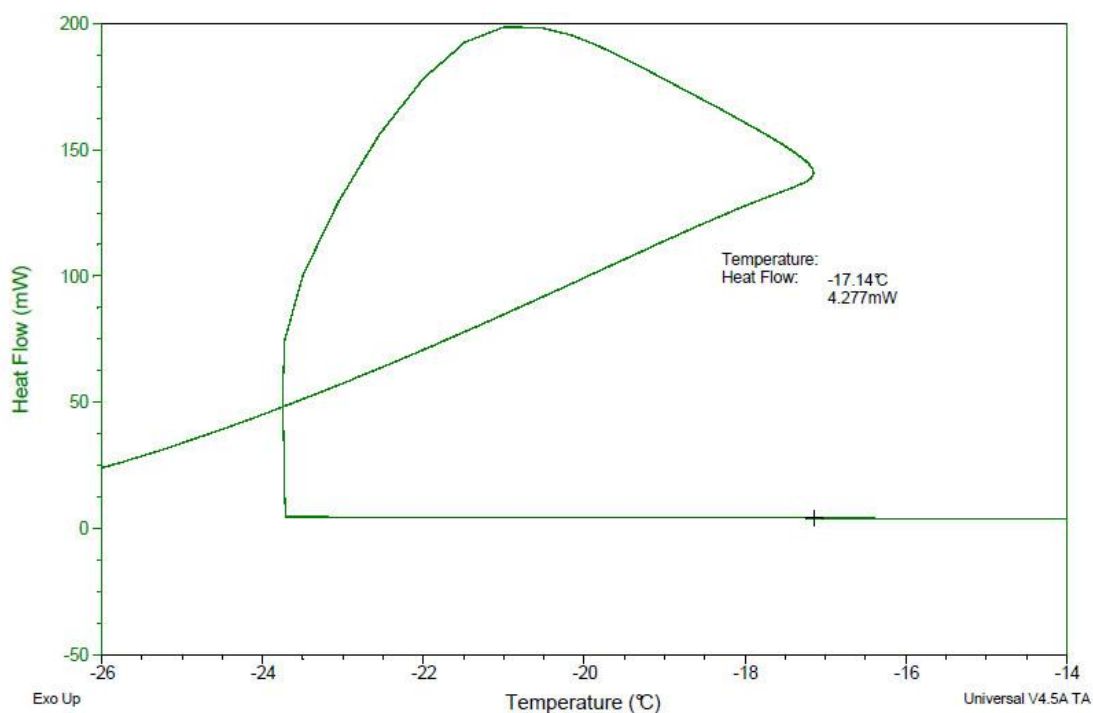
Figure 122. Freezing profile for 30 µl of 0.5 mol/kg Sodium Chloride sealed in an aluminium pan and cooled from 35°C to -30°C at a rate of 5°C/min. Analysis was carried out by reading off temperature at the highest temperature achieved by the solution during the freezing process.
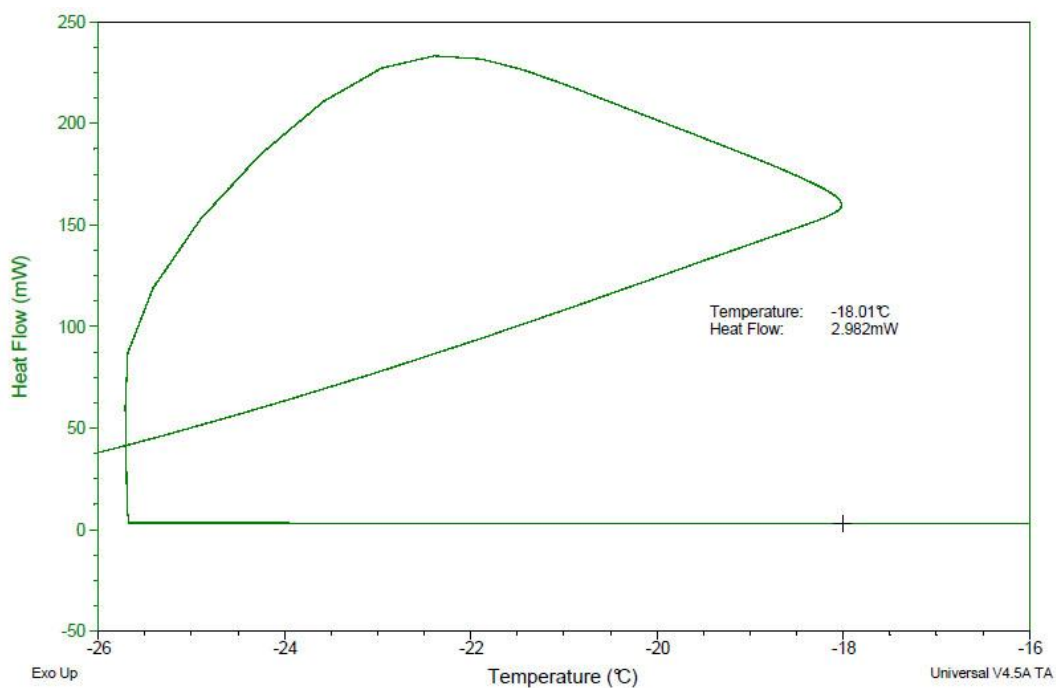
0.6 mol/kg Sodium Chloride Solution

Figure 123. Freezing profile for 30 µl of 0.6 mol/kg Sodium Chloride sealed in an aluminium pan and cooled from 35°C to -30°C at a rate of 5°C/min. Analysis was carried out by reading off temperature at the highest temperature achieved by the solution during the freezing process.
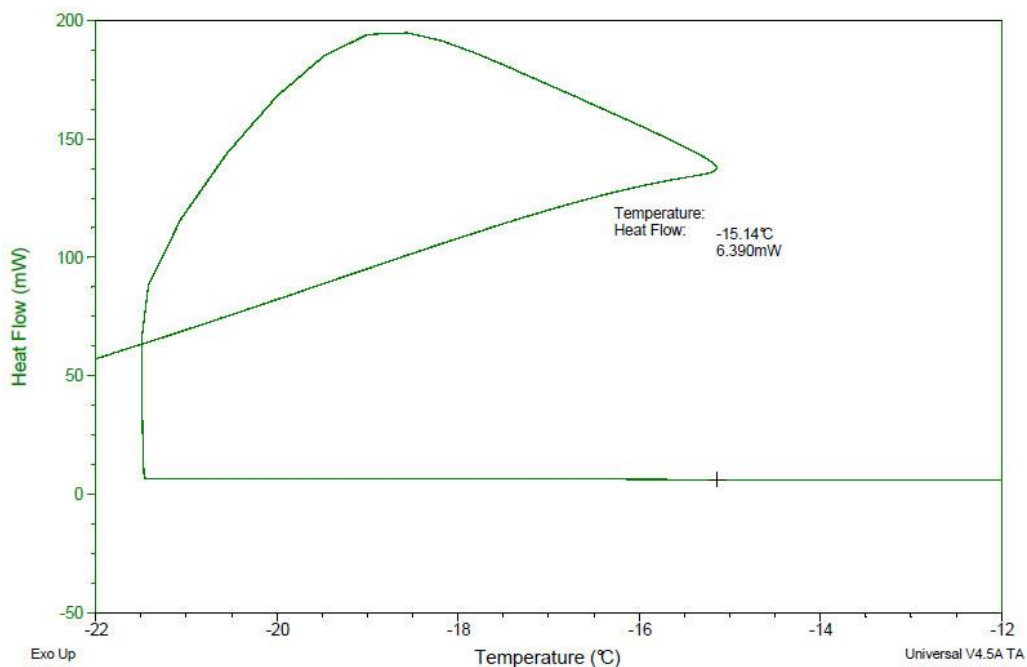
Figure 124. Freezing profile for 30 µl of 0.6 mol/kg Sodium Chloride sealed in an aluminium pan and cooled from 35°C to -30°C at a rate of 5°C/min. Analysis was carried out by reading off temperature at the highest temperature achieved by the solution during the freezing process.

0.7 Sodium Chloride Solution

Figure 125. Freezing profile for 30 µl of 0.7 mol/kg Sodium Chloride sealed in an aluminium pan and cooled from 35°C to -30°C at a rate of 5°C/min. Analysis was carried out by reading off temperature at the highest temperature achieved by the solution during the freezing process.
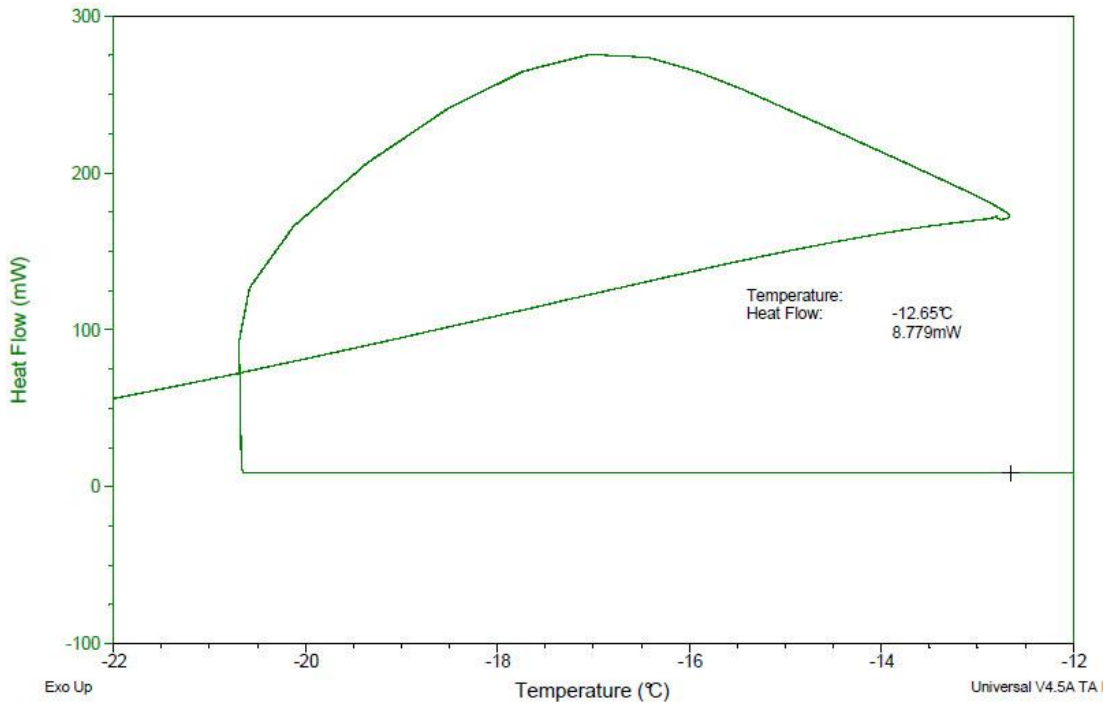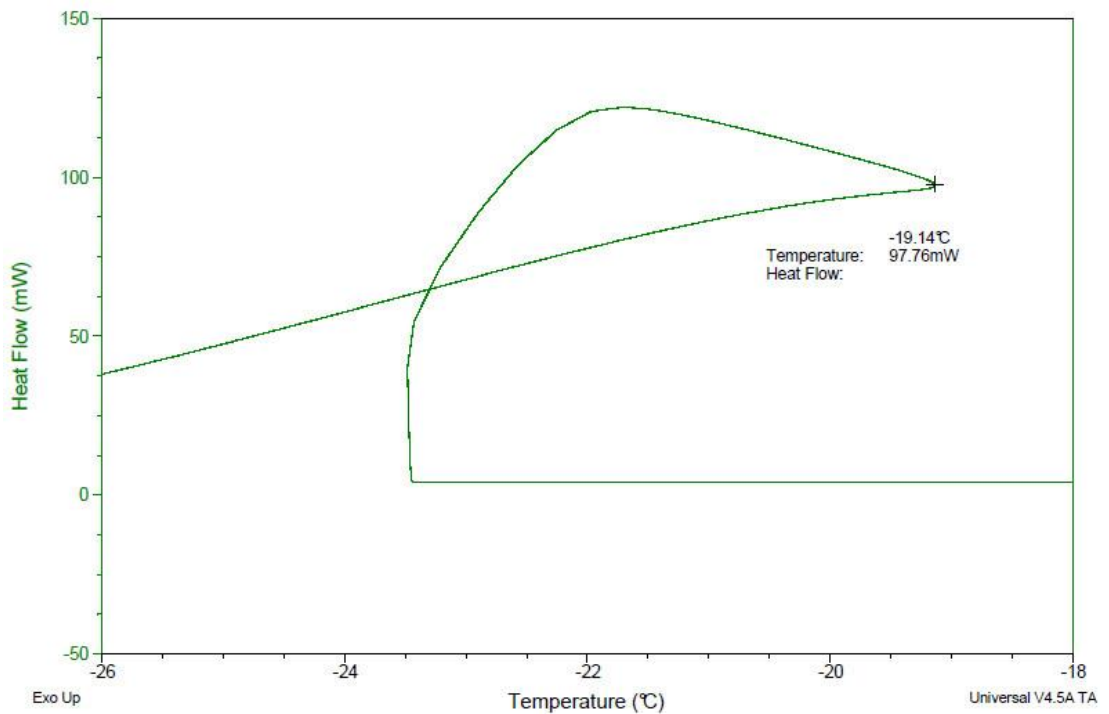
Figure 126. Freezing profile for 30 μl of 0.7 mol/kg Sodium Chloride sealed in an aluminium pan and cooled from 35°C to -30°C at a rate of 5°C/min. Analysis was carried out by reading off temperature at the highest temperature achieved by the solution during the freezing process.

0.8 mol/kg Sodium Chloride Solution

Figure 127. Freezing profile for 30 μl of 0.8 mol/kg Sodium Chloride sealed in an aluminium pan and cooled from 35°C to -30°C at a rate of 5°C/min. Analysis was carried out by reading off temperature at the highest temperature achieved by the solution during the freezing process.
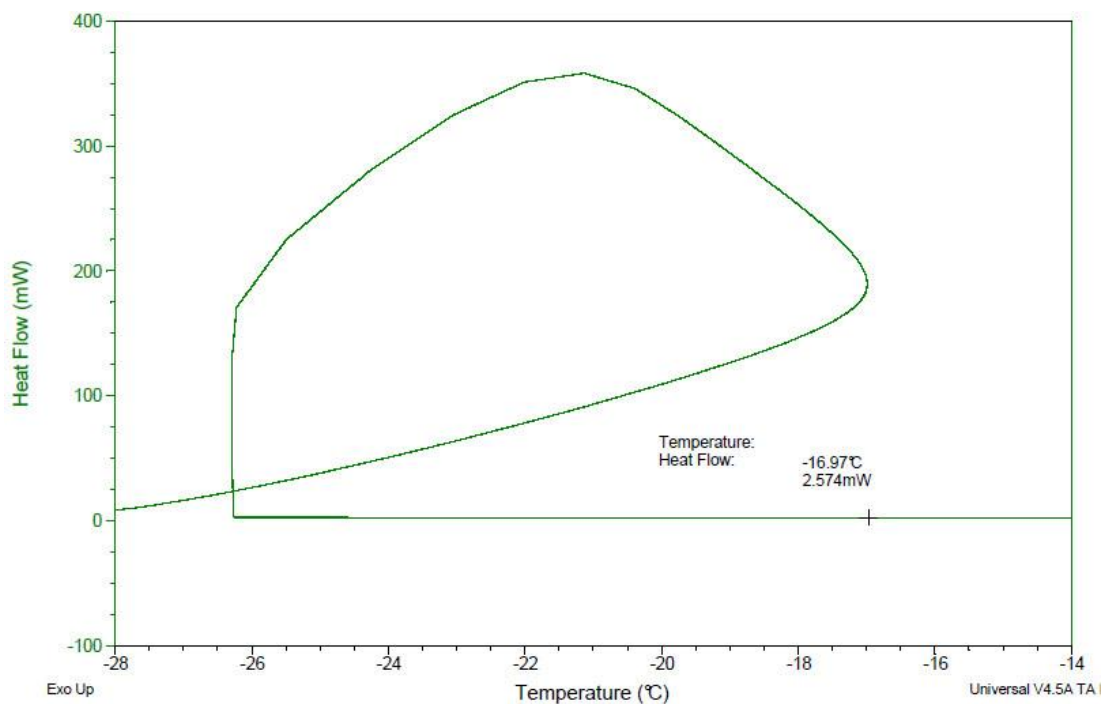
Figure 128. Freezing profile for 30 μl of 0.8 mol/kg Sodium Chloride sealed in an aluminium pan and cooled from 35°C to -30°C at a rate of 5°C/min. Analysis was carried out by reading off temperature at the highest temperature achieved by the solution during the freezing process.

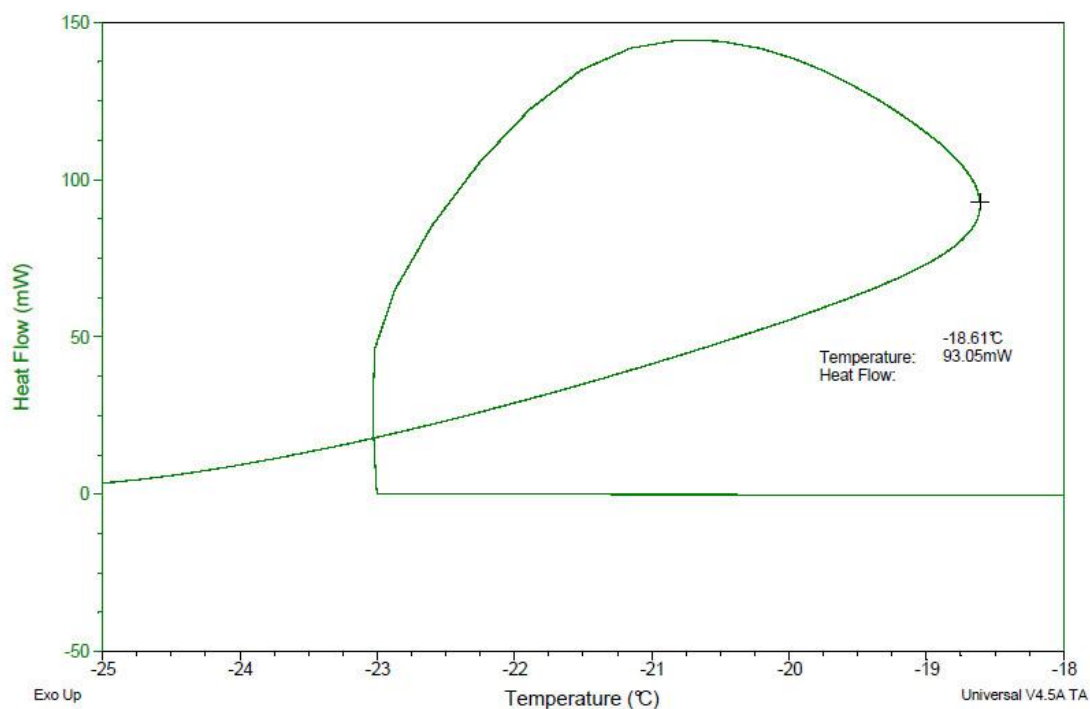## 0.9 mol/kg Sodium Chloride Solution

Figure 129. Freezing profile for 30 μl of 0.9 mol/kg Sodium Chloride sealed in an aluminium pan and cooled from 35°C to -30°C at a rate of 5°C/min. Analysis was carried out by reading off temperature at the highest temperature achieved by the solution during the freezing process.
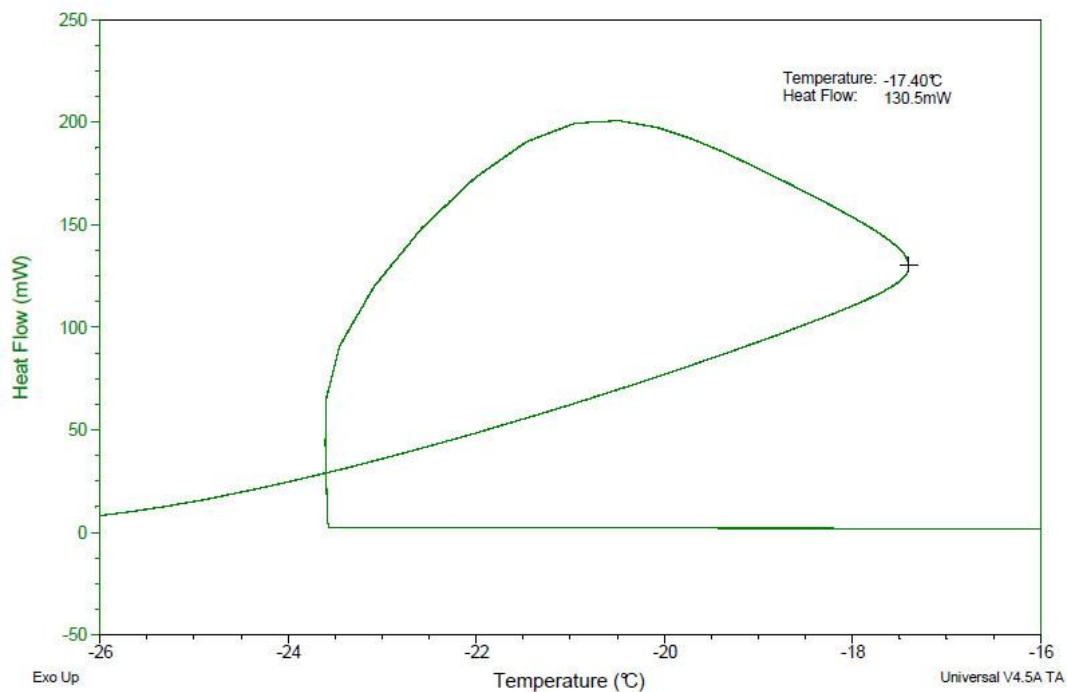
Figure 130. Freezing profile for 30 µl of 0.9 mol/kg Sodium Chloride sealed in an aluminium pan and cooled from 35°C to -30°C at a rate of 5°C/min. Analysis was carried out by reading off temperature at the highest temperature achieved by the solution during the freezing process.

1.0 mol/kg Sodium Chloride Solution
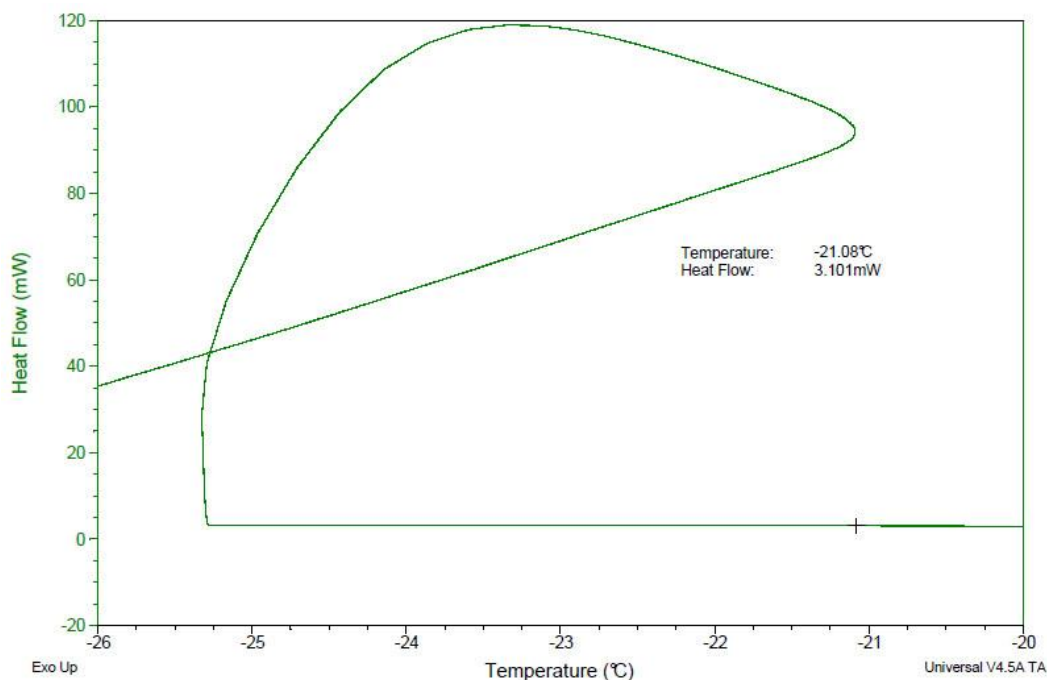

Figure 131. Freezing profile for 30 µl of 1.0 mol/kg Sodium Chloride sealed in an aluminium pan and cooled from 35°C to -30°C at a rate of 5°C/min. Analysis was carried out by reading off temperature at the highest temperature achieved by the solution during the freezing process.

Figure 132. Freezing profile for 30 μl of 1.0 mol/kg Sodium Chloride sealed in an aluminium pan and cooled from 35°C to -30°C at a rate of 5°C/min. Analysis was carried out by reading off temperature at the highest temperature achieved by the solution during the freezing process.
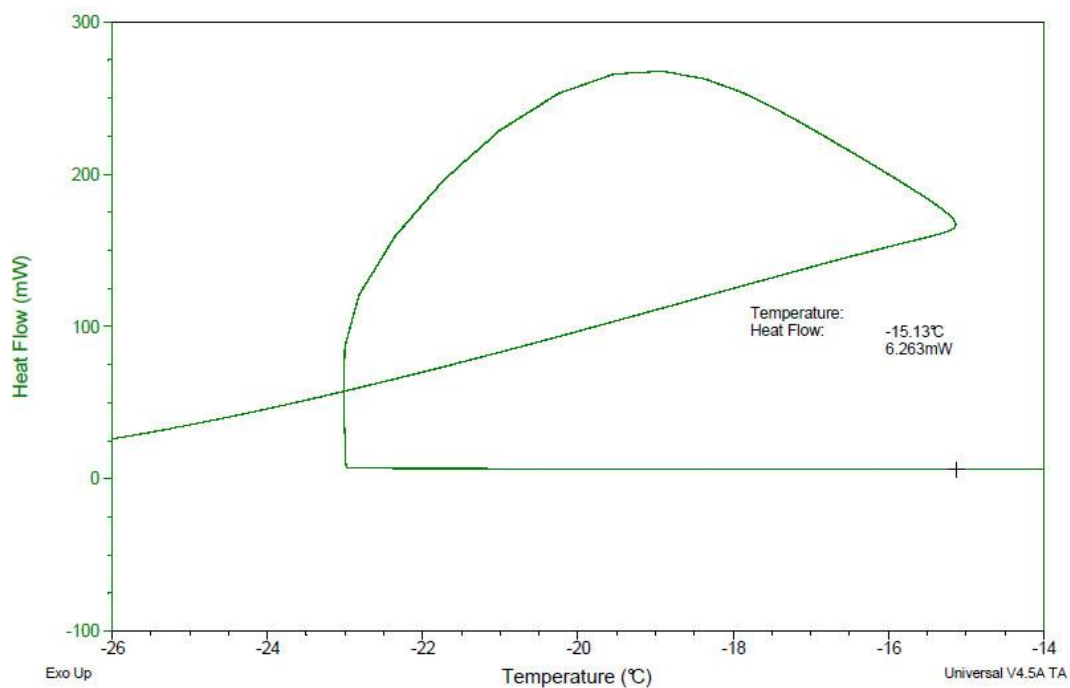
1.2 mol/kg Sodium Chloride Solution
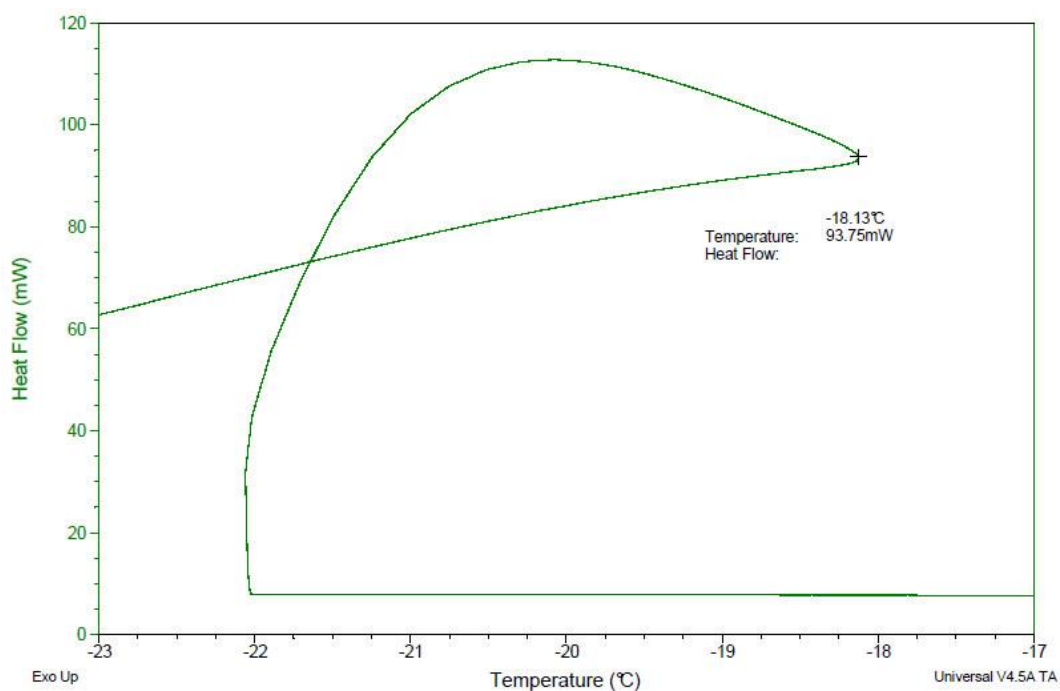

Figure 133. Freezing profile for 30 μl of 1.2 mol/kg Sodium Chloride sealed in an aluminium pan and cooled from 35°C to -30°C at a rate of 5°C/min. Analysis was carried out by reading off temperature at the highest temperature achieved by the solution during the freezing process.

203

Figure 134. Freezing profile for 30 μl of 1.2 mol/kg Sodium Chloride sealed in an aluminium pan and cooled from 35°C to -30°C at a rate of 5°C/min. Analysis was carried out by reading off temperature at the highest temperature achieved by the solution during the freezing process.
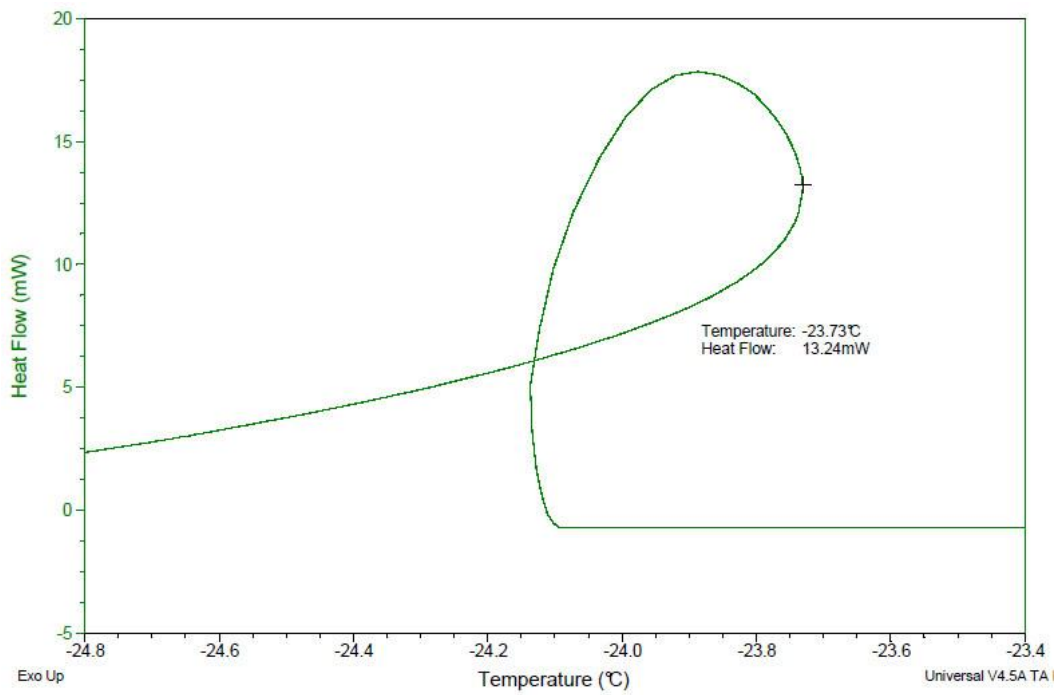
1.4 mol/kg Sodium Chloride Solution

Figure 135. Freezing profile for 30 μl of 1.4 mol/kg Sodium Chloride sealed in an aluminium pan and cooled from 35°C to -30°C at a rate of 5°C/min. Analysis was carried out by reading off temperature at the highest temperature achieved by the solution during the freezing process.
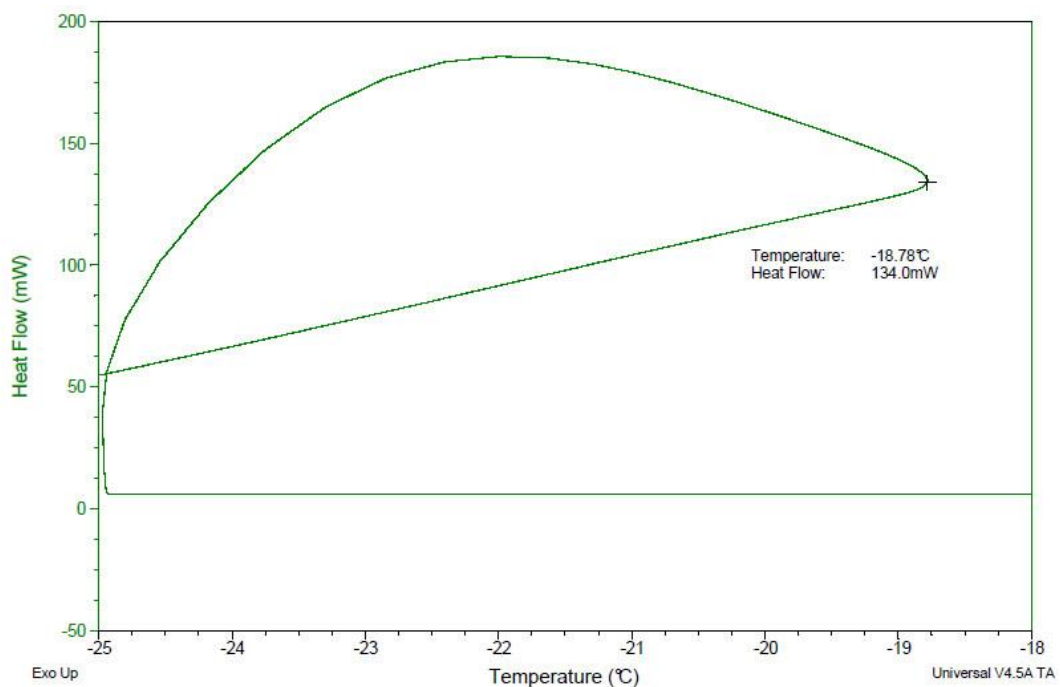
Figure 136. Freezing profile for 30 µl of 1.4 mol/kg Sodium Chloride sealed in an aluminium pan and cooled from 35°C to -30°C at a rate of 5°C/min. Analysis was carried out by reading off temperature at the highest temperature achieved by the solution during the freezing process.
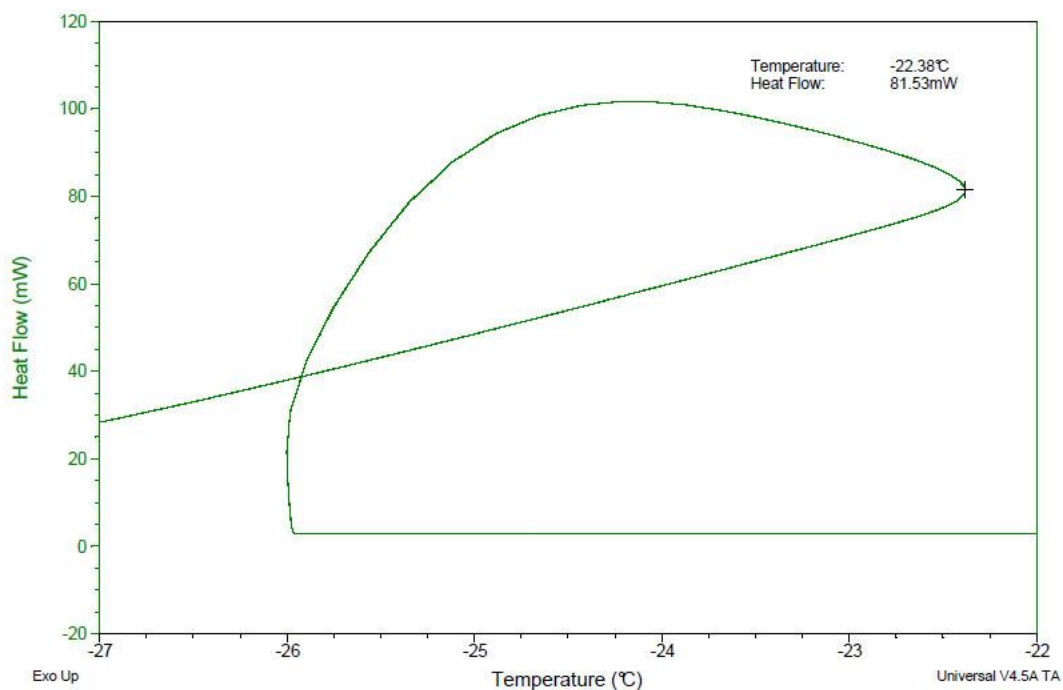
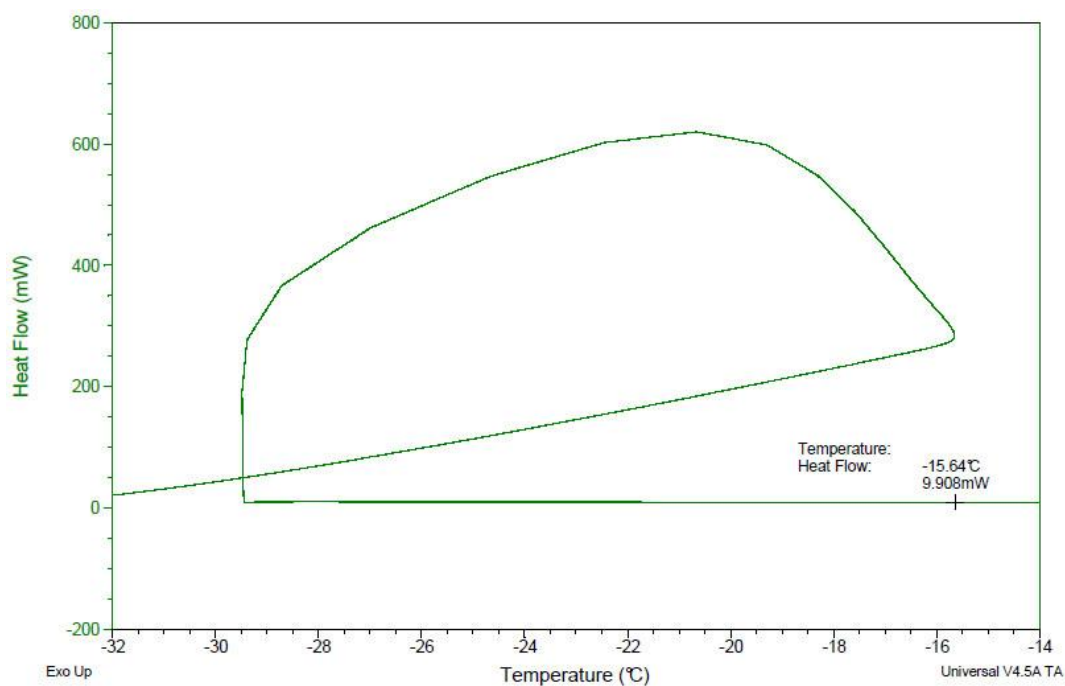## 1.6 mol/kg Sodium Chloride Solution

Figure 137. Freezing profile for 30 µl of 1.6 mol/kg Sodium Chloride sealed in an aluminium pan and cooled from 35°C to -30°C at a rate of 5°C/min. Analysis was carried out by reading off temperature at the highest temperature achieved by the solution during the freezing process.

Figure 138. Freezing profile for 30 µl of 1.6 mol/kg Sodium Chloride sealed in an aluminium pan and cooled from 35°C to -30°C at a rate of 5°C/min. Analysis was carried out by reading off temperature at the highest temperature achieved by the solution during the freezing process.

1.8 mol/kg Sodium Chloride Solution

Figure 139. Freezing profile for 30 µl of 1.8 mol/kg Sodium Chloride sealed in an aluminium pan and cooled from 35°C to -30°C at a rate of 5°C/min. Analysis was carried out by reading off temperature at the highest temperature achieved by the solution during the freezing process.
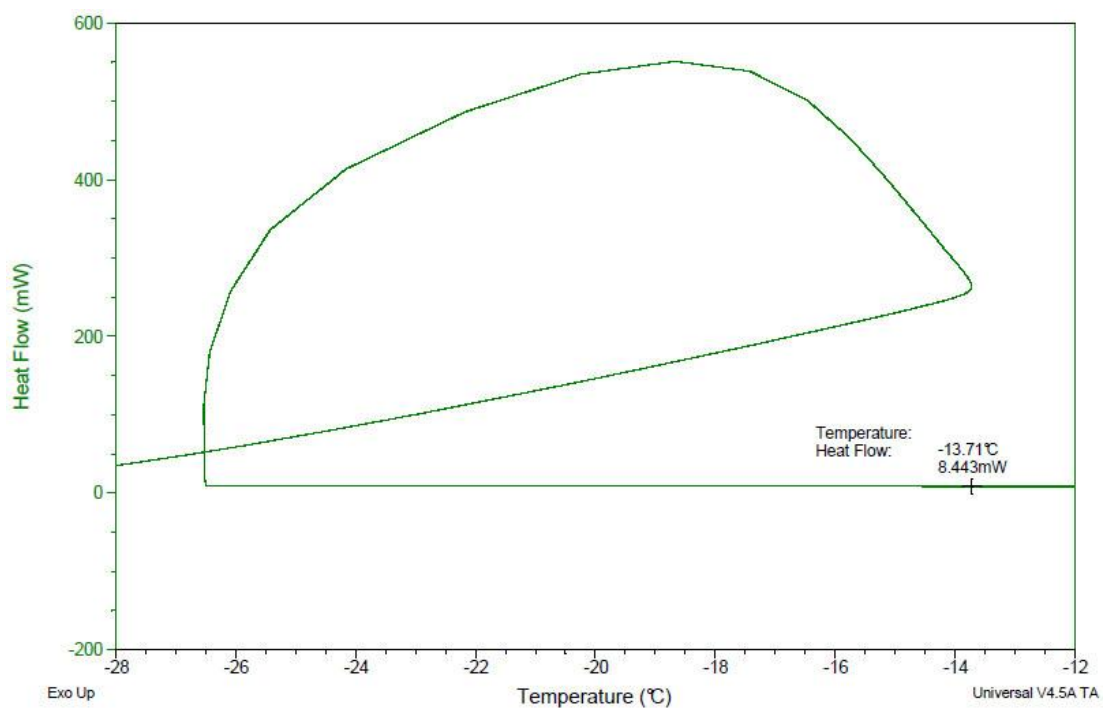
Figure 140. Freezing profile for 30 µl of 1.8 mol/kg Sodium Chloride sealed in an aluminium pan and cooled from 35°C to -30°C at a rate of 5°C/min. Analysis was carried out by reading off temperature at the highest temperature achieved by the solution during the freezing process.

2.0 mol/kg Sodium Chloride Solution

Figure 141. Freezing profile for 30 µl of 2.0 mol/kg Sodium Chloride sealed in an aluminium pan and cooled from 35°C to -40°C at a rate of 5°C/min. Analysis was carried out by reading off temperature at the highest temperature achieved by the solution during the freezing process.

Figure 142. Freezing profile for 30 μl of 2.0 mol/kg Sodium Chloride sealed in an aluminium pan and cooled from 35°C to -30°C at a rate of 5°C/min. Analysis was carried out by reading off temperature at the highest temperature achieved by the solution during the freezing process.

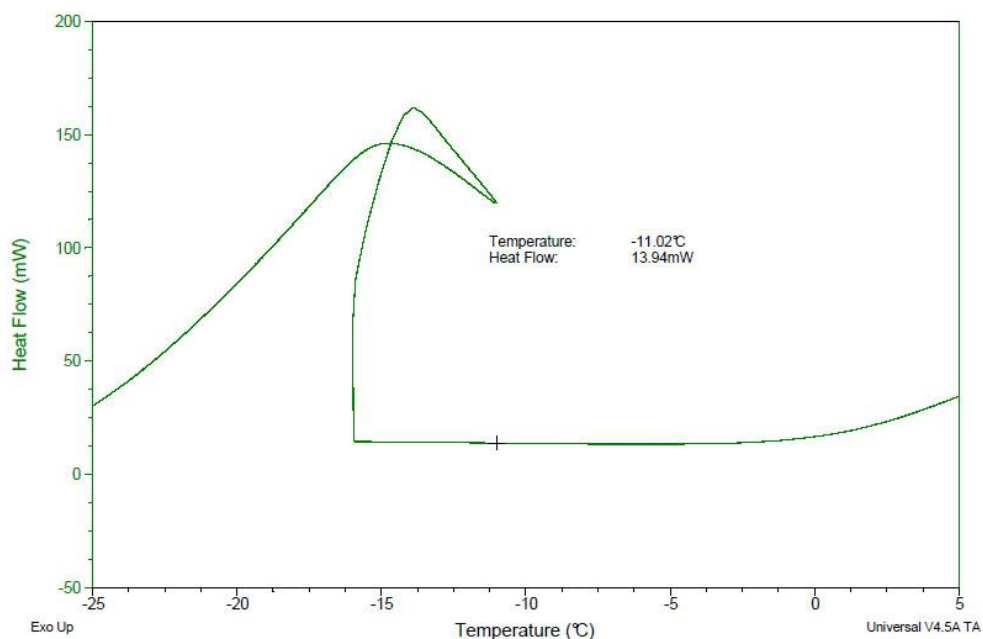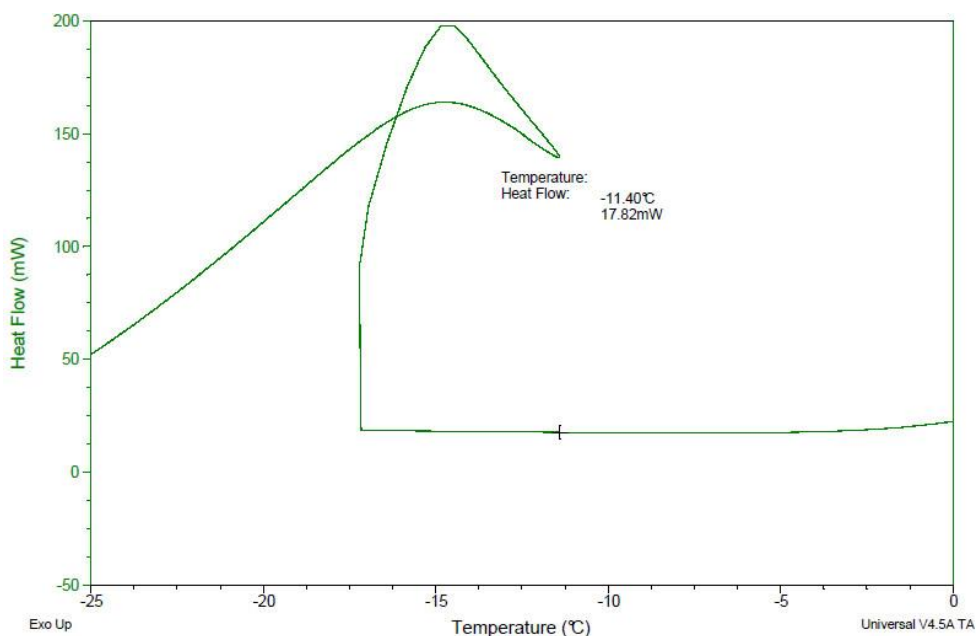**Method 3 - DSC Traces**

0.1 mol/kg Sodium Chloride Solution

Figure 143. Freezing profile for 100 µl of 0.1 mol/kg Sodium Chloride solution sealed in an aluminium pan with 0.3g of iron filings. Temperature was ramped from 35°C to 5°C at a rate of 100°C/min and then ramped from 5°C to -30°C at a rate of 2°C/min. Analysis was carried out by reading off temperature at the highest temperature achieved by the solution during the freezing process.
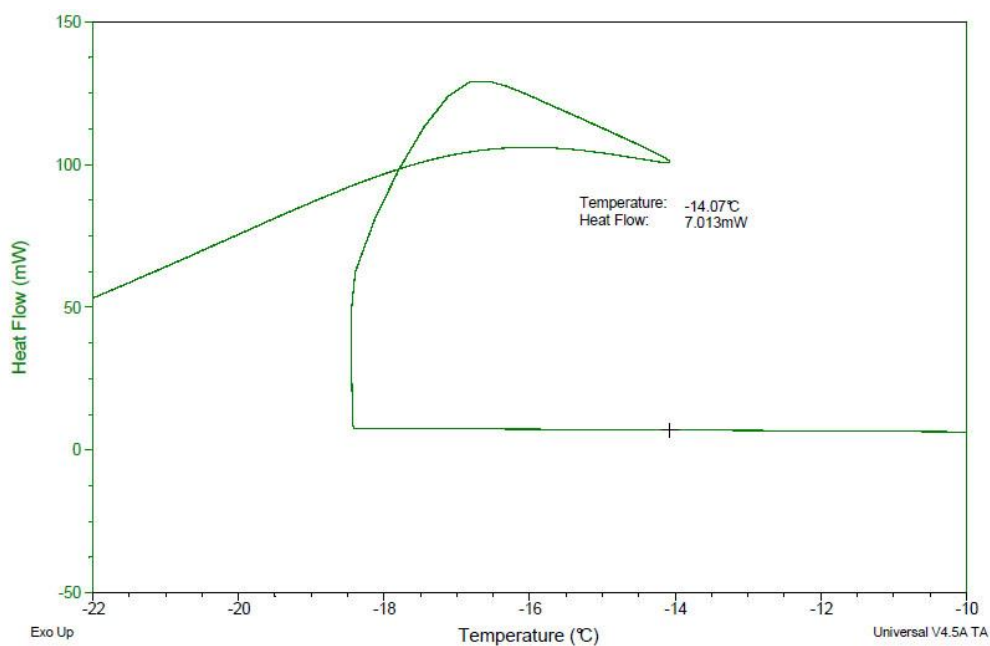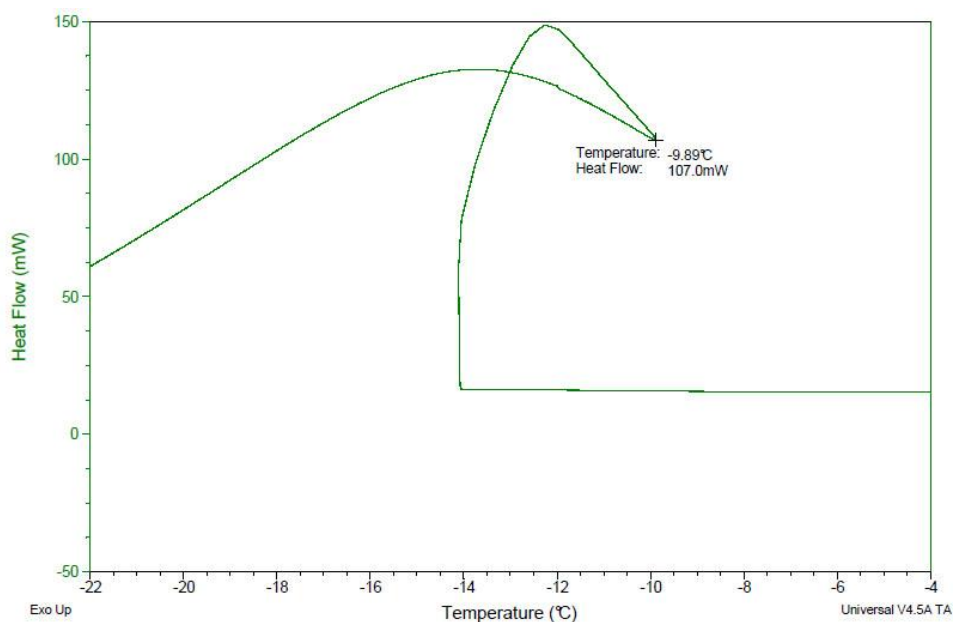
0.2 mol/kg Sodium Chloride Solution

Figure 144. Freezing profile for 100 µl of 0.2 mol/kg Sodium Chloride solution sealed in an aluminium pan with 0.3g of iron filings. Temperature was ramped from 35°C to 5°C at a rate of 100°C/min and then ramped from 5°C to -30°C at a rate of 2°C/min. Analysis was carried out by reading off temperature at the highest temperature achieved by the solution during the freezing process.
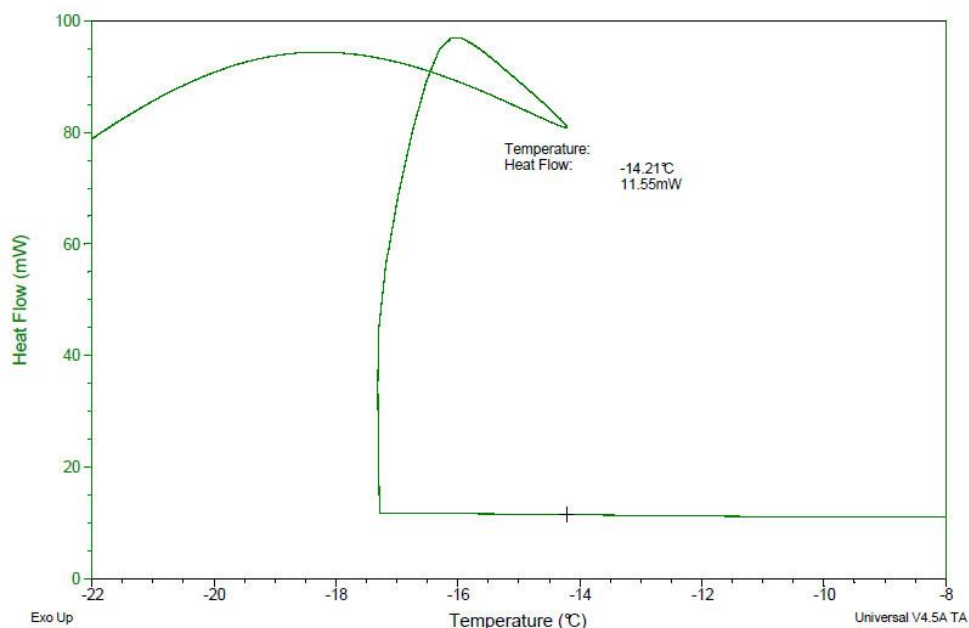
209

0.3 mol/kg Sodium Chloride Solution

Figure 145. Freezing profile for 100 µl of 0.3 mol/kg Sodium Chloride solution sealed in an aluminium pan with 0.3g of iron filings. Temperature was ramped from 35°C to 5°C at a rate of 100°C/min and then ramped from 5°C to -30°C at a rate of 2°C/min. Analysis was carried out by reading off temperature at the highest temperature achieved by the solution during the freezing process.

0.4 mol/kg Sodium Chloride Solution

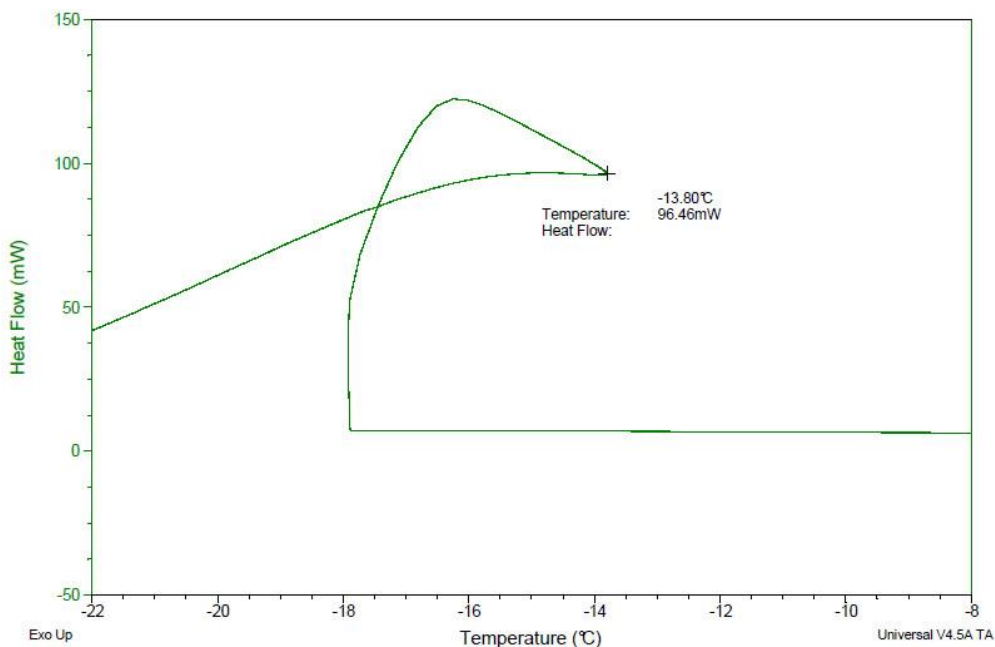Figure 146. Freezing profile for 100 µl of 0.4 mol/kg Sodium Chloride solution sealed in an aluminium pan with 0.3g of iron filings. Temperature was ramped from 35°C to 5°C at a rate of 100°C/min and then ramped from 5°C to -30°C at a rate of 2°C/min. Analysis was carried out by reading off temperature at the highest temperature achieved by the solution during the freezing process.
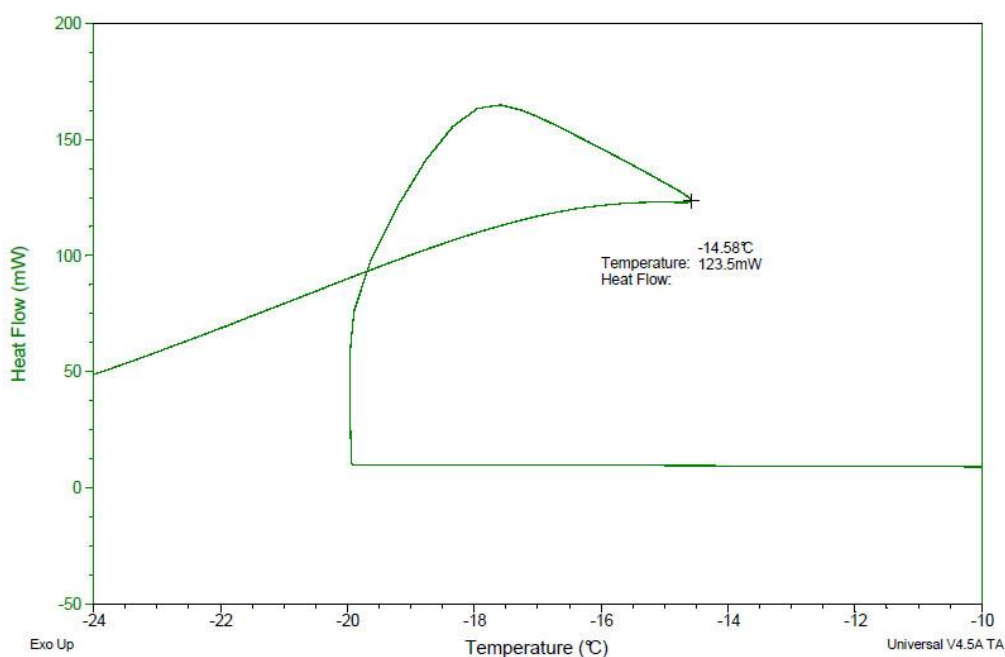
210

0.5 mol/kg Sodium Chloride Solution

Figure 147. Freezing profile for 100 μl of 0.5 mol/kg Sodium Chloride solution sealed in an aluminium pan with 0.3g of iron filings. Temperature was ramped from 35°C to 5°C at a rate of 100°C/min and then ramped from 5°C to -30°C at a rate of 2°C/min. Analysis was carried out by reading off temperature at the highest temperature achieved by the solution during the freezing process.

0.6 mol/kg Sodium Chloride Solution

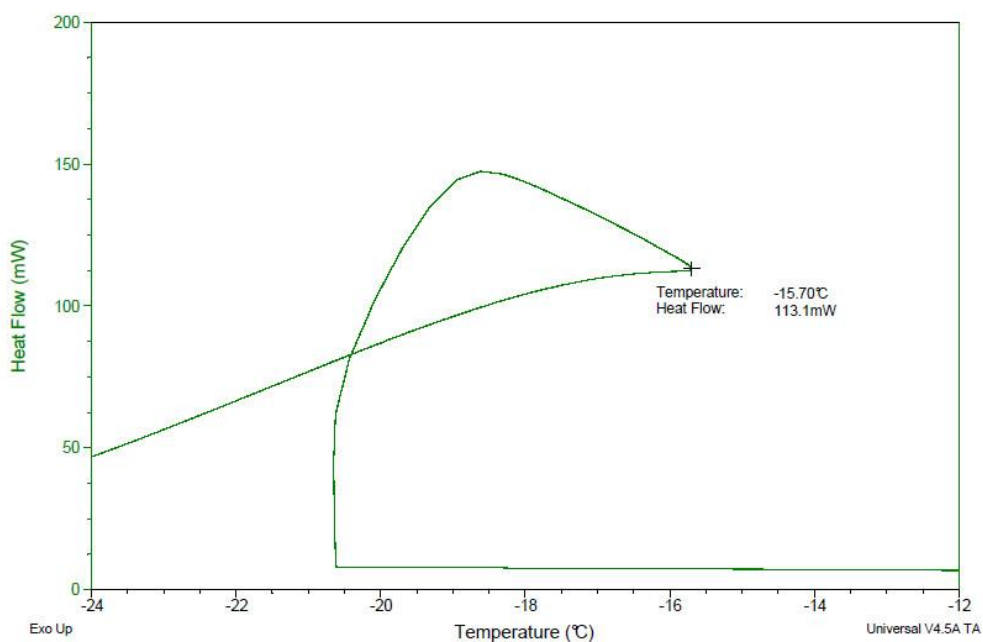Figure 148. Freezing profile for 100 μl of 0.6 mol/kg Sodium Chloride solution sealed in an aluminium pan with 0.3g of iron filings. Temperature was ramped from 35oC to 5oC at a rate of 100oC/min and then ramped from 5oC to -30oC at a rate of 2oC/min. Analysis was carried out by reading off temperature at the highest temperature achieved by the solution during the freezing process.
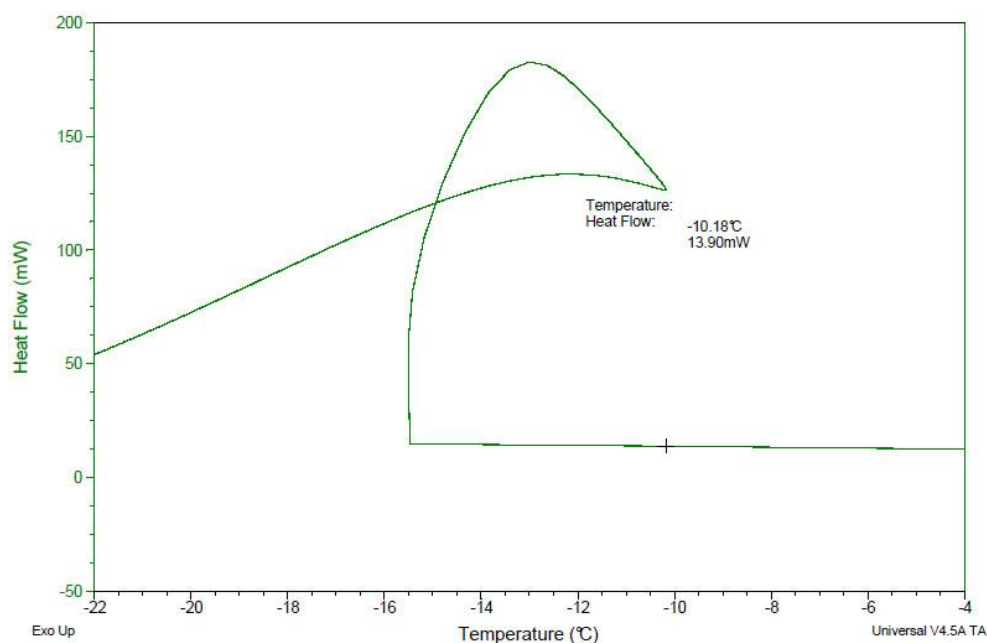
211

0.7 mol/kg Sodium Chloride Solution

Figure 149. Freezing profile for 100 μl of 0.7 mol/kg Sodium Chloride solution sealed in an aluminium pan with 0.3g of iron filings. Temperature was ramped from 35°C to 5°C at a rate of 100°C/min and then ramped from 5°C to -30°C at a rate of 2°C/min. Analysis was carried out by reading off temperature at the highest temperature achieved by the solution during the freezing process.

0.8 mol/kg Sodium Chloride Solution

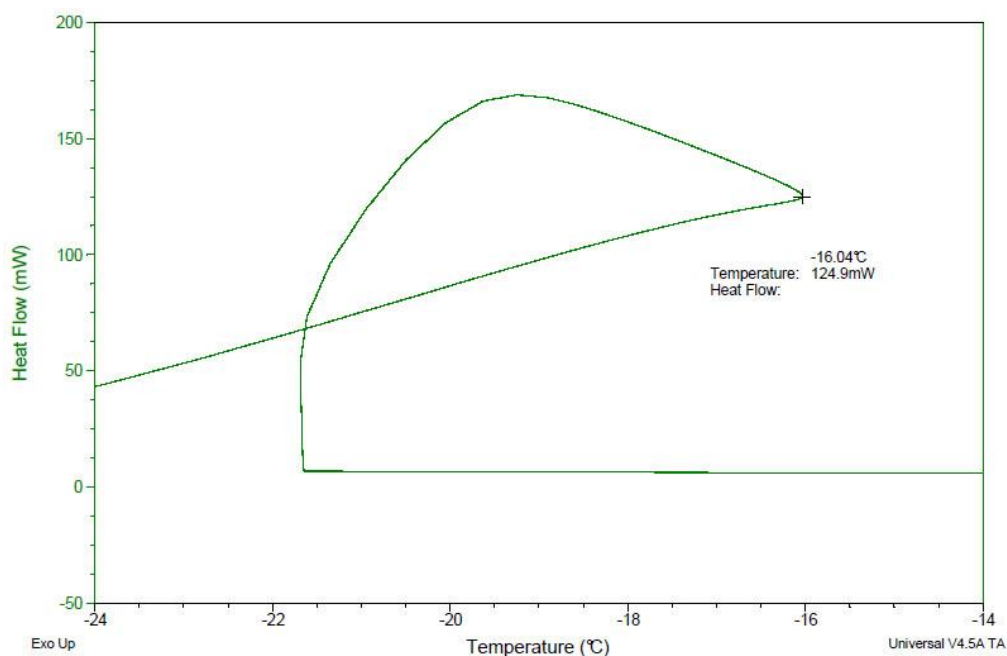Figure 150. Freezing profile for 100 μl of 0.8 mol/kg Sodium Chloride solution sealed in an aluminium pan with 0.3g of iron filings. Temperature was ramped from 35°C to 5°C at a rate of 100°C/min and then ramped from 5°C to -30°C at a rate of 2°C/min. Analysis was carried out by reading off temperature at the highest temperature achieved by the solution during the freezing process.

0.9 mol/kg Sodium Chloride Solution

Figure 151. Freezing profile for 100 µl of 0.9 mol/kg Sodium Chloride solution sealed in an aluminium pan with 0.3g of iron filings. Temperature was ramped from 35°C to 5°C at a rate of 100°C/min and then ramped from 5°C to -30°C at a rate of 2°C/min. Analysis was carried out by reading off temperature at the highest temperature achieved by the solution during the freezing process.
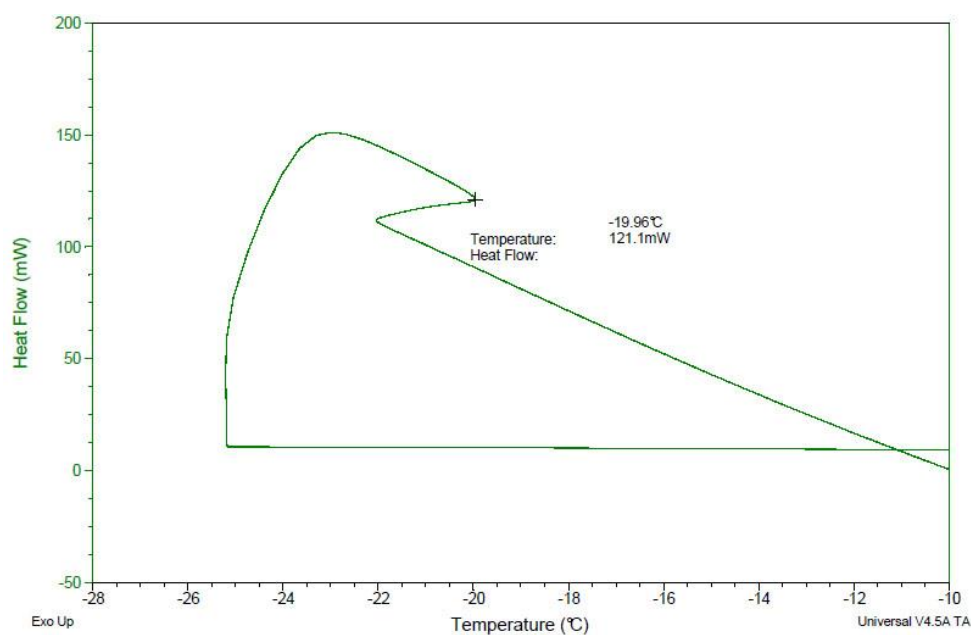
1.0 mol/kg Sodium Chloride Solution

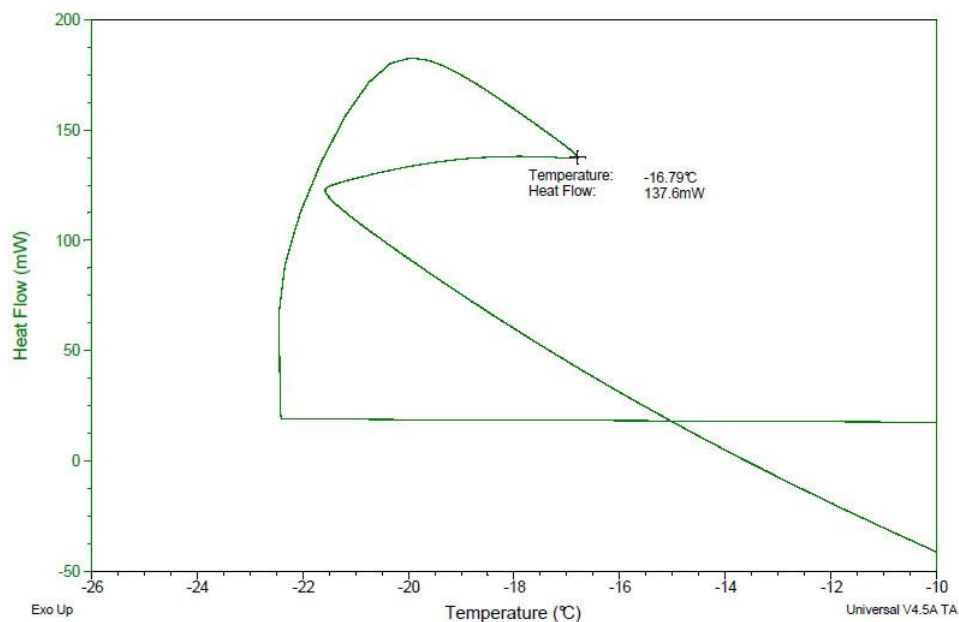Figure 152. Freezing profile for 100 µl of 1.0 mol/kg Sodium Chloride solution sealed in an aluminium pan with 0.3g of iron filings. Temperature was ramped from 35°C to 5°C at a rate of 100°C/min and then ramped from 5°C to -30°C at a rate of 2°C/min. Analysis was carried out by reading off temperature at the highest temperature achieved by the solution during the freezing process.
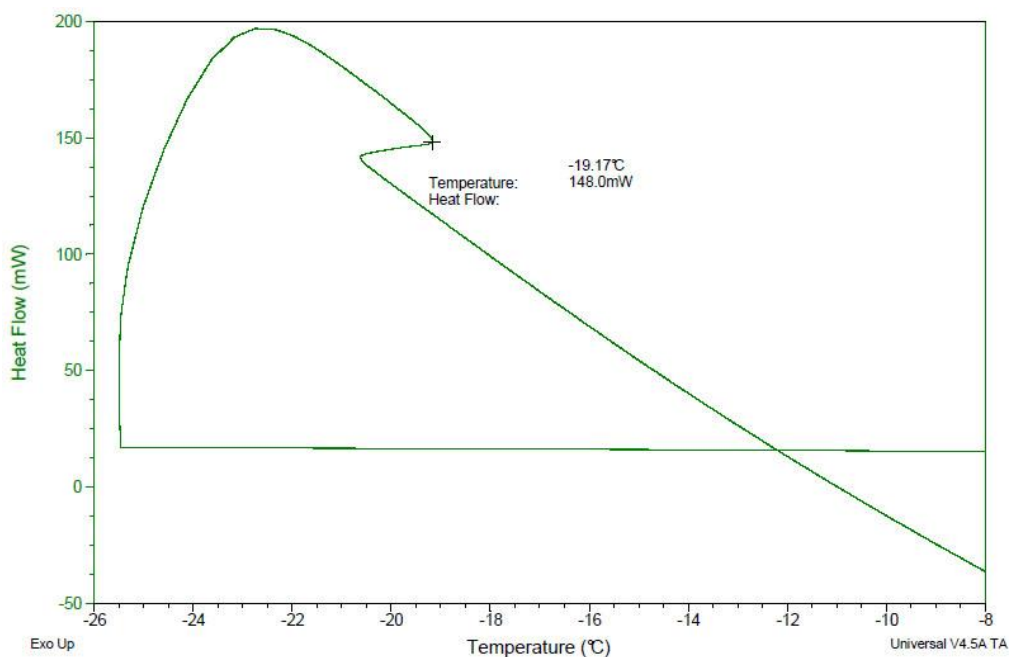
213

1.2 mol/kg Sodium Chloride Solution

Figure 153. Freezing profile for 100 µl of 1.2 mol/kg Sodium Chloride solution sealed in an aluminium pan with 0.3g of iron filings. Temperature was ramped from 35°C to 5°C at a rate of 100°C/min and then ramped from 5°C to -30°C at a rate of 2°C/min. Analysis was carried out by reading off temperature at the highest temperature achieved by the solution during the freezing process.
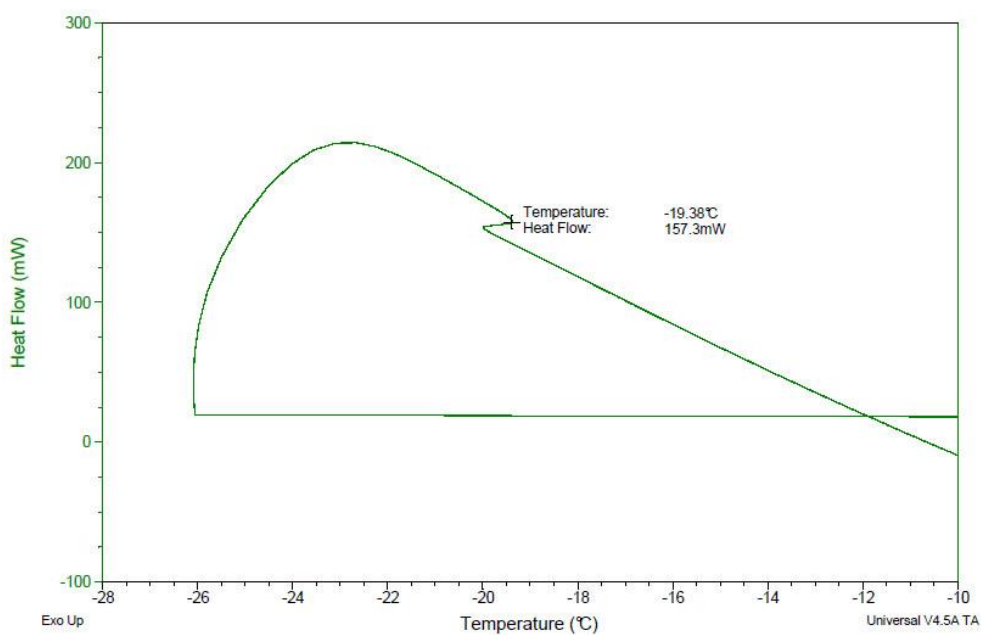
1.4 mol/kg Sodium Chloride Solution

Figure 154. Freezing profile for 100 µl of 1.4 mol/kg Sodium Chloride solution sealed in an aluminium pan with 0.3g of iron filings. Temperature was ramped from 35oC to 5oC at a rate of 100oC/min and then ramped from 5oC to -30oC at a rate of 2oC/min. Analysis was carried out by reading off temperature at the highest temperature achieved by the solution during the freezing process.
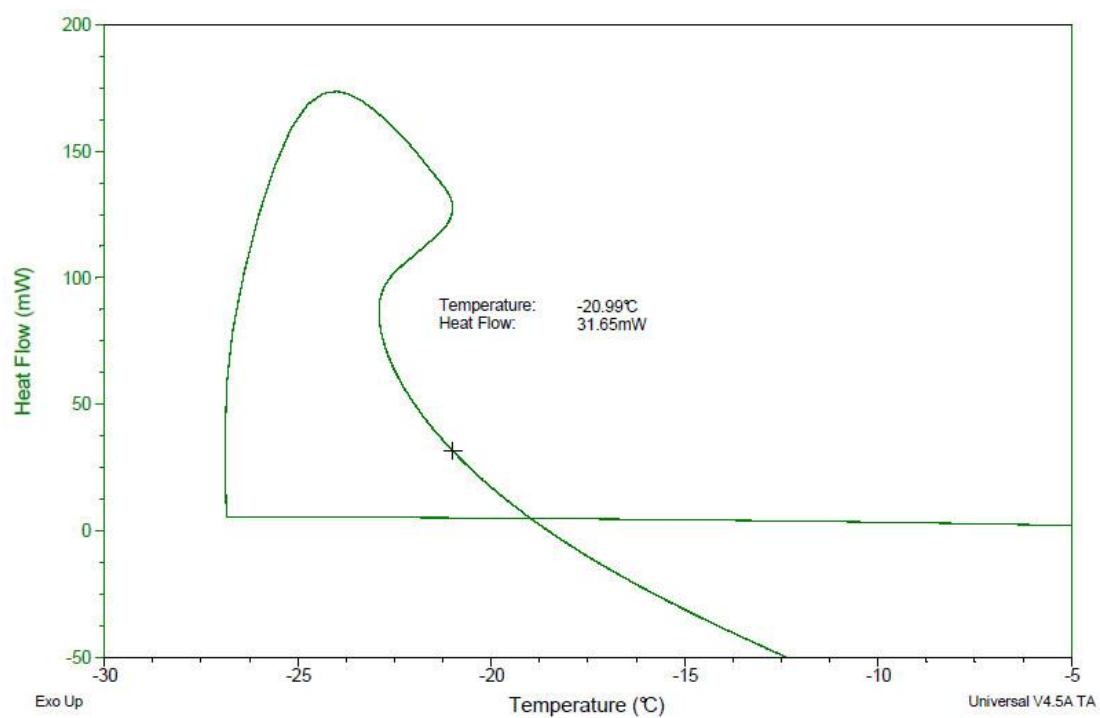
1.6 mol/kg Sodium Chloride Solution

Figure 155. Freezing profile for 100 µl of 1.6 mol/kg Sodium Chloride solution sealed in an aluminium pan with 0.3g of iron filings. Temperature was ramped from 35°C to 5°C at a rate of 100°C/min and then ramped from 5°C to -30°C at a rate of 2°C/min. Analysis was carried out by reading off temperature at the highest temperature achieved by the solution during the freezing process.

1.8 mol/kg Sodium Chloride Solution

Figure 156. Freezing profile for 100 µl of 1.8 mol/kg Sodium Chloride solution sealed in an aluminium pan with 0.3g of iron filings. Temperature was ramped from 35°C to 5°C at a rate of 100°C/min and then ramped from 5°C to -30°C at a rate of 2°C/min. Analysis was carried out by reading off temperature at the highest temperature achieved by the solution during the freezing process.
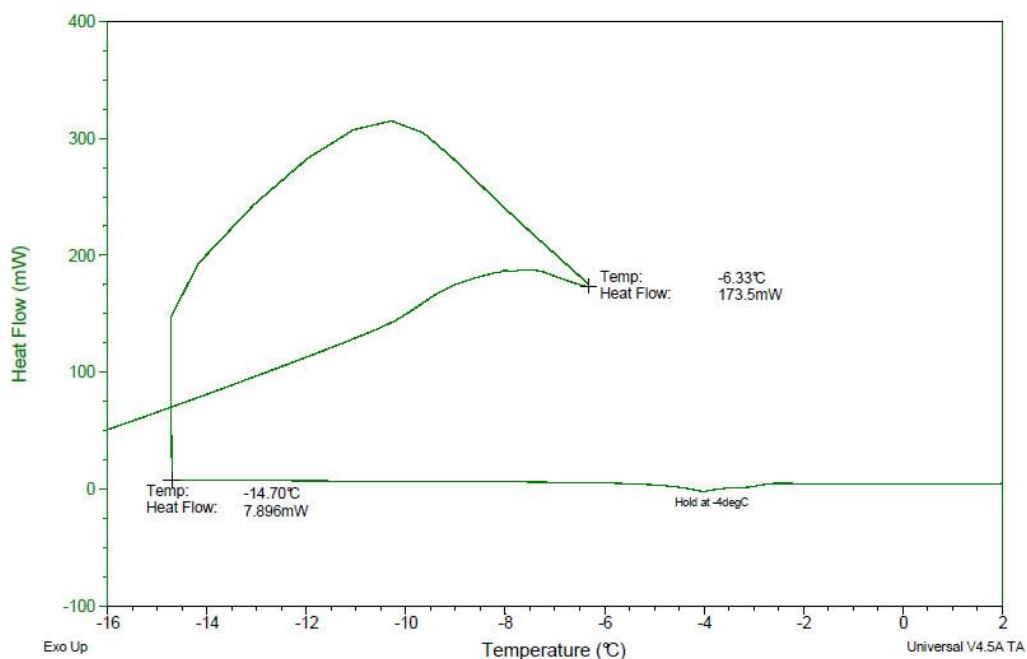
215

2.0 mol/kg Sodium Chloride Solution

Figure 157. Freezing profile for 100 µl of 2.0 mol/kg Sodium Chloride solution sealed in an aluminium pan with 0.3g of iron filings. Temperature was ramped from 35°C to 5°C at a rate of 100°C/min and then ramped from 5°C to -40°C at a rate of 2°C/min. Analysis was carried out by reading off temperature at the highest temperature achieved by the solution during the freezing process.

Method 4 - DSC Traces

Pure Water

Figure 158. Freezing profile for 100 µl of pure water sealed in an aluminium pan. Analysis was carried out by reading off temperature at the highest temperature achieved by the solution during the freezing process.

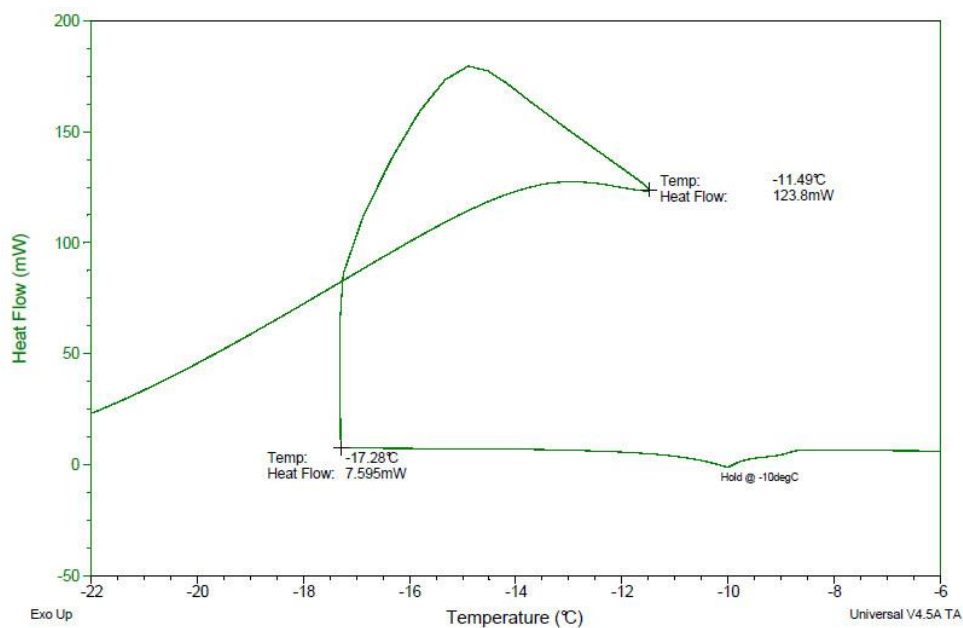**0.3 mol/kg Sodium Chloride (Isothermal hold at -10°C)**
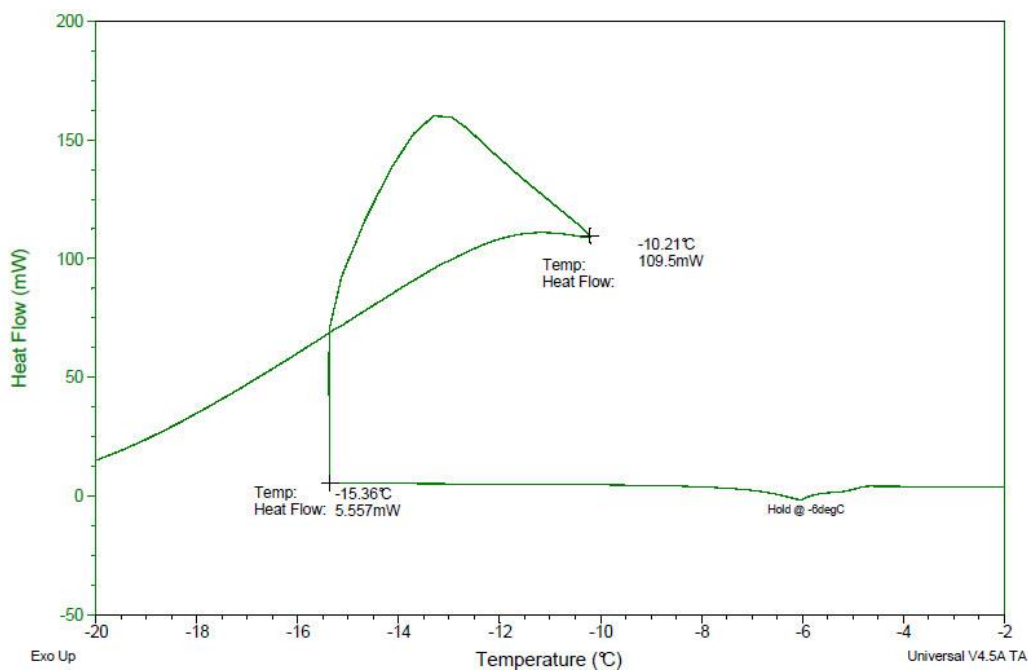

Figure 159. Freezing profile for 100 µl of 0.3 mol/kg Sodium Chloride solution sealed in an aluminium pan. Analysis was carried out by reading off temperature at the highest temperature achieved by the solution during the DSC freezing process.

217
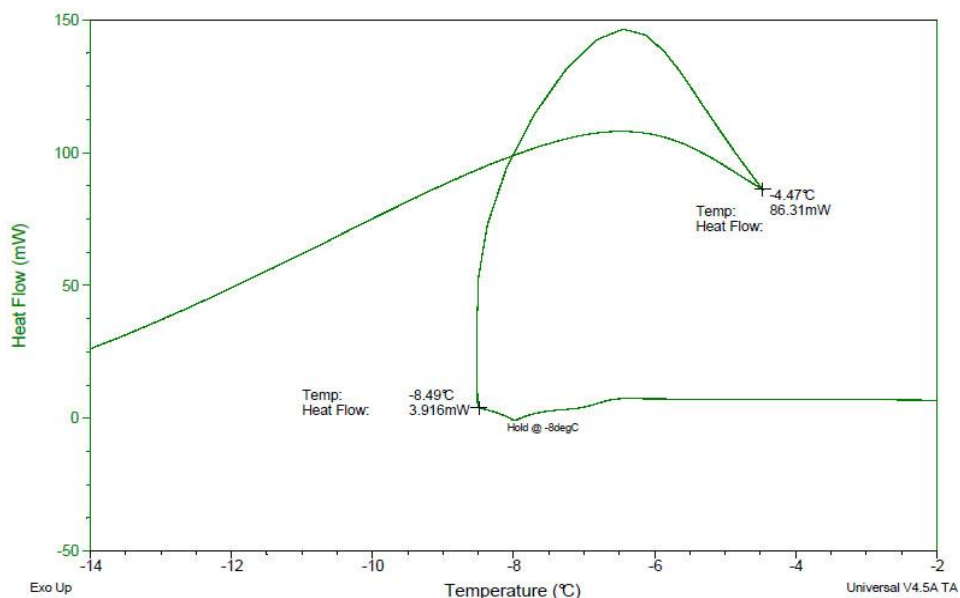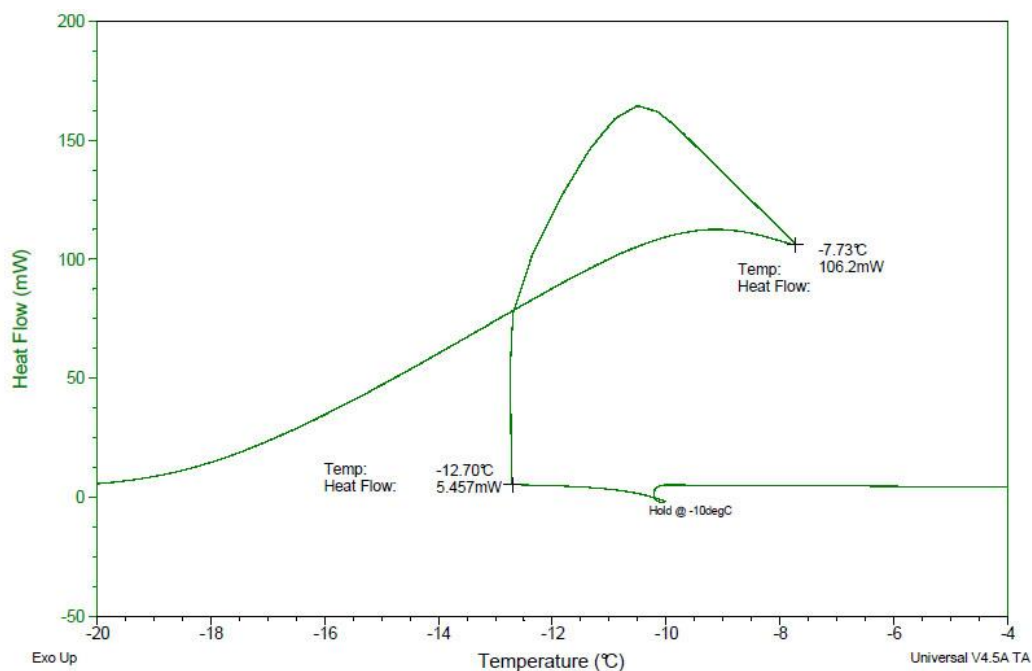
0.3 mol/kg Sodium Chloride (Isothermal hold at -6°C)

Figure 160. Freezing profile for 100 µl of 0.3 mol/kg Sodium Chloride solution sealed in an aluminium pan with 0.3g iron filings. Analysis was carried out by reading off temperature at the highest temperature achieved by the solution during the freezing process.

0.3 mol/kg Sodium Chloride (Isothermal hold at -8°C)

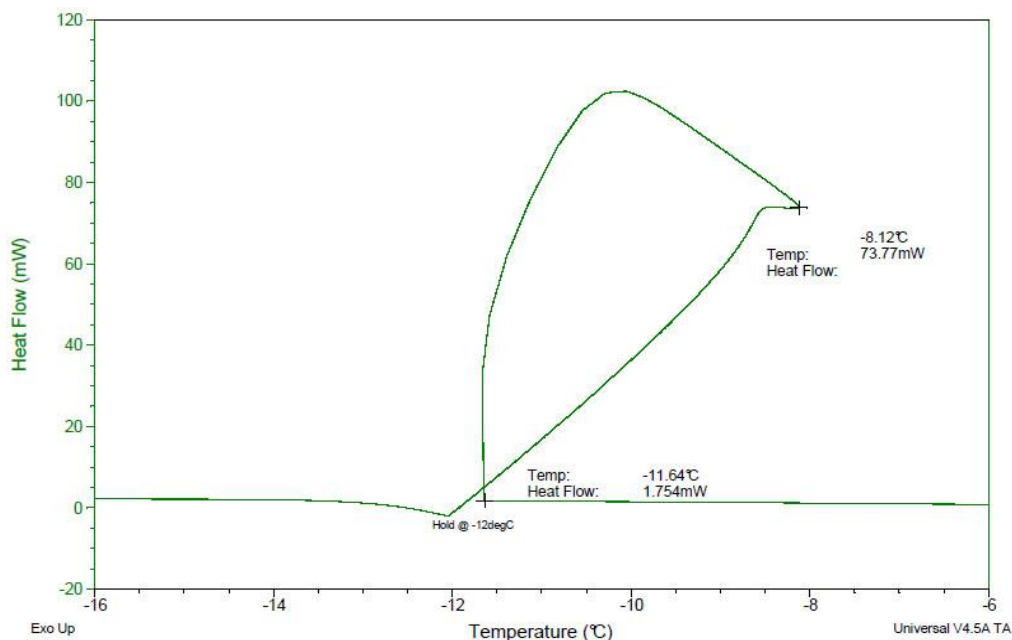
Figure 161. Freezing profile for 100 µl of 0.3 mol/kg Sodium Chloride solution sealed in an aluminium pan with 0.3g iron filings. Analysis was carried out by reading off temperature at the highest temperature achieved by the solution during the freezing process.

0.3 mol/kg Sodium Chloride (Isothermal hold at -10°C)

Figure 162. Freezing profile for 100 µl of 0.3 mol/kg Sodium Chloride solution sealed in an aluminium pan with 0.3g iron filings. Analysis was carried out by reading off temperature at the highest temperature achieved by the solution during the freezing process.

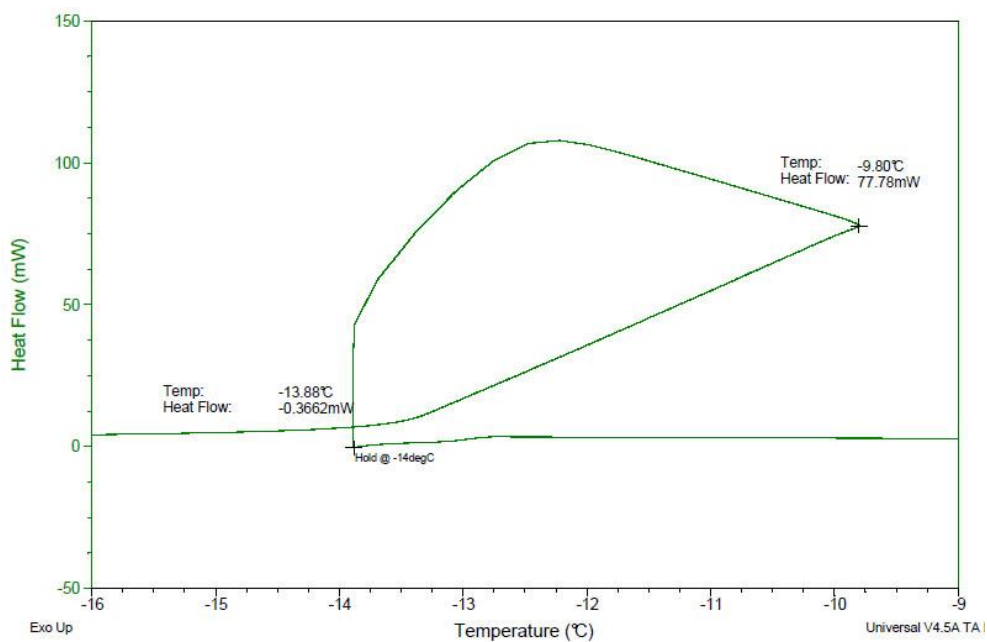## 0.3 mol/kg Sodium Chloride (Isothermal hold at -12°C)

Figure 163. Freezing profile for 100 µl of 0.3 mol/kg Sodium Chloride solution sealed in an aluminium pan with 0.3g iron filings. Analysis was carried out by reading off temperature at the highest temperature achieved by the solution during the freezing process.

0.3 mol/kg Sodium Chloride (Isothermal hold at -14°C)

Figure 164. Freezing profile for 100 µl of 0.3 mol/kg Sodium Chloride solution sealed in an aluminium pan with 0.3g iron filings. Analysis was carried out by reading off temperature at the highest temperature achieved by the solution during the freezing process.

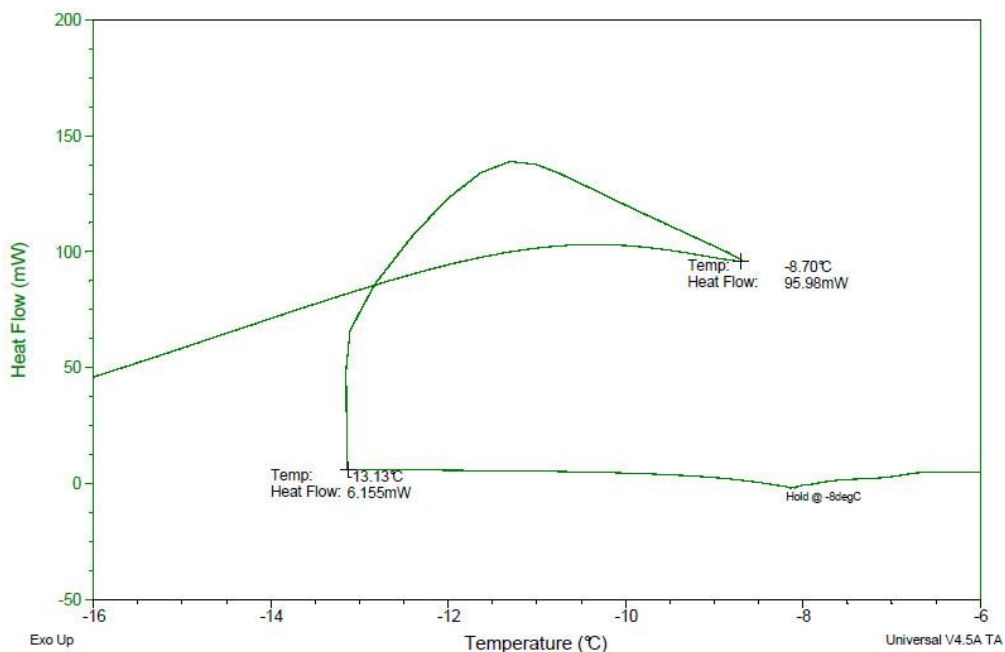**0.3 mol/kg Sodium Chloride (Isothermal hold at -8°C, magnet applied)**

Figure 165. Freezing profile for 100 µl of 0.3 mol/kg Sodium Chloride solution sealed in an aluminium pan with 0.3g iron filings. Analysis was carried out by reading off temperature at the highest temperature achieved by the solution during the freezing process.
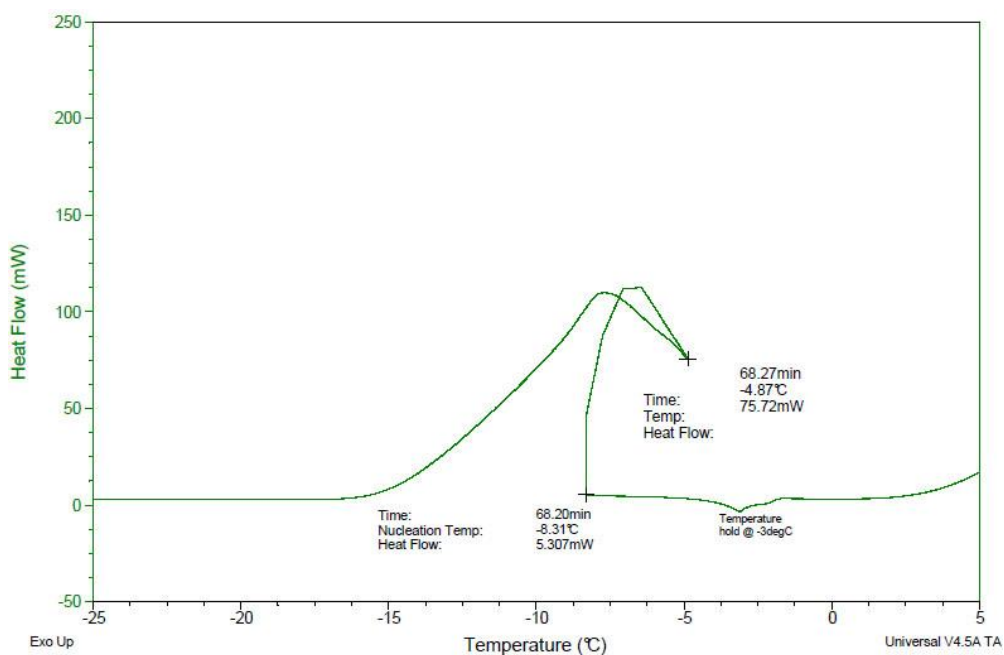
Pure water (1 hour isothermal hold)

Figure 166. Freezing profile for 100 µl of pure water sealed in an aluminium pan with 0.3g iron filings. Analysis was carried out by reading off temperature at the highest temperature achieved by the solution during the freezing process.

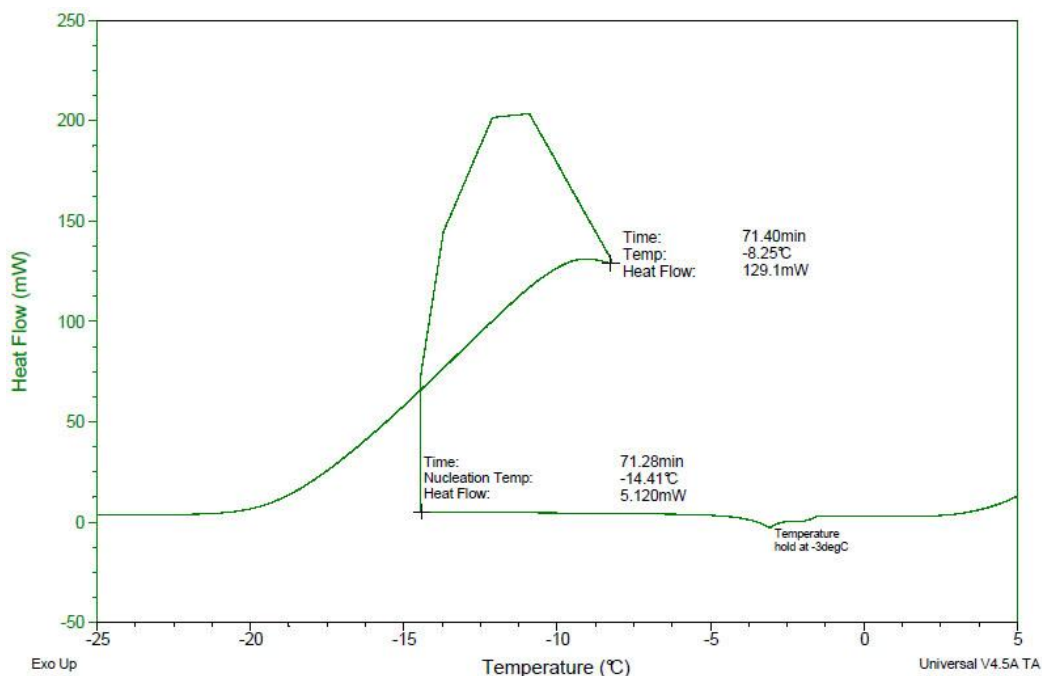**0.3 mol/kg Sodium Chloride (1 hour isothermal hold))**

Figure 167. Freezing profile for 100 µl of Sodium Chloride solution sealed in an aluminium pan with 0.3g iron filings. Analysis was carried out by reading off temperature at the highest temperature achieved by the solution during the freezing process.

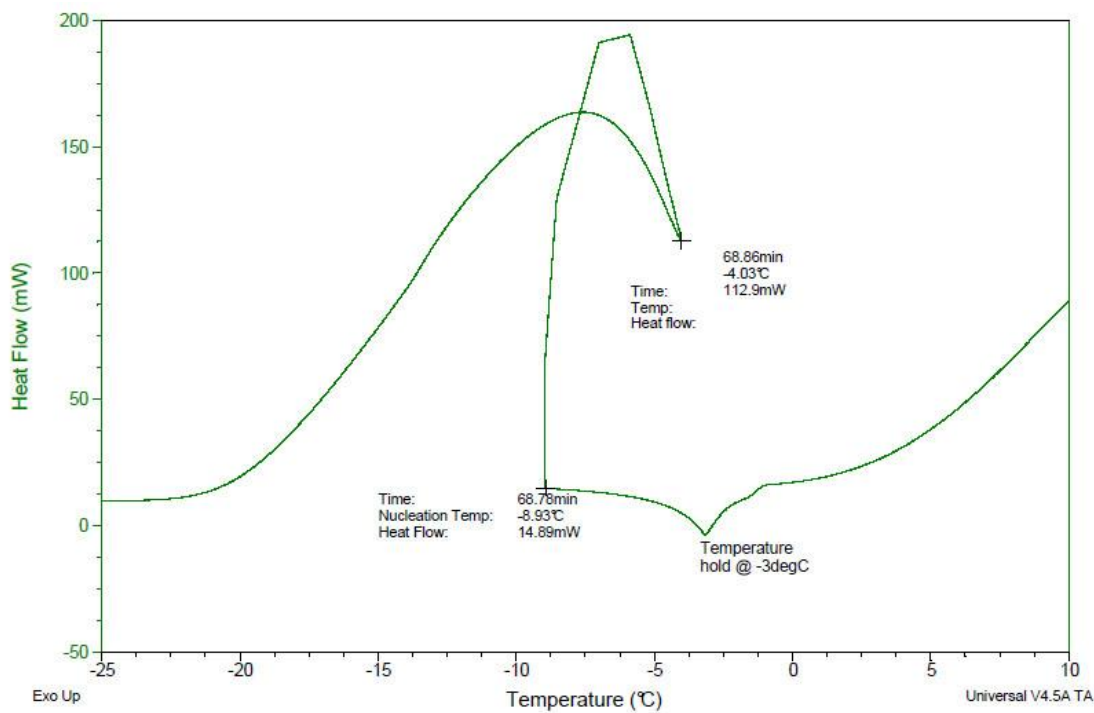221

Method 5 - DSC Traces

Pure water (Open pan)

Figure 168. Freezing profile for 150 µl of pure water in an aluminium pan with 0.3g iron filings. Pan was not sealed. Analysis was carried out by reading off temperature at the highest temperature achieved by the solution during the freezing process.

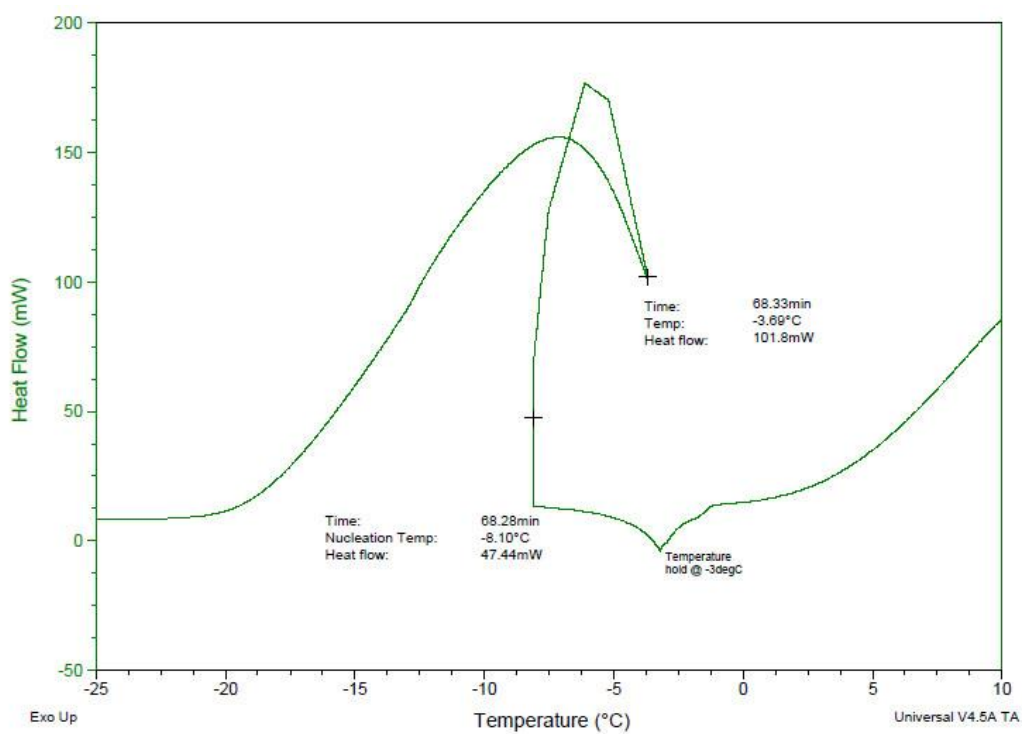**Pure water (Open pan with the use of magnet)**

Figure 169. Freezing profile for 150 µl of pure water in an aluminium pan with 0.3g iron filings. Pan was not sealed. Analysis was carried out by reading off temperature at the highest temperature achieved by the solution during the freezing process.
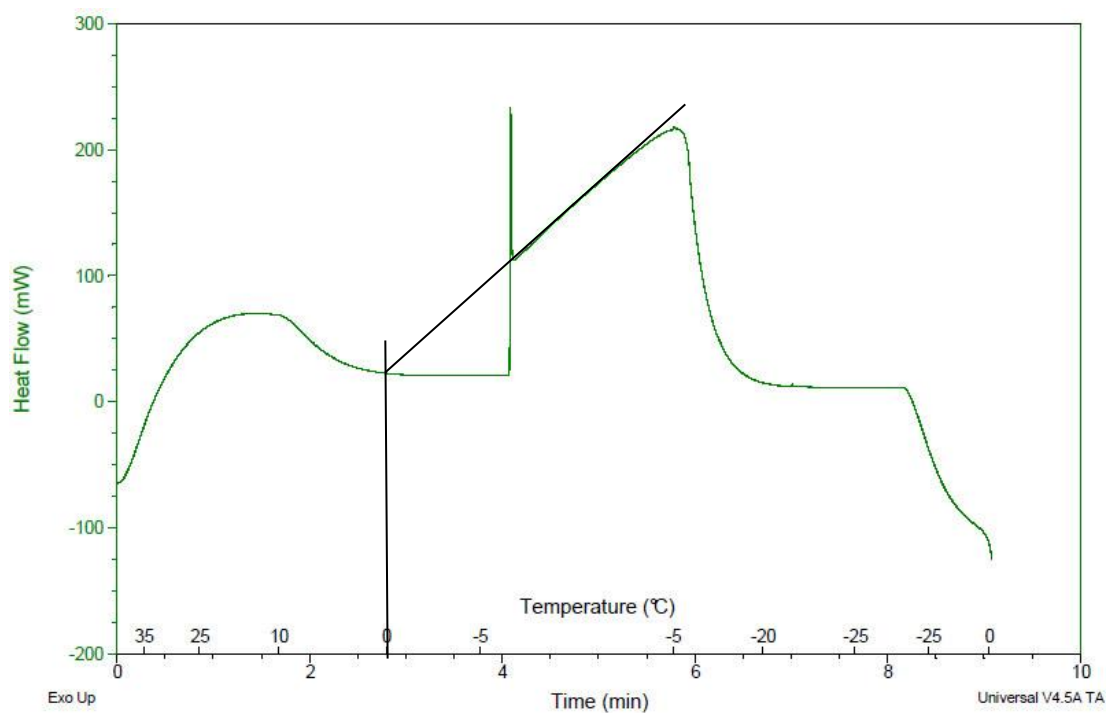
Method 3 - DSC Traces Reanalysed

Pure Water

Figure 170. Freezing profile for 100 µl of pure water sealed in an aluminium pan with 0.3g of iron filings. Analysis was carried out by drawing a tangential line which is extrapolated backwards to intersect with the baseline of the trace
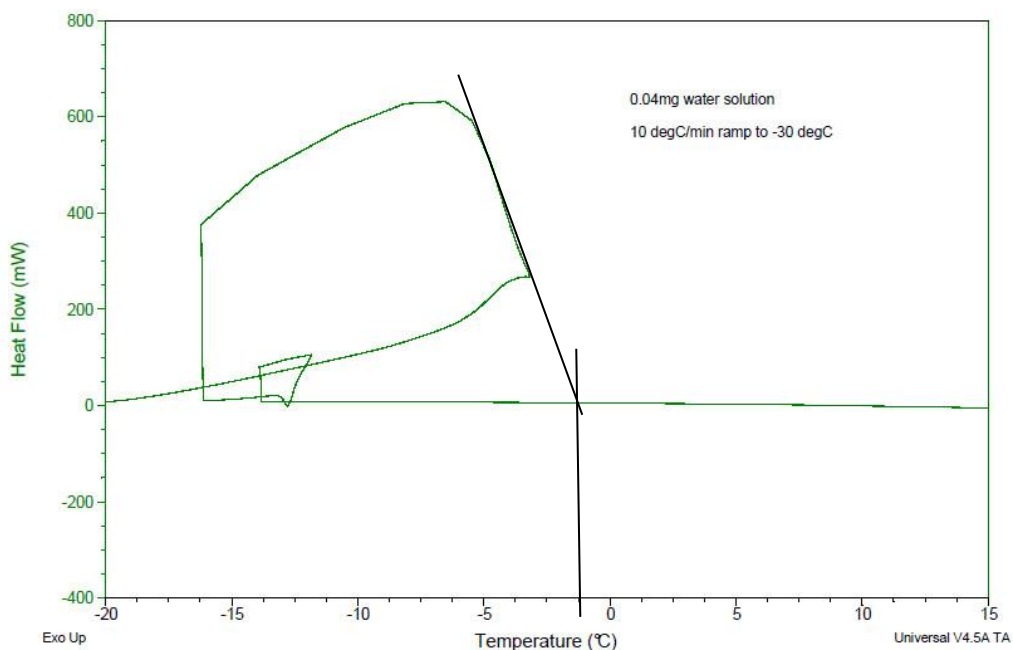
Method 6 - DSC Traces

Pure water

Figure 171. Freezing profile for 50 µl of pure water sealed in an aluminium pan. Temperature was ramped from 35°C to -30°C at a rate of 10°C/min. Heat flow (mW) is plotted against temperature (°C). Analysis was carried out by drawing a tangential line which is extrapolated forward to intersect with the baseline of the trace.
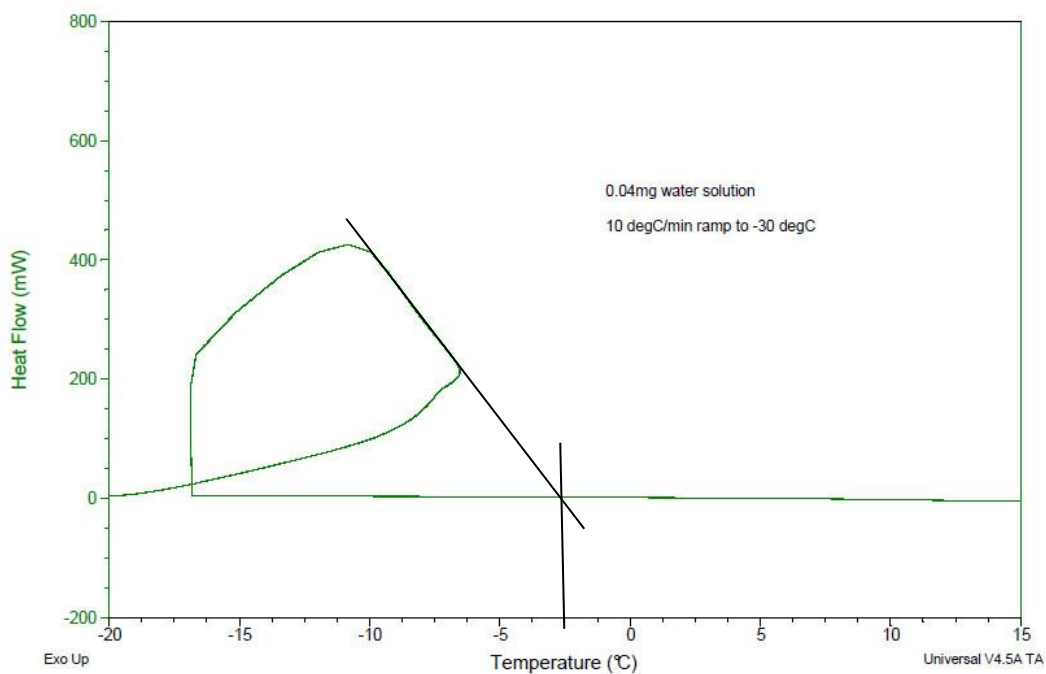

Figure 172. Freezing profile for 50 µl of pure water sealed in an aluminium pan. Temperature was ramped from 35°C to -30°C at a rate of 10°C/min. Heat flow (mW) is plotted against temperature (°C). Analysis was carried out by drawing a tangential line which is extrapolated forward to intersect with the baseline of the trace.
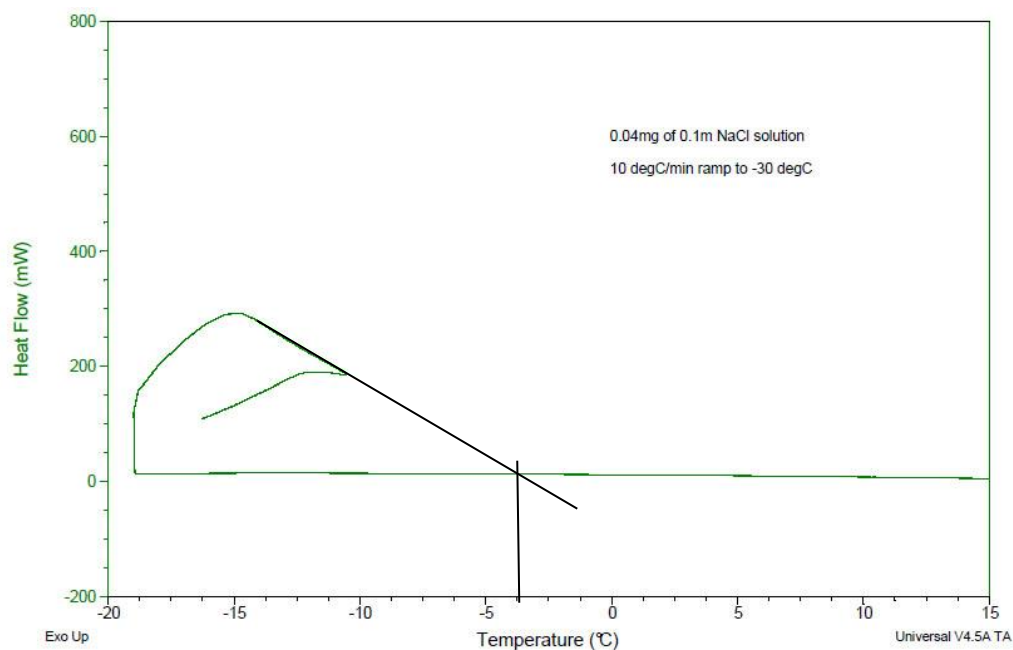
0.1 mol/kg Sodium Chloride

Figure 173. Freezing profile for 50 µl of 0.1 mol/kg Sodium Chloride sealed in an aluminium pan. Temperature was ramped from 35°C to -30°C at a rate of 10°C/min. Heat flow (mW) is plotted against temperature (°C). Analysis was carried out by drawing a tangential line which is extrapolated forward to intersect with the baseline of the trace.
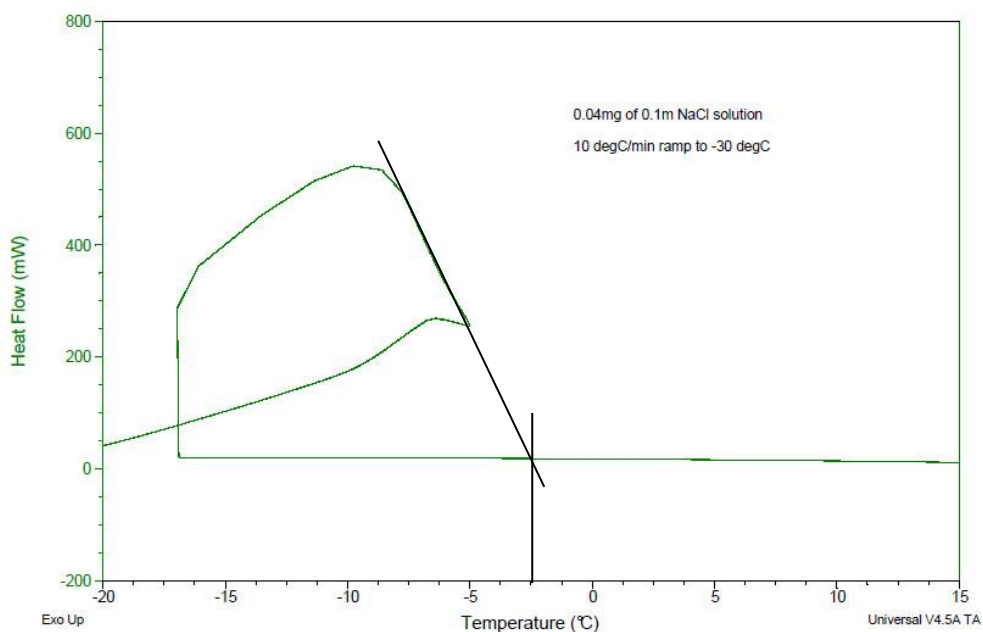

Figure 174. Freezing profile for 50 µl of 0.1 mol/kg Sodium Chloride sealed in an aluminium pan. Temperature was ramped from 35°C to -30°C at a rate of 10°C/min. Heat flow (mW) is plotted against temperature (°C). Analysis was carried out by drawing a tangential line which is extrapolated forward to intersect with the baseline of the trace.